Université de Montréal

# Nouvelles stratégies pour l'analyse des cyanotoxines par spectrométrie de masse

par
Audrey Roy-Lachapelle

Département de Chimie
Faculté des Arts et Sciences

Thèse présentée à la Faculté des Études Supérieures et Postdoctorales
en vue de l'obtention du grade de *Philosophiæ Doctor* (Ph. D.)
en Chimie
option Analytique

avril, 2015

© Audrey Roy-Lachapelle, 2015

# Résumé

Les cyanobactéries ont une place très importante dans les écosystèmes aquatiques et un nombre important d'espèces considéré comme nuisible de par leur production de métabolites toxiques. Ces cyanotoxines possèdent des propriétés très variées et ont souvent été associées à des épisodes d'empoisonnement. L'augmentation des épisodes d'efflorescence d'origine cyanobactériennes et le potentiel qu'ils augmentent avec les changements climatiques a renchéri l'intérêt de l'étude des cyanobactéries et de leurs toxines. Considérant la complexité chimique des cyanotoxines, le développement de méthodes de détection simples, sensibles et rapides est toujours considéré comme étant un défi analytique.

Considérant ces défis, le développement de nouvelles approches analytiques pour la détection de cyanotoxines dans l'eau et les poissons ayant été contaminés par des efflorescences cyanobactériennes nuisibles a été proposé. Une première approche consiste en l'utilisation d'une extraction sur phase solide en ligne couplée à une chromatographie liquide et à une détection en spectrométrie de masse en tandem (SPE-LC-MS/MS) permettant l'analyse de six analogues de microcystines (MC), de l'anatoxine (ANA-a) et de la cylindrospermopsine (CYN). La méthode permet une analyse simple et rapide et ainsi que la séparation chromatographique d'ANA-a et de son interférence isobare, la phénylalanine. Les limites de détection obtenues se trouvaient entre 0,01 et 0,02 $\mu g\ L^{-1}$ et des concentrations retrouvées dans des eaux de lacs du Québec se trouvaient entre 0,024 et 36 $\mu g\ L^{-1}$. Une deuxième méthode a permis l'analyse du β-*N*-méthylamino-L-alanine (BMAA), d'ANA-a, de CYN et de la saxitoxine (STX) dans les eaux de lac contaminés. L'analyse de deux isomères de conformation du BMAA a été effectuée afin d'améliorer la sélectivité de la détection. L'utilisation d'une SPE manuelle permet la purification et préconcentration des échantillons et une dérivatisation à base de chlorure de dansyle permet une chromatographie simplifiée. L'analyse effectuée par LC couplée à la spectrométrie de masse à haute résolution (HRMS) et des limites de détections ont été obtenues entre 0,007 et 0,01 $\mu g\ L^{-1}$. Des échantillons réels ont été analysés avec des concentrations entre 0,01 et 0,3 $\mu g\ L^{-1}$ permettant ainsi la confirmation de la présence du BMAA dans les efflorescences de cyanobactéries au Québec.

Un deuxième volet du projet consiste en l'utilisation d'une technologie d'introduction d'échantillon permettant des analyses ultra-rapides (< 15 secondes/échantillons) sans étape chromatographique, la désorption thermique à diode laser (LDTD) couplée à l'ionisation chimique à pression atmosphérique (APCI) et à la spectrométrie de masse (MS). Un premier projet consiste en l'analyse des MC totales par l'intermédiaire d'une oxydation de Lemieux permettant un bris de la molécule et obtenant une fraction commune aux multiples congénères existants des MC. Cette fraction, le MMPB, est analysée, après une extraction liquide-liquide, par LDTD-APCI-MS/MS. Une limite de détection de 0,2 µg $L^{-1}$ a été obtenue et des concentrations entre 1 et 425 µg $L^{-1}$ ont été trouvées dans des échantillons d'eau de lac contaminés du Québec. De plus, une analyse en parallèle avec des étalons pour divers congénères des MC a permis de suggérer la possible présence de congénères ou d'isomères non détectés. Un deuxième projet consiste en l'analyse directe d'ANA-a par LDTD-APCI-HRMS pour résoudre son interférence isobare, la phénylalanine, grâce à la détection à haute résolution. La LDTD n'offre pas de séparation chromatographique et l'utilisation de la HRMS permet de distinguer les signaux d'ANA-a de ceux de la phénylalanine. Une limite de détection de 0,2 µg $L^{-1}$ a été obtenue et la méthode a été appliquée sur des échantillons réels d'eau avec un échantillon positif en ANA-a avec une concentration de 0,21 µg $L^{-1}$. Finalement, à l'aide de la LDTD-APCI-HRMS, l'analyse des MC totales a été adaptée pour la chair de poisson afin de déterminer la fraction libre et liée des MC et comparer les résultats avec des analyses conventionnelles. L'utilisation d'une digestion par hydroxyde de sodium précédant l'oxydation de Lemieux suivi d'une purification par SPE a permis d'obtenir une limite de détection de 2,7 µg $kg^{-1}$. Des échantillons de poissons contaminés ont été analysés, on a retrouvé des concentrations en MC totales de 2,9 et 13,2 µg $kg^{-1}$ comparativement aux analyses usuelles qui avaient démontré un seul échantillon positif à 2 µg $kg^{-1}$, indiquant la possible présence de MC non détectés en utilisant les méthodes conventionnelles.

**Mots-clés** : Cyanobactéries, cyanotoxines, microcystines, anatoxine-a, cylindrospermopsine, saxitoxine, β-*N*-méthylamino-L-alanine, désorption thermique à diode laser, chromatographie liquide, spectrométrie de masse.

# Abstract

Cyanobacteria have a very important place in aquatic ecosystems and a significant number of species are considered harmful given their production of toxic metabolites. These cyanotoxins have various chemical proprieties and have often been associated with poisoning episodes. The frequency of cyanobacterial blooms is increasing and the study of cyanobacteria and their toxins is of increasing interest, especially considering the potential increase associated with climate changes. Given the chemical complexity of the cyanotoxins, the development of simple, sensitive and fast detection methods is an analytical challenge.

Considering these issues, the development of new analytical approaches for the detection of cyanotoxins in water and fish samples contaminated with harmful cyanobacterial blooms have been proposed. A first approach consists of the use of an on-line solid phase extraction coupled to liquid chromatography and tandem mass spectrometry (SPE-LC-MS/MS) for the analysis of six microcystins (MCs), anatoxin-a (ANA-a) and cylindrospermopsin (CYN). This method allows a simple and rapid analysis and enables the chromatographic separation of ANA-a and its isobaric interference, phenylalanine. The detection limits ranged from 0.01 to 0.02 µg $L^{-1}$ and concentrations in lake waters were found between 0.024 and 36 µg $L^{-1}$. A second method consists of using manual solid phase extraction (SPE) coupled to high resolution mass spectrometry (HRMS) for the determination of β-*N*-methylamino-L-alanine (BMAA), ANA-a, CYN and saxitoxin (STX) in contaminated lake water. The analysis of two conformational isomers of BMAA was done to improve the selectivity. Dansyl chloride-based derivatization allows simplified chromatography. The detection limits were obtained between 0.007 and 0.01 µg $L^{-1}$. The analysis of bloom water samples detected concentrations of cyanotoxins between 0.01 and 0.3 µg $L^{-1}$ allowing the confirmation of the presence of BMAA in algal blooms in Québec.

A second part of the project consists in the use of an alternative sample introduction technology for MS analysis. It enables ultra-fast analysis (< 15 seconds/sample) without the use of a chromatographic step, and is called laser diode thermal desorption (LDTD) coupled with atmospheric pressure chemical ionization (APCI). The first LDTD project consists of the

analysis of total MCs via Lemieux oxidation in order to obtain a common moiety of all MCs existing congeners. This fraction, the MMPB, is analyzed after a liquid-liquid extraction step, with the LDTD-APCI-MS/MS. A value of 0.2 µg $L^{-1}$ was obtained for detection limit and concentrations between 1 and 425 µg $L^{-1}$ have been found in contaminated water samples. In addition, a comparison with a parallel analysis using MCs congeners' standards suggested the possible presence of undetected MCs or isomers. A second project involves the direct analysis of ANA-a using LDTD-APCI-HRMS in order to solve the isobaric interference, phenylalanine, which is possible due to the high resolution detection. The LDTD offers no chromatographic separation and by using HRMS, we can distinguish ANA-a signals from those of phenylalanine. A value of 0.2 µg $L^{-1}$ was obtained as detection limit and the method has been applied on water bloom samples with a positive concentration of 0.21 µg $L^{-1}$. Finally, using the LDTD-APCI-HRMS combination, analysis of total MCs has been adapted to fish tissues to determine the unbound and bound MCs and compare the results with standard analysis. The use of digestion with sodium hydroxide prior to Lemieux oxidation followed by SPE purification yielded a detection limit of 2.7 µg $kg^{-1}$. Total MCs concentrations were found between 2.9 and 13.2 µg $kg^{-1}$ in real field-collected contaminated fish samples and comparison was made with standard analysis which yield a single positive sample with a concentration of 2 µg $kg^{-1}$. This indicates the possible presence of undetected MCs using conventional analytical methods.

**Keywords**: Cyanobacteria, cyanotoxins, microcystins, anatoxin-a, cylindrospermopsin, saxitoxin, β-*N*-methylamino-L-alanine, laser diode thermal desorption, liquid chromatography, mass spectrometry.

# Table des matières

# Liste des tableaux

# Liste des figures

# Liste des abréviations, sigles et acronymes

Les mots dans la langue anglaise et en latin sont indiqués en italique. Certains termes n'apparaissent que dans une langue parce qu'ils n'ont pas été utilisés dans l'autre langue.

| | |
|---|---|
| 4-PB | *4-Phenylbutyric acid* |
| 6-ACQ | 6-Aminoquinoly-*N*-hydroxysuccinimidyle |
| ACN | Acétonitrile / *Acetonitrile* |
| Adda | Acide (2S,3S,8S,9S)-3-amino-9-méthoxy-2,6,8-triméthyl-10-phényldéca-4,6-diénoique / *(2S,3S,8S,9S)-3-Amino-9-methoxy-2,6,8-trimethyl-10-phenyldeca-4,6-diénoic acid* |
| AEG | N-(2-Aminoéthyle)glycine / *N-(2-Aminoethyl)glycine* |
| AGC | *Automatic gain control* |
| AIF | *All ion fragmentation* |
| ALS/PDC | *Amyotrophic lateral sclerosis/Parkinson's disease complex* |
| amu | *Atomic mass unit* |
| ANA-a | Anatoxine-a / *Anatoxin-a* |
| ANOVA | *Analysis of variance* |
| APCI | Ionisation chimique à pression atmosphérique / *Atmospheric pressure chemical ionization* |
| APTX | Aplysiatoxine |
| BAMA | β-Amino-*N*-méthylalanine / *β-Amino-N-methylalanine* |
| BMAA | β-Méthylamino-*N*-alanine / *β-Methylamino-N-alanine* |
| C18 | Phase stationnaire à base d'octadécylsilane |
| C8 | Phase stationnaire à base d'octasilane |
| CA | *Cellulose acetate* |
| CEAEQ | Centre d'Expertise en Analyse Environnementale du Québec |
| CYN | Cylindrospermopsine / *Cylindrospermopsine* |
| Da | Dalton |
| DAB | Acide 2,4-diaminobutyrique / *2,4-Diaminobutyric acid* |
| D-Ala | D-Alanine |

| | |
|---|---|
| D-Asp$^3$ | Acide aspartique situé à la 3$^e$ position du cycle peptidique |
| dcSTX | Décarbamoylsaxitoxine |
| dd-$H_2O$ | *Deionized/distilled water* |
| $DL_{50}$ | Dose létale à la médiane |
| DNS | Chlorure de dansyle / *Dansyl chloride* |
| D-MeAsp | Acide D-*érythro*-β-méthylaspartique |
| DMEQ-TAD | 4-[2-(6,7-diméthoxy-4-méthyl-3-oxo-3,4-dihydroquinoxalinyl)éthyl]-1,2,4-triazoline-3,5-dione |
| D-Glu | D-Glucose |
| $E_a$ | Énergie d'activation |
| CE | Électrophorèse capillaire / *Capillary electrophoresis* |
| EtAc | *Ethyl acetate* |
| ECD | Détection par capture d'électrons / *Electron capture dissociation* |
| ELISA | Dosage d'immunoadsorption par enzyme liée / *Enzyme-linked immunosorbent assays* |
| ESI | Ionisation par électronébuliseur / Electrospray ionization |
| FA | *Formic Acid* |
| FLD | Détection par fluorescence / *Fluorescence detection* |
| FMOC | *9-Fluorenylmethyl chloroformate* |
| FS | *Full scan* |
| FWHM | Largeur à mi-hauteur / *Full width at half maximum* |
| GC | Chromatographie gazeuse / *Gas chromatography* |
| GF | *Glass Fiber* |
| GXT | Gonyautoxines |
| H | Heure |
| HCD | *Higher-energy collisional dissociation* |
| HESI | Ionisation par électronébuliseur chauffée / *Heated electrospray ionization* |
| HILIC | Chromatographie par interactions hydrophiles / *Hydrophilic interaction chromatography* |
| HPLC | Chromatographie liquide à haute performance / |

| | |
|---|---|
| | *High performance liquid chromatography* |
| HRMS | Spectrométrie de masse à haute résolution / *High resolution mass spectrometry* |
| IR | Infrarouge / *Infrared* |
| IS | Étalon interne / *Internal standard* |
| IT | *Injection time* |
| KDO | 2-céto-3-désoxyoctanate |
| LC | Chromatographie liquide / *Liquid chromatography* |
| $LD_{50}$ | *Median lethal dose* |
| LDTD | Désorption thermique à diode laser / *laser diode thermal desorption* |
| log $K_{ow}$ | Logarithme de la constante de partition octanol-eau / *Logarithm of the octanol-water partition coefficient* |
| LPS | Lipopolysaccharides |
| LTX | Lyngbyatoxine |
| LWTX | *Lyngbya wollei* |
| M | Valeur en masse |
| $M^+$ | Ion moléculaire |
| MALDI | Désorption-ionisation laser assistée par matrice / *Matrix-Assisted Laser Desorption ionization* |
| $Masse_{exp}$ | Masse expérimentale |
| $Masse_{th}$ | Masse théorique |
| MC | Microcystine / *Microcystin* |
| MC-AR | Microcystine-Alanine/Arginine |
| MCE | *Mixed cellulose ester* |
| MC-FR | Microcystine-Phénylalanine/Arginine |
| MC-HilR | Microcystine-Homoisoleucine/Arginine |
| MC-HtyR | Microcystine-Homotyrosine/Arginine |
| MC-LA | Microcystine-Leucine/Alanine |
| MC-LR | Microcystine-Leucine/Arginine |
| MC-LRéq | Microcystine-Leucine/Arginine équivalent |
| MC-LY | Microcystine-Leucine/Tyrosine |

| | |
|---|---|
| MC-M(O)R | Microcystine-Sulfoxyde de méthionine/Arginine |
| MC-RR | Microcystine-Arginine/Arginine |
| MC-WR | Microcystine-Tryptophane/Arginine |
| MC-YR | Microcystine-Tyrosine/Arginine |
| MC-YA | Microcystine-Tyrosine/Alanine |
| MC-YM(O) | Microcystine-Tyrosine/Sulfoxyde de méthionine |
| MDL | *Method detection limit* |
| MeOH | Méthanol / *Methanol* |
| Mdha | *N*-Méthyldéhydroalanine / *N-methyldehydroalanine* |
| Mdhb | Acide 2-(méthylamino)-2-déhydrobutyrique |
| MDDELCC | Ministère du développement durable, de l'environnement et de la lutte contre les changements climatiques |
| MDDEFP | Ministère du développement durable, de l'environnement, de la faune et des parcs |
| MMPB | Acide 2-méthyl-3-méthoxy-4-phénylbutyrique / *2-Methyl-3-methoxy-4-phenylbutyric acid* |
| MQL | M*ethod quantification limit* |
| MS | Spectrométrie de masse / *Mass spectrometry* |
| MS/MS | Spectrométrie de masse en tandem / *Tandem mass spectrometry* |
| *m/z* | Ratio masse sur charge / *Mass to charge ratio* |
| n | Nombre de réplicat |
| $N_2^{\cdot+}$ | Ion radical diazote |
| NBDF | 4-Fluoro-7-nitro-2,1,3-benzoxadiazole |
| NC | *Nitrocellulose* |
| NCE | *Normalized collision energy* |
| N/D / ND | Données non disponibles / *Not detected* |
| neoSTX | Néosaxitoxine |
| ng inj. | Nanogramme par injection sur colonne chromatographique |
| NI | *Negative ionization* |
| NOD | Nodularine / *Nodularin* |
| NY / NYL | *Nylon* |

| | |
|---|---|
| OMS | Organisation Mondiale de la Santé |
| *P* | *Probability* |
| PDA | Détecteur à barrette de diode / *Photodiode array detector* |
| PHE | Phénylalanine / *Phenylalanine* |
| $pK_a$ | Constante de dissociation d'un acide |
| PC | *Polycarbonate* |
| PP | *Polypropylene* |
| PP1 | Protéine phosphatase 1 / *Protein phosphatase 1* |
| PP2A | Protéine phosphatase 2A / *Protein phosphatase 2A* |
| ppm | Partie par million |
| PVDF | *Polyvinylidene fluoride* |
| Q1 | Premier analyseur quadripôle |
| q2 | Deuxième analyseur quadripôle ou cellule de collision |
| Q3 | Troisième analyseur quadripôle |
| QC | *Quality control* |
| QIT | Quadrupole-trappe ionique / *Quadrupole-ion trap* |
| R | Résolution |
| $R^2$ | *Coefficient of determination* |
| RE | *Relative error* |
| rpm | *Rotation per minute* |
| RSD | *Relative standard deviation* |
| SD | *Standard deviation* |
| SDB-L | *Styrene-divinylbenzene* |
| SIM | *Selected ion monitoring* |
| S/N | Rapport signal sur bruit / *Signal to noise ratio* |
| SPE | Extraction sur phase solide / *Solid phase extraction* |
| SRM | *Selective reaction monitoring* |
| STX | Saxitoxine / *Saxitoxin* |
| STXéq | Saxitoxine équivalent |
| T | Temps |
| TDI | *Tolerable daily intake* |

| | |
|---|---|
| t-$MS^2$ | *Targeted ion fragmentation* |
| TOF | Temps d'envol / *Time of flight* |
| UPLC | *Ultra performance liquid chromatography* |
| UHPLC | *Ultra high-performance liquid chromatography* |
| UV-vis | Ultraviolet-visible |
| v/v | Volume par volume / *Volume per volume* |
| W | Watt |
| WHO | *World health organization* |
| *X* | Acides aminés variables des microcystines |
| *Z* | Acides aminés variables des microcystines |

*À ma famille,*

# Remerciements

Je voudrais tout d'abord remercier le Prof. Sébastien Sauvé pour m'avoir donné l'opportunité de travailler au sein de son groupe de recherche durant toutes ces années. Je le remercie profondément pour la confiance qu'il m'a accordée, ainsi pour son implication et son soutien tout au long de mon parcours. Mes études supérieures m'ont permis de vivre une expérience unique m'amenant à apprendre et à grandir dans le milieu de la recherche et j'en suis très reconnaissante.

Je remercie également les anciens et présents membres du groupe du laboratoire de chimie analytique environnementale du Prof. Sébastien Sauvé, avec qui les discussions autant sérieuses que loufoques m'ont permis à la fois d'avancer dans mon cheminement par de bons conseils et aussi de développer de belles amitiés. Je souhaite plus particulièrement remercier Morgan Solliec, Paul Fayad, Sung Vo Duy et Pedro Segura pour leur soutien et conseils tout au long de mon cheminement au sein du groupe. Je remercie aussi Rachel Benoît, Michel Boisvert, Guillaume Cormier et Simon Comtois-Marotte pour les multiples délires et fou-rires au laboratoire, mais aussi devant un match de hockey!

Je remercie mes amis,  ma famille et mes grands-parents pour leur soutien et leur patience durant les bons moments, mais aussi les plus difficiles. Je remercie aussi ma mère et mon père pour avoir toujours cru en moi et m'avoir encouragée tout au long de mes études. Et un merci particulier à ma mère car sans elle, je n'aurais pas été aussi loin.

Je ne dois pas oublier Manon, ma professeure de piano, qui a été très patiente malgré mes nombreuses absences parce qu'il fallait que je travaille au lieu de pratiquer! Mais grâce à son soutien, je n'ai pas lâché ma passion du piano.

Je remercie finalement Morgan, avec qui j'ai partagé ma vie d'étudiante en laboratoire, mais aussi avec qui je partage ma vie. Il a toujours été là pour m'appuyer, vice versa, et malgré les hauts et les bas, au doctorat on a dit être un duo de la mort, et en plus d'être vrai, ça ne va pas s'arrêter là!

# Chapitre 1. Introduction

## 1.1 Cyanobactéries

### 1.1.1 Description générale

Les cyanobactéries sont des micro-organismes omniprésents partout sur la planète et sont apparues il y a environ 3,5 milliard d'années. Elles sont considérés comme étant des contributeurs importants à la formation de l'atmosphère et à la fixation de l'azote [1]. Les cyanobactéries sont des organismes cellulaires de type procaryotes ne possédant pas de noyaux ni d'organites et font partie des bactéries à Gram négatifs [2]. Leurs capacités photosynthétiques leur permettent d'utiliser l'énergie solaire et de capter le dioxyde de carbone afin de libérer du dioxygène et cette photosynthèse aurait pu être précurseur de la couche d'ozone [3]. La production des pigments phycobiline et phycocyanine procurent à certains une couleur cyan caractéristique d'où l'origine de leur appellation populaire algues bleu-vert. Le pigment phycoérythrine est quelques fois produit, bien qu'aussi accessoire, donnant un pigment rouge à certaines espèces [4]. Elles sont bien adaptées à des environnements extrêmes et résistent à la dessiccation, à de hautes radiations, au manque de lumière, au manque de nutriments, à de hauts taux de salinité et à des conditions acides et alcalines. Il n'est pas étonnant que les cyanobactéries aient résisté à leur environnement et qu'elles puissent se retrouver dans tous types d'environnements soumis à un minimum de lumière [4]. On considère qu'elles sont les organismes les plus importants sur la Terre imposant une biomasse estimée à $3 \times 10^{14}$ g de carbone ou de mille millions de tonnes ($10^{15}$ g) humide [5].

Les cyanobactéries comptent près de 150 genres incluant plus de 2000 espèces [6]. Elles ont tout d'abord été caractérisées par les fortes odeurs et le mauvais goût terreux qu'elles donnent aux eaux où elles prolifèrent, résultant des métabolites secondaires formés incluant la géosmine et le 2-méthylisoborénol [7]. Par la suite, des composés toxiques ont été associés aux cyanobactéries, suggérant la production de cyanotoxines. On estime qu'environ 40 genres de cyanobactéries sont propices à produire ces métabolites secondaires qui ont été

responsables de plusieurs épisodes de décès d'animaux et d'humains [8]. C'est pour ces raisons que les cyanobactéries, depuis quelques décennies, font l'objet d'études approfondies afin de mieux comprendre leurs impacts environnementaux.

### 1.1.2 Efflorescence d'algues bleu-vert

Les cyanobactéries se reproduisent de manière asexuée de deux façons : soit par bipartition étant une division binaire de la bactérie, soit par spores. Elles se retrouvent sous forme unicellulaire ou bien sous forme de filaments de cyanobactéries, comme par exemple l'espèce connue *Nostoc* [4, 9]. Une efflorescence de cyanobactéries consiste en une production significative de biomasse sur une courte période. Une efflorescence est souvent multi espèces et se forme en une couche cellulaire dense à la surface d'un plan d'eau. Les efflorescences massives d'algues bleu-vert se produisent généralement dans des lacs, des étangs et des rivières eutrophiques et hypertrophiques. Les conditions de formation d'une efflorescence de cyanobactéries sont régies par plusieurs facteurs : de hautes concentrations de nutriments disponibles (principalement les nitrates et les phosphates), de la lumière, une température élevée (idéalement au-dessus de 25 °C), la disponibilité de carbone, une eau stagnante avec peu de turbidité et un pH légèrement alcalin [10-12].

Le moment et la durée des efflorescences de cyanobactéries varient beaucoup dépendamment du climat de la région et il est très difficile de prédire précisément le lieu et la durée d'un épisode. Dans les régions à climats tempérés, comme au Québec, les périodes d'efflorescence importantes débutent durant l'été et perdurent jusqu'aux mois de novembre et décembre [13]. Par contre, dans les régions méditerranéennes et subtropicales, les périodes d'efflorescence sont plus longues, allant jusqu'à plus de 6 mois. De ce fait, les pays tropicaux sont fortement touchés par les épisodes d'efflorescence due aux fortes chaleurs et à de long temps d'ensoleillement. Étant donné que les cyanobactéries sont des espèces principalement phototrophes, il est rare de les retrouver dans les cours d'eaux souterrains ou dans la nappe phréatique [10-12]. Par contre, d'importants épisodes d'efflorescence de cyanobactéries ont été rapportés dans des bassins d'eaux usées de différentes usines d'épuration d'eau et des concentrations importantes de cyanotoxines à la sortie du traitement d'eau suggèrent l'omniprésence des cyanobactéries si les conditions de production sont réunies [14, 15]. De

plus, lorsque que la quantité de cyanobactéries est trop importante, un phénomène d'anoxie peut se produire due à l'augmentation de la consommation d'oxygène par les microorganismes qui se nourrissent des cellules mortes présentes dans le milieu [16].

Normalement, les conditions de formation et d'efflorescence des cyanobactéries sont tout à fait naturelles et sont régies par des facteurs environnementaux. Par contre, l'activité humaine a induit une expansion importante des efflorescences de cyanobactéries partout dans le monde. Tout d'abord, les rejets agricoles par ruissellement, riches en phosphates et nitrates, ont causé, depuis plusieurs décennies, une augmentation marquée de la présence des cyanobactéries dans les cours d'eau douces. De plus, les déversements industriels directement dans les cours d'eaux font l'objet de préoccupations pour les mêmes raisons [17]. Plus récemment, un autre phénomène beaucoup plus difficile à contrôler nuit à l'équilibre environnemental face aux cyanobactéries, c'est-à-dire le réchauffement climatique. Plusieurs laboratoires ont étudié le lien entre les changements des écosystèmes liés au réchauffement climatique et la croissance des cyanobactéries. Les conclusions émises indiquent qu'une eutrophisation des cours d'eaux ainsi que l'augmentation de leur température est en croissance affectant ultimement les moments et la dominance des cyanobactéries [18, 19].

Malgré qu'elles prolifèrent généralement en milieux adaptés, les cyanobactéries possèdent des stratégies pour survivre en conditions plus hostiles. Tout d'abord, elles ont la capacité de fixer l'azote atmosphérique et de le transformer en azote assimilable tel les sels d'ammonium ou de nitrates. Dans un milieu où l'apport en nutriments est déficient, cette capacité de fournir les composés azotés après la mort cellulaire permet la survie des colonies [4, 20]. Par la suite, lors d'un refroidissement atmosphérique, comme l'arrivée de l'hiver ou un phénomène de sécheresse, les cyanobactéries se transforment en akinètes, par l'épaississement de leurs parois cellulaires. Ce phénomène crée un état de sommeil cellulaire leur permettant de survivre à des conditions extrêmes [21, 22]. Finalement, les cyanobactéries planctoniques possèdent une mobilité leur permettant de se déplacer où les conditions de survie sont plus favorables. La principale stratégie de mobilité provient de la formation de vésicules gazeuses leur permettant de se déplacer verticalement dans des colonnes d'eau et ainsi contrôler leur apport en luminosité et en nutriments selon leurs besoins et la disponibilité [6, 23].

### 1.1.3 Cyanotoxines

Les cyanotoxines sont des métabolites produits par certains genres de cyanobactéries. Des 150 genres existants, on dénombre 40 genres de cyanobactéries produisant des toxines. Les raisons entourant la production de toxines est toujours incertaine, mais plusieurs hypothèses ont été énoncées sur les facteurs du déclanchement de la production des cyanotoxines. Tout d'abord, il a été démontré que la production de cyanotoxines est liée à la croissance cellulaire des cyanobactéries. Les raisons expliquant cette production incluent la possible atteinte d'une dominance dans le milieu occupé en induisant une compétitivité par la production de toxines ou bien que les toxines aideraient la croissance des cyanobactéries en procurant une régulation intracellulaire [23-25]. Quant à la production spécifique des toxines, elle est régie par la transcription génétique des cyanobactéries, de ce fait, plusieurs espèces peuvent produire la majorité des cyanotoxines connue et d'autres n'en produisent qu'une seule. Le potentiel de cyanotoxines est déterminé par la présence de gènes spécifiques, mais l'expression de ce potentiel est régi par les conditions environnementales présentes tel les concentrations en nutriments, les métaux traces, le pH, la lumière, la température, etc. [12, 24, 25].

Lors de la production de cyanotoxines, la majeure partie ne sera pas sous forme soluble dans les eaux environnantes. En effet, la grande majorité des toxines produites sont intracellulaires (entre 80 et 90 %) et un faible pourcentage est alors excrété hors des parois pour être dissoutes dans le milieu où elles ont été produites [26]. Des concentrations élevées de toxines peuvent être relarguées suite à la lyse des cellules de cyanobactéries causée par un stress ou une dégénérescence [11].

Les cyanotoxines, en plus de posséder une grande diversité de leurs propriétés chimiques, possèdent une grande biodisponibilité. En effet, certaines toxines peuvent s'accumuler dans les chaînes trophiques et être soumises à une bioamplification [11]. Ainsi, des cyanotoxines ont été mesurées dans les eaux naturelles, mais aussi dans des espèces végétales et aquatiques [12, 27]. Ce faisant, leur présence peut être préoccupante pour la santé publique et des écosystèmes étant donné la multiplication des voies d'exposition. Plusieurs cas d'intoxications animales et humaines ont été rapportés et les symptômes observés étaient

variables [12, 28]. À faible exposition, on observe principalement l'irritation de la peau et des problèmes gastro-intestinaux. Par contre, à fortes doses, les symptômes peuvent varier entre des dérèglements neurologiques à court terme jusqu'à des effets cancérogènes d'organes tel le foie ou le système gastrique à long terme [28].

## 1.2 Classification des cyanotoxines

De nombreuses espèces de cyanobactéries possèdent un potentiel génétique de production de toxines. Les cyanotoxines peuvent être classées en plusieurs catégories. Tout d'abord, leurs types de toxicité les divisent en 4 catégories importantes : les hépatotoxines, s'attaquant principalement au foie, les neurotoxines, agissant sur les cellules nerveuses, les cytotoxines, ayant un effet sur les cellules en général et les dermatotoxines possédant des propriétés irritantes. Les cyanotoxines peuvent aussi être classées en fonction de leurs propriétés structurelles : les peptides cycliques, les alcaloïdes, les acides aminés non-protéinogènes et les lipopolysaccharides [6].

### 1.2.1 Peptides cycliques

Les cyanotoxines les plus souvent rencontrées lors d'épisodes d'efflorescences sont les peptides cycliques composés de la famille des microcystines (MC) et celle des nodularines (NOD) et tous deux possèdent des propriétés hépatotoxiques. Les MC sont les plus connues et les plus étudiées à ce jour étant donné leur occurrence et leur répartition [6]. Les NOD, malgré leur structures très apparentée aux MC, sont beaucoup moins répandues, se limitant surtout à l'Australie, la Nouvelle-Zélande et la mer Baltique en eaux marines saumâtres [11].

#### 1.2.1.1 Microcystines

Le nom microcystine (MC) provient de l'espèce *Microcystis aeruginosa*, la première espèce de cyanobactérie ayant été identifiée comme produisant des toxines. Par la suite, on a dénombré plusieurs autres genres capables de produire des MC incluant *Anabaena, Nostoc, Planktothrix, Anabaenopsis, Cyanobium, Arthrospira, Hapalosiphon, Limnothrix, Phormidium* et *Snowella* [10, 29]. Les MC possèdent une structure monocyclique, présentée composée de 7 acides aminés (**Figure 1-1**). La structure générale incluant les acides aminés

est la suivante : cyclo-(-D-alanine-*X*-D-MeAsp-*Z*-Adda-D-glutamate-Mdha) où D-MeAsp est l'acide D-*érythro*-β-méthylaspartique, Mdha est la *N*-méthyldéhydroalanine. Le groupement Adda, où l'acide (2S,3S,8S,9S)-3-amino-9-méthoxy-2,6,8-triméthyl-10-phényldéca-4,6-diénoique, est commun à toutes les MC et est la principale cause de leur toxicité dû à un diène conjugué [30, 31]. Finalement *X* et *Z* se réfèrent à des acides aminés variables dont les multiples combinaisons menant à plus de 100 analogues différents [32]. Cette caractéristique fait des MC les cyanotoxines les plus diversifiées. Pour permettre leur différenciation, chaque variante est identifiée par ses acides aminés *X* et *Z*, par exemple, MC-LR est composé de la leucine (L) et de l'arginine (R). En plus de ces différences structurelles, certaines variantes ont été identifiées, où la partie Mdha ou la D-alanine sont remplacées par la L-sérine. Aussi, des variantes non toxiques ont été identifiées comme par exemple une MC possédant un stéréoisomère 6*Z* de la partie Adda [31, 32]. Plus récemment, de nouvelles MC ont été identifiées, démontrant que tous les sites du cycle peptidique peuvent être des domaines d'adénylation. Chaque souche de cyanobactérie produit environ de deux à sept congénères, le plus souvent MC-LR et MC-RR ainsi que leurs analogues déméthylées. Par exemple, la souche *Anabaena 60* peut produire : MC-LR, [D-Asp$^3$]MC-LR, MC-RR et [D-Asp$^3$]MC-RR, Asp$^3$ étant l'acide aspartique situé à la 3$^e$ position du cycle peptidique [32]. Malgré toute cette diversité et la découverte constante de nouvelles structures des MC, à ce jour, une très faible proportion d'étalons sont disponibles pour leur analyse, soit autour de 12 étalons.

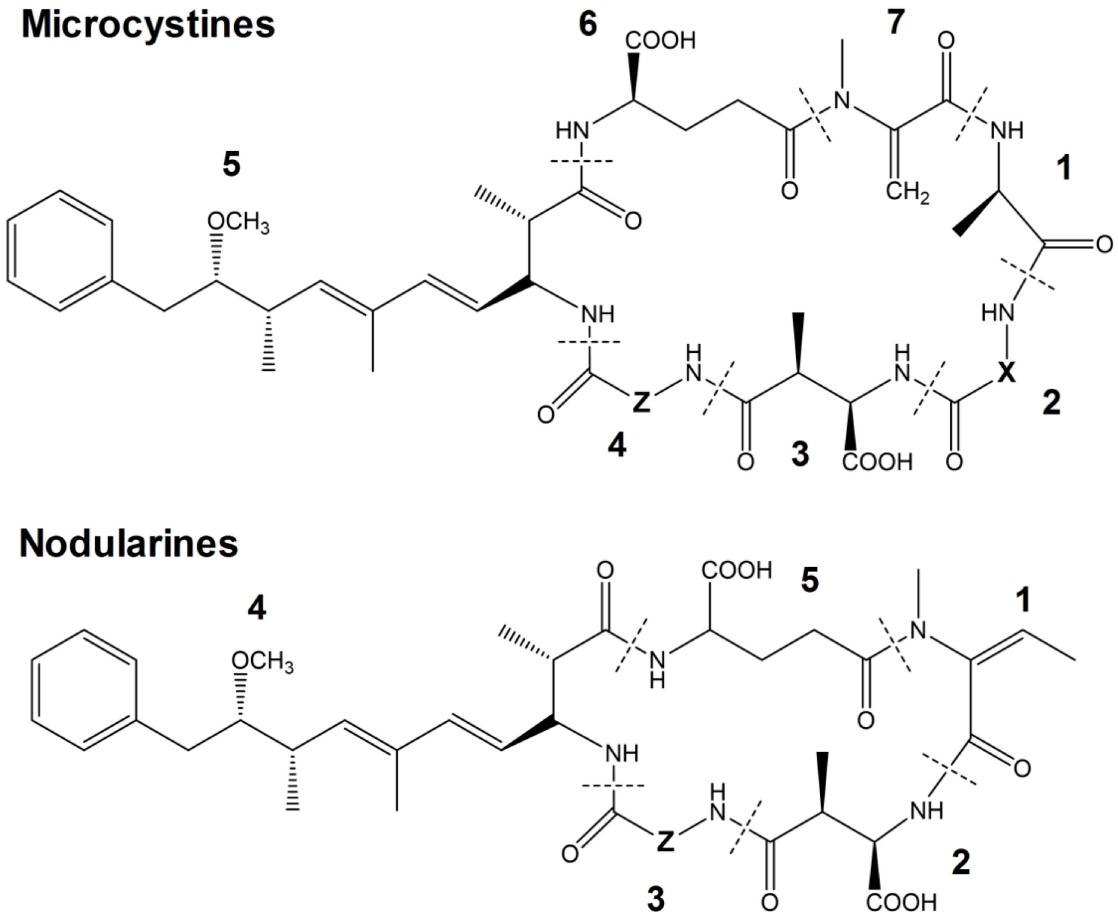


**Figure 1-1.** Structure moléculaire des microcystines : 1 = D-Ala, 2 = *X* (variable), 3 = D-MeAsp, 4 = *Z* (variable), 5 = Adda, 6 = D-Glu et 7 = Mdha. Structure moléculaire des nodularines : 1 = Mdhb, 2 = D-MeAsp, 3 = *Z* (variable), 4 = Adda et 5 = D-Glu.

Dépendamment des variantes, les MC possèdent une masse molaire variant entre 500 et 1400 g $mol^{-1}$. Par contre, en considérant les MC les plus souvent rencontrées, leur masse molaire vont plutôt varier entre 900 et 1100 g $mol^{-1}$ [28]. Deux fonctions carboxyliques dans la majorité des MC leur procurent des propriétés hydrophiles et de ce fait, leur $pK_a$ ont été évalués à environ 3,4 et 12,5. Ces valeurs proviennent toutefois des acides aminés seuls et peuvent varier selon l'environnement dans la chaîne peptidique. Les MC démontrent aussi un caractère hydrophobe important (log $K_{ow} > 4$) malgré les fonctions carboxyliques, amine et amides de la structure. En effet, la fonction Adda très hydrophobe en est la cause et sa combinaison avec les fonctions polaires permet une formation micellaire [24, 33]. Étant donné

leur masse molaire élevée et leur polarité, les MC sont très peu volatiles. Elles sont solubles dans l'eau à 1 g $L^{-1}$, mais aussi dans le méthanol et l'éthanol. Elles possèdent une grande stabilité chimique lorsqu'elles sont exposées à la lumière naturelle, excepté lorsque certains pigments sont présents (e.g. phycocyanine) et elles peuvent résister à plusieurs heures d'ébullition et tolèrent une large gamme de pH [12, 34].

Les cas aigus d'intoxications dues aux MC peuvent entraîner une mort rapide chez les humains et les animaux. Le mode d'exposition principal est par ingestion et par la suite, les toxines sont transportées au foie à l'aide de protéines de transport d'anions organiques. La toxicité hépatique est causée par l'inhibition des protéines phosphatases 1 et 2A (PP1 et PP2A) et créant une hyperphosphorylation des protéines cytosquelettiques et finalement une déformation des hépatocytes. Lorsque que ces cellules se détériorent, le sang des cellules voisines sera aggloméré dans le foie, l'enflant presque au double de son volume, le conduisant finalement à des lésions tissulaires, une défaillance de l'organe et un choc hémorragique [35-38]. Cette inhibition serait due au groupement Adda et à l'acide glutamique. De plus, le groupe Mdha se lie à la cystéine-273 de la PP1 et la cystéine-266 de la PP2A, expliquant le lien covalent des MC dans les tissus hépatiques [39]. Ce lien covalent induit une bioaccumulation des MC, qui a été retrouvée dans les organismes qui servent de nourriture pour les poissons, induisant finalement une bioamplification dans la chaîne trophique en milieux aquatiques [6].

#### 1.2.1.2 Nodularines

Les nodularines (NOD) sont des pentapeptides monocycliques et ont été découvertes par leur isolation dans la cyanobactérie planctonique filamenteuse, *Nodularia spumigena*. On retrouve les NOD dans la mer Baltique durant l'été lorsque des efflorescences de *N. spumigena* se produisent. On peut les retrouver partout dans le monde, malgré qu'elles soient très peu étudiées au Canada. Par contre, l'Australie et la Nouvelle-Zélande sont touchées par les NOD, dans des eaux saumâtres et estuariennes [12, 40]. Les NOD possèdent une structure monocyclique composés de 5 acides aminés qui est très similaire à celle des MC (**Figure 1-1**) et possèdent une toxicité similaire [24, 41]. Leur structure générale est le cyclo-(D-MeAsp-L-arginine-Adda-D-glutamate-Mdhb) où D-MeAsp est le D-*érythro*-β-méthylaspartique, Mdhb

est l'acide 2-(méthylamino)-2-déhydrobutyrique. Tout comme pour les MC, on retrouve le groupement Adda et l'acide glutamiques sont responsables de la toxicité des NOD [24]. On dénombre sept variantes des NOD; deux d'entre elles possèdent une variation du groupement Adda, l'une déméthylée et l'autre étant sa forme stéréoisomère 6*Z*, réduisant significativement la toxicité. L'estérification du carboxyle libre de l'acide glutamique élimine la toxicité, alors que la déméthylation du D-MeAsp n'affecte pas la toxicité [40]. Les deux dernières isoformes retrouvées sont la nodularine-Har, produite par la souche *N. harveyna* et dont le groupement L-arginine est remplacé par le L-homoarginine ainsi que la motuporine, isolée du *Theonella swinhoei* en Papouasie-Nouvelle-Guinée et dont le groupement L-arginine est remplacé par la L-valine. La motuporine possède une cytotoxicité additionnelle causée par la présence de la L-valine [42]. Les NOD ont des propriétés chimiques similaires aux MC, possédant un caractère à la fois polaire et hydrophobe. La masse molaire de la NOD principale est de 824,96 g $mol^{-1}$ et le composé est aussi très peu volatil.

Les NOD possèdent un mode d'action et une toxicité semblables à celles des MC. Elles sont transportées, après ingestion, vers le foie à l'aide de protéines de transport d'anions organiques. Elles inhibent l'activité de la PP1, mais surtout de la PP2A. Le groupement Adda bloque l'activité de l'enzyme en interagissant avec le canal hydrophobe et obstruant l'accès du substrat au site actif. Le groupement Mdhb des NOD se lie à la cystéine-266 de la PP2A de la même manière que le résidu Mdha des MC, mais le lien n'est pas covalent. Cette liaison réversible pourrait expliquer les propriétés cancérigènes additionnelles de cette toxine [43-45]. Une accumulation des NOD dans plusieurs espèces de mollusques et de poissons en milieux aquatiques a été rapportée, mais elles peuvent aussi être facilement extraites ou dégradées. Leur bioamplification serait moins importante comparativement aux MC [46].

### 1.2.2 Alcaloïdes

Les cyanotoxines alcaloïdes ont la caractéristique de posséder un ou plusieurs hétérocycles azotés basiques. Ce sont normalement des composés actifs biologiquement et de par leurs structures très variées, elles possèdent des propriétés toxiques tout aussi diversifiées. Parmi ces toxines alcaloïdes d'origine cyanobactériennes on retrouve l'anatoxine-a, la cylindrospermopsine et la saxitoxine ainsi que tous leurs analogues.

#### 1.2.2.1 Anatoxine-a

L'anatoxine-a (ANA-a) est la première cyanotoxine chimiquement et structurellement définie. Cette neurotoxine a été rapportée partout dans le monde et est principalement produite par trois genres de cyanobactéries : *Anabaena*, *Aphanizomenon* et *Planktothrix* [47]. Elle est une amine secondaire bicyclique, à faible poids moléculaire (masse molaire de 165,24 g $mol^{-1}$) systématiquement nommée 2-acétyl-9-azabicyclo(4,2,1)non-2-ène et sa structure, présentée à la **Figure 1-2**, est analogue à celle de la cocaïne. Une légère hydrophobicité lui confère un log $K_{ow}$ de 1,1 et son $pK_a$ est de 9,4 lui conférant un état protoné à pH physiologique, en plus d'être hautement soluble dans l'eau [48]. La molécule est stable en milieu acide (pH < 3), mais se dégrade rapidement en milieu alcalin, en plus d'être photosensible. En présence de lumière naturelle, ANA-a se dégrade en deux métabolites non toxiques : le dihydroanatoxin-a et l'époxyanatoxine-a (**Figure 1-2**) [49]. Une variante importante d'ANA-a est l'homoanatoxine-a, résultat de la méthylation du carbone à l'extrémité de la fonction cétone (**Figure 1-2**) [50]. La voie d'exposition principale est l'ingestion. Une fois dans l'organisme, elle se fixe de manière irréversible sur les récepteurs acétylcholines sans être dégradée par l'acétylcholinérase [47]. Une fois fixée, ANA-a mime l'effet du neurotransmetteur induisant une stimulation constante et de ce fait, bloque les autres transmissions électriques, nécessaires pour l'activité des muscles squelettiques. Une dose assez élevée peut induire une paralysie musculaire et lorsque ses muscles respiratoires sont touchés, la mort peut se produire par asphyxie [51]. L'homologue homoanatoxine-a quant à lui est un agent de blocage neuromusculaire qui augmente le flux d'ions $Ca^{2+}$ dans les terminaisons nerveuses cholinergiques [12]. Des dérivés moins toxiques de l'homoanatoxine-a ont été identifiés : les 4*S* et 4*R* hydroxyhomoanatoxine-a, la cétohomoanatoxine-a, le dihydrohomoanatoxine-a, l'hydrométhoxyhomoanatoxine-a et le 2,3-époxyhomoanatoxine-a ont été identifiés **(Figure 1-2)** [50, 52].

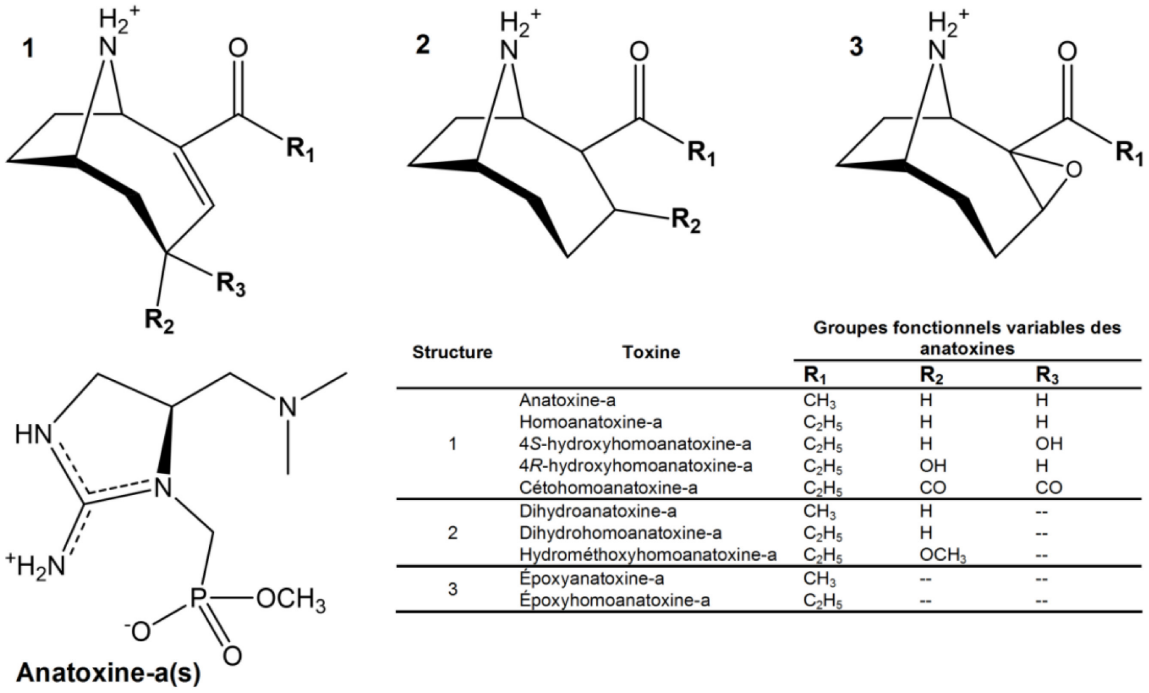


| Structure | Toxine | Groupes fonctionnels variables des anatoxines | | |
|---|---|---|---|---|
| | | $R_1$ | $R_2$ | $R_3$ |
| 1 | Anatoxine-a | $CH_3$ | H | H |
| | Homoanatoxine-a | $C_2H_5$ | H | H |
| | 4*S*-hydroxyhomoanatoxine-a | $C_2H_5$ | H | OH |
| | 4*R*-hydroxyhomoanatoxine-a | $C_2H_5$ | OH | H |
| | Cétohomoanatoxine-a | $C_2H_5$ | CO | CO |
| 2 | Dihydroanatoxine-a | $CH_3$ | H | -- |
| | Dihydrohomoanatoxine-a | $C_2H_5$ | H | -- |
| | Hydrométhoxyhomoanatoxine-a | $C_2H_5$ | $OCH_3$ | -- |
| 3 | Époxyanatoxine-a | $CH_3$ | -- | -- |
| | Époxyhomoanatoxine-a | $C_2H_5$ | -- | -- |

**Figure 1-2.** Structure moléculaire de l'anatoxine-a, de ses variantes et de l'anatoxine-a(s) (adapté de Hiller *et al.* [50]).

### 1.2.2.2 Anatoxine-a(s)

L'anatoxine-a(s) (ANA-a(s)) est une toxine apparentée à ANA-a, produite par les espèces *Anabaena flos-aquae* et *Abanaena lemmermannii*. Elle possède une structure différente étant un ester phosphorique du *N*-hydroxyguanidine et ayant une masse molaire de 252,21 g $mol^{-1}$ **(Figure 1-2)** [53]. La spécification "S" est utilisée parce que la toxine crée des symptômes de salivation excessive chez les vertébrés [12]. Tout comme ANA-a, la molécule est stable en milieu acide, mais se dégrade rapidement en milieu alcalin. De plus, la toxine devient inactive lorsque le milieu est chauffé (>40 °C) [12]. À ce jour, aucune variante structurelle d'ANA-a(s) n'a été identifiée [50]. À l'intérieur de l'organisme, ANA-a(s) inhibe l'action de l'acétylcholinestérase et induit une paralysie musculaire causant potentiellement la mort par asphyxie. N'étant produite que par le genre *Anabaena*, cette toxine est moins répandue qu'ANA-a [11, 54].

### 1.2.2.3 Saxitoxines

La saxitoxine (STX) et ses dérivés font partie du groupe des PSPs (*Paralytic Shellfish Poisons*) car elles sont produites principalement par des organismes marins [55]. Les STXs sont des neurotoxines puissantes détectées partout dans le monde qui sont produites principalement par les espèces *Anabaena circinalis*, *Aphanizomenon flos-aquae*, *Lyngbya wollei* et *Cylindrospermopsis raciborskii* mais aussi par les dinophytes [53, 56]. La toxicité importante de STX lui a valu obtenu une attention militaire et la molécule purifiée a été classée comme arme chimique [57]. STX est le parent d'une famille de plus de 30 dérivés naturels et sa structure tricyclique se compose d'un noyau tétrahydropurique dont 5 positions sont variables par hydroxylation, sulfatation ou carbamylation. Comme présenté à la **Figure 1-3**, les formes retrouvées comprennent la néosaxitoxine (neoSTX), les gonyautoxines (GXT) qui sont sulfatées, les toxines C qui sont doublement sulfatées, les analogues qui ne possèdent pas de carbamate (dcSTX) et les analogues qui sont nommées en fonction de l'espèce *Lyngbya wollei* (LWTX) [11, 50]. La masse molaire de STX est de 299,29 g $mol^{-1}$ tandis que ses dérivés, elle varie entre 241 et 491 g $mol^{-1}$. Ne possédant pas de groupement sulfates, la molécule de STX possède deux $pK_a$ de 8,2 et 11,3 et donc deux charges positives s'y retrouve en milieu à pH physiologique. Pour les variantes mono-sulfatées, on retrouvera une charge tandis que les variantes doublement sulfatés n'auront aucune charge. De plus, la molécule est très hydrophile possédant un log $K_{ow}$ de -4,2, elle est donc très soluble en milieu aqueux [55]. La molécule de STX est très stable et peut être entreposé en solution diluée acide pendant des mois sans perdre de sa toxicité. Par contre, sa variante la plus importante, la neoSTX, est plus instable et peu d'information est retrouvée sur la stabilité des autres variantes [12, 58]. La principale voie d'exposition des STXs est l'ingestion de fruits de mer contaminés. Les premiers signes de toxicité apparaissent 30 minutes après ingestion, incluant des brûlements aux lèvres, à la langue et à la gorge ainsi qu'un engourdissement du visage [24]. Les STX agissent en bloquant les canaux sodiques présents dans les membranes cellulaires nerveuses et ainsi les influx nerveux. À fortes doses, les effets peuvent varier entre des paralysies musculaires et respiratoires amenant à un arrêt respiratoire ou à un arrêt cardiaque [59, 60]. Une fois présentes dans l'eau, les STX peuvent être en contact avec des organismes aquatiques

filtreurs tels les mollusques et on observe une bioaccumulation temporaire dans certaines espèces, mais les traces des toxines disparaissent au bout de 14 jours [12].

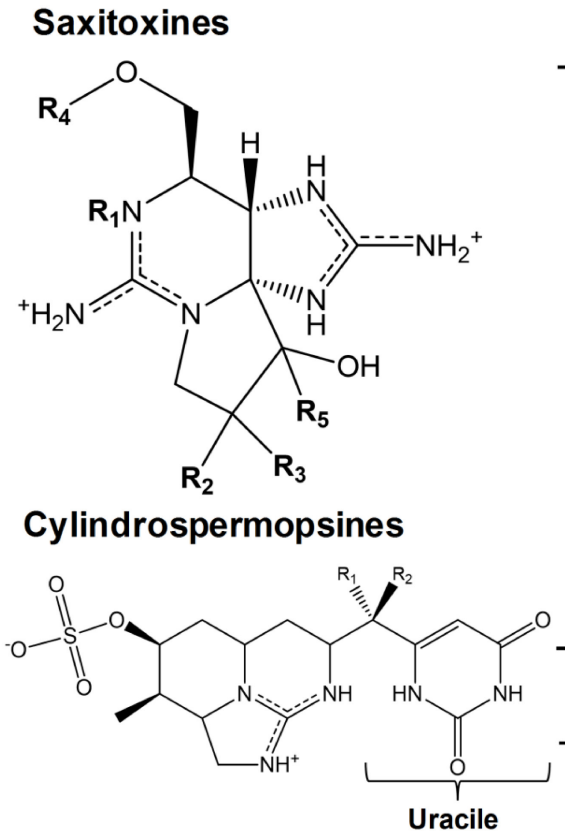


| Toxine | Groupes fonctionnels variables des STXs | | | | |
|---|---|---|---|---|---|
| | $R_1$ | $R_2$ | $R_3$ | $R_4$ | $R_5$ |
| STX | H | H | H | $CONH_2$ | OH |
| GTX2 | H | H | $OSO_3^-$ | $CONHSO_3^-$ | OH |
| GTX3 | H | $OSO_3^-$ | H | $CONH_2$ | OH |
| GTX5 | H | H | H | $CONHSO_3^-$ | OH |
| C1 | H | H | $OSO_3^-$ | $CONHSO_3^-$ | OH |
| C2 | H | $OSO_3^-$ | H | $CONHSO_3^-$ | OH |
| C3 | OH | H | $OSO_3^-$ | $CONHSO_3^-$ | OH |
| C4 | OH | $OSO_3^-$ | H | $CONHSO_3^-$ | OH |
| neoSTX | OH | H | H | $CONH_2$ | OH |
| GTX1 | OH | H | $OSO_3^-$ | $CONH_2$ | OH |
| GTX4 | OH | $OSO_3^-$ | H | $CONH_2$ | OH |
| GTX6 | OH | H | H | $CONHSO_3^-$ | OH |
| dcSTX | H | H | H | H | OH |
| dcneoSTX | OH | H | H | H | OH |
| dcGTX1 | OH | H | $OSO_3^-$ | H | OH |
| dcGTX2 | H | H | $OSO_3^-$ | H | OH |
| dcGTX3 | H | $OSO_3^-$ | H | H | OH |
| dcGTX4 | OH | $OSO_3^-$ | H | H | OH |
| LWTX1 | H | $OSO_3^-$ | H | $COCH_3$ | H |
| LWTX2 | H | $OSO_3^-$ | H | $COCH_3$ | OH |
| LWTX3 | H | H | $OSO_3^-$ | $COCH_3$ | OH |
| LWTX4 | H | H | H | H | H |
| LWTX5 | H | H | H | $COCH_3$ | OH |
| LWTX6 | H | H | H | $COCH_3$ | H |

| Toxine | Groupes fonctionnels variables des CYNs | |
|---|---|---|
| | $R_1$ | $R_2$ |
| Cylindrospermopsine | H | OH |
| 7-épicylindrospermopsine | OH | H |
| 7-déoxycylindrospermopsine | H | H |

**Figure 1-3.** Structure moléculaire des saxitoxines et des cylindrospermopsines (adapté de Hiller *et al.* [50]).

### 1.2.2.4 Cylindrospermopsine

La cylindrospermopsine (CYN) a été identifiée pour la première fois en 1979 lors d'un épisode d'hépatoentérite en Australie, dont les symptômes sont semblables à l'hépatite, qui a touché 148 personnes. Une souche de *Cylindrospermopsis raciborskii* a été isolé de eau potable et la production de la CYN aurait été la cause de cet empoisonnement [61]. En plus de la souche *C. raciborskii*, plusieurs autres cyanobactéries peuvent produire la CYN : *Umezakia natans*, *Aphanizomenon ovalisporum*, *Aphanizomenon flos-aquae*, *Raphidiospis curvata* et *Anabaena bergii* [24]. Ainsi, malgré que la toxine soit retrouvée principalement dans les climats tropicaux et subtropicaux, on la recense de plus en plus dans des climats tempérés tel

qu'en Europe et en Amérique du Nord [12]. La CYN est un polycétide dérivé alcaloïde incluant un groupement guanidine tricyclique combinée à un groupement hydroxyméthyluracile (**Figure 1-3**). Avec une masse molaire de 415,43 g $mol^{-1}$, la CYN possède un $pK_a$ de 8,8 et son caractère hydrophile lui confère une valeur de log $K_{ow}$ de -2,6 le rendant très soluble dans l'eau. À pH physiologique, la CYN possède une charge nulle, mais se retrouve sous forme de zwitterion avec une charge négative sur le groupement sulfate et une charge positive sur la portion guanidine de la molécule. La CYN est stable dans le noir en milieu aqueux mais peut se dégrader en présence de lumière ultra-violette (UV). Par contre, la molécule est relativement stable à la chaleur et aux changements de pH, en plus d'être résistante à certains précédés standards de traitement d'eau [62]. On retrouve la CYN sous une forme naturelle épimérique au pont hydroxyle, le 7-épicyclindrospermopsine, un métabolite mineur toxique produit par la souche *A. ovalisporum*, mais aussi une variante dont un groupement hydroxyle manque à la structure, le 7-déoxycylindrospermopsine (**Figure 1-3**) [11, 50, 62]. L'origine des variantes n'est pas claire, à savoir si elles sont précurseurs à la CYN, des variantes ou des produits de dégradation [62].

La CYN est une cyanotoxine hautement active biologiquement possédant des groupements variés lui conférant des effets hépatotoxiques, cytotoxiques et neurotoxiques et peut ainsi interférer dans plusieurs voies métaboliques [63]. Lorsqu'ingérée, la CYN se déplace dans le système digestif et cause une inhibition de la protéine de synthèse, le glutathion, et aussi des cytochromes P450, responsable de la métabolisation de molécules toxiques. Le groupement uracile et l'hydroxyle en $R_1$ ou $R_2$ (**Figure 1-3**) sont responsables de la toxicité de la molécule [64-66]. Ultimement, un empoisonnement à la CYN peut causer des dommages aux cellules hépatiques et aux muqueuses intestinales, des lésions cellulaires dans les reins créant un dysfonctionnement rénal et aux vaisseaux sanguins induisant des hémorragies [12, 67]. Finalement, quelques études ont démontré la présence d'une bioaccumulation de la CYN dans les mollusques et poissons en contact avec la toxine sans toutefois montrer une bioamplification significative dans la chaîne trophique aquatique [68].

### 1.2.2.5 Autres toxines alcaloïdes

Plusieurs autres cyanotoxines possédant des propriétés dermatotoxiques et neurotoxiques ont été identifiées plus récemment. Tout d'abord, les dermatotoxines aplysiatoxine et débromoaplysiatoxine (APTXs) et les lyngbyatoxines (LTXs) sont des dermatoxines majoritairement produites par la souche *Lyngbya majuscula* qui n'a été identifiée qu'en milieu marin [12]. Les APTXs sont des bilactones phénoliques (**Figure 1-4**) et ils sont connus pour leurs effets irritants et inflammatoires, mais aussi comme promoteurs de tumeurs par l'activation de la protéine kinase C [12, 69]. La structure des LTXs est identique à l'isomère de la téléocidine A retrouvé dans le mycélium de plusieurs souches de *Steptomyces*. On retrouve trois variantes les LTX-a, - et –c (**Figure 1-5**) et a des propriétés légèrement lipophiles induisant une légère pénétration dans la peau pouvant causer des inflammations et dermatites cutanées. Lorsqu'elles sont ingérées, une irritation et inflammation de la bouche et du système gastro-intestinal peut se produire [70, 71]. Due à un manque d'information et leur faible occurrence, ces cyanotoxines ne seront pas à l'étude dans les chapitres suivants.

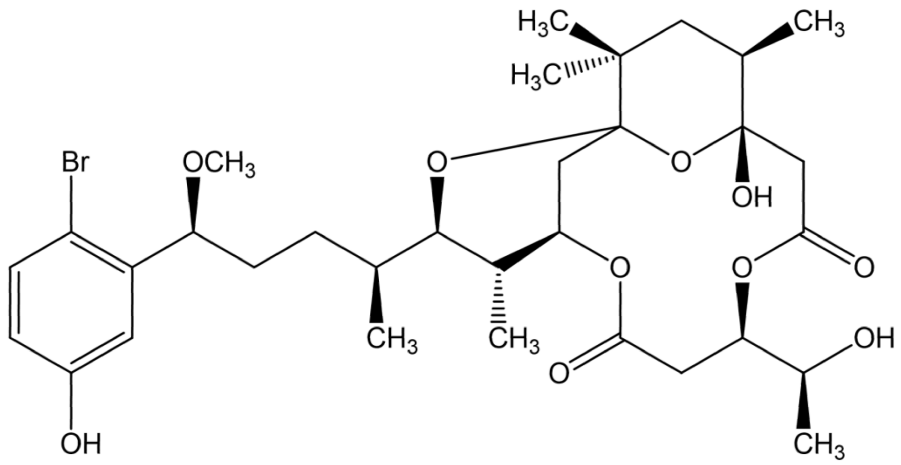


**Figure 1-4.** Structure moléculaire de l'aplysiatoxine [12].

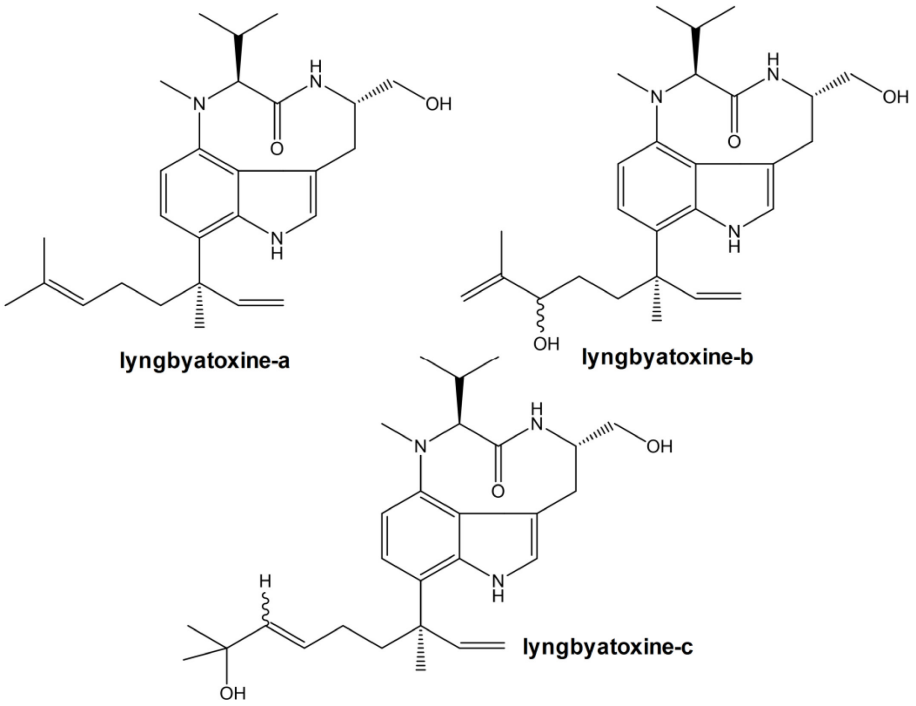


**Figure 1-5.** Structure moléculaire des différentes lyngbyatoxines (adapté de van Apeldoorn *et al.* [12]).

### 1.2.3 Acides aminés non-protéinogènes; BMAA

Les acides aminés non-protéinogènes, ou non naturels, sont des acides aminés qui ne sont pas retrouvés naturellement dans le code génétique des organismes vivants. Certains d'entre eux ont des propriétés toxiques étant donné qu'ils vont avoir les mêmes fonctions que les acides aminés présents dans l'organisme.

L'acide aminé non-protéinogène, le β-*N*-méthylamino-$_L$-alanine (BMAA), est une neurotoxine excitotoxique produit par environ 95% des genres de cyanobactéries nuisibles [72]. Malgré qu'il soit présent partout sur la planète, le BMAA n'a été identifié qu'en 1967 suite à un incident à l'île de Guam. Des cas importants de sclérose latérale amyotrophique et de la maladie de Parkinson, communément appelés Syndrome de Guam, ont été diagnostiqués et la neurotoxine a été rapportée comme la responsable de cet incident. Elle aurait été retrouvée dans des graines de *Cycas circinalis*, ou grand rameau, utilisées pour faire de la

farine par les habitant de l'île [73, 74]. Le BMAA a une faible masse molaire de 118,13 g mol$^{-1}$ et possède un carbone alpha avec un groupement carboxyle, une amine secondaire et une méthylamine dans la chaîne latérale (**Figure 1-6**). Étant une base polaire, la molécule possède deux $pK_a$ de 6,5 et 9,7 et étant fortement hydrophile, elle possède un log $K_{ow}$ de -4. Le BMAA peut se lier facilement à différentes molécules et a une tendance à produire des adduits avec des ions métalliques présents dans son milieu [75]. Le BMAA est une molécule très stable et peut supporter une large plage de pH, de température ainsi que la lumière naturelle [11]. Pour induire sa toxicité, le BMAA est habituellement ingéré, soit par une eau contaminée, mais aussi par des végétaux. Il agit principalement sur les neurones moteurs en se fixant sur les récepteurs glutamates et ainsi induire un effet excitotoxique. De plus, le BMAA pourrait causer un mauvais repliement des protéines intraneuronales associé aux troubles neurodérénératifs [76, 77].

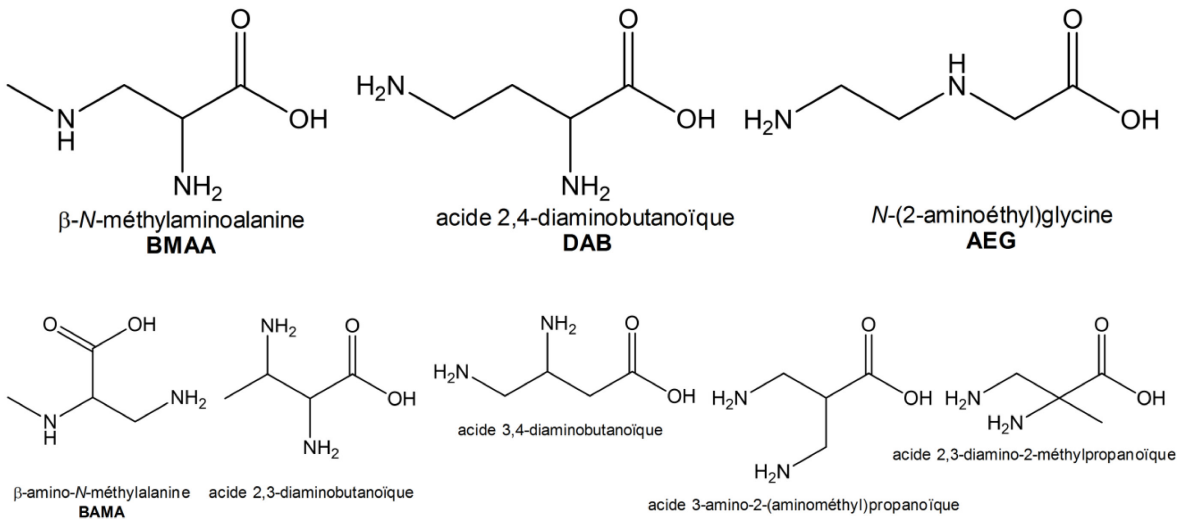


**Figure 1-6.** Structure moléculaire du β-*N*-méthylaminoalanine et de ses isomères de conformation (adapté de Jiang *et al.* [78]).

Plusieurs isomères de conformation du BMAA ont été identifiés pouvant interférer avec sa détection (**Figure 1-6**). On retrouve tout d'abord l'acide 2,4-diamino butyrique, connu comme étant aussi une toxine hépatotoxique et neurotoxique d'origine non-protéique. Elle est retrouvée dans plusieurs organismes procaryotes et eucaryotes, mais n'est pas d'origine cyanobactérienne [78]. Ensuite, on retrouve le N-(2-aminoéthyle)glycine, une molécule non

toxique pouvant être produite par les cyanobactéries et jouant le rôle d'épine dorsale pour les acides nucléiques peptidiques [79, 80]. Finalement, une étude récente a permis d'identifier et différencier cinq autre isomères de conformation du BMAA pouvant se retrouver dans les mêmes milieux soit le β-amino-*N*-méthylalanine (BAMA), l'acide 2,3-diaminobutanoïque, l'acide 3,4-diaminobutanoïque, l'acide 3-amino-2-(aminométhyle)promanoïque et l'acide 3-diamino-2-méthylpropanoïque (**Figure 1-6**) [78].

On retrouve le BMAA autant dans des environnements terrestres qu'aquatiques. La toxine peut facilement être bioaccumulée dans les végétaux, dans les racines, fruits et graines, et ainsi induire une bioamplification assez importante dans la chaîne trophique pour obtenir des niveaux de concentrations suffisamment importante pour être nocif lorsque qu'il y a exposition [72].

### 1.2.4 Lipopolysaccharides

Les lipopolysaccharides (LPS) sont des composantes de la membrane externe cellulaire de la plupart des cyanobactéries mais aussi des bactéries à Gram négatif où ils forment des complexes avec les lipides et les phospholipides. Plusieurs LPS peuvent être retrouvées et leur structure générale, présentée à la **Figure 1-7**, est constituée d'une protéine antigénique, un noyau polysaccharidique contenant une partie 2-céto-3-désoxyoctanate (KDO) liée à une partie glycophospholipidique (Lipide A) qui est le support de la toxicité des LPS [8, 81]. Malgré que les LPS d'origine cyanobactérienne soient moins toxiques que celles d'origines bactériennes, elles peuvent causer d'importantes inflammations de la peau ou du système digestif s'ils sont ingérés [8]. Dues aux caractéristiques structurelles et aux propriétés différentes des cyanotoxines mentionnées dans les sections précédentes, les LPS ne seront pas à l'étude dans les prochains chapitres.

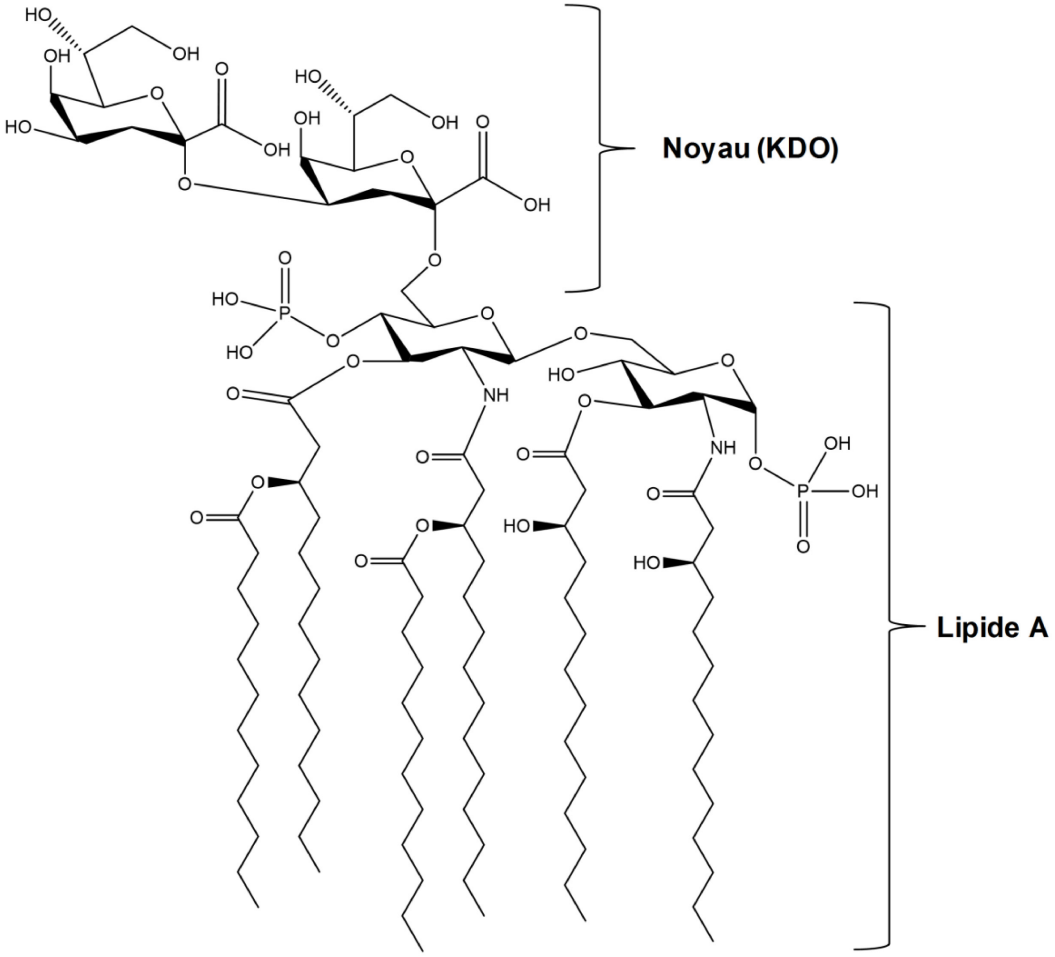


**Figure 1-7.** Structure moléculaire des lipopolysaccharides.

## 1.3 Toxicité et réglementation des cyanotoxines

De nombreux épisodes d'empoisonnement par la consommation d'eau contaminée par les cyanotoxines ont été rapportés depuis plus d'un siècle, ce qui a inspiré de nombreuses générations de chercheurs à étudier les cyanobactéries nuisibles et leur production de toxines [82]. Le cas d'empoisonnement le plus important occasionné par une exposition aux cyanotoxines a été rapporté au Brésil en 1996 lorsque 50 patients sur 130 touchés sont morts due à une hémodialyse dont l'eau était contaminée [83]. La majeure partie des cas d'intoxication sont reliés à la consommation de poissons contaminés ou à des activités

récréatives dans des eaux contaminés et plusieurs cas de morts d'animaux ou d'intoxication humaine ont été répertoriés [12, 28, 84].

Au fil des années, de plus en plus de données toxicologiques ont été répertoriées permettant une meilleure compréhension des modes d'action et des impacts sur la santé. La dose létale à la médiane ($DL_{50}$), c'est-à-dire, la dose causant la mort de 50 % d'une population animale dans des conditions spécifiques, est la méthode utilisée pour décrire la toxicité des cyanotoxines. Ces valeurs sont déterminées par injections intrapéritonéales et sont exprimées en microgrammes de cyanotoxines injectés par kilogramme de la masse animale $\mu g\ kg^{-1}$. Les valeurs de $DL_{50}$ des différentes toxines sont présentées dans le **Tableau 1-1**. Dû à un manque de données toxicologiques, les valeurs pour APTXs et BMAA ne sont pas disponibles.

En fonction des données toxicologiques pour chacune des toxines, plusieurs pays ont établi des réglementations quant à la concentration limite de chacune des toxines dans l'eau potable. L'Organisation Mondiale de la Santé (OMS) a établi, après l'incident du Brésil en 1996, une norme temporaire de 1 $\mu g\ L^{-1}$ en MC-LR équivalent (éq) [6]. Le **Tableau 1-1** présente les différentes réglementations adoptées par plusieurs pays pour certaines toxines [8, 11, 12, 85, 86]. La norme de l'OMS a été adoptée pour les MC-LR par plusieurs pays tel la Nouvelle Zélande, le Brésil, la Grande Bretagne, la France, l'Italie, le Japon, la Corée du Sud, la Chine, la Norvège, la Pologne et la République Tchèque. Le Québec et l'Australie ont établi des niveaux tolérables de 1,5 $\mu g\ L^{-1}$ pour les MC-LRéq et 1,3 $\mu g\ L^{-1}$ pour les MC totales, respectivement. Finalement, aucune réglementation officielle n'a été adoptée par les État-Unis. En Nouvelle Zélande, une norme de 0,1 $\mu g\ L^{-1}$ a été établie en incluant un facteur 10 dû à l'effet promoteur tumoral. Pour les autres toxines, l'OMS n'a pas établi de norme à suivre. Pour ANA-a, au Québec, on tolère des concentrations maximales de 3,7 $\mu g\ L^{-1}$, tandis qu'en Nouvelle Zélande, la concentration maximale tolérée est de 6 $\mu g\ L^{-1}$. Finalement, trois états des États-Unis ont établi une directive de 1 $\mu g\ L^{-1}$ dans l'eau potable. Aucunes réglementations n'ont été établies pour l'homoanatoxine-a et ANA-a(s). Pour les STXs, une norme de 3 $\mu g\ L^{-1}$ en Australie a été adoptée en termes de STXéq. Pour CYN, des niveaux tolérables de 1 $\mu g\ L^{-1}$ au Canada et à la Nouvelle Zélande ainsi que 15 $\mu g\ L^{-1}$ au Brésil ont été

proposés. Finalement, aucune réglementation n'a été identifiée pour NOD, APTXs, LTXs, BMAA et LPS.

**Tableau 1-1.** Récapitulatif des données sur la toxicité ($DL_{50}$) des cyanotoxines et des normes et réglementations internationales dans l'eau potable et récréative [6, 8, 11, 24, 87, 88].

| Cyanotoxine | Toxicité ($DL_{50}$/µg kg$^{-1}$) | Pays et normes/réglementations | Mécanisme de toxicité |
|---|---|---|---|
| Microcystines : | | | |
| MC-LR | 50 | OMS : 1 µg L$^{-1}$ (MC-LRéq) | |
| MC-LA | 50 | | |
| MC-LY | 90 | Brésil, Grande Bretagne, France, Italie, Japon, Corée du Sud, Chine, Norvège, Pologne et République Tchèque : 1 µg L$^{-1}$ (MC-LRéq) | |
| MC-RR | 500 – 800 | | |
| MC-YR | 150 – 200 | | |
| MC-YA | 60 – 70 | | |
| MC-AR | 250 | | |
| MC-FR | 250 | | |
| MC-WR | 150 – 200 | | |
| MC-HilR | 100 | Québec et Australie : 1,5 µg L$^{-1}$ (MC-LRéq) 1,3 µg L$^{-1}$ (MC total) | |
| MC-HtyR | 80 – 100 | | |
| MC-M(O)R | 700 – 800 | | |
| MC-YM(O) | 56 – 110 | | |
| [Dha$^{7}$]MC-LR | 250 | Nouvelle Zélande : 1 et 0,1 µg L$^{-1}$ (MC-LRéq) | |
| [(6*Z*)-Adda]MC-LR | 1200 | | |
| Nodularines | 30 – 70 | N/D | |
| Anatoxine-a | 200 | Québec : 3,7 µg L$^{-1}$ Nouvelle Zélande : 6 µg L$^{-1}$ Californie, Washington, Oregon : 1 µg L$^{-1}$ | Liaison aux récepteurs acétylcholines : paralysie musculaire |
| Homoanatoxine-a | 250 | N/D | |
| Anatoxine-a(s) | 20 | N/D | Inhibition de l'acéthylcholinestérase : paralysie musculaire |
| Saxitoxines | 10 | Australie : 3 µg L$^{-1}$ (STXéq) | Blocage des canaux sodiques : paralysie |
| Cylindrospermopsine | 200 – 2100 | Canada et Nouvelle Zélande : 1 µg L$^{-1}$ Brésil : 15 µg L$^{-1}$ | Inhibition de la synthèse protéique : insuffisance rénale et hépatique |
| Aplysiatoxines | N/D | N/D | Activation de la protéine kinases C : irritation et tumeurs |
| Lyngbyatoxines | 250 | N/D | |
| BMAA | N/D | N/D | Liaison aux récepteurs glutamates : maladies neurodégénératives |
| Lipopoysaccharides | 40 – 190 mg kg$^{-1}$ | N/D | Inflammations |

N/D : Données non disponibles

## 1.4 Analyse des cyanotoxines

Une multitude de méthodes d'analyses sont disponibles pour la détection des cyanotoxines dans diverses matrices, mais aucune n'a pu être développée pour la détermination de toutes les variantes en une seule méthode analytique. Globalement, les méthodes d'analyses utilisées se définissent en deux groupes distincts : les méthodes d'analyses biologiques et les méthodes d'analyses physicochimiques [53]. Ces méthodes varient en termes de l'information fournie et de l'application. Les prochaines sections présenteront de manière générale les différentes méthodes d'analyse des cyanotoxines dans diverses matrices environnementale ainsi qu'une comparaison critique de leurs performances. Le **Tableau 1-2** présente un résumé des différentes techniques utilisées en fonction des toxines ciblées et précise leurs performances analytiques. Ces techniques analytiques et leurs caractéristiques seront décrites dans les sections qui suivent.

### 1.4.1 Méthodes d'extraction

Dépendamment des cyanotoxines ciblées, de la matrice ou se trouve les composés et de la méthode d'analyse utilisée, une méthode de préparation d'échantillon spécifique doit être utilisée avant l'analyse, tant de type biologique que physicochimique. Tout d'abord, dans les échantillons d'eau, les toxines sont présentes sous deux formes, c'est à dire sous forme libres dissoutes, ou extracellulaires, et sous forme liée ou intracellulaire. De manière générale, lorsque qu'un échantillon est simplement filtré avant une analyse, seule la partie dissoute sera prise en compte [11]. Afin d'avoir la totalité des cyanotoxines dans un échantillon, il est préférable d'inclure une étape additionnelle visant une lyse cellulaire pour briser les parois des cellules et de libérer les toxines intracellulaires. La lyse peut être effectuée soit par des cycles de gel et dégel répétés suivi, au besoin, d'une sonication de l'échantillon. Cette étape est primordiale, mais n'est pas toujours efficace due à la robustesse des parois cellulaires des cyanobactéries. Une lyophilisation de l'échantillon suivie d'une sonication en solution aqueuse ou organique est aussi possible si l'échantillon est solide (cellules, sédiments ou tissu animal) [89]. Par la suite l'échantillon peut être filtré avant d'être soumis à l'analyse.

**Tableau 1-2.** Récapitulatif des limites de détections et caractéristiques diverses méthodes d'analyses des cyanotoxines.

| Méthode | Toxine | Limite de détection | Référence | Commentaires |
|---|---|---|---|---|
| ELISA | MC | 0,006 – 0,2 µg $L^{-1}$ | [90-93] | Sensible, peu dispendieux |
| | NOD | | | Peu reproductible |
| | CYN | 0,04 µg $L^{-1}$ | [94] | Sélectivité croisée |
| | STX | 0,003 – 0,01 µg $L^{-1}$ | [95] | |
| GC-ECD | ANA-a | 5 ng inj.* | [96] | Sensible, peu dispendieux<br>Dérivatisation nécessaire |
| GC-MS | MC | 0,1 ng inj. | [47] | Sensible, sélectif et robuste |
| | MMPB | 0,43 ng inj. | [97] | Relativement peu dispendieux |
| | ANA-a | 0,1 ng inj. | [47] | Dérivatisation nécessaire |
| | BMAA | 5 ng inj. | [98] | |
| HPLC-UV | MC | 0,02 – 0,1 µg $L^{-1}$ | [99, 100] | Relativement peu dispendieux |
| | CYN | 0,15 – 0,2 µg $L^{-1}$ | [101, 102] | Non applicable aux matrices complexes |
| HPLC-PDA | MC | 0,02 µg $L^{-1}$ | [103] | Un peu dispendieux, fiable |
| | MMPB | 1 ng inj. | [104] | Manque de standards pouvant gêner la détection |
| | CYN | 1 ng inj. | [105] | |
| HPLC-FLD | MC | 3 µg $L^{-1}$ | [106] | Sensible, relativement peu couteux |
| | MMPB | 0,125 µg $L^{-1}$ | [107] | |
| | ANA-a | 0,01 – 0,02 µg $L^{-1}$ | [47, 108] | Applicable en matrices plus chargées |
| | STX | 0,5 µg $L^{-1}$ | [109, 110] | |
| | BMAA | 0,002 – 1,2 µg $L^{-1}$ | [72, 111, 112] | Dérivatisation nécessaire |
| HPLC-MS | MC | 0,2 – 1 µg $L^{-1}$ | [99] | Sensible, sélectif, robuste et fiable |
| | MMPB | 0,002 µg $L^{-1}$ | [47] | |
| | NOD | 0,3 µg $L^{-1}$ | [113] | Dispendieux, étalons peu disponibles |
| | ANA-a | 0,002 – 0,4 µg $L^{-1}$ | [114, 115] | |
| | BMAA | 0,002 – 0,1 µg $L^{-1}$ | [116, 117] | |
| HPLC-MS/MS | MC | 0,002 – 1,5 µg $L^{-1}$ | [118-122] | Plus sensible, plus sélectif, robuste et fiable |
| | NOD | 0,002 – 0,2 µg $L^{-1}$ | [118, 121, 123] | |
| | ANA-a | 0,008 – 0,13 µg $L^{-1}$ | [122, 124] | Dispendieux, étalons peu disponibles |
| | CYN | 0,2 µg $L^{-1}$ (C18) | [94] | |
| | | 0,01 µg $L^{-1}$ (HILIC) | [94] | |
| | STX | 0,425 µg $L^{-1}$ | [118] | |
| | BMAA | 0,025 µg $L^{-1}$ (C18) | [125] | |
| | BMAA | 0,4 µg $L^{-1}$ (HILIC) | [126] | |
| CE | MC | 1 – 4 mg $L^{-1}$ | [127] | Peu dispendieux |
| | NOD | | | Très peu sensible |
| | ANA-a | | | |
| | CYN | | | |
| | LTX | | | |
| | BMAA | 0,5 mg $L^{-1}$ | [128] | |

*inj. : Quantité d'analyte en injectée dans la colonne chromatographique.

Si les cyanotoxines d'intérêt sont présentes à des concentrations trop faibles pour être détectées à l'aide de la technique analytique choisie, une étape de purification et d'enrichissement peut s'avérer nécessaire. La méthode la plus utilisée est l'extraction sur phase solide (SPE) qui permet de concentrer les analytes jusqu'à trois ordres de grandeurs dépendamment de la quantité de matériel utilisé au départ et le volume de reconstitution après l'extraction. Globalement, l'échantillon est filtré sur une cartouche SPE constituée d'un sorbant possédant des propriétés d'interaction spécifiques aux composés étudiés et généralement, on utilisera des sorbants à phases inverses tel l'octadécylsilane (C18) [11]. Il est cependant possible d'utiliser des cartouches échangeuses d'ions dont la chaîne polymérique de la résine se termine, par exemple, avec un groupement sulfate pour un échange cationique, ou un groupement amine, pour un échange anionique et finalement isoler des composés possédant une charge à un pH donné. En règle générale, l'élution des composés selon les cartouches se fait avec du méthanol (MeOH) qui peut être acidifié ou basifié au besoin. La SPE permet alors d'éliminer les molécules interférentes de la matrice, mais aussi d'améliorer les limites de détection des méthodes analytiques.

Les MC, comparées aux autres cyanotoxines, offrent un défi quant à leur extraction dans différentes matrices biologiques, incluant les tissus d'animaux. En effet, leurs liaisons covalentes irréversibles sur les tissus font en sorte que les méthodes conventionnelles d'extraction sont souvent inefficaces et des méthodes plus agressives ont été développées. Les méthodes conventionnelles d'extraction des MC dans les tissus incluent une lyse cellulaire et une extraction utilisant du MeOH acidifié. Par contre, les recouvrements obtenus sont généralement faibles, parfois aussi peu que 10 %, étant donné que cette méthode ne tient compte que de la portion libre des MC dans les tissus [129]. Des études plus récentes ont proposé l'utilisation d'une méthode d'extraction par oxydation de Lemieux, une réaction chimique d'oxydation à base de permanganate de potassium et de periodate de sodium permettant de cliver les molécules de MC en deux parties au niveau du groupement Adda [130, 131]. On sépare alors la chaîne peptidique d'une molécule commune à toute les MC, l'acide 2-méthyl-3-méthoxy-4-phénylbutyrique (MMPB) qui est illustrée à la **Figure 1-8**. Cette oxydation, précédée d'une digestion enzymatique des tissus à l'aide de trypsine, permet

d'améliorer l'extraction des MC avec des récupérations variant de 20 à 100 % [130, 131]. En effet, la partie liée des tissus étaient prise en compte en plus d'inclure toutes ses variantes. L'inconvénient de la technique provient du travail fastidieux incluant des temps de réactions d'oxydations chimiques jusqu'à 20 h pour toutes les étapes.

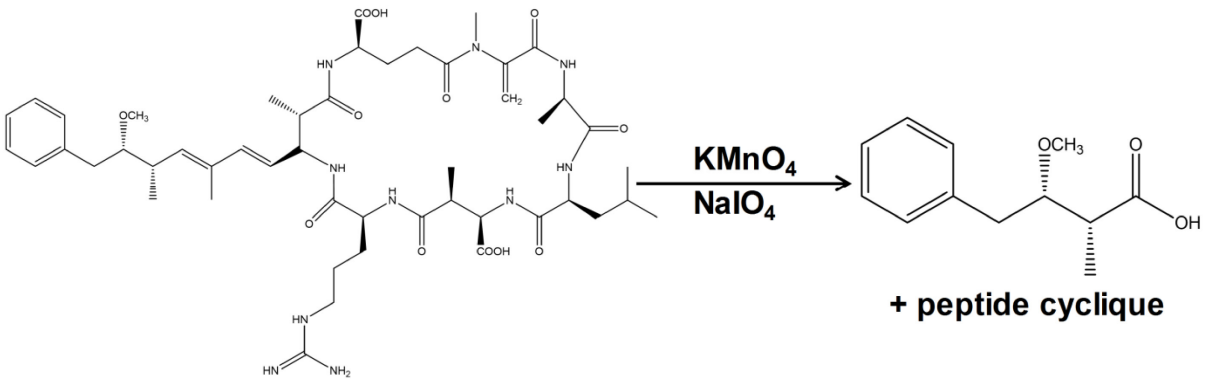


**Figure 1-8.** Schématisation de l'oxydation de Lemieux appliquée aux microcystines pour former leur partie commune, le MMPB.

## 1.4.2 Essais biologiques

Plusieurs approches d'analyses par essais biologiques sont disponibles pour la détection des cyanotoxines incluant les essais biologiques *in vivo*, les essais biochimiques et les essais immunologiques, ces derniers étant les plus répandus.

### 1.4.2.1 Essais biologiques *in vivo*

Cette méthode de dépistage est la plus simple et est plus généralement utilisée par l'intermédiaire d'essais biologiques sur les souris. Cette technique, principalement qualitative, est utilisée pour déterminer l'activité toxicologique des cyanotoxines ($DL_{50}$) et est généralement utilisée sur des organismes vivants, donc elle ne peut être utilisée pour des échantillons environnementaux [11, 53]. Les composés d'intérêts sont alors injectés de manière intrapéritonéale et ce qui permet l'observation des différents symptômes engendrés [89]. Les principaux inconvénients de cette méthode sont une faible sensibilité et une mauvaise sélectivité causée par la sélectivité croisée entre les MC et NOD ou avec d'autres

molécules présentes dans la matrice. De plus, en plus des coûts engendrés par la méthode, il y a une opposition publique due à l'utilisation d'un nombre important de souris, nécessaire pour effectuer ces tests de toxicité [53, 132].

#### 1.4.2.2 Essais biochimiques

Les MC et NOD sont des inhibiteurs de protéines phosphatases et cette propriété peut être utilisée pour leur détection par l'intermédiaire d'un essai par inhibition de la protéine phosphatase PP1A. Les enzymes sont alors exposées à l'aliquote d'un échantillon contenant la toxine et celui-ci est incubé avec un substrat approprié, normalement marqué d'un radio-isotope du $^{32}P$, mais aussi des chromophores et fluorochromes [89, 133]. Les échantillons sont alors analysés par spectrophotométrie et permettent la détection du substrat ou de son produit de transformation et ultimement l'activité de l'enzyme, qui est inversement proportionnelle à la concentration de la toxine. Cette technique permet des analyses rapides, quelques heures pour un grand nombre d'échantillons, en plus d'offrir une bonne sensibilité avec des limites de détection allant jusqu'à 0,01 $\mu g\ L^{-1}$ [133]. Par contre, les résultats sont exprimés en MC-LRéq en plus de ne pas pouvoir distinguer les MC des NOD. Une sélectivité croisée est aussi observée avec la matrice causant des sur ou sous estimations [11]. Des essais biochimiques ont été utilisés aussi pour ANA-a(s) en utilisant la mesure de l'acétylcholinestérase. Ce test n'est pas sélectif car des pesticides organophosphorés souvent présents possèdent le même pouvoir d'inhibition [109]. On retrouve aussi des méthodes d'analyse par activité biologique pour la quantification de la STX en utilisant leur faculté à bloquer les canaux sodiques des membranes cellulaires. Des cellules cancéreuses du type neuroblastes sont utilisées pour leur expression des canaux sodiques et sont incubées avec deux agents qui permettent l'ouverture et le retour du sodium hors des cellules. La concentration de la STX est alors déterminée en fonction de la survie des cellules mesurée par colorimétrie [134].

#### 1.4.2.3 Essais immunologiques

Les essais immunologiques, et plus particulièrement les méthodes immuno-enzymatiques appelées ELISA (*Enzyme-linked immunosorbent assays*) font partie des techniques biochimiques les plus utilisées pour la détermination de différents composés

toxiques. La concentration d'un antigène, étant l'analyte, dans un échantillon est mesuré à l'aide d'une réaction avec des anticorps. Le principe se repose sur la formation d'un complexe entre un anticorps de capture et la molécule d'intérêt. Un anticorps secondaire, couplé avec une enzyme permettant la transformation d'un substrat en produit chromophore, est alors ajouté étant spécifique à la toxine étudiée. La réaction est alors quantifiée et la concentration en cyanotoxines est inversement proportionnelle à l'intensité de la coloration. Deux types d'anticorps sont utilisés pour les analyses par ELISA, les anticorps monoclonaux, ayant un seul site de reconnaissance et les anticorps polyclonaux, étant un mélange d'anticorps possédant plusieurs sites de reconnaissance [135]. L'ELISA permet des analyses moins dispendieuses et faciles d'utilisation en plus d'être très sensibles, pouvant détecter dans certains cas jusqu'à quelques ng $L^{-1}$. Par contre, la méthode souffre en sélectivité, causée par des liaisons non spécifiques entre les anticorps et les antigènes ainsi qu'une réactivité croisée avec d'autres molécules du milieu [53, 89, 136].

Pour le moment, seules les MC, la NOD, la CYN et les STXs sont détectables par cette technique. Les MC ont été les premières toxines à être détectées par ELISA. Les premiers anticorps utilisés étaient spécifiques à la MC-LR, mais on a découvert qu'ils possédaient une réactivité croisée avec d'autres variantes. Par la suite, cette réactivité croisée a confirmé que la détection de plusieurs variantes pouvait être sous-estimée [53]. Étant donné que le choix des anticorps est essentiel à la sélectivité de la méthode, des avancées ont récemment permis la détection de plusieurs variantes des MC ainsi que la NOD avec une haute sensibilité [137]. Plusieurs kits ELISA sont commercialisés et régulièrement utilisés. Par contre, la possibilité de réactions croisées, phénomène observé pour les différentes toxines, fait en sorte que les concentrations sont souvent rapportées en MC-LRéq ou STX-éq par exemple. De plus, ces possibilités d'interférence sont élevées dû à la réactivité des anticorps avec des molécules de la matrice. L'ELISA pourrait donc, grâce à sa sensibilité, être un excellent outil de dépistage des cyanotoxines, mais son utilisation à des fins quantitatives est limitée à cause de son manque de sélectivité [11, 135].

### 1.4.3 Méthodes physicochimiques

Les méthodes d'analyse les plus utilisées pour la plupart des cyanotoxines couplent une séparation chromatographique avec une détection par spectroscopie ou la spectrométrie de masse (MS). Les méthodes séparatives incluent l'électrophorèse capillaire (CE), la chromatographie liquide (LC) et la chromatographie gazeuse (GC).

#### 1.4.3.1 Électrophorèse capillaire

La CE a été appliquée surtout pour les MC, mais aussi pour l'ANA-a, la CYN et le BMAA. La technique permet une séparation en fonction de la grosseur et la charge des molécules et utilisent de petits volumes d'échantillons. Un couplage peut être fait avec une détection par fluorescence ou par MS avec une ionisation par électronébulisation (ESI). Le problème principal de la CE étant la robustesse, les limites de détections obtenues sont souvent beaucoup trop élevées [53]. Une analyse simultanée de la MC-LR, l'ANA-a et la CYN a été possible, avec des limites de détection de 1 à 4 mg $L^{-1}$. En général, l'EC offre des limites de détection allant autour du mg $L^{-1}$ comme pour le cas de l'analyse de la BMAA avec une limite de détection de 0,5 mg $L^{-1}$ [127, 128].

#### 1.4.3.2 Chromatographie gazeuse

La séparation chromatographique par GC a été utilisée surtout pour ANA-a, et les MC à l'aide d'une dérivatisation chimique. Comme son nom l'indique, cette technique permet une séparation de composés volatiles thermiquement stables en phase gazeuse. Quelques microlitres d'échantillon en solvant organique volatile sont injectés et directement évaporés à haute température dans l'injecteur. Un gaz vecteur, généralement inerte, sert de phase mobile et permet la séparation des composés par interaction avec la phase stationnaire souvent à l'aide d'un gradient de température. La température du four en GC doit être légèrement supérieure à la température d'ébullition des composés afin de permettre une bonne séparation tout en évitant que les composés sortent au temps mort.

Les méthodes de détection principalement utilisées pour l'analyse des cyanotoxines en GC sont la MS à simple ou triple quadripôles, dont les concepts généraux seront expliqués

plus en détails à la **Section 1.4.3.5**, et la détection par capture d'électrons (ECD) où la détection se fait par réaction entre l'azote et des particules bêta pour créer des électrons qui réagiront avec les analytes. L'intensité du courant généré est mesurée en continu. L'analyse d'ANA-a et de l'homoanatoxine-a a été appliquée en GC-MS et GC-ECD en utilisant des stratégies de dérivatisation à l'aide de l'acétylation ou l'alkylation des molécules. Globalement les limites de détections en GC-ECD et GC-MS se retrouvent entre 0,1 et 5 ng de composé injecté dans la colonne chromatographique [47].

Les MC ont aussi été analysées par GC-MS, mais étant peu volatiles, une dérivatisation est nécessaire. Pour cette fin, l'utilisation de l'oxydation de Lemieux formant la portion MMPB a donc été utilisée dans diverses études. À la suite de l'oxydation, le MMPB est dérivatisé sous une forme de méthyl ester afin d'améliorer la volatilité de la molécule et ultimement la séparation chromatographique. Une bonne sensibilité est obtenue avec des quantités détectées plus faibles qu'un nanogramme, mais les différentes étapes de traitement d'échantillons rendent la méthode fastidieuse [53, 138]. Afin améliorer les performances de l'oxydation, l'utilisation d'ozone a permis de réduire considérablement le temps de réaction et de préparation d'échantillon [139]. Finalement, une analyse directe du MMPB n'ayant pas subi de dérivatisation post-oxydation de Lemieux a permis une détection au niveau du picomolaire, mais les temps d'analyse allait jusqu'à 30 minutes par échantillon dû à la séparation chromatographique [140]. Le principal avantage d'utiliser une oxydation afin d'analyser le MMPB est l'analyse des MC totales, comptant plus de 100 variantes. Une détermination plus complète et réaliste est donc possible.

#### 1.4.3.3 Chromatographie liquide

Les méthodes de séparation chromatographiques les plus utilisées pour la détermination des cyanotoxines sont les méthodes utilisant la LC et plus précisément la chromatographie liquide à haute performance (HPLC). Un échantillon sous phase liquide est injecté à petit volume (de l'ordre du µL) dans une colonne chromatographique remplie d'une phase stationnaire composé de fine granulométrie (3 à 5 µm) et est transporté par une phase mobile composée d'un ou plusieurs solvants organiques ou aqueux dépendamment de la polarité des composés. La composition de la phase mobile peut être modifiée tout au long du

processus de chromatographie permettant une séparation par gradient de solvants, mais la phase mobile peut aussi rester la même permettant une séparation isocratique. Le débit peut être augmenté pour diminuer le temps de séparation des composés augmentant ainsi la pression imposée à la colonne chromatographique et permettant ainsi une durée chromatographique d'environ 15 minutes. Les composés seront principalement séparés selon leur affinité pour la phase stationnaire. Le choix de la colonne chromatographique ainsi que la composition de la phase mobile, initial et dans le temps, sont donc très importants pour permettre une séparation adéquate dans un temps minimal.

La chromatographie de partage est la plus utilisée pour les analyses de routine et deux types de modes de séparation sont utilisés, soit le mode inverse et le mode normal. Une séparation en phase inverse, le mode le plus utilisés en LC, permet d'utiliser des colonnes apolaires dont une chaine alkyle est greffée sur la phase stationnaire généralement avec un nombre de 8 ou 18 carbones (C8 et C18). La séparation se produira en utilisant un mélange d'eau et de MeOH ou d'acétonitrile (ACN) au début et une augmentation de la force éluante se fera par l'augmentation de la proportion des solvants organiques moins polaires afin de déloger les molécules plus hydrophobes interagissant avec la phase stationnaire. Pour ce qui est de la séparation en phase normale, la colonne est polaire et sépare les composés polaires, donc la composition de la phase mobile sera inversée. Un mélange d'eau et solvant organique est utilisé et la polarité de la phase mobile sera augmentée avec l'apport en eau et pour transporter les molécules polaires hydrophiles lors de la chromatographie. Les phases normales les plus utilisées comportent des groupements silanols ou siloxanes permettant des interactions par liaisons hydrogènes. Une variante des phases normales nommée chromatographie par interactions hydrophiles (HILIC) est de plus en plus utilisée pour la séparation de composés polaires hydrophiles. Tout comme la chromatographie en phase normale, une augmentation de la polarité de la phase mobile permettra de séparer les composés polaires dans la colonne. Plusieurs colonnes à base de silanols, amines, amides, ainsi que des phases à séparation zwittérionique sont retrouvées sur le marché [141]. Le solvant organique le plus utilisé est l'ACN à cause de sa faible viscosité et l'utilisation de tampons tel l'acétate d'ammonium ou le formate d'ammonium permettent de modifier le pH et

ainsi de modifier la polarité des molécules d'intérêt. Il est alors possible d'améliorer les performances séparatives de la méthode pour ces composés.

Un autre type de LC plus performante, l'UPLC ou UHPLC (*Ultra Performance Liquid Chromatography*) est une amélioration de l'HPLC en termes de temps d'analyse, de l'efficacité chromatographique et est de plus en plus utilisée. La phase stationnaire possède une granulométrie plus fine (< 2 µm) ce qui donne des pics très fins, donc permet une meilleure résolution chromatographique. La diminution de la granulométrie permet aussi d'utiliser une gamme de débits plus large sans altérer les performances chromatographiques. L'augmentation du débit permet des temps d'analyse plus rapides, mais augmente aussi la pression, ce qui peut altérer la durée de vie des colonnes chromatographiques.

Pour l'analyse des cyanotoxines, la chromatographie la plus utilisée est à phase inverse avec des colonnes C18 en HPLC en utilisant une phase organique composée de MeOH ou d'ACN. Les méthodes chromatographiques pour la séparation des MC se font généralement avec les étalons disponibles, et pour éviter leur coélution, comme par exemple la MC-LR et la MC-YR. L'utilisation de MeOH est préférée à l'ACN qui leur permet d'avoir une meilleure résolution [142]. La NOD est aussi bien séparée de cette manière. La séparation de l'ANA-a et la CYN se fait aussi par C18, mais elle est plus efficace utilisant une phase organique à base d'ACN [47, 62]. De plus, un interférent commun à l'ANA-a, l'acide aminé naturel phénylalanine, peut coéluer avec cette dernière causant des erreurs dans la quantification et l'ajustement des paramètres chromatographiques est essentiel [143]. Finalement, dû à leur caractère hydrophile, certaines toxines peuvent être séparées à l'aide de colonnes HILIC. C'est le cas de la CYN et l'ANA-a, mais surtout de la STX et du BMAA qui ne peuvent être séparés par des colonnes conventionnelles [47]. La possibilité d'analyser le BMAA en phase inverse a été étudié en utilisant la dérivatisation avec le 6-ACQ, principalement utilisé pour être détecté par spectroscopie, mais permet une séparation hydrophobe sélective du BMAA ainsi que de ses isomères de conformation [141].

#### 1.4.3.4 Détection par les méthodes photométriques

Les détecteurs photométriques couplés à la HPLC incluent la détection par absorption moléculaire dans l'ultraviolet-visible (UV-vis), soit à barrettes de diode (PDA), soit à simple longueur d'onde et par fluorescence moléculaire (FLD). Ces méthodes sont basées sur l'absorption des photons par des chromophores présents dans la molécule et dans le cas de la fluorescence, l'émission spontanée de l'énergie absorbée sera observée. Un spectrophotomètre UV-vis comporte une source lumineuse et un monochromateur permettant la séparation des longueurs d'onde de la lumière transmise dans le domaine spectral de l'ultraviolet (185-400 nm) et du visible (400-700 nm). Un chromatogramme peut alors être enregistré selon les composés séparés et détectés et la quantification se fait par une courbe d'étalonnage. Par contre, il est possible que d'autres molécules qui coéluent avec le composé d'intérêt aient une absorbance à la même longueur d'onde, affectant ainsi la quantification des toxines, surtout à basses concentrations [144].

L'utilisation de la PDA permet une meilleure identification de la présence des cyanotoxines étant donné qu'au lieu d'enregistrer une seule longueur d'onde, elle va enregistrer le spectre complet d'absorption d'un composé séparé par chromatographie. La méthode présente tout de même la même problématique lorsqu'on retrouve les analytes à basses concentrations [89].

Dans le cas de la FLD, l'utilisation d'un rayonnement ultraviolet permettra l'absorption de photons par un groupement fluorochrome spécifique de l'analyte, et ce groupement émettra spontanément l'énergie lumineuse qui sera finalement détecté. La détection par FLD est couramment utilisée et a été développée pour la détection de cyanotoxines comme alternative à la détection par absorption. L'émission permet d'améliorer la sensibilité, car il y a moins d'effets de matrice et d'interférents, mais la détection est limitée par l'absence de fluorochromes pour les molécules d'intérêts et de longues étapes de dérivatisation sont souvent nécessaires.

Les MC et la NOD ont une longueur d'absorption maximum de 238 nm, mais les MC possédant un groupement aromatique tel la MC-LW qui contient l'acide aminé tryptophane,

ont une absorbance maximale à une longueur d'onde plus basse, soit 222 nm [142, 145]. Étant donné que la détection des MC est dépendante de la séparation chromatographique, seulement sept variantes peuvent être quantifiées et les autres sont rapportées en MC-LRéq [11]. D'autres cyanotoxines ont été analysées par HPLC-UV, dont la CYN et l'ANA-a avec des longueurs d'ondes d'absorption maximales de 262 et 227 nm respectivement [47, 62]. La sensibilité de l'ANA-a aux rayonnements UV rend la quantification de cette dernière difficile étant donné qu'elle a tendance à se dégrader sous ces conditions et son analyse en LC-UV est donc très limitée [143]. Finalement, le BMAA a été analysé pour la première fois par spectroscopie en utilisant une dérivatisation à l'aide principalement d'un agent fluorescent, le 6-aminoquinoly-*N*-hydroxysuccinimidyle (6-ACQ) permettant une augmentation de la sensibilité de la détection [141]. Des limites de détection jusqu'à quelques dizaines de ng $L^{-1}$ peuvent être obtenues par cette technique pour les différentes cyanotoxines [53]. Le désavantage de cette technique est la présence d'interférents dans la matrice pouvant nuire à la détection UV créant des limitations en termes de sélectivité lorsque les analytes sont en basses concentrations en milieu chargé [11]. L'utilisation du PDA en mode de détection fonctionne de la même manière qu'avec l'UV-vis, excepté une meilleure identification des toxines étudiées étant donné que la détection se fait sur une plage de longueurs d'ondes au lieu d'une longueur d'onde unique [53]. Finalement, l'utilisation de la FLD permet d'améliorer la sensibilité et de diminuer les interférences lors de l'analyse des cyanotoxines et est utilisée comme alternative à l'UV-vis. La seule limitation est que peu de molécules ont la capacité de réémettre la lumière absorbée en UV à la température de la pièce et une étape de dérivatisation avec une molécule fluorochrome est souvent nécessaire afin d'obtenir un signal détectable [11]. C'est le cas des MC avec l'utilisation du DMEQ-TAD (4-[2-(6,7-diméthoxy-4-méthyl-3-oxo-3,4-dihydroquinoxalinyl)éthyl]-1,2,4-triazoline-3,5-dione) et l'ANA-a avec l'utilisation du NBDF (4-fluoro-7-nitro-2,1,3-benzoxadiazole) permettant une détection beaucoup plus sensible avec des limites de détection allant jusqu'à 10 ng $L^{-1}$ [106, 108].

#### 1.4.3.5 Détection par spectrométrie de masse

En règle générale, pour des fins qualitatives et quantitatives, la GC et la HPLC sont couplées avec une détection en spectrométrie de masse (MS) en simple et triple quadripôles.

La détection se fait par la distinction des composés en phase gazeuse selon leur charge une fois ionisés, donnant une valeur de masse sur charge (*m/z*) et de leur abondance relative aux autres ions dans le système. Les sources d'ionisations peuvent varier, mais les techniques d'ionisations les plus utilisées sont l'impact électronique (EI) en GC-MS et la nébulisation électrostatique (ESI) en HPLC-MS.

L'ionisation par EI en GC-MS se déroule en phase gazeuse et à très basse pression. Des électrons sont soumis à une énergie de 70 eV pour être accélérés et concentrés en faisceau. Ce faisceau atteindra les molécules neutres en phase gazeuse et ce bombardement permettra un transfert d'énergie et l'ionisation des molécules en éjectant un électron et formant un cation radicalaire ($M^{+}$). La haute énergie cinétique des électrons induit des réactions de clivage qui sont prévisibles et les signaux obtenus permettent d'obtenir des informations sur la structure des composés. Les ions ainsi formés se dirigent finalement vers l'analyseur.

En HPLC-MS, le mode d'ionisation le plus utilisé pour les cyanotoxines est l'ESI qui peut être couplé à l'analyseur MS à la sortie du LC. Contrairement à l'EI, cette ionisation nécessite un échantillon en état liquide, d'où l'intérêt de l'utiliser en amont de la HPLC. Sensible aux composés polaires, elle est considérée comme étant une source d'ionisation douce, étant donné que très peu de fragmentation se produit, limitant ainsi l'étude structurelle des composés, mais peut produire des ions multi chargés permettant l'ionisation de composés à haute masse moléculaire (> 100 kDa) [146]. Le solvant provenant de la séparation en HPLC est injecté en continu dans le système d'ionisation, et est dispersé en fines gouttelettes d'aérosols. Des additifs peuvent être ajoutés pour augmenter la conductivité de la solution, tel l'acide formique qui agit comme source de protons supplémentaire pour faciliter l'ionisation. Une différence de potentiel (quelques kV) positive ou négative est appliquée au bout d'une aiguille à décharge corona et conférera une charge aux gouttelettes. Elles sont alors attirées par le vide du détecteur MS qui est alors chauffé à environ 300 °C. Au fur et à mesure que le solvant s'évapore, les gouttelettes chargées deviennent instables par augmentation de densité de charges et après avoir atteint la limite de Rayleigh, les répulsions électrostatiques deviennent plus importantes que la tension de surface et une fission de Coulomb se produit,

créant une explosion des gouttelettes, devenant plus petites et plus stables. Les solvants évaporés, les ions, le plus souvent formés d'un ajout ou d'un retrait de proton selon la polarité du voltage appliqué à l'entrée de l'analyseur, se dirigent vers le premier quadripôle du système MS, où ils seront filtrés.

Suite à l'ionisation, les ions sont sélectionnés et séparés par un analyseur soit à simple quadripôles ou triple quadripôles. L'analyseur, schématisé à la **Figure 1-9**, est constitué de quatre électrodes hyperboliques ou cylindriques parallèles. Une différence de potentiel est appliquée aux électrodes opposés, deux à potentiel positifs et deux à potentiels négatifs. Le champ électrique créé par les différents potentiels appliqués aux électrodes quadripolaires permet de modifier la trajectoire des ions en fonction de leur valeur en *m/z*. En effet, selon le potentiel appliqué, certains ions auront une trajectoire stable et traverseront le quadripôle pour aller au détecteur tandis que les autres ions instables seront éjectés. Ce système sert alors de filtre de masse afin de sélectionner les ions d'intérêts au profit des composés non désirés. Un simple quadripôle permet l'analyse en deux modes, soit en balayage complet ou *full scan* (FS) ou en suivi d'ions sélectionnés ou *selected ion monitoring* (SIM). Le mode en FS est un balayage large permettant d'obtenir une détection de tous les ions présents dans un spectre de masse entre les deux valeurs choisies en *m/z*, qui seront filtrés par le quadripôle. Ce mode sert à des fonctions qualitatives afin d'identifier les composés présents dans un échantillon. Le mode SIM, quant à lui, sélectionne une masse spécifique, avec une fenêtre de sélection en masse autour de l'unité, avant d'être transféré au détecteur, un multiplicateur d'électrons transformant le courant des ions le frappant en intensité. Ce mode, principalement utilisé à des fins quantitatives, est beaucoup plus sensible, car il élimine considérablement le bruit de fond, augmentant ainsi le rapport signal sur bruit (S/N).

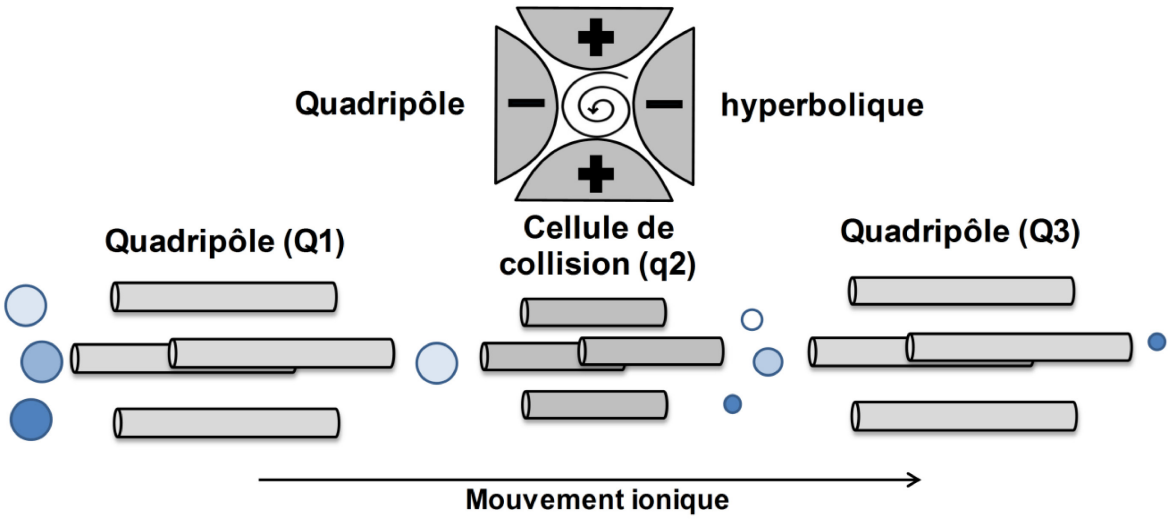


**Figure 1-9.** Schématisation d'un triple quadripôle et le fonctionnement du mode d'acquisition SRM.

Le système en MS le plus populaire de nos jours est le triple quadripôle faisant partie des spectromètres de masse en tandem (MS/MS) due à sa double dimension en terme séparation des ions. Le système, illustré à la **Figure 1-9**, est constitué d'un premier quadripôle (Q1), suivi d'un quadripôle servant de cellule de collision des ions (q2) et finalement un troisième quadripôle (Q3) est utilisé pour une deuxième séparation des ions. La grande différence réside dans la cellule de collision qui permet la fragmentation des ions préalablement sélectionnés par le Q1. Aucun potentiel n'est appliqué afin de stabiliser les ions et un gaz inerte, généralement de l'argon, est soumis à une différence de potentiel (10 à 100 eV) et l'énergie cinétique du gaz induira une fragmentation par collision créant des ions radicaux qui seront transportés vers le Q3.

L'utilisation de quadripôles en série permet de faire des analyses en simple MS ou en MS/MS. En plus des modes obtenus en simple MS, un triple quadripôle permet la sélection d'ions fragments produits, le suivi de réaction ciblée ou *selective reaction monitoring* (SRM). Ainsi, un ion dit précurseur, pourra être fragmenté et ces ions, dits fragments, seront sélectionnés pour être séparés permettant ainsi une double sélectivité d'analyse. Le plus grand avantage d'un détecteur MS/MS est sa grande sélectivité permettant d'éliminer un grand nombre d'interférents. Les résultats obtenus sont aussi beaucoup plus sensibles dû à une

élimination considérable du bruit de fond augmentant ainsi le rapport S/N pour des analyses quantitatives.

L'analyse par MS est largement utilisée pour la détection des cyanotoxines due à sa notable sélectivité et sa grande sensibilité. En effet, la détection utilisant le ratio *m/z* réduit considérablement la probabilité d'avoir des interférents et ce, dans des matrices très chargées. De plus, la MS/MS permet une identification plus spécifique liée aux patrons de fragmentation des cyanotoxines étudiées [11]. Par exemple, les MC ont pu être identifiées individuellement à l'aide des standards disponibles, mais aussi à l'aide de la méthode des MC totales utilisant l'oxydation de Lemieux [53]. Par contre, l'ANA-a possède un interférent, la phénylalanine, dont les masses précurseurs et fragments sont trop proches pour être détectées par MS et MS/MS. C'est pour cette raison que la séparation chromatographique est essentielle pour cette toxine [143]. De plus, la même problématique s'applique au BMAA, qui possède des isomères de conformation possédant des masses identiques [141]. Finalement, des méthodes multi-toxines très sensibles ont aussi été développées pour l'analyse simultanée des MC, de NOD, d'ANA-a, de CYN, et de STX utilisant la HPLC-MS/MS [122, 147-149].

#### 1.4.3.6 MALDI-TOF

Des avancements récents ont permis d'utiliser la MALDI-TOF-MS (*Matrix-Assisted Laser Desorption/Ionization-Time of flight MS)* comme instrument d'identification des toxines et leurs variantes dans des échantillons de cellules cyanobactériennes et de microorganismes [150]. L'analyse se fait directement sur un échantillon, souvent en très petite quantité, séché ou solide où on ajoute une matrice organique qui permet l'absorption de rayons ultraviolets. Un laser, de longueur d'onde appropriée, frappe la matrice qui est co-cristallisée avec les analytes. Des ions sont générés en phase gazeuse et sont finalement pulsés vers l'analyseur qui est un MS à haute résolution. La technique a permis l'identification de plusieurs variantes de MC ainsi que la production d'ANA-a et homoanatoxine-a dans des cultures cyanobactériennes [151, 152]. Malgré que la MALDI-TOF-MS procure une identification précise des cyanotoxines, la méthode ne permet pas d'analyse quantitative.

### 1.4.4 Perspectives de recherche

Les cyanotoxines sont considérées comme étant une menace émergente dans les milieux aquatiques, mais aussi dans les réservoirs et systèmes d'alimentation d'eau. Due à cette problématique, il y a un intérêt croissant envers l'amélioration de la détection de ces toxines pour un contrôle de risques rapide et efficace. Malheureusement, à ce jour, aucune méthode d'analyse de routine n'est disponible pour la détection de toutes les cyanotoxines et il y a toujours du travail à faire pour leur analyse étant donné leur complexité et leur diversité structurelle. En considérant l'état de la recherche et des connaissances sur l'analyse des cyanotoxines, le développement de nouvelles approches analytiques a été proposé afin d'améliorer les méthodes déjà existantes et de proposer par la suite de nouvelles stratégies pour l'obtention de résultats plus complets et une meilleure compréhension de la présence des cyanotoxines dans les matrices environnementales.

Principalement, deux aspects ont été étudiés à cet effet, soit l'utilisation de nouvelles méthodes de traitement d'échantillon afin d'améliorer l'étendue de l'analyse des cyanotoxines et l'utilisation de technologies innovatrices en MS afin d'améliorer la détection en terme de rapidité et de sélectivité. Une première analyse multi-toxines incluant diverses MC, l'ANA-a et la CYN, a été proposée en utilisant une étape SPE en ligne couplée à une détection par UHPLC-ESI-MS/MS afin d'inclure plusieurs cyanotoxines en une seule analyse, résoudre l'interférence d'ANA-a, la phénylalanine, par chromatographie et augmenter la rapidité de l'extraction et l'analyse des échantillons. Une analyse multi-toxines alcaloïdes a été choisie afin d'améliorer la détection du BMAA et de ses isomères, en plus de pouvoir incorporer d'autres toxines dans une même routine analytique. L'utilisation de la MS en haute résolution a été suggérée afin d'améliorer la sélectivité des analyses en plus de comprendre la fragmentation des composés préalablement dérivatisés. Ensuite, l'utilisation de la désorption thermique à diode laser couplée à l'ionisation chimique à pression atmosphérique et à la spectrométrie de masse en tandem ainsi que la spectrométrie de masse à haute résolution (LDTD-APCI-MS/MS et HRMS) comme technologies analytiques ont été suggérées afin d'améliorer le débit analytique dû aux analyses ultra-rapides permise par la LDTD. Tout d'abord, l'analyse directe de l'ANA-a par LDTD-APCI-HRMS a été proposée afin de

résoudre son interférence isobare, la phénylalanine. Ensuite, l'analyse des MC en utilisant l'oxydation de Lemieux a été proposée afin d'obtenir la concentration totale de la toxine dans des échantillons d'eaux et de poissons et ce par LDTD-APCI-MS/MS et HRMS. Ces concentrations, comparées à des analyses de routine standards permettront d'évaluer la sous-évaluation des MC. Les détails des différentes technologies utilisées seront développés à la section suivante.

## 1.5 Nouvelles méthodes analytiques

Cette section décrit et met en contexte les diverses technologies utilisées pour les différentes études de la thèse présentées dans les prochains chapitres.

### 1.5.1 Désorption thermique à diode laser (LDTD)

La LDTD est une interface d'introduction d'échantillon couplée à l'APCI pour effectuer des analyses en MS. Développée par Phytronix Technologies (Québec, Qc, Canada), cette technique n'utilise pas de séparation chromatographique, mais plutôt une désorption thermique pour amener les composés en phase gazeuse. Les échantillons, dont les analytes, sont dissous dans un solvant choisi et déposés à faible volumes (1 et 10 µL) à l'intérieur des puits d'une plaque analytique à 96 puits et les solvants sont alors séchés soit à l'air libre ou dans un four à une température autour de 40 °C. Les puits sont concaves de forme hexagonale permettant de centraliser les composés au fond lors du séchage du solvant. Une fois la plaque insérée dans l'appareil, un laser infrarouge (980 nm, 20 W) frappe l'arrière du puits, étant constitué d'acier inoxydable, permettant ainsi un transfert rapide de la chaleur du laser au métal et ensuite aux composés [153]. Ce laser ne touche pas les analytes, mais seulement le métal en arrière du puits donc la désorption sera produite par le transfert d'énergie thermique entre le puits chauffé rapidement et les composés cristallisés au fond. La puissance et la durée du laser peuvent être contrôlées afin d'obtenir une désorption optimale des composés. Ces composés neutres maintenant volatilisés, un gaz vecteur, normalement composé d'air, permettra de stabiliser leur énergie et de les transporter au travers d'un tube de transfert pour être soumis à une ionisation en APCI et ensuite analysés par MS. Les détails de l'interface

LDTD et une plaque d'analyse sont présentés à la **Figure 1-10** adapté de Picard *et al.* [153] et à la **Figure 1-11** respectivement.

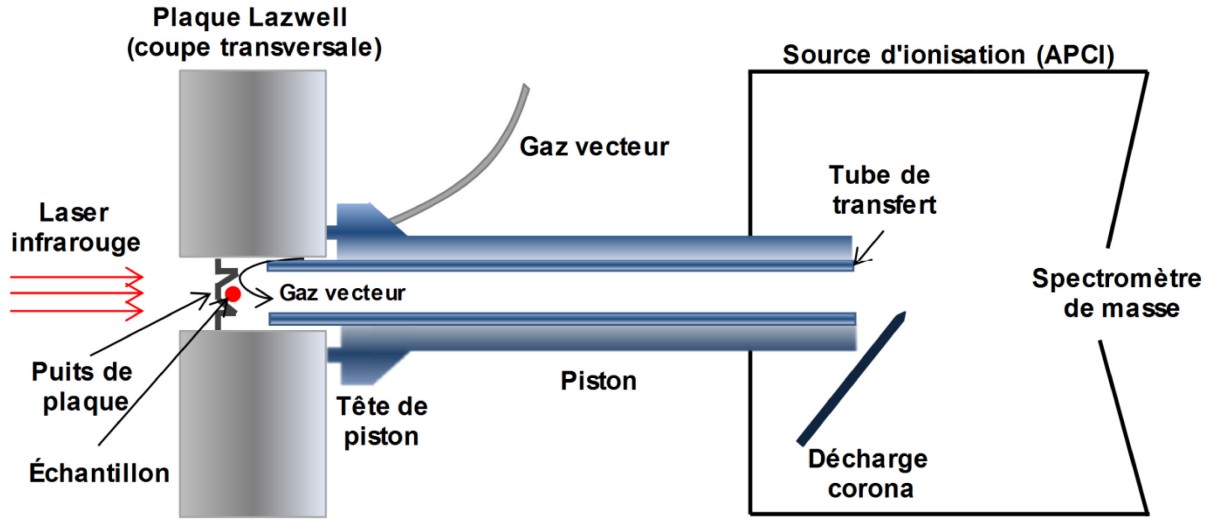


**Figure 1-10.** Schématisation et fonctionnement de la LDTD-APCI (adapté de Picard *et al.* [154]).

**Figure 1-11.** Exemple d'une plaque Lazwell à 96 puits pour les analyses en LDTD-APCI.

L'énergie transférée au puits métallique par le laser infrarouge augmente très rapidement (3000 °C $s^{-1}$) et les températures atteintes sont en dessous du point de fusion de la majorité des molécules analysées en LDTD qui se retrouvent autour de 200 °C [154]. En effet, la chaleur transférée induit des températures de 100 à 180 °C, et cette énergie est exprimée en pourcentage de puissance laser lors de sélection de ce paramètre [154]. Les échantillons sont déposés à très faibles volumes et forment des nanocristaux en séchant dans les puits [154, 155]. Cette propriété permet de réduire la possibilité de dégradation des molécules lors du transfert de chaleur. En effet, le format microscopique des cristaux formés leur procure des propriétés physicochimiques différentes en termes de volatilité comparé à des cristaux macroscopiques [156]. La dégradation et fragmentation des molécules est aussi limitée par le gaz vecteur, possédant un débit entre 2 et 3 L $min^{-1}$. Il sert alors de transporteur, mais aussi empêche la dégradation des molécules en refroidissant considérablement le puits chauffé par le laser et le milieu gazeux [154]. Finalement, le transfert de chaleur diminue aussi les chances de dégradation des composés lors de la désorption thermique [157, 158]. Le concept provient du fait que l'énergie d'activation ($E_a$) de la désorption des composés en phase gazeuse est plus élevée que celle du bris des liens intermoléculaires si l'énergie est transférée est lente, ainsi la fragmentation sera favorisée à la vaporisation des molécules. Le concept est expliqué par la théorie d'Arrhenius sur la compétition cinétique entre la vaporisation et la fragmentation des molécules et schématisé à la **Figure 1-12**. Dans le cas de la LDTD, le transfert d'énergie est suffisamment rapide pour favoriser la vaporisation, avec une valeur de (1/T) plus basse que la valeur critique indiqué par la ligne verticale de la **Figure 1-12**. Ainsi les molécules seront désorbées en phase gazeuse sans subir de fragmentation.

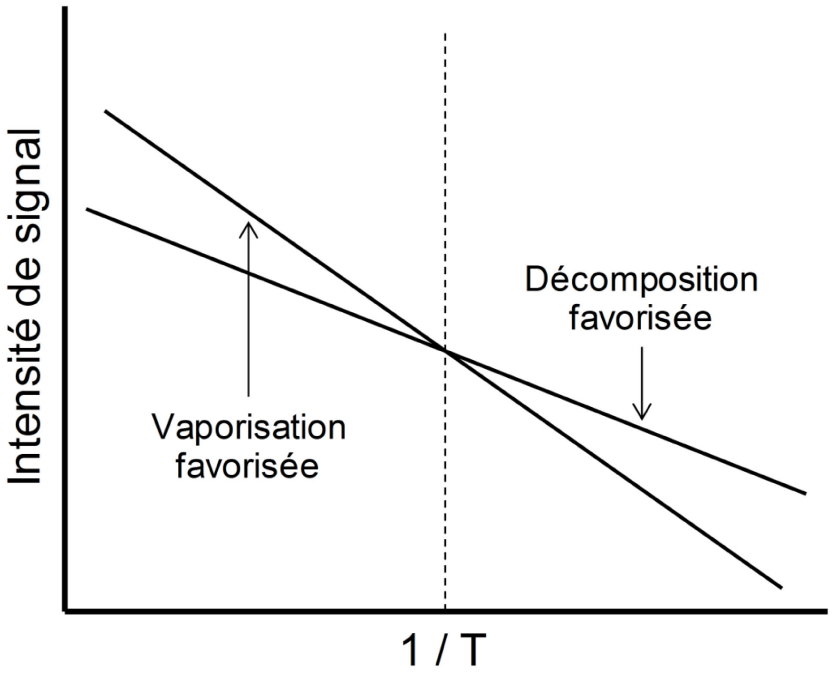


**Figure 1-12.** Représentation de la théorie d'Arrhenius sur la décomposition et vaporisation des composés en fonction de la température (adapté de Daves *et al.* [157]).

Plusieurs avantages sont reliés à l'utilisation de la LDTD comme système d'introduction d'échantillons en MS. Elle permet tout d'abord d'effectuer des analyses ultra-rapides allant en dessous de 15 secondes par échantillon. De plus, l'utilisation des plaques LDTD à 96 puits permettent des analyses à hauts débits. De faibles volumes d'échantillons sont nécessaires si ceux-ci sont analysés directement et l'utilisation de solvants est grandement diminuée. Globalement, la LDTD permet donc des analyses simplifiées tout en possédant une robustesse analytique semblable aux méthodes chromatographiques. Malgré ses avantages reliés à la vitesse d'analyse, la LDTD possède plusieurs inconvénients reliés à l'absence de séparation des composés. En effet, l'analyse de composés isobares, tel des isomères de conformation dont leur masse est impossible à différencier par MS, peut être difficile par LDTD étant donné que des faux positifs s'ajouteraient aux résultats. Une deuxième séparation permise par la MS/MS peut généralement éliminer ces interférences, mais il existe quelques rares cas où les ions précurseurs et fragments peuvent être semblables. Une étude de Lemoine *et al*. [159] ont démontré l'utilisation de la puissance de désorption laser afin d'induire une

pseudo-séparation de composés problématiques. Dans ce cas-ci, le signal d'ANA-a a été séparé de la phénylalanine en favorisant la désorption d'un composé (ANA-a) au détriment de l'autre. Aussi, malgré que l'avantage principal de la LDTD provienne de l'analyse ultra-rapide avec peu de manipulations d'échantillon, il est possible que la matrice soit composée de molécules interférentes demandant ainsi des étapes de purifications supplémentaires des échantillons, comme la SPE. Finalement, les limites de détections obtenues par une analyse directe en LDTD sont comparables aux méthodes chromatographiques ou légèrement supérieures. Il est donc possible de faire un compromis entre le temps d'analyse et la sensibilité en utilisant la SPE comme méthode de préconcentration. Globalement, la LDTD a été appliquée à des matrices complexes telles des matrices biologiques, de sédiments, de lisier, et d'eau avec des limites de détections plus basses que 1 $\mu g\ L^{-1}$ pour des analyses directes, et jusqu'à quelques dizaines de ng $L^{-1}$ en utilisant une étape de préconcentration [155, 159-164]. Par contre, même en ajoutant une étape d'extraction pré-analyse, les temps d'analyses en LDTD reste tout de même très avantageux.

### 1.5.2 Ionisation chimique à pression atmosphérique (APCI)

L'APCI est une technique d'ionisation analogue à l'ESI, mais fonctionne à partir de réactions d'échanges de charges en phase gazeuse et à pression atmosphérique. Ce type d'ionisation est optimal pour des composés polaires possédant une masse moléculaire inférieure à 1500 Da [146]. Considérée comme une ionisation douce, les ions produits en APCI possèdent généralement qu'une charge simple (ex. $z = +1$ ou -1), mais contrairement à l'ESI, il est possible qu'une faible fragmentation survienne durant l'ionisation.

Les analytes en phase liquide, après une séparation chromatographique dans la majorité des cas, sont introduits dans un nébuliseur aidé par un jet d'air ou d'azote pour être converti en un fin aérosol. Les gouttelettes formées se retrouveront dans une chambre à haute température pour subir une désolvatation à l'aide d'un gaz chauffé autour de 120 °C [146]. Les molécules neutres se dirigeront ensuite dans la source, où une différence de potentiel positive ou négative de l'ordre du kV sera appliquée sur une aiguille à décharge corona, et produira des ions réactifs provenant des solvants évaporés et ceux-ci serviront de gaz ionisant. Ces ions enclencheront alors une série de réactions mettant en scène des transferts de charges jusqu'aux

molécules neutres présents dans la source [165]. Dans le mode positif, des ions primaires seront formés par la décharge de l'aiguille corona, soit $N_2^{\cdot+}$ et $O_2^{\cdot+}$ qui réagiront avec les solvants vaporisés pour former des ions secondaires, souvent des molécules d'eau (**Figure 1-12**) [165, 166]. Il s'en suivra un transferts de protons aux molécules d'intérêt produisant ainsi des ions $[M+H]^+$ où M est la molécule d'intérêt et H le proton. Normalement, le transfert de proton se fait en fonction de l'affinité protonique des composés [167]. Ainsi, en mode positif, l'affinité protonique doit être plus grande pour les analytes que pour les ions réactifs. Pour le mode négatif, des ions $O_2^{\cdot-}$ ou $CO_3^{\cdot-}$ par exemple, seront formés en s'appropriant les électrons présents autour de l'aiguille à décharge corona [168]. Ceux-ci arracheront un proton aux molécules de solvant environnantes, souvent des molécules d'eau. Finalement, ces molécules négatives gazeuses arracheront un proton aux molécules environnantes si celles-ci ont une affinité protonique plus faible et des ions $[M-H]^-$ seront formés.

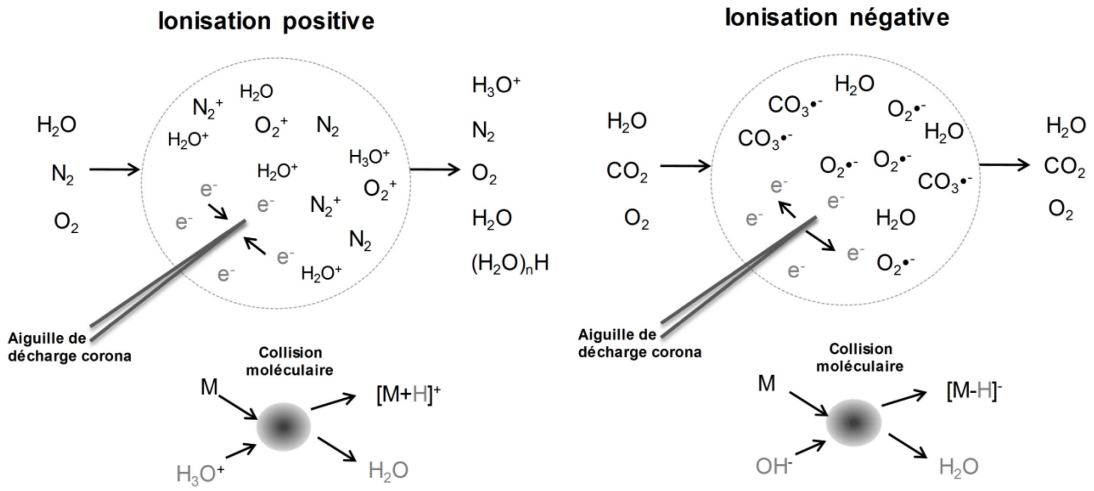


**Figure 1-13.** Mécanismes d'ionisation dans une source APCI en mode positif et négatif (adapté de Byrdwell *et al.* [165]).

Une différence entre l'APCI et l'ESI est le phénomène de suppression ionique lors de l'ionisation. En effet, cette forme d'effet de matrice est causée par la présence de molécules présentes dans un échantillon analysé qui interfèreront avec l'ionisation des composés étudiés, affectant la précision et la sensibilité d'une méthode d'analyse peu importe la force de la séparation chromatographique et du détecteur [169]. Une diminution ou augmentation de

signal peut alors être observée tout dépendamment des mécanismes d'ionisations. L'ionisation par ESI est surtout sensible aux molécules polaires et plusieurs facteurs peuvent influencer une suppression ionique [169, 170]. Tout d'abord, une compétition d'espace ou de charge causée par des quantités élevées de matière peut induire une suppression ionique et aussi peut créer une saturation de signal à concentrations élevées. De plus, une augmentation de la viscosité et de la tension de surface des gouttelettes formées peut diminuer la capacité du solvant à s'évaporer en plus de la présence de matériel non volatile pouvant réduire l'efficacité de la formation des gouttelettes.

Pour l'APCI, la suppression ionique est différente et moins importante qu'en ESI, étant reliée à des mécanismes différents de formation d'ions [171]. En effet, on ne retrouve pas de compétition ni de saturation de charge, mais plutôt une suppression causée par la composition de l'échantillon influençant le transfert de charge par la décharge de l'aiguille corona. De plus, la possibilité de former des solides par coprécipitation avec des composés non volatiles dans l'échantillon peut influencer l'ionisation [172]. Plusieurs stratégies sont utilisées pour réduire la suppression ionique, dont l'utilisation du mode négatif étant donné que moins de composés ionisent dans ce mode, la possibilité de diluer les échantillons sauf en niveau trace. Une préparation adéquate des échantillons avant l'analyse reste la meilleure manière de diminuer les effets de matrices et de surcroît, la suppression ionique.

Dans le cas de la désorption LDTD, les analytes arrivent en phase gazeuse dans la région d'ionisation et aucun solvant n'est disponible, car il n'y a aucune séparation chromatographique. Ce seront les ions hydroniums à différent niveaux de solvatation qui permettront le transfert de charge [173]. Le fait que peu de molécules provenant de la désorption en LDTD se retrouve à l'ionisation APCI permet de diminuer la compétition des transferts de charge provenant des aggrégats d'ions hydroniums et ainsi diminuer grandement les effets de suppression ionique [174]. Par contre, le fait que peu de molécules sont présentes pour les réactions d'ionisation, les réactions secondaires se font principalement par les molécules d'eaux présentes dans l'humidité de l'air et peuvent ainsi influencer le taux d'ionisation des molécules à analyser. Idéalement l'humidité de l'air dans la chambre d'ionisation doit contenir des traces d'eau inférieures à 3 ppm [146]. Beattie *et al.* [175] ont

étudiés la possibilité d'incorporer de la vapeur d'eau dans la chambre d'ionisation APCI afin d'améliorer l'efficacité de l'ionisation des molécules. L'idée a finalement été rejetée puisqu'aucune amélioration significative de l'ionisation n'a été observée.

### 1.5.3 Spectrométrie de masse à haute résolution

La MS est largement utilisée pour l'analyse des cyanotoxines et d'autres composés et ce dans des matrices complexes biologiques et environnementales. Le détecteur le plus utilisé est le triple quadripôle étant donné sa sensibilité, sa sélectivité et sa robustesse pour des analyses de routine. De nouvelles technologies sont apparues en MS s'appuyant sur la détection en masse à haute résolution (HRMS) et sont devenus de plus en plus accessibles depuis plus d'une dizaine d'années. Tout d'abord implantés comme analyseurs à des fins qualitatives dû à leur haut pouvoir de résolution permettant une grande précision à la masse exacte détectée, ces MS à haute résolution permettent de plus en plus des analyses quantitatives par l'implantation de systèmes hybrides.

La résolution est définie, en spectrométrie de masse, comme étant la séparation entre deux signaux en *m/z* possédant des masses voisines $m_1$ et $m_2$. Une bonne résolution signifie donc que ces deux signaux sont séparés à un maximum de 10 % de vallée. Le pouvoir de résolution est défini comme la capacité de l'analyseur à distinguer ces pics de masses voisines et est une valeur utilisée pour en comparer leur performance. Plus le pouvoir de résolution est élevé, plus l'analyseur sera capable de séparer les signaux de deux pics avec des valeurs en *m/z* rapprochées. Le pouvoir de résolution peut être calculé selon les deux méthodes présentées à la **Figure 1-14** où R désigne le pouvoir de résolution et m la plus petite valeur en *m/z* [176, 177]. Pour la première méthode, $\Delta m$ est la plus petite différence entre les deux pics de signaux résolus $m_1$ et $m_2$, en valeurs de *m/z* lorsque le chevauchement à la base est d'un maximum de 10 % de vallée. La deuxième méthode a pour dénominateur $m_{1/2}$ qui est la largeur du pic à la mi-hauteur. La deuxième définition sera utilisée dans les prochains chapitres en mentionnant le pouvoir de résolution à *full width half maximum* (FWHM).

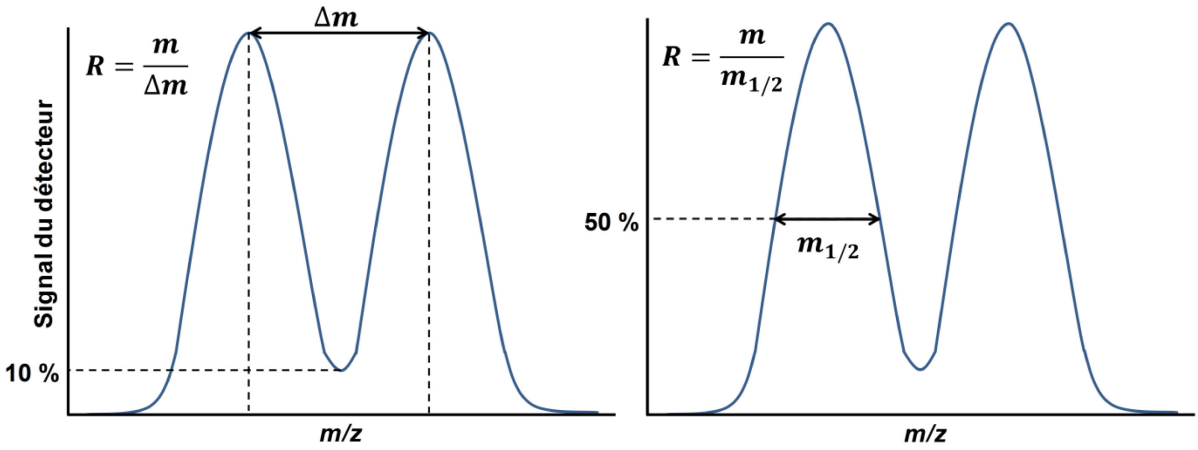


**Figure 1-14**. Deux méthodes pour la détermination du pouvoir de résolution en spectrométrie de masse à haute résolution; la deuxième est la méthode utilisée lors des chapitres suivants (adapté de Harris [176]).

Les valeurs en *m/z* mesurées par les spectromètres de masse à haute résolution permettent des mesures de masses exactes. Avec une grande précision sur la mesure, il est possible de déterminer l'écart des valeurs détectées avec leurs valeurs théorique mono-isotopiques. Cette erreur, exprimée en partie par million (ppm), est calculée en comparant la valeur en *m/z* théorique ($Masse_{th}$) du composé et la valeur expérimentale ($Masse_{exp}$) :

$$Erreur\ (ppm) = \frac{Masse_{th} - Masse_{exp}}{Masse_{exp}} \times 10^6 \text{ [177]}$$

L'utilisation de la HRMS réduit considérablement les interférences isobares, permettant ainsi la distinction de deux *m/z* très proches. Une tolérance de moins de 5 ppm est jugée acceptable et un étalonnage en masse doit être effectué régulièrement afin d'obtenir des analyses spécifiques avec des erreurs acceptables [178].

### 1.5.3.1 Analyseurs à haute résolution

L'utilisation des triples quadripôles en spectrométrie de masse est généralisée pour des analyses de routine et la situation s'applique aussi pour les cyanotoxines. Par contre, quelques utilisations récentes de la haute résolution pour l'étude des MC et d'ANA-a ont permis une identification plus sélective de ces toxines. Comme mentionné à la **Section 1.3.4.6**, le

MALDI-TOF a permis l'identification ciblée de certaines MC, sans permettre une quantification des composés. De plus, les voies de fragmentation d'ANA-a ont été élucidés par l'utilisation de MS hybrides tel le QqTOF (*Triple quadrupole/Time of flight MS*), le QIT-MS (*Quadrupole/Ion trap MS*) ainsi que la trappe ionique standard [143, 179]. En plus d'élucidation structurelle des fragments d'ANA-a, le pouvoir de résolution des MS précédents ont aussi permis de dissocier le signal de la toxine de son interférent isobare, la phénylalanine.

Le principe de la spectrométrie de masse à temps d'envol, ou TOF, permet une séparation des ions en fonction de leur vitesse lorsqu'ils sont propulsés en paquets, par une extraction ionique retardée à la source d'ionisation, dans un tube de vol soumis à un vide. Ces ions sont accélérés à l'aide d'une différence de potentiel appliqué à la source et l'énergie cinétique transmise aux ions étant la même, leur vitesse sera établie en fonction de leur masse, où les plus légers migrent plus rapidement. Le temps nécessaire à atteindre le détecteur sera ensuite traduit en valeur *m/z*. De manière générale, un réflectron est utilisé afin d'améliorer la résolution en diminuant $\Delta m$. Les ions, avec un excès d'énergie cinétique, sont ralentis, puis un effet miroir les renvois en direction opposée vers le tube de vol. Cette technique permet de focaliser les ions ayant la même énergie cinétique ou même valeur *m/z* améliorant ainsi la résolution, au dépend de la sensibilité et de la gamme de masse. La possibilité de former un analyseur MS hybride en couplant un quadripôle avec un analyseur TOF en incorporant un analyseur Q1 et une cellule de collision q2 ont permis d'améliorer à la fois la sensibilité et la sélectivité des analyses en plus de facilement être couplé à une séparation par HPLC [180]. De manière générale, le pouvoir de résolution des analyseurs TOF et QTOF peuvent aller jusqu'à 60 000 FWHM (*Full width at half maximum* – largeur à mi-hauteur) procurant ainsi une exactitude en masse plus faible que 5 ppm [180].

Les détecteurs à trappe d'ions fonctionnent en fragmentant directement les ions dans la trappe par impacts électroniques. Les ions sont piégés au moyen de radio-fréquences, puis fragmentés et ensuite les fragments sont expulsés de la trappe en fonction de leurs masses *m/z* croissant par un balayage de potentiel. Il est possible d'utiliser les trappes d'ions en HRMS en utilisant des expériences du type $MS^n$ qui permettent la fragmentation successive d'un même ion. De plus, il est possible de coupler les trappes d'ions avec un quadripôle linéaire, et ainsi

permettre une première sélection d'ions avant la fragmentation, au lieu de faire une fragmentation totale de tous les ions présents, ce qui améliore grandement la sensibilité [180]. Les analyseurs à trappe d'ions peuvent avoir des pouvoir de résolution allant jusqu'à 50 000 FWHM.

#### 1.5.3.2 Orbitrap

Un type de spectromètre de masse plus récent, breveté il y a 15 ans consiste en une trappe ionique orbitale aussi appelée Orbitrap$^{TM}$ [178]. La **Figure 1-15** schématise l'Orbitrap, et celle-ci est composée d'une électrode extérieure en forme de tonneau et une électrode interne en forme de fuseau. Une différence de potentiel est appliquée entre les deux électrodes à symétrie axiale et leur combinaison crée un potentiel exclusivement électrostatique. Ainsi, les ions stabilisés auront une trajectoire en orbite autour de l'électrode centrale ainsi que des oscillations dans la direction de l'angle z (**Figure 1-15**). Le potentiel dans l'angle z est quadratique, induisant un mouvement des ions tel un oscillateur harmonique, mais ce mouvement est indépendant la coordonnée cylindrique en r. En fait, la fréquence et l'amplitude d'oscillation sont dépendantes du rapport en *m/z* uniquement permettant ainsi des hauts pouvoirs de résolution et une excellente exactitude en masse. Le mouvement des ions d'une moitié de l'électrode externe à l'autre en fonction de l'axe r induira un courant opposé à ces moitiés et ce signal sera détecté par amplification différentielle. L'Orbitrap est peu sensible aux effets de charge dans l'espace en raison des mouvements de rotation autour de l'électrode centrale permettant ainsi leur dispersion [146]. De ce fait, cette trappe possède donc une grande capacité d'emmagasinage d'ions. Les pouvoirs de résolution de l'Orbitrap peuvent aller jusqu'à 600 000 FWHM à 195 *m/z* et une large plage dynamique en *m/z* peut être prise en charge pour leur analyse. De plus, l'exactitude en masse obtenue se retrouve en général près de 1 ppm [178, 180].

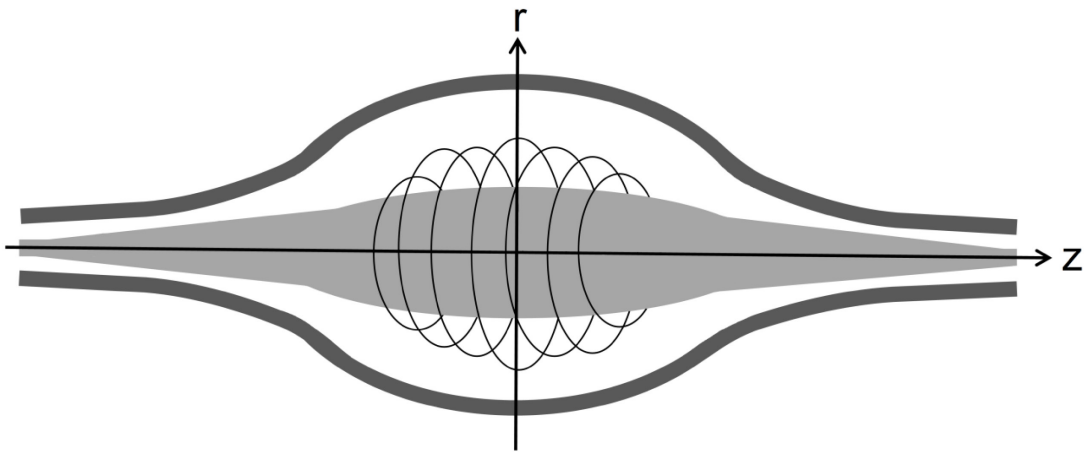


**Figure 1-15.** Schématisation de l'Orbitrap.

La majorité des applications analytiques de l'Orbitrap se font en fonction de son pouvoir de résolution et sa large plage dynamique en *m/z* analysable. Ainsi, on l'utilisera principalement de manière qualitative dans les domaines de la protéomique et de la métabolomique, et généralement l'analyseur est couplé à un système HPLC et une ionisation par ESI [181, 182]. En utilisant un Orbitrap uniquement, seul des analyses en balayage complet des ions sont possibles sans présélection ni fragmentation. Plus récemment, afin d'étendre l'utilisation de cet analyseur en HRMS, la création de divers hybrides incorporant une sélection d'ions à l'aide de quadripôles et l'utilisation de cellules de collisions afin de former des fragments spécifiques ont permis d'étendre les utilisations de l'Orbitrap dans le domaine analytique.

#### 1.5.3.3 Q-Exactive

Un spectromètre de masse, le Q-Exactive, a été présenté par la compagnie Thermo Scientific™ comme étant un hybride formé d'un quadripôle, d'une cellule de collision et d'un Orbitrap comme analyseur. En plus de ses possibilités d'identification grâce à l'Orbitrap, l'appareil permet aussi des analyses quantitatives dans plusieurs domaines, incluant l'analyse environnementale, biologique et médicolégale [183-189]. Le Q-Exactive possède donc des capacités analytiques semblables à un triple quadripôle en plus de permettre une détection à

haute résolution, mais en isolant les ions dans une trappe tandis que les analyses en triple quadripôle se déroulent en continu.

Les détails du Q-Exactive sont schématisés à la **Figure 1-16** modifiée de Michalski *et al.* [187]. Suite à l'étape d'ionisation, les ions sont injectés dans le MS par effet de vide et se déplacent au travers d'un système *S-lens* composé d'une série d'électrodes annulaires planes et génèrant un champ électrique permettant de focaliser les ions en faisceau. Le *S-lens* permet d'augmenter la transmission des ions dans le système et ainsi augmenter la sensibilité de l'analyse en plus d'augmenter le nombre d'acquisitions, car le maximum d'ions à injecter est atteint plus rapidement. Contrairement au *tube lens* utilisé dans les analyseurs MS précédents qui génèrent un champ électrique en gradient, celui du *S-lens* est gardé constant, ce qui facilite son utilisation, car aucune optimisation n'est nécessaire. Ensuite, ces ions sont dirigés vers un quadripôle à haute performance qui permet de présélectionner des composés désirés et ceux-ci seront alors transportés à une cellule *C-Trap*. Cette trappe permet de ralentir les ions et les accumuler pour les injecter dans l'Orbitrap, soit directement, ou après une étape de fragmentation. La *C-Trap* peut accumuler les ions successivement lors de leur sortie du quadripôle permettant une analyse en multiplexage, jusqu'à 10 composés par acquisition, et ainsi améliorer la sensibilité de l'analyse. Les ions peuvent aussi se diriger vers la cellule de collision nommée HCD (*Higher-energy collisional dissociation*) composée d'un multipôle et se diriger à nouveau dans la *C-Trap* afin d'être injectés dans l'Orbitrap.

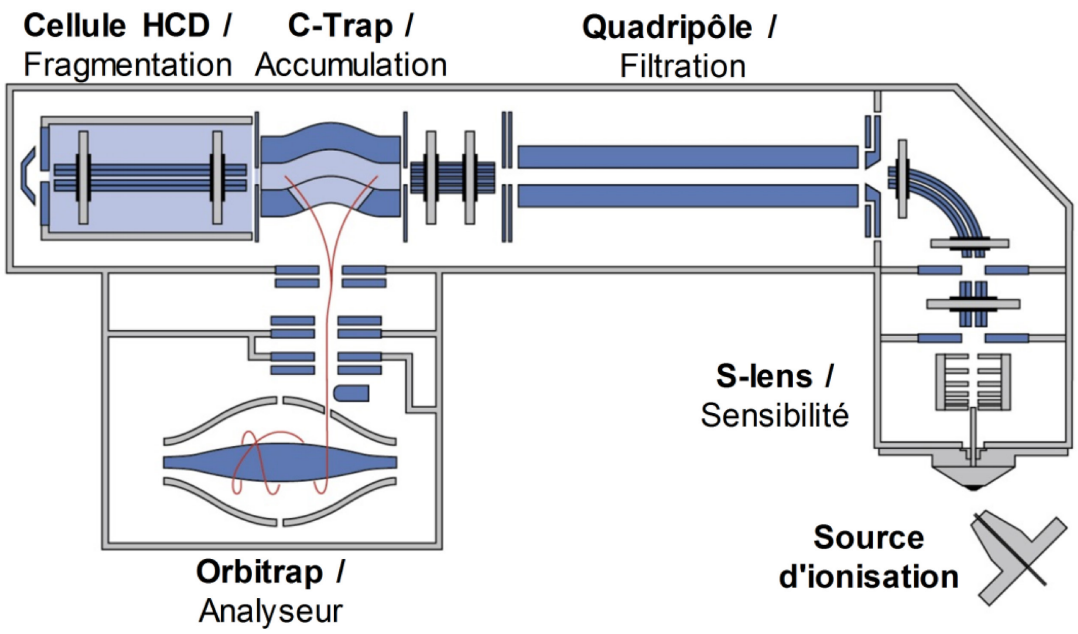


**Figure 1-16.** Schématisation du Q-Exactive (adapté de Michalski *et al.* [187]).

Le pouvoir de résolution de ce détecteur peut être réglé entre 17 500 et 140 000 FWHM à 200 *m/z* dépendamment de l'exactitude en masse désirée. En général, cette valeur se retrouve entre 1 et 3 ppm, mais peut facilement être plus faible que 1 ppm. Dans le cas où l'erreur sur la masse est trop importante, il est possible d'utiliser un correcteur en masse nommé *lock mass*. Ce composé doit être stable et se retrouver dans le signal de fond de manière constante lors des analyses. En ajoutant la masse exacte de ce composé dans la méthode d'analyse, la différence entre cette valeur et la masse expérimentale servira à la correction pour les autres masses analysées. Il est possible d'utiliser une molécule volatile présente dans l'atmosphère, une molécule de plastifiant présente dans le système ou un composé choisi ajouté lors des analyses. Une multitude d'expériences peuvent être sélectionnées tout dépendamment des besoins analytiques grâce à la présence de la présélection par quadripôle et la fragmentation dans la cellule HCD du Q-Exactive. Tout d'abord, le mode FS peut être utilisé pour effectuer une analyse dans une plage large en masse. Contrairement à un Orbitrap simple où toutes les masses atteignent directement au détecteur, une sélection de la gamme de masse choisie pour l'analyse, allant de 50 à 6000 *m/z*, devra se faire au niveau du quadripôle. Ce mode permet entre autre la détection simultanée d'une multitude de composés par analyse, et c'est le cas de Wang *et al.* [183] qui ont développé une

méthode de détection pour 451 résidus de pesticides sur des fruits et légumes. Ensuite, il est possible d'utiliser le mode de fragmentation totale de tous les ions (AIF ou *all ion fragmentation*) où les ions en FS vont être fragmentés ensemble et un spectre total de tous les fragments sera présenté. Ensuite, un mode SIM est utilisé en sélectionnant les masses à l'étude au niveau du quadripôle. Ce mode d'analyse devient plus intéressant en l'utilisant avec un multiplexage au niveau de la *C-Trap*, emmagasinant ainsi jusqu'à 10 composés à la fois choisis par le mode SIM améliorant ainsi la sensibilité des analyses. Finalement, il est possible d'effectuer une expérience comparable à la MS/MS, utilisant le mode de fragmentation t-$MS^2$ (*targeted ion fragmentation*). La procédure consiste à sélectionner les ions au niveau du quadripôle, et ceux-ci seront fragmentés dans la cellule HCD pour être finalement détectés par l'Orbitrap. Cette expérience permet d'obtenir des analyses spécifiques quantitatives de composés ciblés, et aussi d'obtenir le patron de fragmentation complet d'un composé. Fedorova *et al.* [185] ont étudié l'utilisation de ce mode d'analyse sur la Q-Exactive et leur méthode permet la détection de 36 composés dans des eaux naturelles avec des performances parfois meilleures que le mode en FS. Finalement, le Q-Exactive devient de plus en plus un outil intéressant pour la détection et la quantification de petites et grosses molécules dans des matrices complexes, grâce à sa grande sélectivité et sa versatilité en plus de sa facilité d'utilisation.

## 1.6 Structure de la thèse

Les chapitres de la thèse sont organisés en fonction de la nouveauté et de l'originalité du développement analytique des cyanotoxines dans les matrices d'eau et de poisson.

Le **Chapitre 2**, article soumis dans *Toxicon* vise à améliorer l'analyse des MC par UHPLC-HESI-MS/MS dans l'eau en utilisant six étalons différents et en ajoutant les cyanotoxines alcaloïdes ANA-a et CYN. Le couplage de la SPE en ligne avec la méthode analytique augmente la rapidité des analyses et la sensibilité. Une séparation chromatographique utilisant l'ACN comme solvant en premier temps permet la séparation de CYN, d'ANA-a et de son interférence isobare, la phénylalanine et du MeOH par la suite permet la séparation des MC.

Le **Chapitre 3**, article soumis dans *Analytical Bioanalytical Chemistry*, démontre l'utilisation d'une dérivatisation par chlorure de dansyle pour l'analyse de la neurotoxine BMAA, ainsi que ses isomères de conformation DAB et AEG et finalement ANA-a, CYN et STX. L'analyse, dans les eaux de lac, se fait par UHPLC-HESI-HRMS afin d'offrir une analyse plus sélective des composés en plus de proposer les structures des fragments des composés dérivatisés.

Le **Chapitre 4**, article publié dans *Analytica Chimica Acta*, présente une nouvelle méthode d'analyse rapide utilisant la LDTD-APCI-MS/MS des MC totales dans les eaux de lac. Les microcystines subissent une oxydation pour libérer la partie MMPB commune à toutes les microcystines. Une présentation de l'optimisation de l'oxydation et des paramètres analytiques est décrite.

Le **Chapitre 5**, article publié dans *Talanta*, explore le couplage de la LDTD-APCI à un spectromètre de masse à haute résolution, le Q-Exactive, pour l'analyse d'ANA-a dans les eaux de lac. Une analyse ultra-rapide sans étapes de préconcentration est présentée ainsi que l'élimination de l'interférence isobare d'ANA-a, la phénylalanine, grâce au pouvoir de résolution de la Q-Exactive.

Le **Chapitre 6**, article publié dans *Agricultural and Food Chemistry*, présente une nouvelle méthode d'analyse des MC totales dans la chair de poisson utilisant une digestion par hydroxide de sodium, une oxidation pour libérer la partie MMPB commune à toute les MC et une analyse par LDTD-APCI-HRMS afin d'améliorer la sélectivité et la sensibilité.

Le **Chapitre 7** présente une conclusion générale de la thèse et met en perspective les résultats obtenus et le travail à suivre pour des projets futurs.

# Chapitre 2. Méthode automatisée de pré-concentration couplée à la chromatographie liquide avec la spectrométrie de masse en tandem pour l'analyse de cyanotoxines dans les eaux d'efflorescences de cyanobactéries

Une version de ce chapitre se trouve dans l'article intitulé :

On-line solid-phase extraction coupled to liquid chromatography tandem mass spectrometry for the analysis of cyanotoxins in algal blooms

Paul B. Fayad, Audrey Roy-Lachapelle, Sung Vo Duy, Michèle Prévost et Sébastien Sauvé, *Toxicon*, 2015. Soumis pour publication.

**Note sur ma contribution**

Ma participation aux travaux de recherche: J'ai réalisé les manipulations pour la validation de la méthode et une partie de l'interprétation des résultats dans ce projet qui était démarré avant le début de mon doctorat.

Rédaction : J'ai rédigé une partie de l'article en m'appuyant sur les commentaires du Prof. Sauvé, mon directeur de thèse.

Collaboration des co-auteurs: Paul B. Fayad a réalisé le développement de la méthode analytique avec l'appui financier du Prof. Michèle Prévost, sa codirectrice de recherche, et a rédigé une partie de l'article. Sung Vo Duy a contribué au développement de la méthode.

# Abstract

An analytical method based on on-line SPE-LC-HESI-MS/MS has been developed for the detection and quantification of eight selected cyanotoxins in algal bloom waters that include mycrocystins, anatoxin-a and cylindrospermopsin. The injection volume was 2 mL according to the expected concentration of cyanotoxins in matrix. The method provides an analysis time of 7 min per sample, acceptable recovery values (91-101%), good precision (RSD < 13%) and method limits of detection at the sub-microgram per liter levels (0.01-0.02 $\mu g\ L^{-1}$). A detailed discussion on optimization parameters that have an impact on the overall performance of the method are presented. In particular, method optimization permitted the chromatographic separation of anatoxin-a and phenylalanine, an isobaric interference with a similar chromatographic characteristics. All optimization and validation experiments for the on-line SPE method and chromatographic separation were performed in environmentally relevant algal bloom water matrices. The applicability of the method was tested on several algal bloom water samples from monitored lakes across the province of Québec (Québec, Canada) known to produce cyanotoxins. All of the targeted cyanotoxins were detected with the exception of cylindrospermopsin. In addition, it was found that total microcystin concentrations in several surface water samples exceeded the proposed guidelines established by the province of Québec in Canada of 1.5 $\mu g\ L^{-1}$ as well as the World Health Organization of 1 $\mu g\ L^{-1}$ for both free and cell-bound microcystin-LR equivalent.

## 2.1 Introduction

Cyanobacteria, also known as blue green algae, are of a major concern worldwide due to their capacity to produce toxic cyanobacterial blooms in eutrophic water [190]. Many different toxins are produced with different structures and harmful proprieties resulting in three major families; hepatotoxins, neurotoxins and cytotoxins [191].

Microcystins (MCs) are the most well-known cyanotoxins and they are widely distributed in water sources, marine animal tissues and sediments [84, 192, 193]. Their structure consists of a cyclic heptapeptide with two uncommon amino acids resulting in over 100 conjugates known to date [32, 194]. Their hepatotoxicity ultimately results in liver failure caused by the inhibition of two specific protein phosphatases [12]. The $LD_{50}$ values of MCs range from 45 to 1000 μg $kg^{-1}$ body weight for mice and considering their toxicity, the World Health Organization (WHO) proposed a guideline of 1 μg $L^{-1}$ in drinking water for both free and cell-bound MC-LR [14, 85]. In the province of Québec in Canada, a guideline of 1.5 μg $L^{-1}$ is used expressed as MC-LR equivalent in drinking water [195].

Anatoxin-a (ANA-a) is an alkaloid neurotoxin with a wide distribution in water sources due to the large number of cyanobacteria responsible for its production [10, 47]. If ingested at high doses, continuous stimulation of the respiratory muscles may occur causing immediate asphyxiation. With a high toxicity, an $LD_{50}$ of 200-250 μg $kg^{-1}$ body weight for mice, many documented animal mortalities have been attributed to ANA-a [51, 196, 197]. The WHO has not established guideline for the risk management of ANA-a in drinking water, but several jurisdictions have implemented such guidelines: Québec, Canada (3.7 μg $L^{-1}$) and New Zealand (6 μg $L^{-1}$) and three U.S. states; California, Oregon and Washington (1 μg $L^{-1}$) [6, 195].

Cylindrospermopsin (CYN) is also an alkaloid compound that shows cytotoxic, neurotoxic and hepatotoxic effects [24]. The first cyanobacterial species known to be a CYN producer is the *Cylindrospermopsis raciborskii*, which was originally found in tropical and subtropical climates and reports of occurrence have been made in Australia, New Zealand, Brazil, Japan and Israel. However, the presence of CYN has also been reported more recently

in Europe and North America where the climate is more temperate [62]. Its toxicity results from it being a tumor promoter as well as being suspected to be carcinogen. It affects principally the lungs, the liver, the kidneys, the heart and the intestines by inhibiting protein synthesis [15]. The $LD_{50}$ values range from 200 to 2100 μg $kg^{-1}$ body weight for mice and based on its toxicity, a guideline value was proposed by Humpage and Falconer (2003) at 1 μg $L^{-1}$ in drinking water [15].

Many analytical methods have been developed and used for these three toxins. Due to their different structures, their determination is often made separately. The most commonly used technique for total MCs is enzyme-linked immunosorbent assays (ELISA) due to its low cost, quickness and sensitivity [91, 135, 136]. However, ELISA has quantitative limits and sometimes, results have to be supported by an additional accurate analysis [198, 199]. As for ANA-a and CYN, only a limited number of bioassay methods have been developed and routinely used [53, 62, 200]. To date, the preferred technique for the identification and quantification of cyanotoxins is high-performance liquid chromatography (HPLC) coupled with tandem mass spectrometry (MS/MS). This is considered the detection method of choice for cyanotoxin identification in complex matrices [53]. Considering the complexity of environmental water samples, solid phase extraction (SPE) is generally used before the analysis for pre-concentration and cleanup. The off-line SPE method sample enrichment process uses 100 to 2000 mL of samples to reach the low-nanogram per liter levels of detection. The major issue with this technique is the time consuming and often laborious steps required for each sample. On-line SPE integrates into an automated procedure all the steps (conditioning, sample enrichment, wash and elution) involved in the traditional off-line method. This on-line SPE approach is quicker, allows for reduced sample size, handling and preparation, improved reproducibility, higher sample throughput as well as less waste and solvent consumption. On-line SPE coupled with HPLC previously allowed simultaneous analysis of multiple cyanotoxins including MCs, ANA-a and CYN with a total analysis time of 70 min per sample with low method detection limits (2–100 ng $L^{-1}$) [201]. Furthermore, ultra-high performance liquid chromatography (UHPLC) can shorten the analysis time per sample considerably, up to less than 15 minutes per sample for environmental matrices [202-204]. UHPLC-MS/MS has been investigated and demonstrated to be a powerful tool for the

quantification of MCs, ANA-a and CYN [122]. Also, the coupling of on-line SPE with UHPLC was developed for the quantification of six different MCs with low method detection limits (2–40 ng $L^{-1}$) [121], but did not include CYN, ANA-a or the isobaric interference from phenylalanine (PHE). Indeed, PHE, an essential amino acid naturally present in natural waters, is an isobaric interference of ANA-a and they cannot be resolved by relying on the selectivity of a triple-quadrupole mass spectrometer [143]. In addition, given their similar molecular masses, identical fragmentation products as well as their comparable liquid chromatography (LC) retention times, it can potentially lead to the misidentification or overestimation of ANA-a. Different LC strategies have been proposed to achieve sufficient separation of ANA-a and PHE, but further work is needed since the required analyses are usually long and costly [47, 143].

This paper presents the application of an optimized rapid chromatographic method using on-line SPE-UHPLC-MS/MS for the determination of different cyanotoxins in water bloom samples, i.e. six MCs (-RR, -YR, -LR, -LY, -LW and -LF), ANA-a (while considering the possible interference of PHE) and CYN. The method validation was done using the hepatotoxin nodularin (NOD) as an internal standard as proposed in reported MCs analytical methods [122, 205, 206]. The method validation includes the search for an adequate filter used for sample treatment, optimisation of the on-line SPE parameters and development of an efficient chromatographic separation coupled with SPE for fast analysis with higher recovery. The proposed chromatographic gradient uses two different solvents: acetonitrile for the separation of CYN, ANA-a and PHE, and methanol for the separation of six MCs. This type of separation enhanced the chromatographic performance and also allowed a complete separation of ANA-a from its isobaric interference, the naturally encountered amino acid, PHE. The determination a few nanograms to high micrograms per liter levels in several algal bloom water samples showed the reliability and versatility of the method in a wide linearity range for complex environmental water samples.

## 2.2 Experimental

### 2.2.1 Chemicals, reagents and stock solutions

All selected standards (99%) for microcystins (MCs-RR, -YR, -LR, -LY, -LW and -LF), anatoxin-a (ANA-a) and cylindrospermopsin (CYN) were purchased form Abcam Biochemicals (Cambridge, MA, USA). DL-Phenylalanine standard (99%) and nodularin (99%), were obtained from Sigma-Aldrich Chemical Co. (Oakville, ON, Canada). Individual stock solutions were prepared in methanol (MeOH) at a concentration of 1000 mg $L^{-1}$ and kept at -20ºC for a maximum of six months. A primary mix of cyanotoxin working solution was prepared weekly at a concentration of 12.5 mg $L^{-1}$ by dilution in water of individual stock solution aliquots. Subsequent working solutions were prepared daily in water to give solutions of desired concentration. All organic solvents and water used for dilutions were of HPLC grade purity from Fisher Scientific (Whitby, ON, Canada).

### 2.2.2 Instrumental conditions

The pre-concentration and analysis of the selected cyanotoxins in water samples was performed using the Equan$^{TM}$ (Thermo Fisher Scientific, Waltham, MA) system. It consists of a sample delivery system, a dual switching-column array and an LC-MS/MS system. An HTC Thermopal autosampler manufactured by CTC analytics AG (Zwingen, Switzeraland) was used for in-loop sample injection and an Accela 600 quaternary pump (Thermo Finnigan, San Jose, CA) was used to load the SPE column with the contents of the sample loop, as part of the delivery system. The column switching system was composed of a six-port valve and a ten-port valve,both with two positions (VICI® Valco Instruments Co. Inc., Houston, TX) and a second Accela 1200 quaternary pump used for sample elution from the SPE column and separation on the analytical column. The on-line SPE was achieved using a Hypersil Gold aQ with C18 column selectivity (20mm x 2mm, 12µm particle size) and chromatographic separation was done with a Hypersil Gold with C18 column selectivity (100mm x 2.1mm, 1.9µm particle size) kept at 55 $^{o}$C. All columns were manufactured by Thermo Fisher Scientific. Ionization of the selected eluting cyanotoxins was achieved using a heated electrospray ionization source (HESI-II) mounted on a Quantum Ultra AM triple quadrupole

mass spectrometer (Thermo Fisher Scientific) operated in selected reaction monitoring (SRM) mode for quantification and detection.

#### 2.2.2.1 On-line solid phase extraction and chromatographic conditions

In order to improve signal intensities and method detection limits (MDLs), we tested different loop injection volumes (1, 2, 5 and 10 mL) of a 500 ng $L^{-1}$ cyanotoxin solution mixture in HPLC water. This allowed us to establish that the maximum loading volume without loss of analyte was 2 mL. The sample transfer time (loading speed) from the injection loop to the SPE column was tested between 1.0 and 2.5 mL $min^{-1}$, for a concentration of cyanotoxins (500 ng $L^{-1}$) spiked in HPLC grade water in order to reduce total analysis time. The maximum sample loading flow rate from the sample loop (2 mL) to the SPE column was 2 mL $min^{-1}$. Following the sample loading step, the pre-concentration column were back-flushed and the eluting analytes were transferred using the analytical pump gradient directly through the analytical column using the solvents MeOH (A), water (B) and ACN (C), with the addition of 0.1% formic acid (FA), at a flow rate of 525 µL $min^{-1}$. The chromatographic run time (7 min) was divided into four time segments as described below.

The on-line SPE loading and elution gradients are detailed in **Tableau 2-1**. To eliminate carryover effects, the 5 mL syringe and the six-port sample loop injection valve were cleaned twice between each injection, during the chromatographic separation step. Cleaning was initially done with a strong mixture of solvents, i.e. acetonitrile:methanol:isopropanol (1:1:1, v/v/v), and then with HPLC grade water with 0.1% FA. The sampling step, the SPE column conditioning, loading and elution steps as well as the LC-MS/MS analysis are all automated. This configuration allowed for a short total analysis time, i.e. 7 min per sample, using a 2 mL injection loop.

**Tableau 2-1.** Valve program, on-line SPE (loading pump) and LC (analytical pump) gradient elution conditions used for the pre-concentration and separation of selected cyanotoxins. Solvents consist of: MeOH (A), water (B) and ACN (C) with the addition of 0.1% FA.

| Loading pump (to six port valve) | | | | | Analytical pump (to ten port valve) | | | | | |
|---|---|---|---|---|---|---|---|---|---|---|
| | Time (min) | A (%) | B (%) | Flow rate (µL min$^{-1}$) | Time (min) | A (%) | B (%) | C (%) | Flow rate (µL min$^{-1}$) | |
| On-line SPE loading step | 0.00 | 0 | 100 | 2 000 | 0.00 | 0 | 75 | 25 | 525 | Column re-equilibration |
| | 1.10 | 0 | 100 | 2 000 | 1.10 | 0 | 75 | 25 | 525 | |
| Loop wash | 1.12 | 100 | 0 | 2 000 | 1.35 | 0 | 45 | 55 | 525 | Elution and chromatographic separation |
| | 6.30 | 100 | 0 | 2 000 | 2.15 | 0 | 45 | 55 | 525 | |
| | | | | | 2.16 | 45 | 55 | 0 | 525 | |
| SPE column and loop conditionning | 6.31 | 0 | 100 | 2 000 | 3.95 | 45 | 55 | 0 | 525 | |
| | | | | | 5.51 | 95 | 5 | 0 | 525 | |
| | 7.00 | 0 | 100 | 2 000 | 5.66 | 0 | 75 | 25 | 525 | Column re-equilibration |
| | | | | | 7.00 | 0 | 75 | 25 | 525 | |

#### 2.2.2.2 Mass spectrometry

Ionization of the cyanotoxins was achieved with the HESI source in positive mode. The initial compound-dependent parameters (tube lens and collision energy) for MS and MS/MS optimization conditions were determined by direct infusion of the cyanotoxin standards and the IS at a concentration of 1 mg L$^{-1}$ with a mobile phase of 50:50 (v/v) MeOH (A) and water (B) with 0.1% FA and are presented in **Tableau 2-2**. The final HESI parameters used to maximize signal intensity were as follows: capillary temperature, 350 $^{o}$C; vaporizer temperature, 450 $^{o}$C; sheath gas pressure, 35 arbitrary units; aux gas pressure (10 arbitrary units), ion sweep gas pressure, 0 arbitrary units; and spray voltage, 3200 V. The scan time was adjusted to 0.02 s, giving a minimum of 15 points across a chromatographic peak, and the first and third quadrupoles (Q1 and Q3) were operated at unit resolution (0.7 Da FWHM), with the second quadrupole (q2) collision gas pressure set at 1.5 mTorr.

**Tableau 2-2.** Optimized MS/MS parameters for the analysis of selected cyanotoxin analytes in positive ionization mode with HESI including the tube lens (TL) and the collision energy (CE).

| Compounds | Precursor ion (*m/z*) | Product ion (*m/z*) | Intensity ratio (%) | TL (V) | CE (eV) |
|---|---|---|---|---|---|
| ANA-a / PHE | 166 | 149 | 100 | 86 | 11 |
| | $[M+H]^+$ | 120 | 22 ± 2 / 15 ± 3 | 86 | 13 |
| CYN | 416 | 194 | 100 | 151 | 31 |
| | $[M+H]^+$ | 176 | 29 ± 3 | 151 | 31 |
| MC-RR | 520 | 135 | 100 | 138 | 31 |
| | $[M+2H]^+$ | 103 | 15 ± 1 | 138 | 70 |
| MC-YR | 1045 | 135 | 100 | 183 | 58 |
| | $[M+H]^+$ | 213 | 75 ± 10 | 183 | 58 |
| MC-LR | 996 | 134 | 100 | 198 | 57 |
| | $[M-H]^+$ | 213 | 18 ± 2 | 198 | 39 |
| MC-LY | 1003 | 265 | 100 | 118 | 50 |
| | $[M+H]^+$ | 135 | 27 ± 3 | 118 | 37 |
| MC-LW | 1026 | 891 | 100 | 164 | 24 |
| | $[M-H]^+$ | 213 | 65 ± 8 | 164 | 43 |
| MC-LF | 987 | 213 | 100 | 150 | 34 |
| | $[M+H]^+$ | 375 | 71 ± 11 | 150 | 22 |
| NOD (IS) | 825 | 135 | 100 | 148 | 50 |
| | $[M+H]^+$ | | | | |

## 2.2.3 Data analysis and method validation

The positive identification of target analytes was confirmed by matching chromatographic retention times within ± 2% of those from standard spiked in analyte free matrix and using a minimum of two SRM transitions as well as the relative intensities of their ratios. The most abundant product ion was used for quantification whereas the second most abundant was used for confirmation. In accordance with the European Commission [25], the SRM ratios were acceptable if for relative intensities greater than 50%, the error was within ± 20% and within ± 50% for relative intensities inferior to 10%. Data acquisition was performed in SRM mode. Resulting MS/MS peaks were integrated using the ICIS algorithm of the Xcalibur 1.2 software from Thermo Fisher Scientific. Data processing was carried out with the ratio of the analyte area to that of the IS.

A filtration step was used prior to analysis to remove suspended cells from the samples. To evaluate the impact of filter material on the retention of the selected cyanotoxins in the initial filtration step before SPE, several types of filters were tested (all 0.22 µm with a 25 mm diameter except for grade 75 glass fiber at 0.3 µm with a 47 mm diameter), i.e. cellulose acetate (CA), mixed cellulose ester (MCE), nylon (NYL), polycarbonate (PC), polyvinylidene fluoride (PVDF) and glass fiber (GF), all obtained from Sterlitech (Sterlitech Corporation, Kent, WA). The selected cyanotoxins were spiked at two concentration levels (10 and 50 µg $L^{-1}$) in HPLC grade water prior to filtration. The resulting filtrate aliquots, were analyzed (n=3 at 10 and 50 µg $L^{-1}$) and their mean peak areas were compared to those of the non-filtered solutions of equal concentration to determine recovery values. Recovery values were reported as percentages.

The matrix effects for the on-line SPE method were evaluated at two concentration level, 10 and 50 µg $L^{-1}$, spiked into HPLC water and analyte-free bloom water, different from the samples used for method validation and containing cyanobacteria without the presence of cyanotoxins, confirmed and validated by the Centre d'Expertise en Analyse Environnementale du Québec (CEAEQ, Québec, Qc, Canada). The cells count in the analyte-free bloom water samples was approximately of 5 000 000 cells $mL^{-1}$ for an approximate cells biovolume of 500 $mm^3$ $L^{-1}$ for a relevant matrix effect compared to analyzed cyanobacterial bloom samples. Extraction recoveries were determined by comparing the mean peak areas (n=3) of the selected cyanotoxins from a direct chromatographic injection without SPE (25 µL at 40 and 400 µg $L^{-1}$) with those of the on-line high volume injection (2 mL at 0.5 and 5 µg $L^{-1}$) used for the standard sample analysis. The same mass of analyte was injected in each case. Matrix effects were calculated by comparing peak areas of spiked affluent wastewater to the peak areas found in HPLC water according to a 2 mL injection volume. Recoveries and matrix effect values were reported as percentages.

The method validation was done according to the recommendation of validation protocol for environmental chemistry analysis from the province of Québec's Ministry of the Environment guidelines (*Ministère du Développement Durable, de l'Environnement, et de lutte aux changements climatiques*, MDDELCC) [207]. Two product ions, with the highest

signal intensity, were selected as quantification and confirmation fragment ions (**Tableau 2-2**) and the relative intensities of their ratios were used for confirmation of the targeted compounds and to avoid false positives. The quantification ion, with higher signal intensity, was used to establish the limits of detection and quantification. Method detection limits (MDLs) and method quantification limit (MQLs) were established by calculating 3 and 10 times, respectively, the standard deviation of the mean calculated concentration value of 6 spiked blank matrix samples (n=6) containing approximately 5 times the estimated concentration for detection limit (0.1 µg $L^{-1}$). Accuracy, interday/intraday variations, and matrix effects were determined with three different concentrations on the linearity range (0.1, 1 and 10 µg $L^{-1}$, n=6) in blank relevant matrix. Accuracy values were determined by the relative error (%) and precision values were defined as the relative standard deviation (%). For the calibration curve, the back-calculated concentrations of calibrant standards were acceptable if within 15% of the nominal value, except for the determined MDLs for which a 20% error was deemed satisfactory.

The Statistical Package for Social Science (SPSS 21.0, Chicago, IL) software was used to realize ANOVA tests to compare the optimization parameters of the method and we also performed Tukey's b post hoc tests. Statistical significance was reported for *P* value of $< 0.05$.

### 2.2.4 Sample collection, preparation and quantification

Environmental scum and water samples were provided by the monitoring program at MDDELCC (Québec, Canada). All targeted lakes were chosen for their high occurrence of cyanobacterial blooms in different regions from the province of Québec, Canada. Cell counts were carried out for all samples, including potential toxic genera and other genera of cyanobacteria in order to manage risks using established limits proposed by the WHO, which begin with 50 000 cells $mL^{-1}$ to consider a potential toxicity and 100 000 cells $mL^{-1}$ to consider a cyanobacterial to pose a risk caused by toxin producing species [6]. **Tableau 2S-1** in supplementary material shows the cell count for the most abundant cyanobacteria species encountered in the different samples. The taxonomic composition of the environmental samples shows very high densities of various toxin producing species often dominated by two or more species. Afterwards, the counts were converted to biovolume estimates according to

the CEAEQ protocol, using standard cell sizes of each species calculated as a function of their shape and dimensions expressed as $mm^3$ $L^{-1}$ in samples [208]. **Tableau 2-4** lists the total cell counts as well as corresponding biovolume and confirms that the environmental matrices tested can be considered representative of extreme amounts of algal organic matter. The samples were acidified for preservation (0.1% FA, pH~2) and then submitted to a freeze-thaw lysis three times to break the cells walls and leach the toxins, followed by filtration through a 0.22 µm pore size nylon filter (Sterlitech Corporation, Kent, WA) to eliminate particulate material (i.e. remaining cyanobacterial cells and organic matter) before storage at 4ºC. No prior treatment of sample matrix was necessary before applying the on-line SPE procedure.

In order to correct for matrix effects, the selected cyanotoxins were quantified using a nine point internal calibration curve, with each calibration point injected twice and the unknowns analyzed in triplicate (n=3). A least-square linear regression model was applied, with coefficients of determination ($R^2$) required to be greater than 0.9950 for all analytes, with IS added to all calibration levels, blanks and unknowns prior to analysis.

## 2.3 Results and discussion

### 2.3.1. Filtration conditions

Although sometimes overlooked, the filtration step involved prior to sample pre-treatment for analysis can have an impact on adsorption and loss of analytes due to undesirable interactions between the filter material and the analytes of interest. This has been discussed previously in the analysis of steroid hormones in water matrices [204] and should be investigated when filtration is applied in the analysis of cyanotoxins (or any trace contaminant). Several filter materials have been used to isolate the unbound water-soluble fraction of cyanotoxins from the particulate phase in water analysis, such as glass fiber [209-211], nylon [121], cellulose [212] or PVDF [112].

The impact of filter material on the retention of the cyanotoxins in the initial filtration step was tested on several filter types in spiked HPLC grade water at two concentration levels (10 and 50 µg $L^{-1}$). The results for the samples spiked at 10 µg $L^{-1}$ are presented in **Figure 2-1**.

At both spiked levels, more consistent recovery values for the selected cyanotoxins were obtained when using the NYL filter (n=3). Mean recovery values ranged from 90 to 101% when NYL was used (with SD < 9% in all cases). This made NYL the most reliable filter material for the elimination of suspended material while minimizing losses of dissolved analyte due to sorption onto the filter. The nature of the sorption and interaction mechanisms involved between the cyanotoxins and the selected filter material can be complex and are not completely understood. These mechanisms include hydrophobic interactions, hydrogen bonding and π–π stacking, all of which are dependent on the nature of the analytes and the physicochemical characteristics of the filter material. The emphasis of this study was to evaluate the impact of filter material on the retention of the cyanotoxins prior to chromatographic quantification, and a more detailed discussion on the different sorption mechanisms between analytes and filter material can be found elsewhere [213].

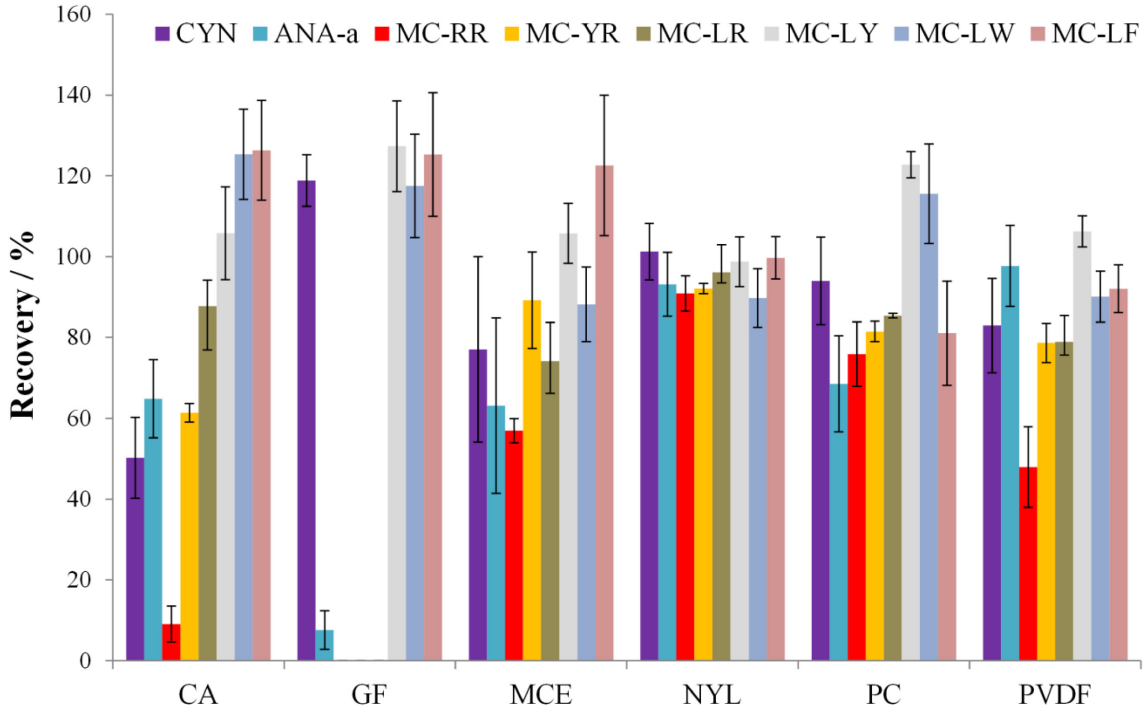


**Figure 2-1.** Comparison of recovery values (mean ± SD, n=3) on different filter materials, cellulose acetate (CA), glass fiber (GF), mixed cellulose ester (MCE), nylon (NYL), polycarbonate (PC) and polyvinylidene fluoride (PVDF), for cyanotoxins. Tests were done in spiked (10 µg $L^{-1}$) analyte-free HPLC grade water. The nylon filter gave more constant recovery values for all cyanotoxins. The same results were observed at 50 µg $L^{-1}$ (results not shown).

## 2.3.2 Optimization of the on-line SPE procedure

### 2.3.2.1 SPE loading speed and breakthrough volume

The time limiting factor in on-line SPE is the sample transfer time from the injection loop to the SPE column in the sample enrichment step. The faster the loading speed from the injection loop to the SPE column, the less time is spent on each sample, increasing sample throughput. This parameter must be optimized so as not to generate sample loss from diminished sample contact time with sorbent phase at higher loading flow rates or, inversely, increased retention behavior from the sorbent phase due to lower flow rates which

subsequently affects elution efficiency. Also, since the breakthrough volume could be a flow rate dependent step [214], the loading speed should be tested under the conditions used for sample analysis. The optimum loading speed values, in terms of both extraction efficiency and speed, was evaluated on a spiked cyanotoxin solution (n=3, 10 µg $L^{-1}$) in HPLC grade water, using a 2 mL injection sample loop. As shown in **Figure 2-2**, for the loading speeds of the selected cyanotoxins, there was no significant difference (n=3; $P < 0.05$) between 500 and 2500 µL $min^{-1}$ and these flow rates yield the highest analyte peak area responses. Therefore, a flow rate of 2000 µL $min^{-1}$ was selected in order to decrease sample loading time while not affecting analyte response for all analyzed compounds.

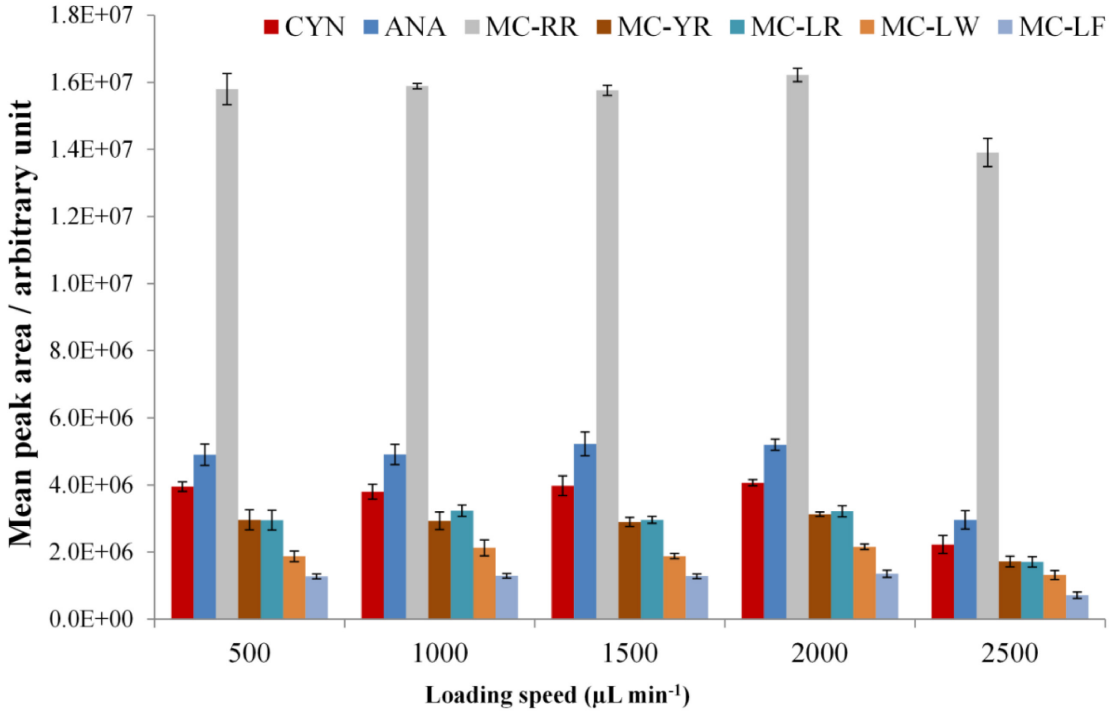


**Figure 2-2.** Effect of loading speed (500 to 2500 µL $min^{-1}$) for spiked cyanotoxins in HPLC grade water on peak areas (mean ± SD, n=3, 10 µg $L^{-1}$) between the sample loop (2 mL) and on-line SPE column. Significantly ($P < 0.05$, n=3 with RSD < 13 in all cases) smaller peak areas were observed at the highest loading speed (2500 µL $min^{-1}$).

The breakthrough volume is important in that it is directly related to the pre-concentration factor, thus influencing the MDLs and the MQLs both of which are related to signal-to-noise ratio (S/N), as well as sensitivity. The breakthrough volume for the selected

cyanotoxins was established by injecting a fixed volume (1 mL) of a sample (at constant concentration, n=3, 10 μg $L^{-1}$) in HPLC grade water, using different sizes of sample injection loops (from 1 to 10 mL). Considering peak areas, a maximum injection volume of 2 mL was chosen (results not shown).

#### 2.3.2.2 SPE matrix effect and recovery

The nature of the composition of the sample matrix can have a negative (ion suppression) or positive (ion enhancement) impact on analyte signal and will influence the reproducibility, linearity and accuracy of a method as well as possibly producing false positives. The matrix effects for the on-line SPE-LC-MS/MS method were evaluated at two concentration levels, 10 and 50 μg $L^{-1}$, in spiked HPLC grade water, in analyte-free wastewater (affluent and effluent, results not shown) and in analyte-free bloom water (containing cyanobacteria but without the presence of cyanotoxins). Matrix effects were calculated by comparing chromatographic peak areas of spiked algal bloom waters to the peak areas found in spiked HPLC water for a 2 mL injection volume. The results (**Tableau 2-3**) show that for all the analytes of interest there was signal suppression (ANA-a, CYN, MC-LR and MC-RR) as well as signal enhancement (MC-LF, MC-LW and MC-LY), with matrix effects varying from 62 to 124% for both concentrations (average values of the spiked concentrations at 10 and 50 μg $L^{-1}$). To compensate for these matrix effects, a single internal standard (NOD) was used for quantification and detection of the selected cyanotoxins in algal bloom water samples.

**Tableau 2-3.** Method validation results for linearity ($R^2$), method detection (MDLs) and quantification (MQLs) limits for cyanotoxins in water bloom matrix (cyanotoxin free). Recovery values, matrix effects, precision and accuracy (Bias %) have also been evaluated for the three spiked concentrations: 0.1, 1 and 10 µg $L^{-1}$.

| Cyanotoxins | $R^2$ | MDL (µg $L^{-1}$) | MQL (µg $L^{-1}$) | Recovery value (%) | Matrix effect (%) | Precision | | | | | | Bias (%) | | |
|---|---|---|---|---|---|---|---|---|---|---|---|---|---|---|
| | | | | | | Intraday (%) | | | Interday (%) | | | | | |
| | | | | | | 0.1 µg $L^{-1}$ | 1 µg $L^{-1}$ | 10 µg $L^{-1}$ | 0.1 µg $L^{-1}$ | 1 µg $L^{-1}$ | 10 µg $L^{-1}$ | 0.1 µg $L^{-1}$ | 1 µg $L^{-1}$ | 10 µg $L^{-1}$ |
| ANA-a | 0.9995 | 0.01 | 0.03 | 72 ± 3 | 92 | 4 | 6 | 5 | 13 | 11 | 9 | 9 | 8 | 9 |
| CYN | 0.9990 | 0.02 | 0.05 | 74 ± 5 | 62 | 8 | 9 | 4 | 12 | 13 | 11 | 11 | 12 | 8 |
| MC-RR | 0.9990 | 0.02 | 0.05 | 100 ± 9 | 97 | 7 | 7 | 3 | 9 | 7 | 8 | 9 | 6 | 5 |
| MC-YR | 0.9990 | 0.02 | 0.07 | 100 ± 9 | 112 | 7 | 5 | 4 | 10 | 10 | 8 | 8 | 8 | 5 |
| MC-LR | 0.9994 | 0.02 | 0.05 | 94 ± 5 | 92 | 6 | 8 | 3 | 11 | 8 | 9 | 7 | 8 | 6 |
| MC-LY | 0.9995 | 0.02 | 0.06 | 96 ± 1 | 113 | 6 | 5 | 7 | 13 | 8 | 6 | 7 | 7 | 5 |
| MC-LW | 0.9994 | 0.01 | 0.04 | 98 ± 10 | 102 | 5 | 9 | 3 | 8 | 8 | 6 | 9 | 8 | 9 |
| MC-LF | 0.9993 | 0.02 | 0.05 | 102 ± 6 | 124 | 6 | 7 | 3 | 12 | 11 | 9 | 8 | 6 | 7 |

Extraction recoveries have an impact on the MDLs and MQLs. They were evaluated with matrix-matched solutions using cyanotoxin free algal bloom water using the on-line SPE method. The recoveries ranged from 72 to 102% for the selected cyanotoxins. The more polar compounds, i.e. ANA-a and CYN, had less affinity with the reverse-phase SPE column which is also confirmed by the fact that they are the compounds that elute first from the cartridge and have the shortest retention times (**Figure 2-3**).

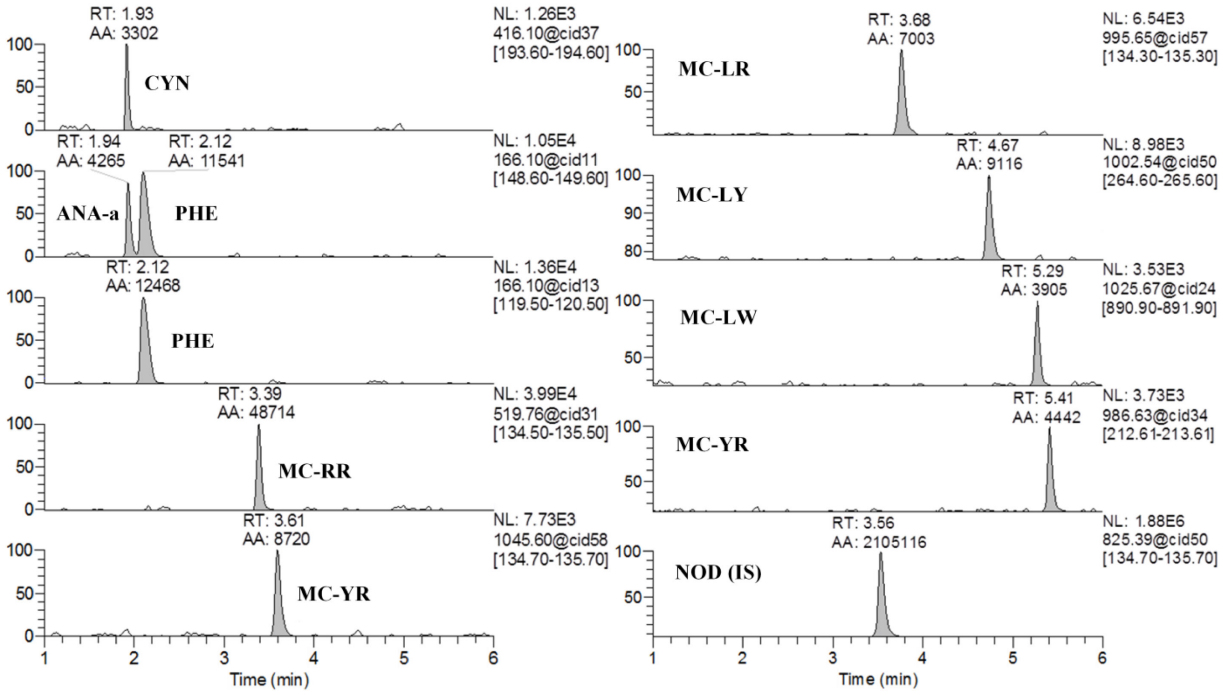


**Figure 2-3.** Representative extracted ion (SRM) chromatograms of the lowest calibration curve standard concentration (0.05 µg $L^{-1}$) for the eight selected cyanotoxins as well as phenylalanine. The analytes are represented by the integrated peaks with corresponding retention times (RT) and area (AA). ANA-a and PHE are baseline separated with a chromatographic resolution of 1.52, thus avoiding any contribution from the isobaric compound PHE to ANA-a.

### 2.3.3 Chromatographic and MS/MS conditions

Optimizing the chromatographic separation was the most challenging step of this study, especially to adjust the elution gradient conditions. Several different LC strategies have been proposed to accomplish ANA-a and PHE separation, but they require long analyse times, complex gradients or the use of normal phase (HILIC) chromatography [15, 24, 51, 62]. Indeed, PHE is an isobaric compound to ANA-a that is a predominantly present within algal bloom water extracts that could mask the detection, and result in false-positives during MS detection if not chromatographically resolved from ANA-a. This is further complicated by the on-line SPE method, since a minimum of 55% of the organic modifier in the initial elution step (**Tableau 2-1**) is needed to simultaneously elute all the cyanotoxins from the SPE column prior to reaching the analytical column and minimize tailing and peak broadening. With this amount of organic modifier, the separation of ANA-a and PHE was not achievable if using MeOH as the organic modifier. In addition, given the short analysis time and their similar column affinity, ANA-a and PHE were unresolved MeOH was used, under all tested conditions during method optimization. Considering the chemical structures of both ANA-a and PHE, we elected to use acetonitrile, instead of MeOH, as the initial organic modifier for the elution step from the SPE column. This adjustment had an impact on the retention behavior of the co-eluting compounds and can be explained by considering the two competing mechanisms involved in the chromatographic separation step, i.e. the hydrophobic interactions and π–π interactions. When MeOH was used, the interactions between the analytes and the stationary phase are significantly stronger compared to those with the methanol molecules. Inversely, by choosing acetonitrile, the π–π interactions between ANA-a, PHE and acetonitrile molecules are favored and thus baseline separation is achieved (Figure 3). This explanation is supported by a previous study on the separation of pharmaceutically active ingredients using reverse phase liquid chromatography [215]. Although it was now possible to achieve baseline separation between ANA-a and PHE, the signal intensity and MDLs were significantly better when using MeOH for the remaining MCs. This is why some MeOH was re-introduced in the mobile phase composition (**Tableau 2-1**).

The chromatographic run was 7 min with all analytes eluting in 5.51 min and column re-equilibration performed during the next sample transfer step from the sample loop to the SPE column. The positive identification of target cyanotoxins in real samples was confirmed by matching chromatographic retention times within ± 2% of those observed in standards spiked in analyte-free matrix.

### 2.3.4 On-line SPE-LC-HESI-MS/MS method validation

Method validation was done by evaluating linearity, precision (interday and intraday), accuracy, method detection (MDLs) and quantification limits (MQLs) in water bloom cyanotoxin-free matrix (**Tableau 2-3**).

The calibration curves of the spiked cyanotoxins showed good linearity in all water matrices, with $R^2 \geq 0.9990$ (**Tableau 2-3**). The precision and accuracy (% bias) of the method was determined at three concentration levels (0.1, 1 and 10 µg $L^{-1}$) by analyzing replicates of spiked algal bloom water samples (n=3, **Tableau 2-1**). The precision and accuracy (as % bias) from the expected concentration for all analytes were deemed suitable, ranging from 3 to 13% and between 5 and 12%, respectively. The MDLs and MQLs values ranged from 0.01 to 0.02 µg $L^{-1}$ and 0.03 to 0.07 µg $L^{-1}$, respectively (**Tableau 2-3**). The evaluated MDLs and MQLs of the present developed method are substantially lower than the guidelines established by the province of Québec in Canada (1.5 µg $L^{-1}$) as well as by the WHO (1 µg $L^{-1}$) [14, 85, 195] and those of ANA-a in Canada (3.7 µg $L^{-1}$), New Zealand (6 µg $L^{-1}$) and three U.S. states; California, Oregon and Washington (1 µg $L^{-1}$) [6, 195], making it a valid approach for the screening ANA-a for risk management purposes as well as the other cyanotoxins.

Ideally an isotopically-labelled compound would be the preferred approach when selecting an internal standard. In this work, this was not a practical approach given that commercially available isotopically-labelled compounds for cyanotoxins are scarce and excessively costly. Therefore, the use of NOD, a compound having an analogous structure to that of cyanotoxins, was proposed as internal standard and has been used in the past [205, 216]. A previous publication on toxic algal blooms has reported the possible presence of NOD in some freshwater samples making it a less attractive choice to use as an internal standard

[217]. To account for this, an external calibration curve for NOD was run during the analysis of real algal bloom water samples to determine its concentration and confirm the amount added in each sample. In the present work, we did not detect any samples containing NOD that could have contributed to the measured spiked NOD concentration used for the internal calibration curves.

### 2.3.5 Method application to environmental samples

The optimized and validated on-line SPE-LC-HESI-MS/MS method was applied to analyze the targeted cyanotoxins in algal bloom water samples from several monitored lakes across the province of Québec (Québec, Canada) known to produce cyanotoxins. The concentrations found in this work for cyanotoxins in 12 different water blooms are reported in **Tableau 2-4**. Among the selected cyanotoxins, CYN was the only one that was not detected in any of the analyzed samples while all the others were observed at least once. ANA-a, MC-LR, MC-RR, and MC-YR were detected in 50% or more of the samples tested, which was not surprising as the samples were selected for their known occurrence of cyanobacteria problems. In nine of the ten surface water samples where MCs were detected, total MC concentrations exceeded the proposed guideline from the province of Québec in Canada, being 1.5 μg $L^{-1}$ for MC-LR equivalent. This could be of importance for this toxin in recreational lake water samples for public health and animal safety [85, 193]. For ANA-a, none the samples exceeded the proposed guideline [6, 195], with concentrations ranging from 0.028 to 0.44 μg $L^{-1}$. However, as anatoxin cannot be readily oxidized by chlorination, its detection in 10/12 environmental samples merits consideration. The presented results clearly show the presence of cyanotoxins in analysis and demonstrate the sensitivity and applicability of the developed on-line SPE analytical method.

**Tableau 2-4.** Concentration (± SD) of detected cyanotoxins and cyanobacterial cells content in several filtered water bloom samples from lakes in the province of Québec (Québec, Canada).[a,b]

| Cyanotoxins | Water bloom sample concentrations (µg $L^{-1}$) | | | | | | | | | | | | Frequency of detection in samples[c] |
|---|---|---|---|---|---|---|---|---|---|---|---|---|---|
| | 1 | 2 | 3 | 4 | 5 | 6 | 7 | 8 | 9 | 10 | 11 | 12 | |
| ANA-a | 0.15 (0.02) | 0.09 (0.01) | 0.33 (0.03) | ND | 0.30 (0.03) | 0.22 (0.02) | *0.024 (0.001)* | *0.028 (0.001)* | 0.44 (0.03) | 0.16 (0.02) | 0.18 (0.02) | ND | 10 / 12 |
| CYN | ND | ND | ND | ND | ND | ND | ND | ND | ND | ND | ND | ND | 0 / 12 |
| MC-RR | 0.26 (0.02) | ND | ND | 0.08 (0.01) | ND | 12.4 (0.9) | 2.8 (0.1) | 0.10 (0.01) | 0.17 (0.02) | 2.8 (0.3) | 2.8 (0.3) | 0.42 (0.04) | 9 / 12 |
| MC-YR | ND | ND | 1.01 (0.09) | ND | ND | 13.8 (0.1) | 4.6 (0.2) | *0.030 (0.003)* | *0.0350 (0.0009)* | 4.9 (0.4) | 1.1 (0.1) | 0.50 (0.05) | 8 / 12 |
| MC-LR | *0.029 (0.002)* | ND | 11.9 (0.4) | 1.5 (0.1) | ND | 36 (2) | 5.1 (0.3) | 1.2 (0.1) | 3.5 (0.3) | 5.6 (0.3) | 3.4 (0.3) | 9.9 (0.5) | 10 / 12 |
| MC-LY | ND | ND | *0.052 (0.005)* | 0.057 (0.004) | ND | ND | ND | 0.25 (0.02) | 0.39 (0.05) | ND | ND | 2.0 (0.2) | 5 / 12 |
| MC-LW | ND | ND | 0.10 (0.01) | ND | ND | 0.63 (0.04) | ND | ND | *0.032 (0.003)* | 0.051 (0.005) | ND | 0.21 (0.02) | 5 / 12 |
| MC-LF | ND | ND | ND | ND | ND | ND | ND | 0.058 (0.006) | ND | ND | ND | 0.33 (0.02) | 2 / 12 |
| | Cyanobacterial cells content | | | | | | | | | | | | |
| | 1 | 2 | 3 | 4 | 5 | 6 | 7 | 8 | 9 | 10 | 11 | 12 | |
| Total count (cells $mL^{-1}$) | 20 600 | 12 000 | 1 785 000 | 2 022 000 | 5 000 000 | 4 980 000 | 1 370 000 | 3 178 000 | 21 410 000 | 13 300 000 | 6 280 000 | 16 790 000 | |
| Biovolume ($mm^3$ $L^{-1}$) | 2 | 1 | 202 | 133 | 755 | 522 | 228 | 324 | 2 029 | 1 744 | 936 | 1 462 | |

[a]ND: not-detected (< MDLs)

[b]Values in italic represent concentrations above the MDLs but under the MQLs.

[c]Number of samples with positive concentration of cyanotoxines out of the 12 samples.

## 2.4 Conclusion

An analytical method based on on-line SPE-LC-HESI-MS/MS has been developed for the detection and quantification of eight selected cyanotoxins (microcystin-RR, -YR, -LR, -LY, -LW and -LF, anatoxin-a and cylindrospermopsin) in algal bloom water samples. A detailed discussion, as a function of water matrix, on optimization of parameters often overlooked and that have an impact on the overall performance of the method (filtration step, SPE loading speeds and maximum injection volume) has been presented. All optimization and validation experiments for the on-line SPE method and chromatographic separation were performed in environmentally relevant algal bloom water matrices. The proposed method is simple and provides a high throughput approach (7 min per injection) for the determination, at low-nanogram per liter levels, of selected cyanotoxins in field-collected algal bloom water samples.

An interesting chromatographic approach was adopted for the first time with an on-line SPE method using acetonitrile to separate anatoxin-a from the naturally occurring isobaric interference phenylalanine quickly and without a complex mobile phase gradient. This is essential given the possibility of a false positive and thus overestimation of anatoxin-a in water bloom samples due to the presence of the interference from un-resolved phenylalanine.

The applicability of the method was demonstrated on samples from twelve lakes known and monitored for cyanotoxins contamination. The results revealed that seven of the eight cyanotoxins included in our method were positively detected in real algal bloom water samples. Moreover, in several surface water samples where microcystins were detected, concentrations exceeded the proposed guideline from the province of Québec, Canada, of 1.5 $\mu g\ L^{-1}$.

## 2.5 Acknowledgments

This work was made possible through the financial support from the *Fond de Recherche Québec Nature et technologies* (FQRNT), the Natural Sciences and Engineering Research Council of Canada (NSERC), the NSERC Industrial Chair on Drinking Water at Polytechnique Montréal and the Canadian Foundation for Innovation (equipment). Marc Sinotte and Christian Deblois from the *Ministère du Développement Durable, de l'Environnement, et de lutte aux changements climatiques,* (MDDELCC – The province of Québec Ministry of the Environment) are acknowledged for providing the samples used in this project and for their scientific support.

## 2.6 Supplementary material

**Tableau 2S-1.** Cell count of cyanobacterial species according to the abundance of potentially toxic cells classes.

| Sample | Cell count (cells $mL^{-1}$) | | | | | | | | |
|---|---|---|---|---|---|---|---|---|---|
| | Anabaena flos-aquae | Aphanizomenon flos-aquae | Aphanocapsa incerta | Aphanothece minutissima | Gloetrichia echinulata | Microcystis aeruginosa | Planktothrix aghardii | Woronichinia naegeliana | Nontoxic |
| 1 | 8 400 | | | | | 3 100 | | 9 100 | |
| 2 | | | 1 700 | 2 200 | | | | 3 100 | 5 000 |
| 3 | 1 000 000 | 15 000 | | | | 770 000 | | | |
| 4 | 22 000 | | | | | 2 000 000 | | | |
| 5 | 5 000 000 | | | | | | | | |
| 6 | 2 100 000 | 250 000 | | | | 2 000 000 | | 630 000 | |
| 7 | 250 000 | 94 000 | | | | 1 000 000 | | 26 000 | |
| 8 | 730 000 | 1 300 000 | | | | 68 000 | 200 000 | 880 000 | |
| 9 | 4 100 000 | 6 300 000 | | | | 3 800 000 | 210 000 | 7 000 000 | |
| 10 | 10 000 000 | | | | | 2 200 000 | | 1 100 000 | |
| 11 | 6 100 000 | | | | | | | 180 000 | |
| 12 | 1 200 000 | 990 000 | | | 2 000 000 | 2 700 000 | | 9 900 000 | |

# Chapitre 3. Détermination du BMAA et de trois cyanotoxines alcaloïdes dans l'eau à l'aide d'une dérivatisation au chlorure de dansyle et d'une détection par spectrométrie de masse à haute résolution

Une version de ce chapitre se trouve dans l'article intitulé :

Determination of BMAA and three alkaloid cyanotoxins in lake water using dansyl chloride derivatization and high-resolution mass spectrometry

Audrey Roy-Lachapelle, Morgan Solliec et Sébastien Sauvé*, Analytical Bioanalytical Chemistry*, 2015. **407**(18): p. 5487-5501.

**Note sur ma contribution**

Ma participation aux travaux de recherche: J'ai conçu le design expérimental en collaboration avec le Prof. Sauvé et Morgan Solliec et j'ai réalisé les manipulations, l'analyse, l'interprétation des résultats.

Rédaction : J'ai rédigé l'article en m'appuyant sur les commentaires du Prof. Sauvé, mon directeur de thèse.

Collaboration des co-auteurs: Morgan Solliec m'a assisté dans le développement du projet et la rédaction de l'article.

# Abstract

A new analytical method was developed for the detection of alkaloid cyanotoxins in harmful algal blooms. The detection of the nonproteinogenic amino acid β-*N*-methylamino-L-alanine (BMAA), and two of its conformation isomers, 2,4-diaminobutyric acid (DAB), and *N*-(2-aminoethyl) glycine (AEG), as well as three alkaloid cyanotoxins, anatoxin-a (ANA-a), cylindrospermopsin (CYN), and saxitoxin (STX), is presented. The use of a chemical derivatization with dansyl chloride (DNS) allows easier separation with reversed phase liquid chromatography. Detection with high resolution mass spectrometry (HRMS) with the Q-Exactive enables high selectivity with specific fragmentation as well as exact mass detection reducing considerably the possibilities of isobaric interferences. Previous to analysis, a solid phase extraction (SPE) step is used for purification, and preconcentration. After DNS derivatization, samples are submitted to ultra high-performance liquid chromatography coupled with heated electrospray ionisation, and the Q-Exactive mass spectrometer (UHPLC-HESI-HRMS). With an internal calibration using isotopically-labeled DAB-$D_3$, the method was validated with good linearity ($R^2$ > 0.998), and method limits of detection and quantification (MDL and MQL) for target compounds ranged from 0.007 to 0.01 µg $L^{-1}$ and from 0.02 to 0.04 µg $L^{-1}$ respectively. Accuracy and within-day/between-days variation coefficients were below 15%. SPE recovery values ranged between 86 and 103% and matrix effects recovery values ranged between 75 and 96%. The developed analytical method was successfully validated with 12 different lakes samples, and concentrations were found ranging between 0.009 and 0.3 µg $L^{-1}$ except for STX which was not found in any sample.


**Keywords :** Water, Organic compounds / trace organic compounds, Mass spectrometry, Blue-green Algae

## 3.1 Introduction

The nonproteinogenic amino acid (BMAA) is an excitotoxic neurotoxin produced by harmful cyanobacterial blooms [218]. The first identification of BMAA was in 1967 with a major incidence of amyotrophic lateral sclerosis/Parkinson's disease complex (ALS/PDC) on the island of Guam [73, 74]. The neurotoxin was reported to be produced by the cyanobacterial genus *Nostoc* symbiont in the seeds of a cycad tree (*Cycas circinalis*), used to make flour by the Chamorro people from Guam [219]. Furthermore, the discovery of the biomagnification of BMAA through the food chain suggested that concentrations could accumulate to levels sufficient to cause neurodegenerative damages [220]. In summary, BMAA causes the hyperexcitation of the neuronal activity by elevating intracellular calcium levels, and it was found that concentrations as low as 10 and 30 μM, administrated to cortical cell cultures, could induce damages and the death of the motor neurons [76, 221]. Recent studies reported that more than 95% of cyanobacterial genera can produce BMAA, suggesting its presence in aquatic environments [72]. BMAA is a small hydrophilic molecule, which makes it challenging to analyze, and due to its controversial link to neurodegenerative diseases, it becomes crucial to use highly selective and robust analytical methods for its detection [74, 77, 222]. Furthermore, the presence of constitutional isomers, such as 2,4-diaminobutyric acid (DAB), *N*-(2-aminoethyl) glycine (AEG), and β-amino-*N*-methyl-alanine (BAMA) can induce false positives if the analytical method has difficulty in discriminating the different forms [78].

Other alkaloid cyanotoxins have been routinely identified in water bodies including anatoxin-a (ANA-a), cylindrospermopsin (CYN), and saxitoxin (STX). ANA-a is a neurotoxin produced by at least ten genera of cyanobacteria. With a high toxicity ($LD_{50}$) of 200-250 μg $kg^{-1}$ for mice, this neurotoxin can cause permanent stimulation of respiratory muscles leading to asphyxiation [51, 196, 197]. To date, Canada and New Zealand tolerate concentrations below 3.7 and 6 μg $L^{-1}$, respectively, in drinking water, and for three US states, (California, Oregon, and Washington) the threshold is 1 μg $L^{-1}$ [86]. CYN is an alkaloid toxin with cytotoxic, neurotoxic, and hepatotoxic effects [15, 24, 62]. With at least 6 cyanobacterial genera responsible for its presence, this toxin is linked to tumor promotion and carcinogenic

effects in the digestive system due to the inhibition of protein synthesis. The $LD_{50}$ values range from 200 to 2100 μg $kg^{-1}$ for mice, and based on its toxicity, a guideline of 1 μg $L^{-1}$ in drinking water was proposed [223]. Finally, STX is also a potent neurotoxin belonging to a group of paralytic shellfish poisoning (PSP) toxins, and known for its severe food poisoning [224]. With a high level of toxicity ($LD_{50}$ value of 10 μg $kg^{-1}$), STX causes numbness, and respiratory failure by disrupting the nervous system; it inhibits the sodium transport by blocking the sodium channels [225, 226]. A guideline of 3 μg $L^{-1}$ in drinking water is used in Australia, however, no guidelines are available in Canada [227].

Several analytical methods have been published for the detection of BMAA, but few consensuses have been made on the reported concentrations. Many separation, and detection methods have been developed such as capillary electrophoresis (EC) [128], gas chromatography (GC) [228, 229], and liquid chromatography (LC) in combination with fluorescence detection [77, 111, 112, 230-233], UV spectroscopy [230, 232], and mass spectrometry [77, 78, 112, 117, 126, 230, 232-240]. Precolumn derivatization was routinely used with 6-amino-quinolyl-*N*-hydrosuccinimidyl (6-AQC) [77, 112, 230, 232, 233, 236-238], 9-fluorenylmethyl chloroformate (FMOC) [231, 235], and propyl chloroformate (EzFaast™) [228, 232]. The most commonly used derivatization technique involves a derivatization with 6-AQC which is widely used for the analysis of amino acids [141]. Derivatization enables easier liquid chromatography separation with reverse phase columns, and the mostly used detectors involve fluorescence detection (HPLC-FD), and mass spectrometry (HPLC-MS) [141]. For the most commonly used analytical method, HPLC-FD, BMAA concentrations were overestimated, due to the derivatization of other amino acids or small molecules present in complex matrices causing false positives, and unspecific detection. However, the use of tandem mass spectrometry (MS/MS) detection showed different results, due to higher selectivity, with significantly lower detected concentrations of BMAA [233-235, 241]. Several studies presented the possibility of eliminating the derivatization step by using hydrophilic separation with HILIC columns coupled with mass spectrometric detection [111, 117, 126, 233-235, 238, 240]. The advantage of the HILIC technique is the simplicity of the sample preparation since the compounds are directly injected, and analyzed. However, the major drawback comes from the high dependency on the chromatographic, and MS/MS separation

abilities [75, 141]. Furthermore, the presence of numerous low mass isobaric compounds, and isomers can compromise the selectivity of the analytical methods. More specifically, DAB, and AEG have been previously studied, and known to interfere with the analysis of BMAA due to problems of coelution [141]. Many studies using derivatization (6-AQC), and HILIC have been able to distinguish BMAA from DAB, but few have been able to differentiate the three isomers [78, 126, 232, 240]. In a recent study, a new approach was used for the analysis of BMAA using DNS derivatization, and ultra performance liquid chromatography coupled with tandem mass spectrometry (UPLC-ESI-MS/MS) [239]. This derivatization was previously reported for the analysis of amines by fluorescence detection [242, 243]. It was also documented for its use on the improvement of chromatographic separation, and enhancement of ionization efficiency in mass spectrometry detection [244-247]. With easier preparation steps, and faster reaction time (4 min at 60°C) as well as a specific fragmentation patterns for BMAA, and DAB, DNS derivatization was shown to be a usable alternative to 6-AQC method [239].

Considering the challenge toward the analysis of BMAA, there is a need for reliable analytical methods usable routinely for clinical reasons. As described by Cohen [141], BMAA is present at low concentrations in complex matrices in presence of possible isobaric interferences; therefore effective sample clean-up is primordial prior to analysis to avoid those compounds. Moreover, a selective method is primordial with good chromatographic separation, and mass spectrometric detection with specific product ions. High-resolution mass spectrometry (HRMS) detection is proposed in this study with the use of the hybrid mass spectrometer, the Q-Exactive. In summary, it is a benchtop Orbitrap detector which is combined to a quadrupole precursor selection, and a high-energy collisional dissociation cell (HCD). The advantage of this hybrid mass spectrometer resides in the combination of a quadrupole *m/z* value filtration prior to an HCD cell, thus offering the possibility of fragmenting selected precursor ions. With resolving power up to 140,000 full width half maximum (FWHM) at *m/z* 200, the mass accuracy obtained with the Q-Exactive is between 1 and 3 ppm [248]. These features allow high sensitivity, and selectivity detection, and quantification. It was previously used for its capability of high selectivity in peptides sequencing and metabolomics, and a few methods were developed for small molecules

quantification in environmental matrices [185, 187, 249-251]. The objective of this study was to develop an analytical method using ultra high-performance liquid chromatography coupled with heated electrospray ionization and the Q-Exactive (UHPLC-HESI-HRMS) for the detection and quantification of BMAA and two of its constitutional isomers, DAB and AEG, as well as three other alkaloid cyanotoxins; ANA-a, CYN, and STX (**Figure 3-1**). A solid phase extraction (SPE) step was used for the clean-up and preconcentration of environmental water samples then the extract was submitted to a derivatization step with DNS. The use of HRMS in a fragmentation mode (t-$MS^2$) allows us to determine the fragmentation pattern of the different derivative compounds and thereafter suggest the structures of the principal product ions detected with high mass accuracy. The method was validated with the use of deuterated 2,4-diaminobutyric acid (DAB-$D_3$) as internal standard. The extraction recovery, the method detection and quantification limits (MDL and MQL), the linear dynamic range, the accuracy, the precision and matrix effects were evaluated with spiked real bloom water samples. The method was finally applied to real field-collected cyanobacterial bloom water samples to assess the quantity of each of the studied cyanotoxins.

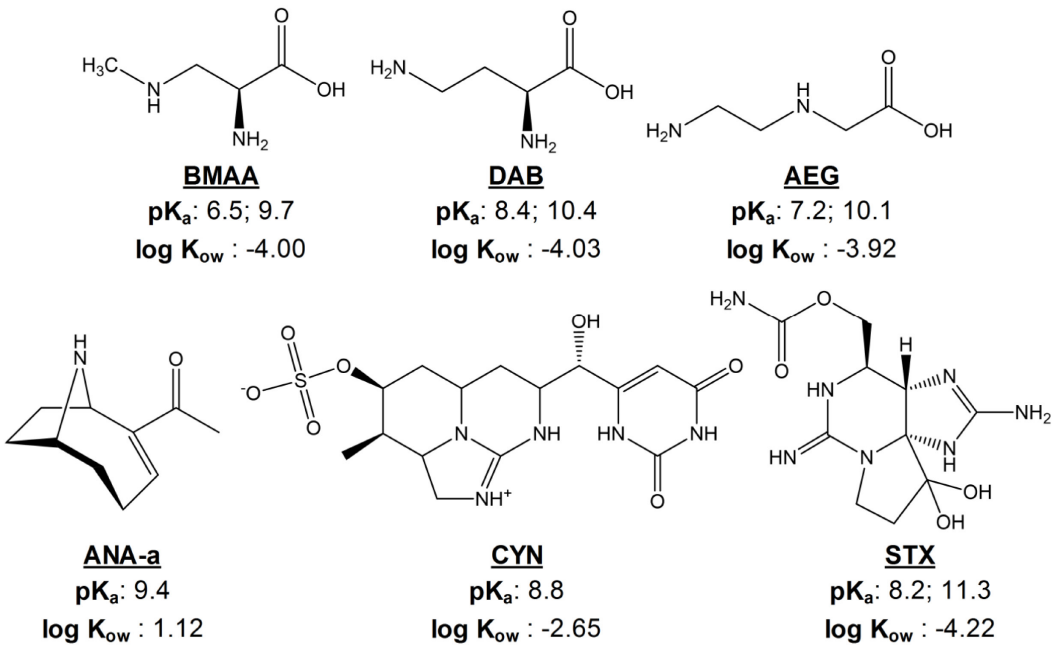


**Figure 3-1.** Chemical structures, p$K_a$ and partition coefficients (log $K_{ow}$) of the studied cyanotoxins: β-*N*-methylamino-L-alanine (BMAA), 2,4-diaminobutyric acid (DAB) and *N*-(2-

aminoethyl) glycine (AEG), anatoxin-a (ANA-a), cylindrospermopsin (CYN) and saxitoxin (STX).

## 3.2 Materials and methods

### 3.2.1 Chemicals, reagents and stock solutions

L-BMAA hydrochloride (BMAA, purity ≥ 97%), DL-2,4-diaminobutyric acid dihydrochloride (DAB, purity ≥ 97%) and DL-phenylalanine (PHE, purity ≥ 99%) were purchased from Sigma-Aldrich Chemical Co. (Oakville, ON, Canada). *N*-(2-Aminoethyl) glycine (AEG, purity ≥ 95%) was purchased from TCI America (Portland, OR, USA), (±)-anatoxin-a/furamate salt (ANA-a, purity ≥ 99%) was purchased from Abcam Biochemicals (Cambridge, MA, USA), cylindrospermopsin (CYN, purity ≥ 97%) was purchased from Enzo Life Sciences, Inc. (Farmingdale, NY, USA) and 2,4 diaminobutyric acid-2,4,4-$D_3$ dihydrochloride (DAB-$D_3$, 99 atom % D) was purchased from CDN isotopes (Pointe-Claire, QC, Canada). Ampoules of certified standard solutions of saxitoxin dihydrochloride (STX, 66.3 µM in 3 mM hydrochloric acid) were obtained from the Certified Reference Materials Program (NRC, Halifax, NS, Canada). Sodium tetraborate (Borax, purity ≥ 99%), dansyl chloride (DNS, purity ≥ 99%), citric acid (purity ≥ 99.5%), and formic acid (HCOOH, purity ≥ 95.0%) were purchased from Sigma–Aldrich (Oakville, ON, Canada). All solvents used were of high-performance liquid chromatography (HPLC) grade purity from Fisher Scientific (Whitby, ON, Canada). Individual stock solutions of BMAA, DAB, AEG, CYN and DAB-$D_3$ were prepared in HPLC grade water and ANA-a was prepared with acidified water (0.1 M formic acid) all at a concentration of 100 mg $L^{-1}$ prior their storage at −20°C. STX solutions from ampoules were transferred to amber glass bottles prior their storage at −20°C. A 100 mg $L^{-1}$ stock solution of PHE was prepared daily in HPLC grade water prior to analysis. All BMAA, DAB, and AEG solutions were prepared and stored in polypropylene bottles and vials knowing that BMAA can strongly adhere on glass surfaces [141]. As for ANA-a, CYN, and STX solutions, they were prepared and stored in glass bottles and vials. According to compound stability, new stock solutions were prepared every 4 months [62, 239, 250]. All

working solutions were prepared by dilution with HPLC-grade water from individual stock solutions. The solvents for the chromatographic mobile phases were prepared daily.

### 3.2.2 Cyanobacterial bloom samples

Environmental samples were provided by the monitoring program realized by the *Ministère du Développement Durable, de l'Environnement, et de lutte aux changements climatiques,* (MDDELCC – The Ministry of the Environment of the province of Québec, Québec, Canada). The lakes were sampled from 2009 to 2013 as part of a project to monitor cyanobacteria genera and their toxins around the province of Québec, Canada, and they were chosen for their high occurrence of cyanobacterial blooms. The whole samples have been stored at −20°C until analysis to reduce degradation. Before each analysis, the samples were submitted three times to a freeze-thaw lysis followed by filtration using 0.22 µm nitrocellulose membrane obtained from Millipore (Billerica, MA, USA) [11, 12, 89, 141, 252]. All recovery data and validation parameters were acquired using spiked relevant environmental matrix which consisted of lake water bloom samples containing nonharmful cyanobacterial cells. This matrix assures the method development to take account of matrix effects without cyanotoxins contamination.

### 3.2.3 Solid-phase extraction procedures

A strong cation-exchange polymeric sorbent Strata-X-C cartridge (Phenomenex, Torrance, CA, USA) with 200 mg bed mass and a volume of 6 mL was used for sample clean-up and preconcentration. Other strong cation-exchange sorbents were previously used for sample pretreatment for the analysis of BMAA by LC-MS/MS and the SPE conditions were inspired from these studies [111, 116, 236, 238]. The procedure was done using a 12-position manifold manufactured by Phenomenex (Torrance, CA, USA). The SPE was performed with 100 mL aliquots of samples with pH adjusted to 4 with citric acid. The conditioning step was done with 5 mL of methanol (MeOH) for cartridge activation followed by 5 mL of acidified water with citric acid (pH 4). The acidified samples were then loaded on the cartridge columns at a rate of 2 mL $min^{-1}$ using a mechanical pump. The cartridges were washed with 5 mL of acidified water (pH 4) containing 15% MeOH (v/v). Elution was performed with 5 mL of

MeOH containing 3% $NH_4OH$ into conical-bottom polypropylene centrifuge tubes. The eluates were completely dried under a gentle stream of nitrogen at room temperature with a nine-port Reacti-Vap unit from Pierce (Rockford, IL, USA). The dried fractions were then reconstituted with the DNS reactive solution.

### 3.2.4 Dansyl chloride derivatization

The derivative procedures with DNS were previously described and optimised by Salomonsson *et al.* [239] for the derivatization of BMAA. A direct derivatization was done with the dried fractions obtained after the SPE procedures by adding 250 µL of a Borax buffer (0.2 M, pH 9.5) and 250 µL of DNS in acetone (1 mg $mL^{-1}$). The tubes were vortexed and placed in an Innova 4230 refrigerated incubator shaker from New Brunswick Scientific (Edison, NJ, USA) at 60 °C for 10 min with agitation at 150 rpm. A slightly longer derivatization time was used compared to Salomonsson *et al.* [239] (4 min) due to the temperature equilibration of the incubator and the solutions. The efficiency of the reaction could not be directly evaluated; however, the reaction completion was evaluated over time (1-30 min) by spiking the analytes in solution (100 µg $L^{-1}$) and using the plateau of signal intensity. The samples were finally cooled at room temperature and then directly submitted to the UHPLC-HESI-HRMS analysis for the target compounds: BMAA-DNS, DAB-DNS, AEG-DNS, ANA-a-DNS, CYN-DNS, STX-DNS, and DAB-$D_3$-DNS. The complete workflow is illustrated in **Figure 3-2** with the reaction scheme of DNS derivatization presented in **Figure 3-3**.

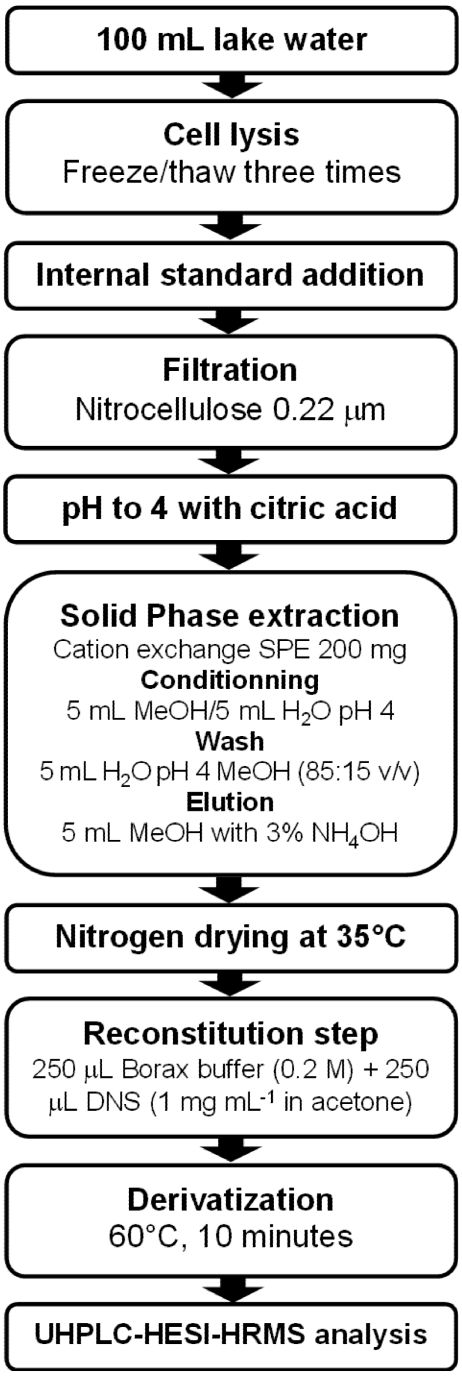


**Figure 3-2.** Analytical method workflow including sample preparation, clean-up procedure, and derivatization.

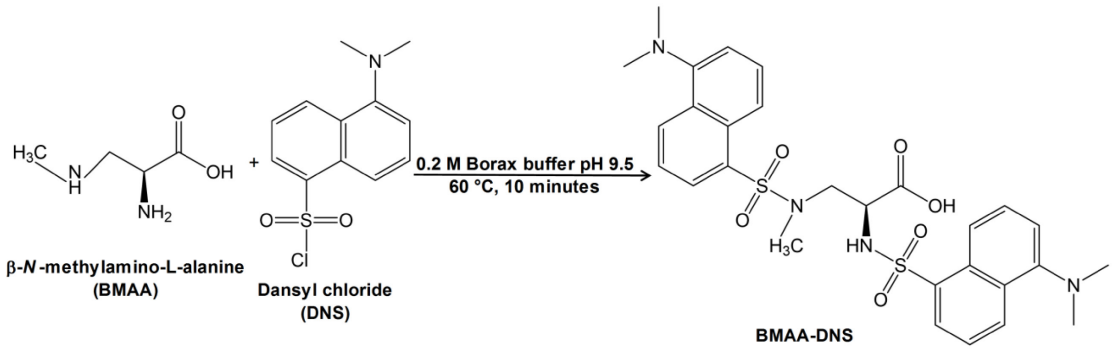


**Figure 3-3.** Reaction scheme of DNS derivatization procedure with BMAA.

### 3.2.5 UHPLC-HESI parameters

The chromatographic separation was performed with a Thermo Scientific Dionex Ultimate 3000 Series RS pump coupled with a Thermo Scientific Dionex Ultimate 3000 Series TCC-3000RS column compartments and a Thermo Fisher Scientific Ultimate 3000 Series WPS-3000RS autosampler controlled by Chromeleon 7.2 Software (Thermo Fisher Scientific, Waltham, MA, USA and Dionex Softron GMbH Part of Thermo Fisher Scientific, Germany). The chromatographic column was a Hypersil GOLD$^{TM}$ C18 column (100 mm, 2.1 mm, 1.9 µm particles) preceded by a guard column (5 mm, 2.1 mm, 3 µm particles) (Thermo Fisher Scientific, Waltham, MA, USA), both at 40 °C. The mobile phase for the analysis of DNS derivatives consisted of $H_2O$ with 0.1% formic acid as mobile phase A and acetonitrile (ACN) with 0.1% formic acid as mobile phase B. A solvent gradient was used starting from 30% of B, increasing to 90% from 0 to 2 min, then increasing to 100% from 2 to 4 min and it was held constant for 2 min. Finally, the mobile phase was brought back to initial conditions and maintained 4 min for equilibration resulting in a total run time of 10 min. The flow rate was 0.5 mL min$^{-1}$ and the injection volume of sample was chosen to be 25 µL. The ionization was performed by a heated electrospray ionization source (HESI-II) configured in positive mode. The voltage was optimized at +3000 V, the capillary and vaporizer temperatures were set at 400 °C and 350 °C, respectively, and the sheath gas and auxiliary gas flow were set at 30 and 60 arbitrary units, respectively.

### 3.2.6 High-resolution mass spectrometry detection

Detection was performed using a Q-Exactive mass spectrometer controlled by the Excalibur 2.3 Software (Thermo Fisher Scientific, Waltham, MA, USA), and exact masses were calculated using Qualbrowser in Xcalibur 2.3. Instrument calibration in positive mode was done every 5 days with a direct infusion of a LTQ Velos ESI positive ion calibration solution (Pierce Biotechnology Inc., Rockford, IL, USA). Targeted ion fragmentation (t-$MS^2$) mode was used for compound quantification and was optimized using individual standards solutions at a concentration of 100 µg $L^{-1}$. The solutions were directly infused with a syringe at a flow rate of 0.01 mL $min^{-1}$ through a T-union connected to the UHPLC system with a mobile phase flow rate of 0.5 mL $min^{-1}$. The product ions and their collision energy were chosen by increasing the normalized collision energy (NCE) using the Q-Exactive Tune 2.3 software (Thermo Fisher Scientific, Waltham, MA, USA). All optimized collision energies, precursor ions and fragment ions, are shown in **Tableau 3-1**. The theoretical exact *m/z* values of the precursor and product ions are presented in supplementary material **Tableau 3S-1** with their respective chemical formulas. In the t-$MS^2$ mode, the data were acquired at a resolving power of 17,500 FWHM at *m/z* 200. The automatic gain control (AGC) target, for a maximum capacity in C-trap, was set at 2 x $10^5$ ions for a maximum injection time of 100 ms. A mass inclusion list was used including the precursor ion *m/z* values, their expected retention time with a 1 min window and their specific fragmentation energy (HCD). The precursor ions are filtered by the quadrupole which operates at an isolation width of 0.4 amu.

**Tableau 3-1.** Parameters of HRMS detection of compounds as DNS derivatives.

| Derivative compounds | RT (min) | Experimental precursor ion (*m/z*) | Quantification product ion (*m/z*) | Confirmation product ion (*m/z*) | Relative intensity ratio[a] | NCE[b] (%) | Average mass accuracy[c] (ppm) | Confirmation ion[d] (*m/z*) |
|---|---|---|---|---|---|---|---|---|
| BMAA | 3.78 | 585.1836 | 277.1007 | 71.0131 | 5.4 ± 0.6 | 30 | 1.26 | 278.1039 |
| DAB | 3.60 | 585.1836 | 277.1006 | 88.0395 | 2.8 ± 0.2 | 30 | 1.80 | 278.1037 |
| AEG | 3.78 | 585.1835 | 289.1005 | 88.0394 | 3.3 ± 0.3 | 30 | 1.95 | 290.1032 |
| ANA-a | 3.77 | 399.1737 | 149.0964 | 131.0856 | 1.2 ± 0.2 | 35 | 1.47 | 150.0989 |
| CYN | 1.27 | 649.1744 | 194.1291 | 176.1184 | 1.6 ± 0.2 | 35 | 1.03 | 195.1230 |
| STX | 2.99 | 533.1925 | 204.0877 | 138.0665 | 2.3 ± 0.2 | 35 | 1.46 | 205.0899 |
| DAB-$D_3$ | 3.60 | 588.2024 | 279.1130 | 88.0396 | 2.3 ± 0.3 | 25 | 1.42 | 280.1159 |

[a] Ratio (quantification product ion/confirmation product ion)
[b] Fragmentation energy for precursor ion in HCD cell
[c] Accuracy of average measured *m/z* values for quantification product ion
[d] Second abundant ion in isotopic pattern from quantification product ion

### 3.2.7 Data analysis and method validation

The data treatment was performed using the Excalibur 2.3 Software (Thermo Fisher Scientific, Waltham, MA, USA). The method validation was done according to the recommendation of validation protocol for environmental chemistry analysis from the Québec's MDDELCC ministry guidelines. For DAB-DNS, ANA-a-DNS, CYN-DNS, and STX-DNS, two product ions with the highest signal intensity were selected as the quantification and the confirmation ions, the first being used to establish the method limits of detection and quantification. The relative intensities of their ratio were used for compound confirmation to avoid false positives. The second most abundant ion from isotopic pattern was used as confirmation ion for the target compounds, and the isotopic ratio was confirmed with <10% of intensity variations. The structural identification of the product ions from derivative compounds was done using Mass Frontier$^{TM}$ 7.0 Software (HighChem, Bratislava, Slovakia). For a good selectivity in data analysis, a mass tolerance window was set to 5 ppm (± 2.5 ppm) for the extracted *m/z* values from acquisition [185]. The recovery values for the SPE method were evaluated using dd-$H_2O$ water and nonharmful cyanobacterial bloom (or bloom water blank), at three concentrations of 0.05, 0.25, and 1.25 µg $L^{-1}$. Extraction recoveries and matrix effects were determined with the mean peak areas of the targeted compounds spiked prior to extraction in matrix-free (dd-$H_2O$) and matrix-containing (bloom water blank) samples

compared to spiked postextraction matrix-free samples, all in triplicate, and results are reported as percentages. A 7-point internal calibration curve was obtained by passing through the SPE method and was prepared with bloom water blanks with concentration levels ranging from 0.025 to 2.5 µg $L^{-1}$ and analyzed in triplicate. The concentration of internal standard (IS) DAB-$D_3$, 0.750 µg $L^{-1}$, was selected for its capacity of signal correction (data not shown). Method detection limit (MDL) and method quantification limit (MQL) were established by calculating three and ten times, respectively, the standard deviation of the mean value of five spiked blank matrix samples (n=5) containing approximately five times the estimated concentration for detection limit (0.05 µg $L^{-1}$). Accuracy, expressed as relative error (%), and within-day/between-days variations, expressed as the relative standard deviation (%), were determined with three different concentrations on the linearity range (0.05, 0.25, and 1,25 µg $L^{-1}$, n=5) in blank matrix samples. Between-days reproducibility was estimated over 5 weeks. Statistical comparison was used when needed with the Statistical Package for Social Science (SPSS 21.0, Chicago, IL, USA) for Windows. ANOVA test and Tukey's post hoc tests were used with statistical significance defined as $P < 0.05$.

## 3.3 Results and discussion

### 3.3.1 Sample treatment

After the sample lysis, which promotes the breaking of the cyanobacterial cells and leaches the cell-bound toxins, a filtration step is needed to remove the suspended particles. Filtration conditions were studied for all compounds of interest to ensure sample integrity and accuracy. This step can have an impact on the loss of analytes due to undesirable interactions between the target compounds and the filter membrane material. Seven different filters were tested to isolate the unbound extracellular fraction: glass fiber (GF), cellulose acetate (CA), polycarbonate (PC), nitrocellulose (NC), mixed cellulose ester (MCE), nylon (NY), and polypropylene (PP). All compounds were spiked at a concentration of 100 µg $L^{-1}$ in bloom water blanks before filtration, and their mean peak areas were compared to blank samples spiked after filtration. Mean recovery values for each filter and compounds are presented in **Figure 3-4**. Three of the seven filter membranes gave significantly higher recovery values

with 92 - 102% for NC, 78 - 118% for PC, and 65 - 107% for NY ($P > 0.05$). However, the four other filter membranes showed much lower recovery values with 20 - 71% for GF, 11 - 31% for CA, 26 - 110% for MCE, and 0 - 22% for PP. Taking into account these results, NC was deemed the most reliable membrane material for the filtration of the suspended particles in samples while minimizing the loss of the molecules of interest onto the filter.

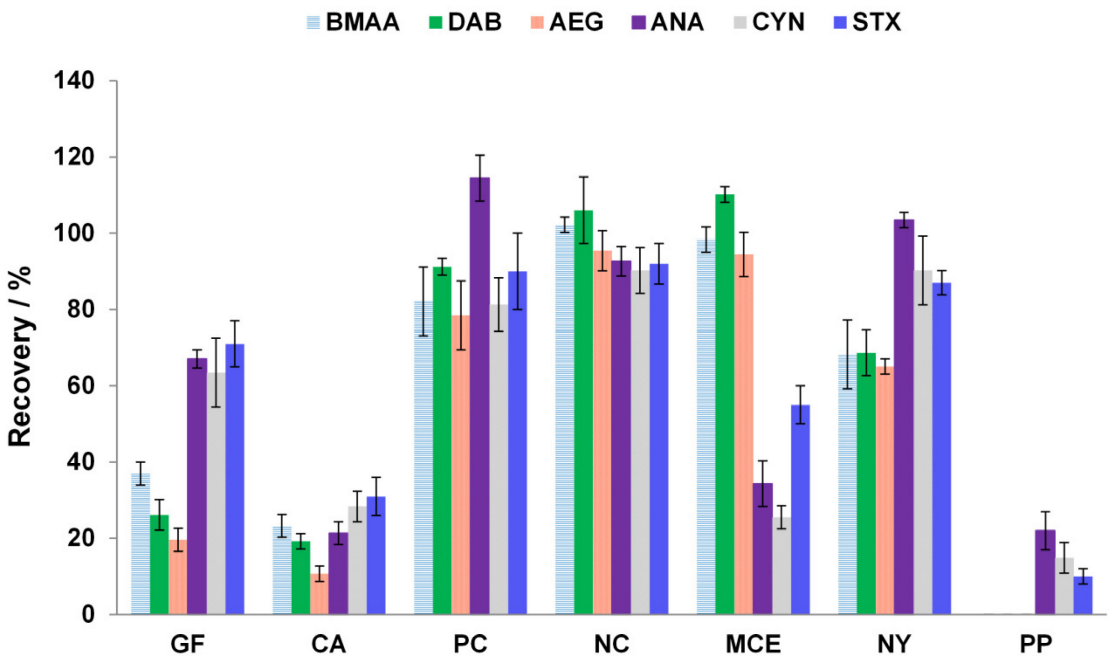


**Figure 3-4.** Comparison of recovery values for the target cyanotoxins on different filter materials, glass fiber (GF), cellulose acetate (CA), polycarbonate (PC), nitrocellulose (NC), mixed cellulose ester (MCE), nylon (NY), and polypropylene (PP). Vertical error bars represent standard deviations from the mean ($n = 3$).

The bloom water samples are complex matrices with a high presence of organic matter. A solid-phase extraction step is then used to clean-up the samples and also to preconcentrate the analytes of interest and consequently enhance sensitivity by decreasing their method detection and quantification limits (MDL and MQL). A Strata X-C cartridge was used, which contain a strong cation exchange sorbent, and has the advantage of allowing the use of organic solvents during the washing step, thus removing a large portion of interfering organic matter

from the matrix. Given that ionic bonds are stronger then van der Waals interactions, this permits us to use a high percentage of organic solvent during the washing step. In order to positively charge the compounds of interest, citric acid was added to set the pH of the solutions to 4, below the $pK_a$s of the target compounds (**Figure 3-1**). For the washing step of the SPE sorbent, 5 mL of water acidified with citric acid (pH 4) containing 15% MeOH was used to eliminate a maximum of interfering compounds from the matrix. The elution step was done with 5 mL of 3% $NH_4OH$ in MeOH in order to change the charge of the compounds and then release them from the sorbent. The use of basified water was suggested by Li *et al.* [238] since it has higher eluent strength, but with the use of 5 mL of MeOH instead, the elution can be completed, and subsequently, the evaporation step is still faster. The recovery values for the SPE procedure were calculated using the mean peak area of targeted compounds spiked in pure water before the extraction compared to pure water spiked after extraction. The results for the different recoveries are shown in **Tableau 3-2** and gave good results for the three concentration levels (0.05, 0.25, and 1.25 µg $L^{-1}$) with values ranging from 86 to 103%. The matrix effects were also determined by comparing the mean peak area of targeted compounds in bloom water blank samples spiked before the extraction compared to pure water spiked after extraction. The signal recoveries for the same three concentration levels are shown in **Tableau 3-2** and ranged from 75 to 96%. This small drop of signal could be caused by ion suppression during the ionization due to the presence of interfering molecules from the matrix, as explained by Cohen [141].

**Tableau 3-2.** Recoveries from SPE procedures and matrix effects of target analytes evaluated at three different concentrations (ng $L^{-1}$) with standard deviation (SD) (n = 3).

| Compounds | SPE recovery ± SD (%) | | | Signal recovery from matrix effects ± SD (%) | | |
|---|---|---|---|---|---|---|
| | 25 | 250 | 1250 | 25 | 250 | 1250 |
| BMAA | 97 ± 11 | 99 ± 10 | 102 ± 6 | 86 ± 10 | 85 ± 8 | 90 ± 9 |
| DAB | 95 ± 13 | 99 ± 9 | 99 ± 5 | 79 ± 12 | 78 ± 12 | 82 ± 9 |
| AEG | 93 ± 12 | 97 ± 7 | 102 ± 6 | 86 ± 10 | 85 ± 10 | 90 ± 7 |
| ANA-a | 99 ± 10 | 103 ± 12 | 101 ± 9 | 90 ± 9 | 95 ± 8 | 96 ± 9 |
| CYN | 92 ± 9 | 91 ± 8 | 94 ± 9 | 84 ± 10 | 83 ± 11 | 87 ± 10 |
| STX | 87 ± 11 | 86 ± 9 | 90 ± 10 | 75 ± 12 | 80 ± 10 | 81 ± 11 |

### 3.3.2 Derivatization

The use of DNS for the derivatization of BMAA and DAB was previously described and optimized by Salomonsson *et al.* [239]. As explained, this derivatization is a good choice for its ease, rapidity, and low cost. It was demonstrated by Guo and Li [245] as a simple method, which produces little to no side-reaction products. In this study, the procedure was adapted from the derivatization proposed by Salomonsson *et al*. [239]. Due to the use of a different source of heat, which was an incubator instead of a heating block, the reaction time was evaluated using the variation of the mean peak areas of the studied compounds between 1 to 30 min. Results are shown in **Figure 3S-1** (see supplementary material), and a reaction time of 10 min was necessary to maximize the signal, and after 10 min, no significant increase occurred but higher signal variability was observed ($P < 0.05$).

### 3.3.3 High-resolution mass spectrometric detection

The Q-Exactive can operate in multiple acquisition modes depending on the analytical needs. In this study, the fragmentation of precursor ions was necessary in order to differentiate the BMAA isomers and give a higher selectivity in the detection. The t-$MS^2$ mode, given by the mass spectrometer, was then chosen for our purposes due to its selectivity and reliability in small molecule quantification [249]. Some parameters need to be optimized to enhance sensitivity: the AGC target, the maximum injection time (IT) of the ions in the C-trap, and the resolving power (RP). These parameters will affect the duty cycle of the Orbitrap detection,

which affect the number of data acquisitions for each chromatographic peak, essential for a precise quantification. For more details about the operation and technical details, see previous studies of analytical methods using the Q-Exactive [249, 250]. Since the t-$MS^2$ scan mode produces much fewer ions transferred to the Orbitrap analyzer than a full-scan mode, a smaller AGC target and injection time can be used. This scan mode is quite useful for enhancing sensitivity when highly charged matrices are analyzed. For our purpose, 1 x $10^5$ ions were transferred to the C-trap for a maximum injection time of 50 ms. As for the selected RP, the main criterion is the number of acquisition points for each chromatographic peak, which as to be 7 or higher for a quantitative analysis with an acceptable relative standard variation (RSD) [253]. In our case, our chromatographic peaks are narrow (<10 s), thus giving approximately 12 acquisition data points per peak using a RP of 17,500 *m/z* 200 (**Figure 3S-2**). This RP was then selected given that, together with precursor fragmentation, the selectivity of an exact *m/z* value is deemed acceptable [250]. Moreover, the mass accuracies were measured below 2 ppm, which is considered acceptable according to the manufacturer recommendations (between 1 and 3 ppm). Finally, selectivity is highly dependent on the mass tolerance (MT), which enables the selection of extracted *m/z* values from acquisition data. By narrowing the mass tolerance of a monitored ion in a mass extraction window, the presence of false positives is reduced. An adequate mass tolerance was chosen to be 5 ppm (±2.5 ppm), which is in accordance with many studies [185, 254].

The DNS derivatives were ionized in positive mode $[M + H]^+$ before being selected by the quadrupole, and then, the fragmentation took place in the HCD cell. The fragmentation energies were carried out to obtain the optimal normalized collision energy (NCE) for complete fragmentation of precursor ions, and results are shown in **Tableau 3-1**. Fragmentation spectra for BMAA-DNS, DAB-DNS, and AEG-DNS (**Figure 3-5**) showed similar pattern of fragmentation. Considering these, the selected product ions were *m/z* 585.1836 > 277.1007; 71.0131 for BMAA-DNS, *m/z* 585.1836 > 277.1006; 88.0395 for DAB-DNS and *m/z* 585.1835 > 289.1005; 88.0394 for AEG-DNS (exact *m/z* values and mass accuracies are presented in **Tableau 3-1**). Specific product ions were selected for each compound in order to avoid signal enhancement caused by mutual contributions. Both *m/z* 277 and 289 are found in their own fragmentation pattern; however, their intensities are

significantly different, with a difference of two orders of magnitude for both, which can be assumed by a fragmentation pattern promoting fragment *m/z* 277 for BMAA-DNS and *m/z* 289 for AEG-DNS. In this case, a specific confirmation ion is essential in order to avoid a cross selectivity of the two isomers. In this case, *m/z* 71 for BMAA-DNS and *m/z* 88 for AEG-DNS were found to be unique product ions and their mean peak area ratios (**Tableau 3-1**) were closely studied for every sample in order to confirm the presence of BMAA-DNS without any signal contribution of AEG-DNS, and vice versa. Since the product ions were selected from the derivatives and not from the compounds alone, a structural search using the software Mass Frontier$^{TM}$ was done to confirm their specificity and results are shown in **Figures 3-5 and 3-6**. In the case of ANA-a-DNS, CYN-DNS, and STX-DNS, the fragmentation patterns were very similar to those without derivatization. The selected ions were *m/z* 399.1737 > 149.0964; 131.0856 for ANA-a-DNS, *m/z* 649.1744 > 194.1291; 176.1184 for CYN-DNS and *m/z* 533.1925 > 204.0877; 138.0665 for STX-DNS. The selected product ions of these three compounds were associated to the toxins molecules without the DNS. For all the fragmentation spectra, specific product ions coming from the DNS reactive were present confirming the derivatization step, including these *m/z* values: *m/z* 170, 172, 235, 236, and 237. These ions were rejected during the product ions selection of derivative compounds as they are only specific to DNS and not to target compounds. Finally, for all the compounds, the second most abundant observed ion was used as confirmation, and the isotopic ratio was confirmed with <10% of intensity variations (**Tableau 3-1**).

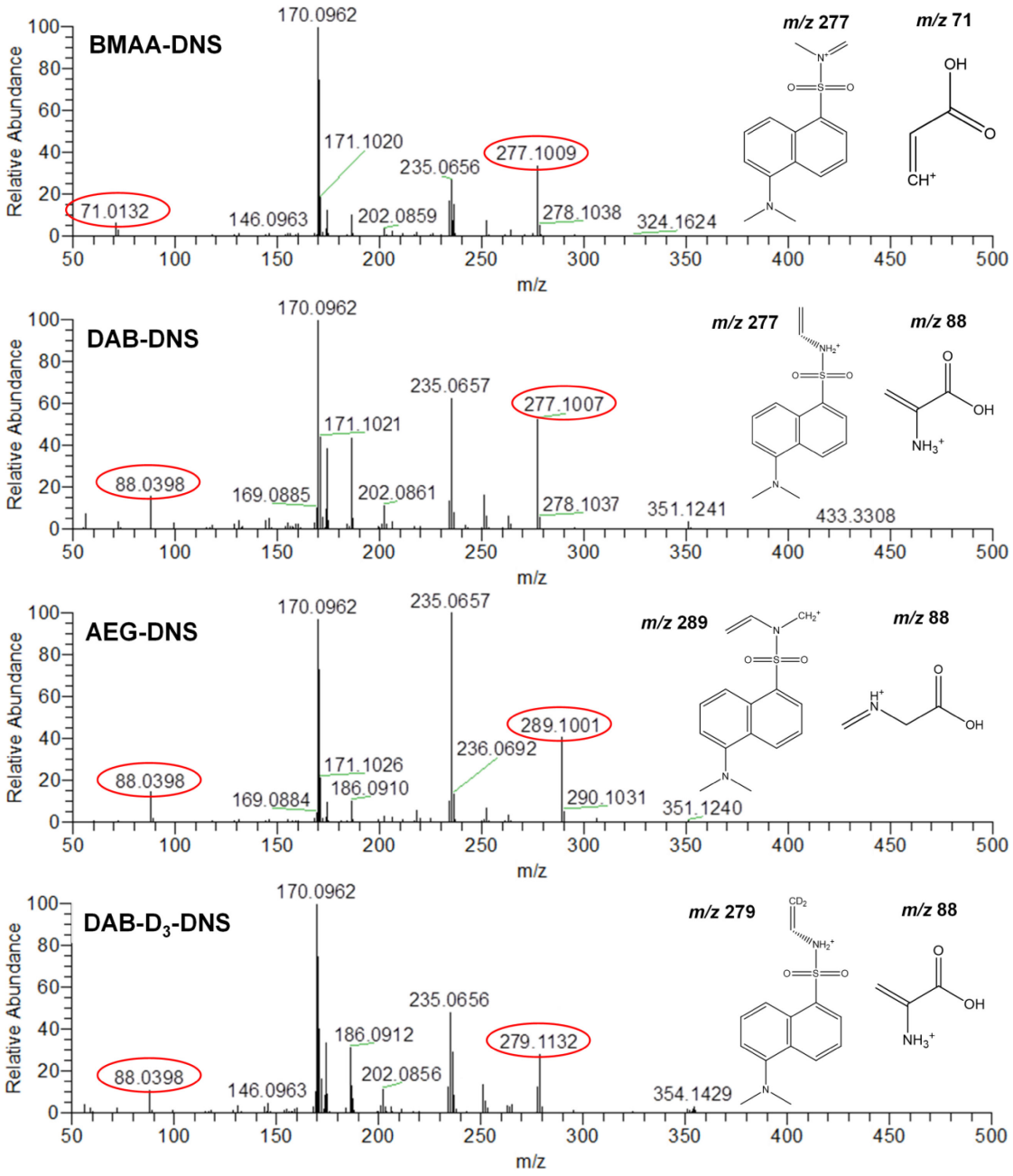


**Figure 3-5.** Fragmentation mass spectra of BMAA-DNS, DAB-DNS, AEG-DNS, and DAB-$D_3$-DNS with the structures of their quantification and confirmation product ions.

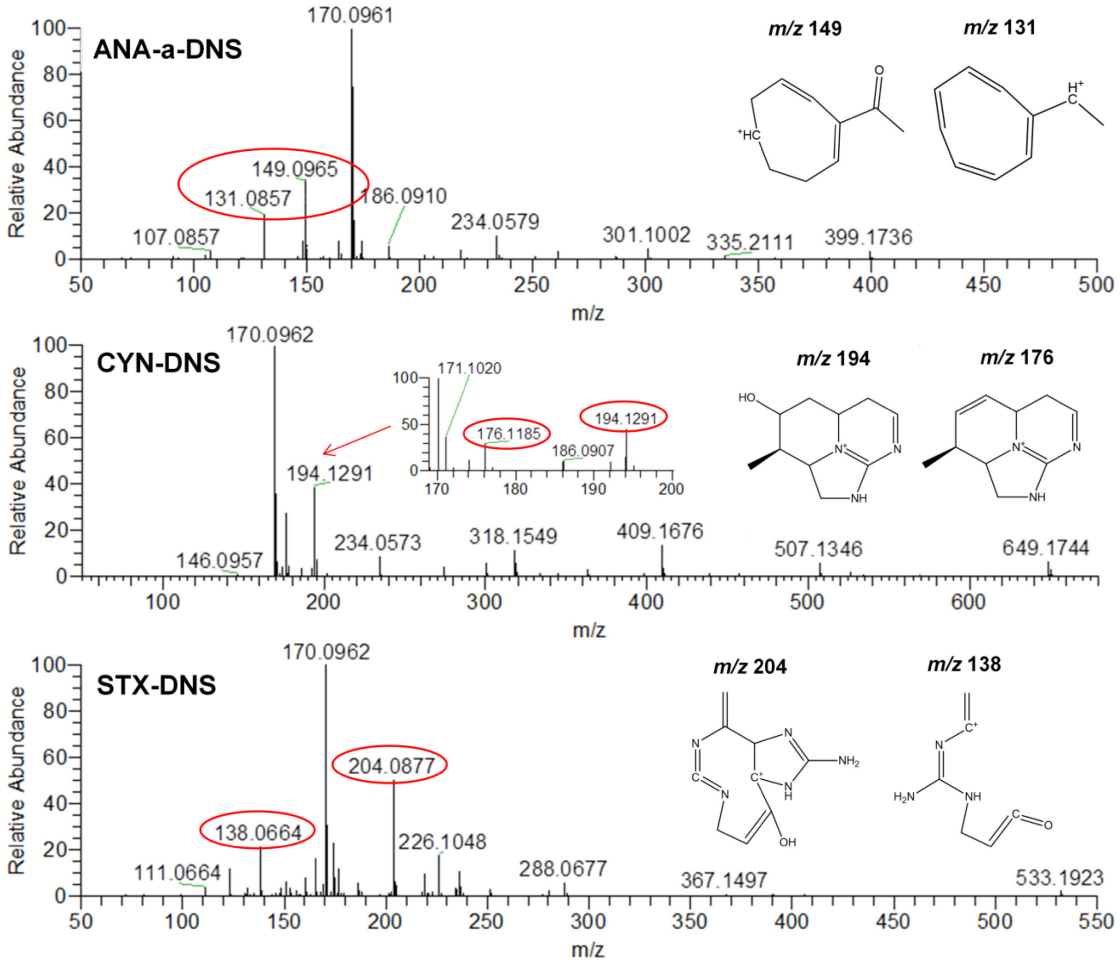


**Figure 3-6.** Fragmentation mass spectra of ANA-a-DNS, CYN-DNS, and STX-DNS with the structures of their quantification and confirmation product ions.

### 3.3.4 Chromatographic separation

A C18 chromatography column was used for the derivative compounds, and the mobile phase included 0.1% formic acid in water and 0.1% formic acid in acetonitrile (ACN). A minimum of 30% of ACN in the beginning of elution was necessary to enable a proper elution of the compounds within the gradient ramp, which was divided in two phases for the same reasons. The gradient was adjusted to achieve the separation of BMAA-DNS and its isomers DAB-DNS, and AEG-DNS. Solvent flow rate, gradients, and elution time were tested, and the parameters were chosen to be optimal for elution time, compounds separation, and compounds peak shape. BMAA-DNS and DAB-DNS were completely resolved; however, chromatographic separation was laborious between BMAA-DNS and AEG-DNS. Therefore,

different chromatographic columns were tested including C18, C8, and phenyl as well as different organic solvents including ACN, MeOH, ethanol, and 2-propanol. Finally, a slow gradient was tested for over 40 min to assess chromatographic separation, without success. Ultimately, to overcome this issue, the use of t-$MS^2$ mode from the Q-Exactive was necessary, and as explained in the previous section, the choice of specific product ions from both derivative compounds enabled selective quantification. The chromatographic separation is illustrated in **Figure 3S-3** for all derivative compounds, and their retention times sustained no significant variation (approximately ±0.02 min) for 4 months of experiments including approximately 1 000 injections on the same column. In the mass inclusion list of the precursor ions, the acquisition time window was set at 1 min center on each retention time of target analytes. Retention time variation was below 0.01 min for 1 day of analysis. The chromatographic run was short with < 4 min for compounds elution and a total of 10 min including the column equilibration. This elution time is similar to the previous UPLC methods with HILIC and reverse phase columns [239, 240]. Finally, the amino acid phenylalanine (PHE), which is considered as an isobaric interference of ANA-a, was derivatized and analyzed to confirm that it would not contribute as a false positive for the detection of ANA-a. Their retention times as DNS derivatives are 3.29 min for PHE-DNS and 3.77 min for ANA-a-DNS making them fully separated, and ultimately, PHE will not interfere during the analysis. If a coelution would have occurred, ANA-a-DNS and PHE-DNS product ions *m/z* values would have been distinguished from each other, given the high resolving power of the Q-Exactive, as explained in a previous study [250].

### 3.3.5 Method validation

The performances of the UHPLC-HESI-HRMS method were evaluated based on these parameters: linearity, sensitivity, precision, accuracy, matrix effects, and selectivity. The matrix effects were previously discussed in the sample treatment section with the evaluation of the SPE treatment. The use of an isotopically labeled internal standard is highly recommended for the quantitative detection of BMAA; the DAB-$D_3$ was then selected according to this criterion. As explained previously, all validation parameters were evaluated using bloom water blanks to take account of matrix effects. A 7-point standard addition calibration curve spiked

prior to the SPE procedure was used with a linearity dynamic range between 0.025 and 2.5 µg $L^{-1}$ analyzed in triplicates. The concentration of DAB-$D_3$ used in every measure was optimized to be 0.75 µg $L^{-1}$ depending on the lowest variability of signal ratios throughout the linearity range of the calibration curve (data not shown). **Tableau 3-3** summarizes the validation parameters for all the derivative compounds. The calibration curves showed good linearity, with correlation coefficients close to unity ($R^2 > 0.998$). The good linearity throughout the dynamic range confirms the efficiency of the derivatization step for low to high concentrations. The MDL and MQL of the compounds were between 0.007 and 0.01 µg $L^{-1}$ and 0.02 and 0.04 µg $L^{-1}$, respectively, which is a significant improvement compared with previous studies using analytical methods for the analysis of BMAA in water bodies, which ranged from 0.2 µg $L^{-1}$ and higher [112, 231, 240]. Chromatograms of the different derivative compounds spiked at their respective MDL are shown in **Figure 3-7**. The accuracy and within-day/between-days precisions are presented in **Tableau 3-3** and were evaluated using three different concentrations to be representative of the linearity range (0.05, 0.25, and 1.25 µg $L^{-1}$). The accuracy, expressed as the relative errors (RE %), ranged between 2 and 11%, within-day repeatability and between-days reproducibility, expressed as relative standard deviations (RSD %) ranged between 2 and 10% and 5 and 15%, respectively.

**Tableau 3-3.** Method validation parameters with accuracy and precision determined at three different concentrations (µg $L^{-1}$).

| Compounds | Accuracy (RE %) | | | Within-day (RSD %) | | | Between-days (RSD %) | | | $R^2$ | Linearity range (µg $L^{-1}$) | MDL (µg $L^{-1}$) | MQL (µg $L^{-1}$) |
|---|---|---|---|---|---|---|---|---|---|---|---|---|---|
| | 50 | 250 | 1250 | 50 | 250 | 1250 | 50 | 250 | 1250 | | | | |
| BMAA | 8 | 4 | 3 | 5 | 2 | 2 | 9 | 5 | 6 | 0.9992 | 0.02 – 2.5 | 0.008 | 0.02 |
| DAB | 8 | 5 | 2 | 6 | 2 | 3 | 9 | 7 | 7 | 0.9991 | 0.03 – 2.5 | 0.009 | 0.03 |
| AEG | 9 | 3 | 2 | 5 | 4 | 2 | 12 | 8 | 6 | 0.9994 | 0.02 – 2.5 | 0.007 | 0.02 |
| ANA-a | 5 | 7 | 3 | 8 | 7 | 4 | 11 | 12 | 8 | 0.9995 | 0.02 – 2.5 | 0.007 | 0.02 |
| CYN | 10 | 7 | 5 | 8 | 9 | 7 | 13 | 11 | 12 | 0.9990 | 0.03 – 2.5 | 0.01 | 0.03 |
| STX | 11 | 8 | 6 | 10 | 8 | 6 | 15 | 14 | 11 | 0.9989 | 0.04 – 2.5 | 0.01 | 0.04 |

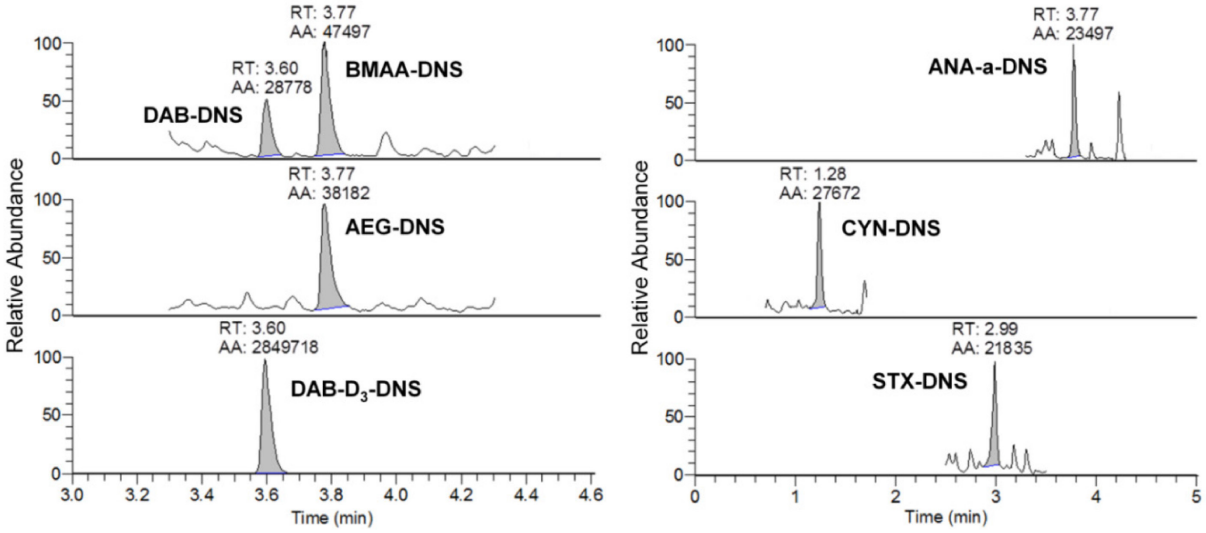


**Figure 3-7.** Chromatograms of DNS derivatives using UHPLC-HESI-HRMS method. Standards were spiked at their detection limit and internal standard (DAB-$D_3$) was spiked at 100 µg $L^{-1}$ in bloom water blank samples.

The analytical method was tested on cyanobacterial bloom samples, which contained harmful algal blooms assessed by the MDDELCC. The samples were from 12 different lakes around the province of Québec during the algal proliferation season, and results are shown in **Tableau 3-4**. STX was absent in all the samples, which is not unusual since this toxin is produced by very specific genera of cyanobacteria and its presence is knowingly less frequent than other cyanotoxins. CYN was found in two samples, with 0.1 and 0.2 µg $L^{-1}$. As for ANA-

a, it was found at low concentrations ranging from 0.02 to 0.2 μg $L^{-1}$ in six samples. Finally, our main target, the nonproteinogenic amino acid BMAA, was found in four samples at low concentrations ranging from 0.01 to 0.3 μg $L^{-1}$. On the other hand, DAB and AEG were found in other samples, at relatively lower concentrations ranging from 0.008 to 0.04 μg $L^{-1}$ for DAB and from 0.009 to 0.08 μg $L^{-1}$ for AEG. Chromatograms of the real samples 8 and 12 are presented in **Figure 3-8** as examples of signals for all the target derivative compounds (except for STX, which was not present in any samples). It was observed that some samples contained BMAA and not AEG, and vice versa. Moreover, using mean peak area ratios of their selected product ions, we can then assume that there were no contribution of signals for each of these two compounds, and ultimately, the developed analytical method can quantitate BMAA with high selectivity. With the use of DNS derivatization, it was possible to develop a selective analytical method for alkaloid cyanotoxins, and the use of HRMS detection gave a selective detection of targeted compounds and a better understanding of their fragmentation.

**Tableau 3-4.** Cyanotoxins detection in lake samples (µg $L^{-1}$) with relative standard deviation (RSD-%).

| No. sample | Location | Date | BMAA | DAB | AEG | ANA-a | CYN | STX |
|---|---|---|---|---|---|---|---|---|
| 1 | Lanaudière | 2009-09-04 | ND | ND | ND | ND | ND | ND |
| 2 | Montérégie | 2009-09-24 | ND | 0.01 (7) | 0.08 (8) | 0.1 (8) | ND | ND |
| 3 | Montérégie | 2009-09-24 | 0.2 (9) | ND | ND | ND | ND | ND |
| 4 | Montérégie | 2009-09-24 | ND | ND | 0.05 (10) | ND | ND | ND |
| 5 | Estrie | 2013-06-14 | ND | ND | ND | 0.08 (9) | ND | ND |
| 6 | Estrie | 2013-06-14 | 0.03 (8) | 0.04 (8) | 0.05 (9) | 0.02 (7) | ND | ND |
| 7 | Saguenay | 2013-06-20 | ND | 0.009 (10) | 0.06 (8) | ND | ND | ND |
| 8 | Saguenay | 2013-06-20 | 0.3 (10) | 0.008 (11) | 0.009 (11) | ND | 0.2 (9) | ND |
| 9 | Abitibi-Témiscamingue | 2013-06-24 | ND | ND | ND | 0.2 (6) | ND | ND |
| 10 | Abitibi-Témiscamingue | 2013-07-31 | 0.01 (8) | ND | ND | ND | ND | ND |
| 11 | Abitibi-Témiscamingue | 2013-07-31 | ND | 0.03 (9) | ND | 0.03 (8) | 0.1 (11) | ND |
| 12 | Montérégie | 2013-08-01 | ND | ND | 0.01 (5) | 0.01 (6) | ND | ND |

ND not detected

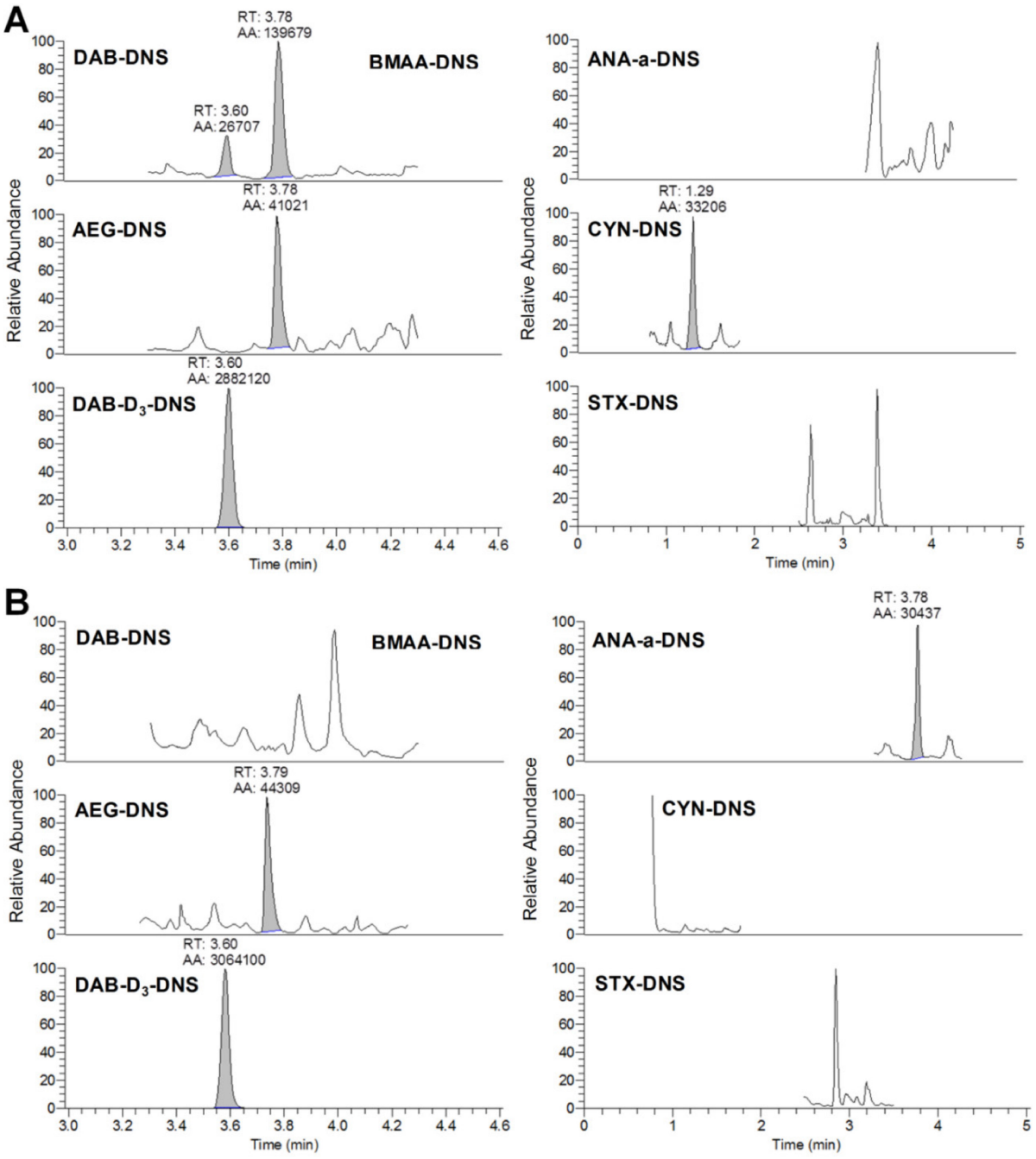


**Figure 3-8.** Example of results for the analysis of A) sample 8 and B) sample 12 analyzed according to the validated method using DNS derivatization and UHPLC-HESI-HRMS analysis.

## 3.4 Conclusion

A new method for the analysis of the nonproteinogenic amino acid BMAA and two of its conformation isomers DAB and AEG, as well as three alkaloid toxins, ANA-a, CYN, and STX, is presented. The use of DNS derivatization permitted easier liquid chromatography with the help of a reverse phase column. With high-resolution detection using the Q-Exactive mass spectrometer in a fragmentation mode (t-$MS^2$), a highly sensitive and selective detection of the toxins was possible, and the structures for the quantification and confirmation product ions of the derivative compounds were proposed using their exact *m/z* values. The chromatographic separation was successfully used with the derivative toxins except for BMAA-DNS and AEG-DNS. However, the use of favored product ions confirmed by their signal ratios permitted selective detection of the two compounds without significant signal contribution. An internal calibration was used with isotopically labeled DAB-$D_3$ and the validated method gave linear correlation coefficients ($R^2$) above 0.998. MDL and MQL for the target compounds ranged between 0.007 and 0.01 µg $L^{-1}$ and 0.02 and 0.04 µg $L^{-1}$ respectively, which is an improvement of one order of magnitude compared to similar analytical methods sensitivity. Accuracy and within-day/between-days variation coefficients for target compounds were below 15%. SPE recovery values ranged between 86 and 103%, and matrix effects recovery values ranged between 75 and 96% showing small signal suppression due to ionisation. The high-resolution detection allowed high mass accuracy, which was below 2 ppm. The developed method was successfully validated for the toxins with concentration found to be between 0.009 and 0.3 µg $L^{-1}$ in 12 tested field-collected samples from lakes where cyanobacterial blooms frequently occur. Only STX was not found in any sample, its presence apparently uncommon in algal blooms. Finally, this new analytical method using DNS derivatization as well as HRMS detection shows great potential for alkaloid cyanotoxins, and could be applied to more complex matrices such as shellfish and sediments, for sensitive and selective detection.

## 3.5 Acknowledgments

The Fond de Recherche Québec Nature et technologies (FQRNT) and the Natural Sciences and Engineering Research Council of Canada (NSERC) are acknowledged for financial support. Marc Sinotte and Christian Deblois from the *Ministère du Développement Durable, de l'Environnement, et de lutte aux changements climatiques,* (MDDELCC – The province of Québec Ministry of the Environment) are acknowledged for providing the samples used in this project and for their scientific support. We thank Thermo Fisher Scientific and Phytronix Technologies for their support. We also thank Paul B. Fayad and Sung Vo Duy for their technical help and scientific support.

## 3.6 Supplementary material

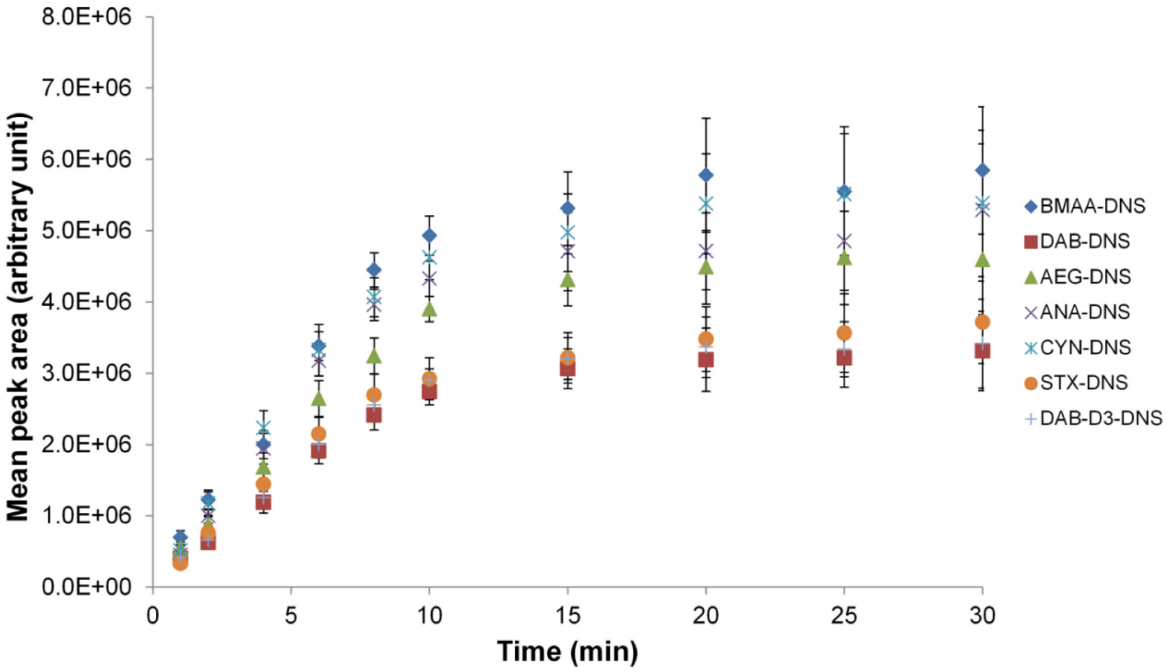


**Figure 3S-1.** Evaluation of the derivatization time with DNS using the variation of the mean peak areas of the target compounds. Vertical error bars represent standard deviations from the mean ($n$ = 3).

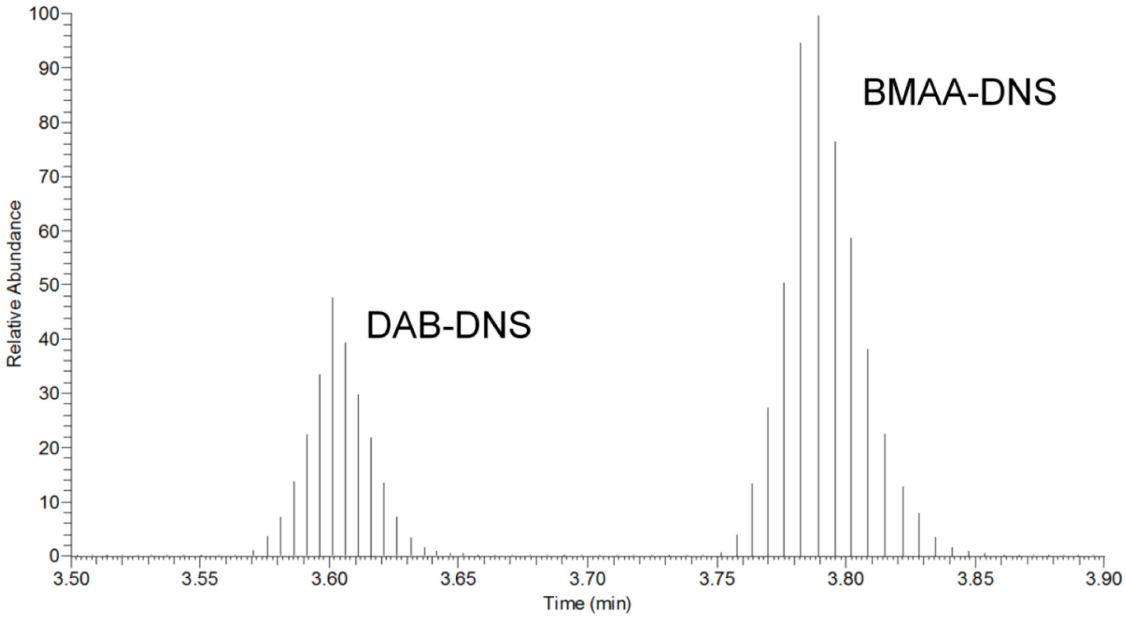


**Figure 3S-2.** Example of the number of data acquisition for DAB-DNS and BMAA-DNS peaks using a resolving power of 17,500 FWHM (*m/z* 200) scanned with the t-$MS^2$ mode.

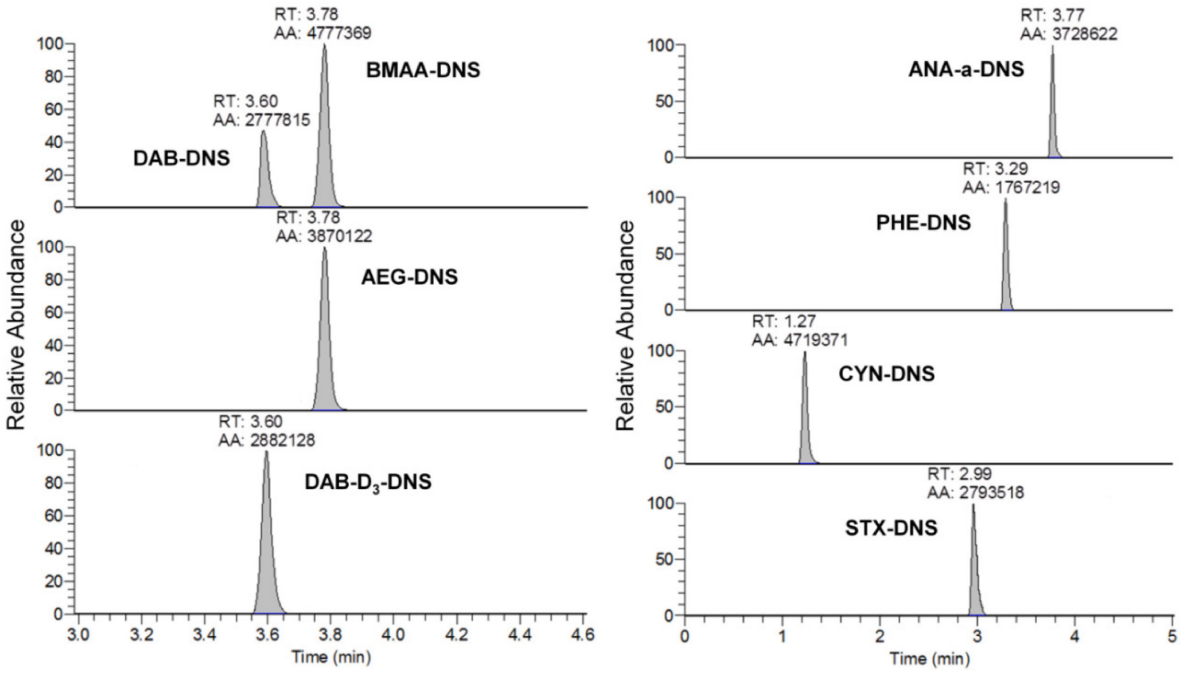


**Figure 3S-3.** Chromatograms of DNS derivatives using UHPLC-HESI-HRMS method. Standards were spiked at (100 µg $L^{-1}$) in bloom water blank samples.

**Tableau 3S-1.** Chemical formulas and calculated exact masses of precursor and fragment ions for derivative compounds.

| Derivative compounds | Chemical formula of precursor ion | Precursor ion exact mass (*m/z*) | Chemical formula of quantitative fragment | Quantitative fragment exact mass (*m/z*) | Chemical formula of confirmation fragment | Confirmation fragment exact mass (*m/z*) |
|---|---|---|---|---|---|---|
| BMAA | $C_{28}H_{32}N_4O_6S_2$+H | 585.18415 | $C_{14}H_{17}N_2O_2S^+$ | 277.10107 | $C_3H_3O_2^+$ | 71.01330 |
| DAB | $C_{28}H_{32}N_4O_6S_2$+H | 585.18415 | $C_{14}H_{17}N_2O_2S^+$ | 277.10107 | $C_3H_6NO_2^+$ | 88.03985 |
| AEG | $C_{28}H_{32}N_4O_6S_2$+H | 585.18415 | $C_{15}H_{17}N_2O_2S^+$ | 289.10107 | $C_3H_6NO_2^+$ | 88.03985 |
| ANA-a | $C_{22}H_{26}N_2O_3S$+H | 399.17424 | $C_{10}H_{13}O^+$ | 149.09664 | $C_{10}H_{11}^+$ | 131.08608 |
| CYN | $C_{27}H_{32}N_6O_9S_2$+H | 649.17505 | $C_{10}H_{14}N_3^+$ | 194.12933 | $C_{10}H_{14}N_3^+$ | 176.11877 |
| STX | $C_{22}H_{28}N_8O_6S$+H | 533.19308 | $C_9H_{10}N_5O^+$ | 204.08854 | $C_6H_8N_3O^+$ | 138.06674 |
| DAB-$D_3$ | $C_{28}H_{29}N_4O_6S_2D_3$+H | 588.20298 | $C_{14}H_{15}N_2O_2SD_2^+$ | 279.11363 | $C_3H_6NO_2^+$ | 88.03985 |

# Chapitre 4. Analyse des microcystines totales dans l'eau utilisant la désorption thermique à diode laser couplée à une ionisation à pression atmosphérique et à la spectrométrie de masse en tandem

Une version de ce chapitre se trouve dans l'article intitulé :

Total Microcystins Analysis in Water using Laser Diode Thermal Desorption-Atmospheric Pressure Chemical Ionization-Tandem Mass Spectrometry

Audrey Roy-Lachapelle, Paul B. Fayad, Marc Sinotte, Christian Deblois et Sébastien Sauvé, *Analytica Chimica Acta,* 2014. **820**; p. 76-82.

**Note sur ma contribution**

Ma participation aux travaux de recherche: J'ai conçu le design expérimental en collaboration avec le Prof. Sauvé et j'ai réalisé les manipulations, l'analyse, l'interprétation des résultats.
Rédaction : J'ai rédigé l'article en m'appuyant sur les commentaires du Prof. Sauvé, mon directeur de thèse.
Collaboration des co-auteurs: Paul B. Fayad m'a assisté dans le développement du projet et la rédaction de l'article, Marc Sinotte a contribué à l'écriture de l'article et Christian Deblois m'a fourni des résultats présentés dans l'article.

# Abstract

A new approach for the analysis of the cyanobacterial microcystins (MCs) in environmental water matrices has been developed. It offers a cost efficient alternative method for the fast quantification of total MCs using mass spectrometry. This approach permits the quantification of total MCs concentrations without requiring any derivatization or the use of a suite of MCs standards. The oxidation product 2-methyl-3-methoxy-4-phenylbutyric acid (MMPB) was formed through a Lemieux oxidation and represented the total concentration of free and bound MCs in water samples. MMPB was analyzed using laser diode thermal desorption-atmospheric pressure chemical ionization coupled to tandem mass spectrometry (LDTD-APCI-MS/MS). LDTD is a robust and reliable sample introduction method with ultra-fast analysis time (< 15 seconds/sample). Several oxidation and LDTD parameters were optimized to improve recoveries and signal intensity. MCs oxidation recovery yield was 103%, showing a complete reaction. Internal calibration with standard addition was achieved with the use of 4-phenylbutyric acid (4-PB) as internal standard and showed good linearity ($R^2$ > 0.999). Limits of detection and quantification were 0.2 and 0.9 µg $L^{-1}$, respectively. These values are comparable with the WHO (World Health Organization) guideline of 1 µg $L^{-1}$ for total microcystin-LR congener in drinking water. Accuracy and interday/intraday variation coefficients were below 15%. Matrix effect was determined with a recovery of 91% showing no significant signal suppression. This work demonstrates the use of the LDTD-APCI-MS/MS interface for the screening, detection and quantification of total MCs in complex environmental matrices.

**Keywords :** Total microcystins, LDTD, APCI, Mass Spectrometry, Cyanobacterial bloom

## 4.1 Introduction

Microcystins (MCs) are cyclic heptapeptide hepatotoxins produced by cyanobacteria, (blue-green algae) and are the most frequently observed cyanobacterial toxins [255]. A cyanobacterial bloom can occur in surface waters rich in nutrients and the toxins can be released from the cells to the natural waters or even in drinking water reservoirs [84, 190]. The cyclic structure of MCs consists of uncommon amino acids, of which two vary from one species to another (X and Z in **Figure 4-1**) thus potentially generating over 80 known MCs structures [6, 190]. The β-amino acid Adda (3-amino-9-methoxy-2,6,8-trimethyl-10-phenyldeca-4(E),6(E)-dienoic acid [256]) is the only part common to all MCs hepatotoxin congeners, and is responsible for their toxicity. This toxicity is caused by the toxin's ability to inhibit specific protein phosphatases in animal tissues, and it is aggravated by its tendency to bioaccumulate in the liver, thus potentially leading to liver failure [12, 257]. MCs $LD_{50}$ ranges from 45 to 1 000 µg $kg^{-1}$ for mice, depending on the specific congener tested [14]. The World Health Organization (WHO) recommends an upper limit of 1 µg $L^{-1}$ for microcystin-LR in drinking water, the most studied and thought to be the most frequently occurring MC [85]. In a recent study, it was mentioned that it was possible to observe significant cyanobacterial bloom within a water treatment facilities, suggesting significant risks of toxin release, thus contributing to high MC concentrations in drinking water [258].

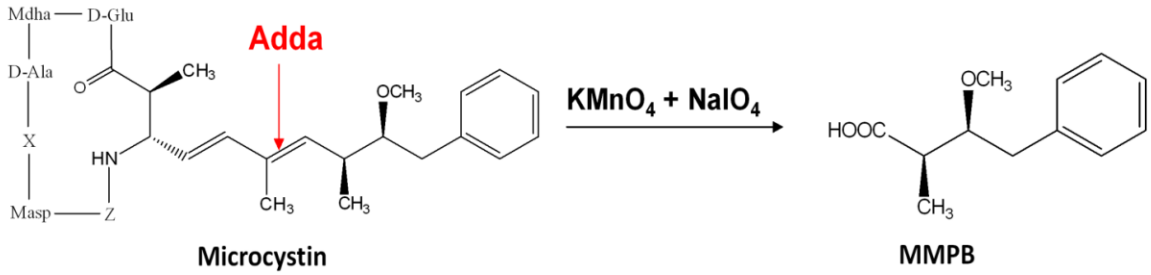


**Figure 4-1.** Reaction scheme of Lemieux oxidation reaction to produce the MMPB used for total microcystin analysis.

There are many techniques available for the screening of MCs in natural water. Solid phase extraction for preconcentration and cleanup and quantification using high-performance liquid chromatography coupled with mass spectrometry (HPLC-MS) is used for the specific analysis of several MCs species [12, 259-261]. However, this analysis is limited to the MCs for which MCs standards are available. Currently, HPLC-MS analysis can roughly detect 10 different congeners over more than 80 possible forms. Gas chromatography coupled with mass spectrometry is used for the analysis of total MCs with the oxidation product 2-methyl-3-methoxy-4-phenylbutyric acid (MMPB) [97, 139, 262]. Since the toxin itself is not volatile enough to be separated by gas chromatography, an oxidation reaction prior to analysis is necessary to obtain the volatile compound MMPB from Adda, a structure common to all the different MC congeners. However, the technique requires an extra derivatization step to make the MMPB more volatile using an ester addition. Traditional chromatography techniques are also time consuming, requiring sample pre-treatment, solid phase extraction and a chromatographic separation which takes several minutes for each analysis, as well as relying on a restricted number of available standards and not taking into account other MCs congeners. In mass spectrometry analysis, MALDI-TOF-MS has also been used recently for the identification of microcystins. However, the technique can be only used for qualitative purposes and the possibility for automated routine HPLC-MALDI interface is still limited for quantification of microcystins [150]. Finally, the most commonly used technique for the nearly instant detection of MCs is enzyme-linked immunosorbent assays (ELISA) [135, 260, 263, 264]. This technique is fast and sensitive, but encounters cross-selectivity which tends to overestimate MCs concentration. The ELISA method mostly uses the microcystin-LR standard, so the quantification assumes that every congener is reacting like MC-LR and results are expressed in MC-LReq.

The laser diode thermal desorption-atmospheric pressure chemical ionization coupled to tandem mass spectrometry (LDTD-APCI-MS/MS) interface is an alternative technique proposed for the quantitative analysis of total MCs. The LDTD is a sample introduction method using thermal desorption, thus eliminating the use of chromatographic separation prior to mass spectrometry detection. This approach results in ultra-fast sample analysis (< 15 seconds/sample) with simple sample preparation, reducing time and material costs otherwise

required for chromatography while also reducing solvent consumption. The LDTD method was previously developed for the analysis of a cyanobacterial neurotoxin, anatoxin-a, in water matrices [159]. It was also developed for several pharmaceutical and pesticide compounds in different environmental matrices including wastewater, sludge, sediments and soils samples [155, 161-163, 265]. The schematic and assembly of the LDTD-APCI source apparatus have been detailed previously [153].

The aim of this study is to develop and validate a new method using the LDTD-APCI-MS/MS apparatus allowing for a simple, rapid and high-throughput detection and quantification of total MCs in complex environmental water matrices. MCs oxidation and MMPB extraction were optimized as a function of the MCs reaction yield and MMPB recovery yield. Several LDTD parameters were studied in order to optimize the thermal desorption and enhance the compound signal; the solvent position, the deposition volume, the laser power, the laser pattern and the carrier gas flow. The method was validated using 4-phenylburytic acid (4-PB) as the internal standard. The method validation was done by evaluating the detection and quantification limits (MDL and MQL), linear dynamic range, accuracy, precision and matrix effect. This ultrafast technique could be used for the quicker screening and quantification of MCs applied for environmental and public health purpose.

## 4.2 Materials and methods

### 4.2.1 Chemicals, reagents and stock solutions

MMPB (2-methyl-3-methoxy-4-phenylbutyric acid) sodium salt standards, 94%, were purchased from Wako Pure Chemical Industries, Ltd. (Osaka, Japan). 4-PB (4-phenylbutyric acid) standard, 99%, was obtained from Sigma-Aldrich (Oakville, ON, Canada). Sodium (meta)periodate (purity ≥ 99,0), sodium bisulfate (A.C.S. reagent), potassium carbonate (purity ≥ 99,0) and sulfuric acid standard solution (1.000 mol $L^{-1}$) were obtained from Sigma-Aldrich (Oakville, ON, Canada). Potassium permanganate (A.C.S. reagent) was obtained from Biopharm (Montreal, Qc, Canada). Methanol (MeOH) and ethyl acetate (EtAc) were of analytical grade purity from Fisher Scientific (Whitby, ON, Canada). Deionized/distilled water (dd-$H_2O$) was used for dilution. Individual stock standard solutions were prepared in MeOH at

a concentration of 100 mg $L^{-1}$ and kept at -20°C for 12 months for the MMPB standards with no significative degradation ($P > 0.5$) and a maximum of 6 months for the 4-PB standards (see supplementary material, **Figure 4S-1**).

### 4.2.2 Cyanobacterial bloom samples

Environmental samples were provided from the monitoring program realized by the *Ministère du Développement Durable, de l'Environnement, de la Faune et des Parcs* (MDDEFP – The province of Quebec Ministry of the Environment) (Québec, Canada). The samples were collected from lakes encountering cyanobacterial blooms and were sampled in glass bottles that were kept in the dark at 4°C until analysis. The lakes were targeted in different regions from the province of Québec, Canada, and were chosen for their high occurrence of cyanobacterial blooms. Microcystins (HilR, HtyR, LA, LF, LR, LR (D-Asp3), LW, LY, RR, RR (D-Asp3), WR, YR) were previously quantified by LC-MS/MS by the Centre d'Expertise en Analyse Environnementale du Québec (CEAEQ), the analytical services of the MDDEFP.

### 4.2.3 Optimization of Lemieux oxidation and MMPB extraction

Microcystins (MCs) were obtained from a cyanobacterial bloom sample where the surface water was sampled. The cells were submitted to freeze-thraw lysis and then filtered with nylon filters of 0.2 µm obtained from Whatman (Florham Park, NJ, USA). Solutions were kept at -20 °C for 6 months. The solutions were analyzed by LC-MS/MS and the MCs (MC-RR, MC-YR, MC-LR, MC-LY, MC-LW and MC-LF) were quantified with a total concentration of 22 mg $L^{-1}$. These MCs were used to optimize the Lemieux oxidation parameters. The reaction scheme of the Lemieux oxidation is presented in **Figure 4-1**. The MCs solutions were spiked into a river water blank matrix to obtain a total MCs concentration of 150 µg $L^{-1}$. All reactions were conducted with $KMnO_4$ (50mM) and $NaIO_4$ (50mM) in alkaline conditions (pH 9) by adding $K_2CO_3$, at room temperature for 1 h, in the absence of light. The reaction was quenched with a saturated sodium bisulfite solution until all the purple color of the solution disappeared. A solution of 10% sulfuric acid was added until the pH

became acidic (~2) [97]. Each reaction test consisted of three replicates and all solutions were conducted with a total volume of 1 mL. A volume of 100 µL of a saturated NaCl solution was added in the aqueous phase to enhance the liquid-liquid extraction. The liquid-liquid extraction was done with 1 mL of EtAc, and then the solutions were submitted to a vortex at 2500 rpm for 2 minutes. The supernatants were then used directly for analysis by LDTD-APCI-MS/MS.

### 4.2.4 Oxidation recovery yield and matrix effect

The sample oxidation recovery yield was measured as the proportion of MCs converted to MMPB and extracted by liquid-liquid extraction. Recovery was determined by spiking blank environmental water matrix with a known amount of MCs (120 µg $L^{-1}$ and 483 µg $L^{-1}$) and of internal standard (4-PB – 150 µg $L^{-1}$) before oxidation and compared to the same blank samples spiked with the corresponding amount of MMPB (25 µg $L^{-1}$ and 100 µg $L^{-1}$) and 4-PB (150 µg $L^{-1}$) after the oxidation and the liquid-liquid extraction with ethyl acetate. The concentration ratios were expressed as recovery percentage. The matrix effect was determined by comparing blank environmental water matrix samples with pure solvent samples both spiked with MMPB (25 µg $L^{-1}$ and 100 µg $L^{-1}$) and 4-PB (150 µg $L^{-1}$). The concentration ratios gave the signal recovery and were expressed in percentage.

### 4.2.5 LDTD-APCI-MS/MS

Desorption and ionization of MMPB and 4-PB were achieved with the T-960 LDTD-APCI interface model, controlled by the LazSoft 4 Software (Phytronix Technologies, Quebec, Qc, Canada) integrated with the Excalibur 2.0 software (Thermo Fisher Scientific, Waltham, MA, USA). Negative mode ionization was achieved with the APCI source. Compound detection was performed using a Quantum Ultra AM triple quadrupole mass spectrometer (Thermo Fisher Scientific, Waltham, MA). Sample solution aliquots for the extraction supernatants (2 µL) were spotted into a LazWell 96-well plate containing inserts made of a thin proprietary stainless steel alloy. The samples were heated at 40°C for 5 minutes until complete evaporation of solvent. Details on the operation of the LDTD apparatus (**Figure 4S-2**) were described in previous studies [153, 155, 159]. Briefly, an infrared laser (980 nm,

20 W, continuous) heats the back of the hexagonal shaped concave well and a thermal desorption of the compounds occurs. The uncharged samples, in gas phase, are transported through a transfer tube by a carrier gas (medical grade purified air) and are then ionized in the APCI corona discharge. The ionized analytes are then transported to the MS detector.

The optimization of the LDTD-APCI parameters was conducted by adding 2 µL of a MMPB (250 µg $L^{-1}$) and 4-PB (150 µg $L^{-1}$) solutions made from blank environmental water matrix subjected to oxidation and extraction to take account of matrix effect. The LDTD-APCI desorption parameters were optimized to the following settings: the maximum laser power used was 35% for the laser pattern (2 s at 0%, 2 s ramping from 0% to 35%, 0.1 s from 35% to 0%, and 2 s at 0% for a total of 6 s), the carrier gas flow rate was 2 L $min^{-1}$ with a temperature of 50°C. The ion source parameters were set with the following settings: ion sweep gas 0.3 (arbitrary unit) and sheath gas, auxiliary gas, skimmer offset and vaporizer temperature were set to 0. Capillary temperature was set to 350 °C with a discharge current of 4 µA in negative ionization (NI) mode.

Selected reaction monitoring (SRM) mode was used, and two product ions for MMPB and 4-PB were selected as quantification and confirmation ions. The quantification ion, with the highest signal intensity, was used to determine the limits of detection and quantification. The relative intensity ratios of product ions, with constant values, were used for confirmation to the targeted compound and to avoid false positives. Optimization of MS/MS parameters was done with the following settings: collision gas (Ar) pressure at 1.5 mTorr, resolution for Q1/Q3 was set at 0.7 amu and scan time was set at 0.005 s. The different SRM transitions and their optimized parameters for the quantification and confirmation of MMPB are shown in **Tableau 4-1**. MMPB and 4-PB structures are presented with their respective fragments in **Figure 4S-3**.

**Tableau 4-1.** Selected reaction monitoring (SRM) optimal parameters for the MMPB analysis by APCI-MS/MS in negative ionization mode (NI) → $[M]^-$.

| Compound | Precursor ion → Product ion *(m/z)* | Collision Energy (V) | Tube Lens (V) |
|---|---|---|---|
| MMPB | 207.1 → 131.1[a] | -15 | -39 |
| | 207.1 → 175.1[b] | -13 | |
| 4-PB | 163.1 → 91.1[a] | -16 | -22 |
| | 163.1 → 119.1[b] | -12 | |

[a] Quantification ion
[b] Confirmation ion

## 4.2.6. Method validation

The method validation was done according to the recommendation of validation protocol for environmental chemistry analysis from the Quebec's MDDEFP guidelines [207]. Data analysis was performed with LCQuan 2.5 software (Thermo Fisher Scientific, Waltham, MA, USA). Internal calibration with standard addition method was used with a seven-point calibration curve, ranging from 1 and 500 µg $L^{-1}$ in triplicates with a bloom matrix submitted to Lemieux oxidation, liquid-liquid extraction and spiked with MMPB and 4-PB. Method detection limit (MDL) and method quantification limit (MQL) were evaluated as 3 and 10 times the standard deviation of the mean value of 10 matrix samples spiked with about 10 times the estimated detection limit (we targeted 10 µg $L^{-1}$). Accuracy was determined by the relative error (RE - %) using the MC spiked bloom sample previously quantified by LC-MS/MS and then quantified by internal calibration with standard addition method. Precision (interday/intraday) and accuracy were expressed as the % relative standard deviation (RSD) and were the evaluated using concentrations of 25 µg $L^{-1}$, 100 µg $L^{-1}$ and 250 µg $L^{-1}$ of MMPB as quality control (QC). The solutions were spiked in a blank river water matrix submitted to oxidation and extraction and analyzed 6 times with internal standard (IS) with a concentration of 150 µg $L^{-1}$.

For a statistical comparison, the Statistical Package for Social Science (SPSS 17.0, Chicago, IL) for Windows was used, when needed, for the ANOVA test as well as the Tukey's post-hoc test with statistical significance defined as $P < 0.05$.

## 4.3 Results and discussion

### 4.3.1 Microcystins oxidation and MMPB extraction optimization

All the Lemieux oxidation parameters were optimized in order to have the best reaction efficiency. It was shown that weakly alkaline conditions (pH ~ 9) were the most efficient for MC oxidation. The different pH conditions during the oxidation reaction were tested between 2 and 10.5; pH 9 was confirmed as the best value (**Figure 4-2a**). Potassium permanganate and sodium periodate concentrations, as well as reaction time, were optimized in order to have the best reaction yield. Each oxidant was tested with a concentration between 10 mM and 100 mM and for each concentration, the reaction lasted between 0.5 h and 5 h. The optimal concentration was set at 50 mM for a reaction time of 1h (**Figure 4-2b**). The use of a higher oxidant concentration could induce compound degradation and provoke higher signal variability. Between 1 to 3 hours for each concentration, no significant reaction yield enhancement was observed ($P > 0.05$) and it was decided to choose the fastest reaction time in order to minimize sample preparation time. It was also important to choose a reaction time that would not induce compound degradation, which was observed after 3 h with higher oxidant concentrations (**Figure 4-2b**). Finally, in several studies, it was shown that the temperature was not a significant parameter when maintained higher than 25 °C for the Lemieux oxidation reaction yield [266]. These results were similar to those of several previous studies [97, 131, 192, 262]. Thus, the optimal reaction conditions used for the determination of total MCs in natural water matrices were using an alkaline condition of pH 9, 50 mM of $KMnO_4$ and $NaIO_4$ each, and a total reaction time of 1 h at room temperature.

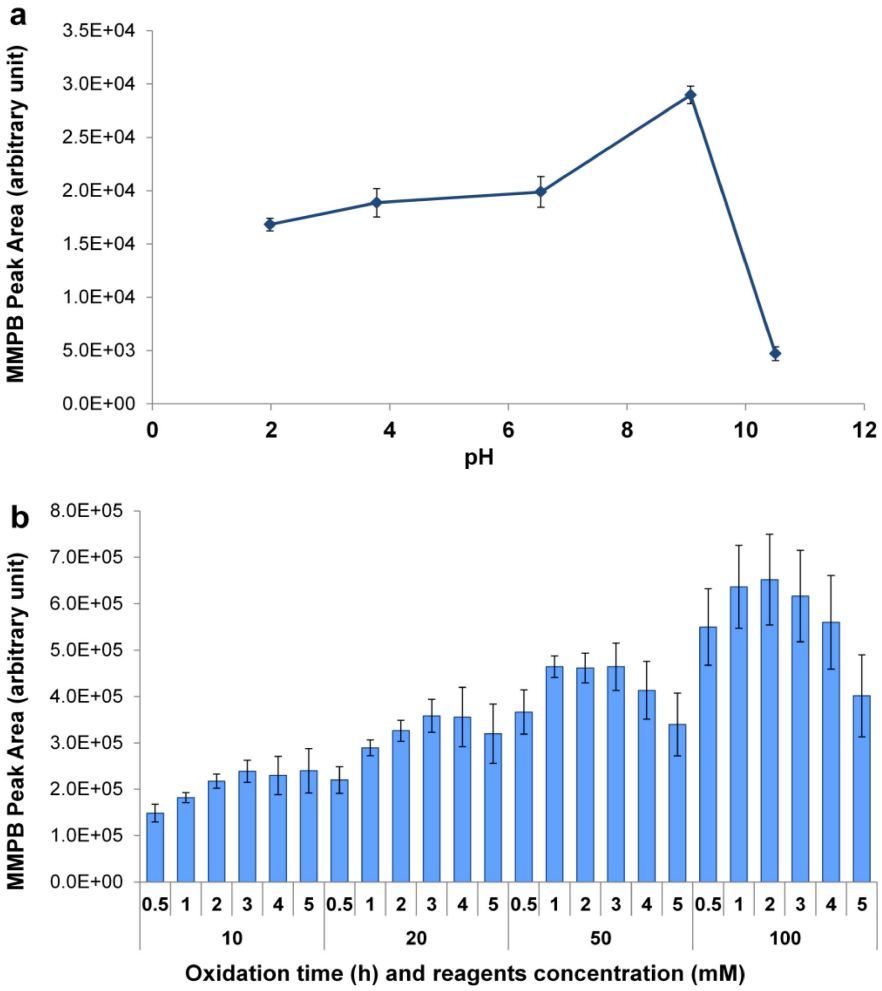


**Figure 4-2.** Different MCs oxidation parameters optimized in order to enhance peak area of the produced MMPB (a) effect of pH between 2 and 10.5 (b) effect of oxidative reagent concentrations (potassium permanganate and sodium periodate) between 10 mM and 100 mM depending on the reaction time between 0.5 h and 5 h, at pH 9. Vertical error bars represent standard deviations from the mean (n=6).

A liquid-liquid extraction was used after MCs oxidation to extract the formed MMPB. Several organic solvents were tested according to their non-miscibility with water; EtAc, hexane, cyclohexane, heptane, diethyl ether, methylene chloride and chloroform. However, only EtAc and hexane showed recovery values for MMPB extraction. Finally, EtAc was chosen as a compromise with the optimal deposition solvent for the LDTD (**S**). To enhance extraction recovery of MMPB and 4-PB, the addition of a solution of saturated NaCl in the

aqueous phase was tested (**Figure 4S-4**). By adding saturated salt in the aqueous phase of the reaction solution, neutral compounds are less soluble and the organic extraction is enhanced [267]. In addition, since the oxidative solution was adjusted to pH 2 following the quenching reaction, the compounds were now in their neutral form which improved the migration from the aqueous phase to the organic phase.

### 4.3.2 Optimization of LDTD/APCI parameters

In order to obtain optimal LDTD desorption and APCI ionization of target compounds, several LDTD parameters were optimized to achieve signal enhancement while minimizing variability. The laser power, laser pattern, deposition solvent, deposition volume and carrier gas flow were all evaluated. All LDTD parameters were optimized in NI mode by spiking 250 µg $L^{-1}$ of MMPB in river water matrix that was subjected to the Lemieux oxidation and liquid-liquid extraction and sample aliquots were deposited in Lazwell plates. Each sample was analyzed 6 times (n=6), in SRM mode using the optimized MS/MS parameters corresponding to parent and fragment *m/z* with indicated optimized tube lens and collision energies (**Tableau 4-1**).

The laser power along with the laser pattern are compound dependent parameters that will have an impact on how the compounds are desorbed when subjected to heat, thus affecting signal intensity. The laser efficiently heats the metal back of the well and some of that energy is transferred to the compounds which are thermally desorbed and transferred by the gas flow to the APCI ionization. The amount of energy transferred is dependent on the laser power setting of the instrument (%), a fairly critical parameter since it must give enough energy to desorb the compound but not so much so as to cause its degradation or fragmentation. Usually, a stable working laser power is obtained with the range of 5 to 65% and this is estimated to correspond to generated well temperature between approximately 50 to 220 °C [154]. Depending on the nature of the matrix, increasing laser power can cause a decrease in signal to noise response because of a higher amount of interfering compounds being desorbed and transferred to the corona discharge along with the compounds of interest [155]. By adjusting the laser ramp pattern and the hold time at maximum laser power, it is

possible to increase the amount of desorbed compounds and control the amount of simultaneously desorbed interfering analytes. For MMPB, these parameters were evaluated by spiking 250 µg $L^{-1}$ of MMPB in blank river water matrix submitted to oxidation and extraction in order to properly consider any matrix interference. The tested parameters were optimized using 6 replicates. Laser power was evaluated between 10 and 60% (**Figure 4-3**). The optimal laser power for maximum compound desorption was set at 35%. Lower laser power did not allow for maximum compound desorption and a higher laser power caused higher variability and decreased signal intensity which we presume can be attributed to heat-promoted compound degradation. Optimized laser pattern was 2 s at 0%, with a ramp of 2 s from 0 to 35%, with no hold time required at maximum power, and a direct decrease of 0.1 s from 35 to 0% with finally 2 s at 0%. **Figure 4-4** shows graphically the laser pattern with its corresponding signal. Overall, with a 6 s LDTD desorption, a chromatogram-like signal is observed covering a time span of less than 15 s. This signal is subsequently quantified the same way a chromatogram would be, illustrating the fast analysis time the LDTD can offer.

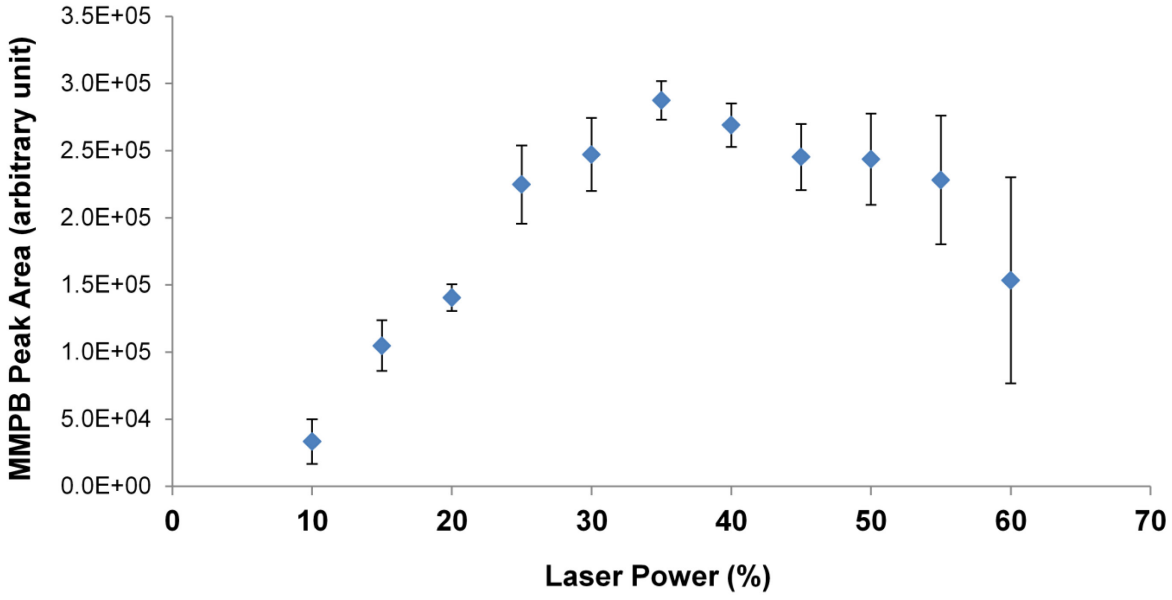


**Figure 4-3.** Effect of LDTD laser power on average peak area of the target compound, MMPB at 250 µg $L^{-1}$. Vertical error bars represent standard deviations from the mean (n=6).

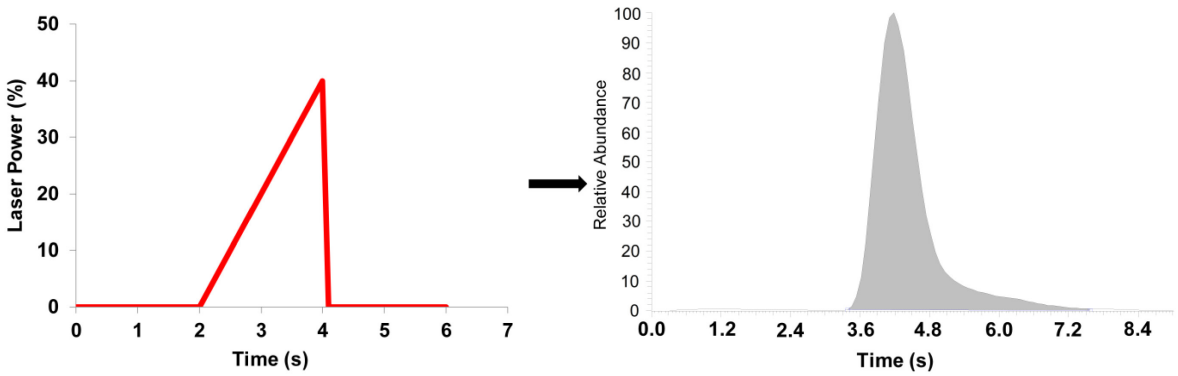


**Figure 4-4.** Illustration of the LDTD laser pattern with its corresponding SRM signal and peak shape obtained using APCI-MS/MS analysis.

Using an adequate deposition solvent is an important parameter affecting compound desorption [155]. Depending on the solvent used for deposition, the nanocrystals formed after drying in the well can have a different effect upon crystallization, repartition into the well and adherence to the metal surface of the well [154]. The compound solubility in a specific solvent can also influence surface well coverage after dryness. If a specific compound is less soluble in a chosen solvent, after deposition in the hexagonal well, it will crystallize first as a donut around the well, therefore, when the laser hits the center of the well, it could be possible that not all analytes will be desorbed because of the heterogeneous crystal formation. Also, depending on the solvent, the shape and superposition of nanocrystals formed after dryness could be different, thus creating several crystal layers with bound analytes hindering total desorption. Many solvents were tested for deposition, and in order to use the same solvent for the optimal MMPB extraction after oxidation, the use of ethyl acetate was deemed most appropriate (**Figure 4-5**).

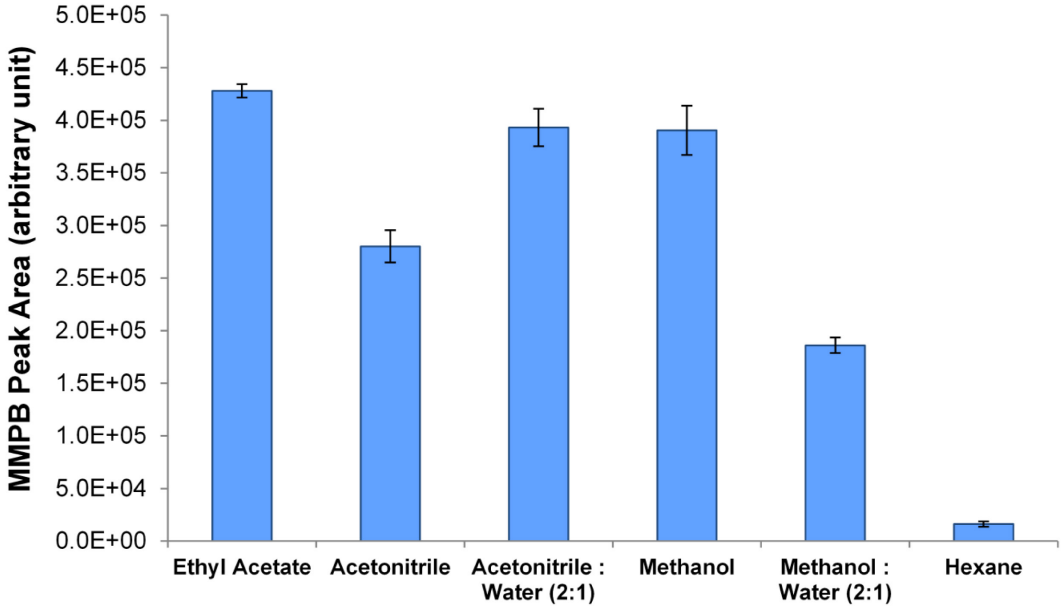


**Figure 4-5.** Effect of using different solvents for the deposition of the analytes in the LDTD Lazwell plate wells with MMPB at 250 µg $L^{-1}$. Vertical error bars represent standard deviations from the mean (n=6).

The sample deposition volume in the wells will influence the amount of analytes thermally desorbed by LDTD. The deposition volume will therefore influence the effectiveness of the APCI ionization and the MS signal intensity of the target compound. Adding a large amount of sample means a higher amount of compounds that would reach ionization, increasing the signal, therefore, increasing sensitivity and enhancing method detection limit (MDL). More compounds in the ionization area can also induce a charge competition during the APCI discharge and also a chance of trapping the compounds into nonvolatile matrix products, all of which would affect signal intensity [155]. The deposition volume was tested between 1 and 8 µL in steps of 1 µL with the spiked matrix. **Figure 4-6a** illustrates the MMPB signal intensity as a function of the deposition volume. The signal response progressively decreases by increasing the volume above 2 µL. These results suggest a signal suppression by matrix effect and this is in concordance with previous work [155, 162]. As a result, 2 µL was set as the optimal deposition volume with significantly higher signal intensity ($P < 0.05$).

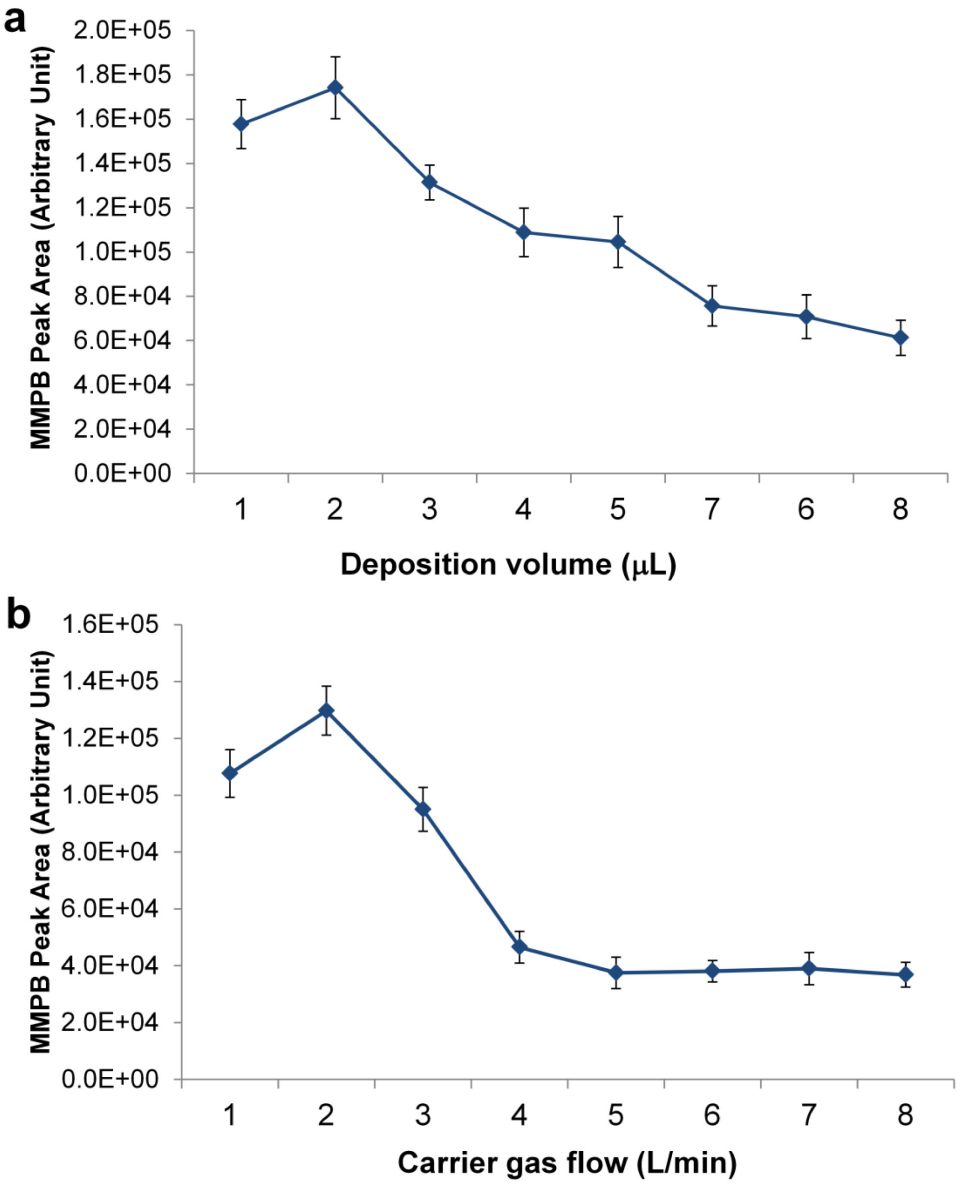


**Figure 4-6.** Average peak area of the target compound, MMPB at 250 µg $L^{-1}$, as influenced by: (a) the deposition volume in the LDTD (1 to 8 µL), and (b) LDTD gas flow (1 to 8 L $min^{-1}$). Vertical error bars represent standard deviations from the mean (n=6).

Carrier gas flow rates have an impact on the transfer of the thermally desorbed molecules to the corona discharge region for ionization. It also allows thermalization of the desorbed and vaporized analytes, thus reducing thermal degradation [164]. Carrier gas flow was optimized between 1 and 8 L $min^{-1}$ (**Figure 4-6b**). This parameter is also optimized for

sensitivity enhancement. Carrier gas flow was optimal at 2 L $min^{-1}$ with a significantly higher signal response ($P < 0.05$), and a significant signal drop occurs above 3 L $min^{-1}$. These results are in concordance with a previous study of BTEX analysis in air where carrier gas flow had an influence on the APCI ionization rate [174]. In fact, it was shown that compound signal intensity was dependent of the residence time in the corona discharge region where ionization occurs. It was also discussed that optimal flow was between 2 and 3 L $min^{-1}$, as high as possible to maximize the mass of analytes but not so fast as to prevent ionization from occurring, as discussed earlier [155, 159, 162-164]. This parameter is not expected to be compound-dependent but rather a physical factor necessary to optimize the ionization in the APCI source. Since LDTD-APCI ionization occurs in dry conditions, the amount of available reactive water molecules becomes an important factor in terms of signal enhancement. In previous work, the possibility of increasing water concentration in the corona discharge area was tested, but had no significant impact above a minimal level [175]. It is therefore important to control the time of residence in the ionization area to optimize ionization rate, thus, allowing sensitivity enhancement.

### 4.3.3 Method validation

We used 4-phenylbutyric acid as IS because of the unavailability of isotopically-labeled MMPB, however, 4-PB has been successfully used in previous work [268]. We used a seven-point internal calibration curve based on a standard addition method of MCs spiked in river water submitted to the optimized oxidation and extraction so as to account for matrix effects and validate the method. Each point of the linear dynamic range (between 1 and 500 µg $L^{-1}$) was analyzed in triplicates. Correlation coefficients showed a good linearity with $R^2 > 0.999$. The precision of the measurements, expressed in terms of relative standard deviation (RSD - %) was deemed satisfactory with 9%. Method detection limit (MDL) and method quantification limit (MQL) were respectively 0.2 and 0.9 µg $L^{-1}$. **Figure 4S-5** shows an example of the LDTD signal at MQL concentration (1 µg $L^{-1}$). The MDL is comparable to other similar analytical techniques ranging from 0.02 to 15 µg $L^{-1}$ [53, 131]. Validation parameters were determined with three concentration levels (25 µg $L^{-1}$, 100 µg $L^{-1}$ and 250 µg $L^{-1}$) with calibration curves and results are shown in **Tableau 4-2**. Accuracy, expressed in

terms of relative error (RE - %), was below 10%. Intraday precision was below 6% and interday precision was below 11%. The Lemieux oxidation reaction yields 103% with a completed reaction and signal recovery of MMPB at 91%, thus showing no significant matrix effect in the analysis. The precision of reaction yield and signal recovery were 7% and 6% respectively. The method was tested on MCs present in an environmental samples from cyanobacterial bloom where the sampled surface water was submitted to a cell lysis, filtered to remove excess cells debris and quantified in parallel by LC-MS/MS. This method was applied to determine the total microcystins present in 9 natural cyanobacterial bloom samples during the proliferation season in order to assess their levels in several water sources. **Tableau 4-3** shows the different results obtained from the quantification of total microcystins using LDTD-APCI-MS/MS. These results are compared with previous analysis of the same samples using standard LC-MS/MS analysis. We observe that for 5 out of 6 samples for which results from both methods were above detection limits, the LC-MS/MS method which is relying on only the 12 MC standards available, significantly underestimated total MCs when compared to LDTD-APCI-MS/MS. For these five samples, the percentage of MC certified and quantified with standards using LC-MS/MS by CEAEQ represents between 15 to 38% of the total MC via MMPB (**Tableau 4-3**). Although CEAEQ had tentatively identified what seem to be isomers of MC-RR and MC-YR, they could not certify them in the absence of the specific standards. When concentrations of MC and MC isomers are added to give Total MC via LC-MS/MS, the results of both methods are quite similar exception made of sample no 8 for which total MC still only represents 22% of MC via MMPB since no congener isomers were detected by the CEAEQ laboratory. Our results show that the presence of isomers of MC or other congeners for which standards are not available could be missed altogether, potentially leading to substantial underestimations of MCs in water samples. Overall, the LDTD-APCI-MS/MS is a robust method that allows high throughput analysis with less than 15 seconds/sample and could be a powerful tool for a fast screening of cyanobacterial toxins including some MC congeners that would otherwise go undetected.

**Tableau 4-2.** Validation parameters using internal calibration with three different concentrations (n = 6).

| QC concentrations (µg $L^{-1}$) | Accuracy RE (%) | Intraday RSD (%) | Interday RSD (%) | Oxidation recovery yield (%) | Signal recovery from matrix effect (%) |
|---|---|---|---|---|---|
| 25 | 10 | 5 | 13 | 109 | 87 |
| 100 | 8 | 6 | 11 | 102 | 90 |
| 250 | 6 | 4 | 9 | 97 | 97 |

**Tableau 4-3.** Comparison of total microcystins analysis of lakes samples using LDTD-APCI-MS/MS and LC-MS/MS.

| No. Sample | Location | Date | Total MC via MMPB (µg $L^{-1}$)[a] (RSD - %) | Total MC with standards (µg $L^{-1}$)[b] | MC isomer without standards (µg $L^{-1}$)[c] | Total MC (µg $L^{-1}$)[d] | Percentage of MC with standards (□)[e] |
|---|---|---|---|---|---|---|---|
| 1 | Estrie | 20130614 | 425 (9) | 70 | 340 (RR[f]) | 410 | 16 |
| 2 | Estrie | 20130614 | 1.0 (5) | 0.15 | 0.5 (RR[f]) | 0.65 | 15 |
| 3 | Saguenay | 20130620 | 5.4 (7) | 1.6 | 3.3 (YR[f]) | 4.9 | 30 |
| 4 | Saguenay | 20130620 | 4.7 (8) | 1.8 | 2.5 (YR[f]) | 4.3 | 38 |
| 5 | Abitibi-Temiscamingue | 20130624 | ND | ND | ND | ND | - |
| 6 | Laurentides | 20130731 | 37.4 (7) | 35.4 | ND | 35.4 | 95 |
| 7 | Abitibi-Temiscamingue | 20130731 | 0.9 (8) | ND | ND | ND | - |
| 8 | Abitibi-Temiscamingue | 20130731 | 2.7 (7) | 0.59 | ND | 0.59 | 22 |
| 9 | Montérégie | 20130801 | ND | 0.1 | ND | 0.1 | - |

ND – Not detected

[a] Total microcystins determined via MMPB using LDTD-APCI-MS/MS.

[b] Microcystins determined via the summation of all microcystins for which standards allowed detection and quantification (i.e. HilR, HtyR, LA, LF, LR, LR (D-Asp3), LW, LY, RR, RR (D-Asp3), WR, YR) using LC-MS/MS.

[c] Microcystin isomer for which identification and concentration could not be certified due to the absence of appropriate standards using LC-MS/MS. Although their characteristics are slightly different from the available standard, there is a very high probability that these are isomers of LC-RR and LC-YR.

[d] Total microcystins determined via the summation of all microcystins for which standards allowed detection and quantification and also for the suspected isomer tentatively identified using LC-MS/MS.

[e] Percentage is calculated as : (MC isomer with standards / Total MC via MMPB) X 100.

[f] Suspected isomer of the specified congener.

## 4.4 Conclusion

A new method for the screening of total microcystins in natural water has been demonstrated and validated using LDTD-APCI-MS/MS. This method uses an oxidation step but this is a simple sample pre-treatment has been kept relatively easy to implement. The MS analysis is simple, fast and allows high-throughput analysis (< 15 seconds/sample). Oxidation and instrumental parameters were optimized in order to enhance sample treatment efficiency and signal response. An internal calibration with standard addition of MMPB and using 4-PB as IS gave an excellent linearity with a correlation coefficient ($R^2$) above 0,999. MDL and MQL were measured to be 0.2 and 0.9 µg $L^{-1}$ respectively. Accuracy and precision were below 10%. Interday and intraday precision were evaluated below 15%. The limit of quantification is below the WHO microcystin-LR guideline for drinking water making the proposed method a useful approach for a rapid total microcystins screening in drinking water, surface waters and water treatment facilities. It could give a fast quantification response prior to applying any LC-MS analysis for characterization of the MCs congeners, eliminating costly and lengthy analysis while providing more selectivity and accuracy than ELISA detection which does not utilize MS/MS detection. The method is based on total MCs and could therefore also identify contaminated samples related to MC congeners which are not usually included in the LC-MS analytical protocol, thus preventing some false negative. The ultrafast analysis combined with a robust quantification and relatively simple sample pre-treatment makes this method a usable alternative for environmental safety and health concerns caused by the presence of microcystins in cyanobacterial blooms occurring in surface waters.

## 4.5 Acknowledgments

The Fond de Recherche Québec Nature et technologies and the Natural Sciences and Engineering Research Council of Canada (NSERC) are acknowledged for financial support. We thank Thermo Fisher Scientific and Phytronix Technologies for their support. We also thank Morgan Solliec, Khadija Aboulfadl, Lucilla Coral and Gabriela Vázquez for their technical help and scientific support.

## 4.6 Supplementary material

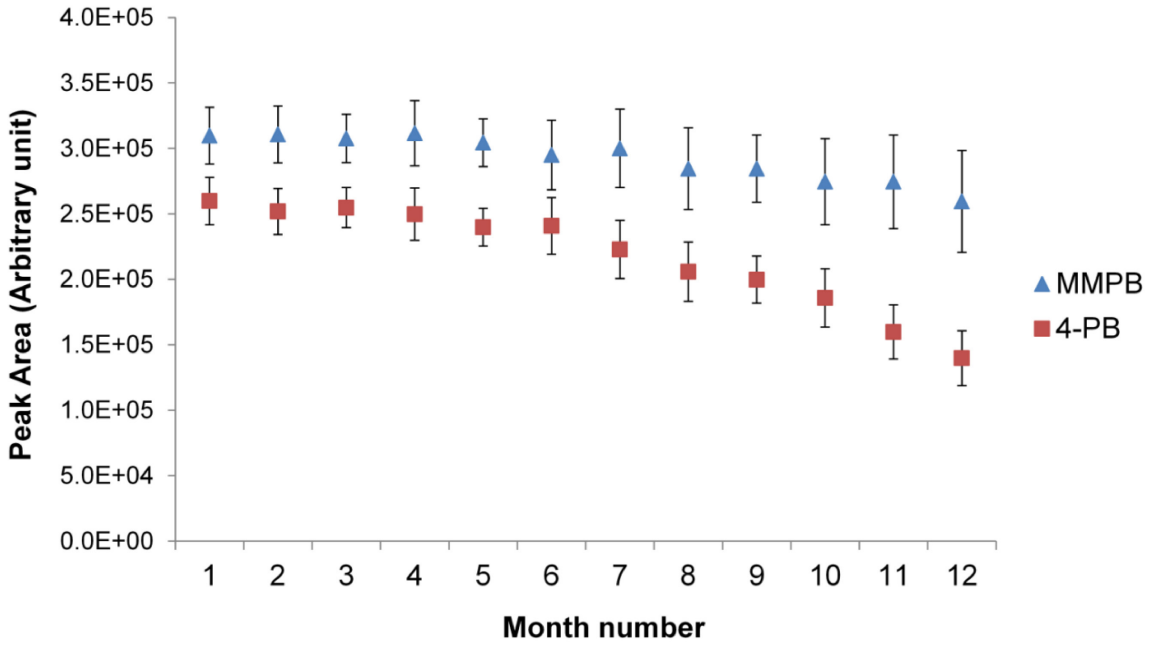


**Figure 4S-1.** Degradation assessment of MMPB and 4-PB over a year at a concentration of 150 µg $L^{-1}$ in ethyl acetate for both compounds. Vertical error bars represent standard deviations from the mean (n=6).

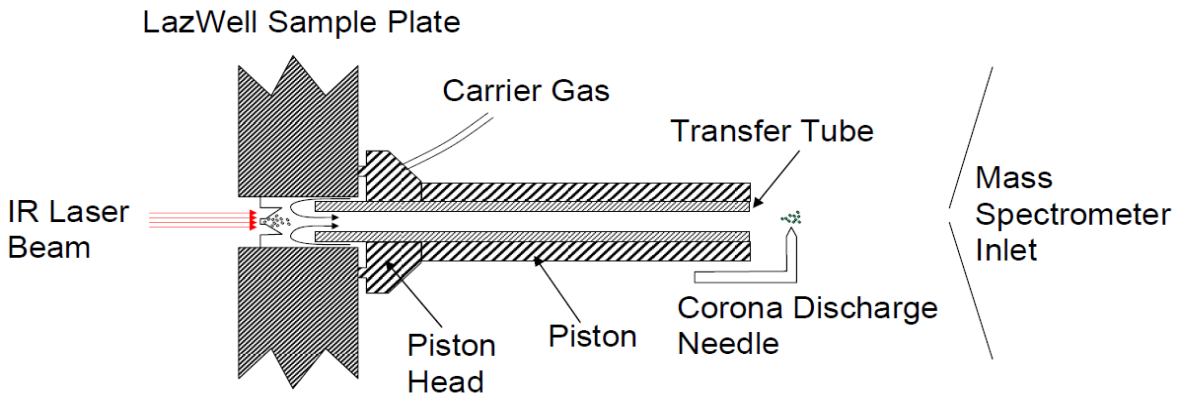


**Figure 4S-2.** Schematic of the LDTD-APCI apparatus.

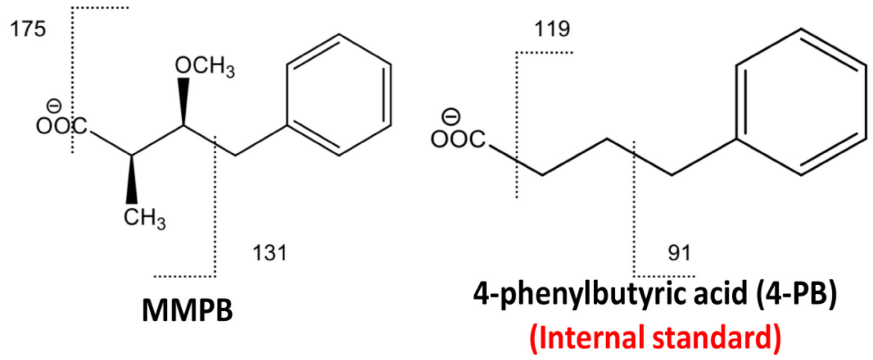


**Figure 4S-3.** Molecular structures of MMPB and 4-PB with their respective SRM fragments.

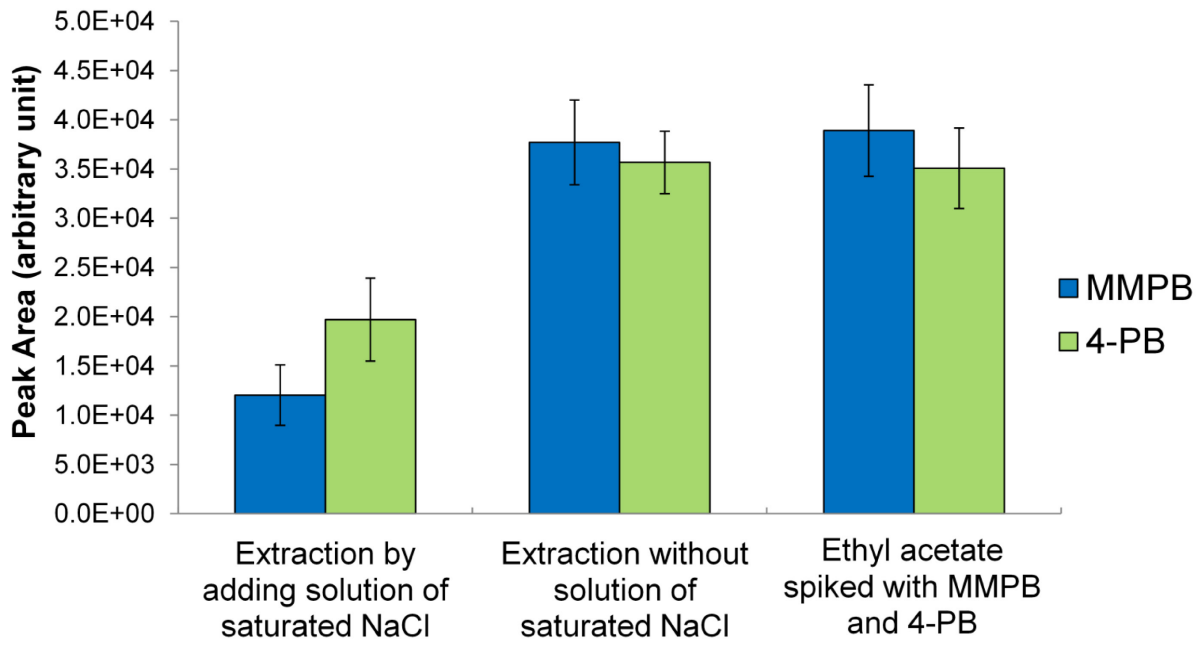


**Figure 4S-4.** Enhancement of liquid-liquid extraction recovery by the addition of a saturated solution of NaCl. Vertical error bars represent standard deviations from the mean (n=6).

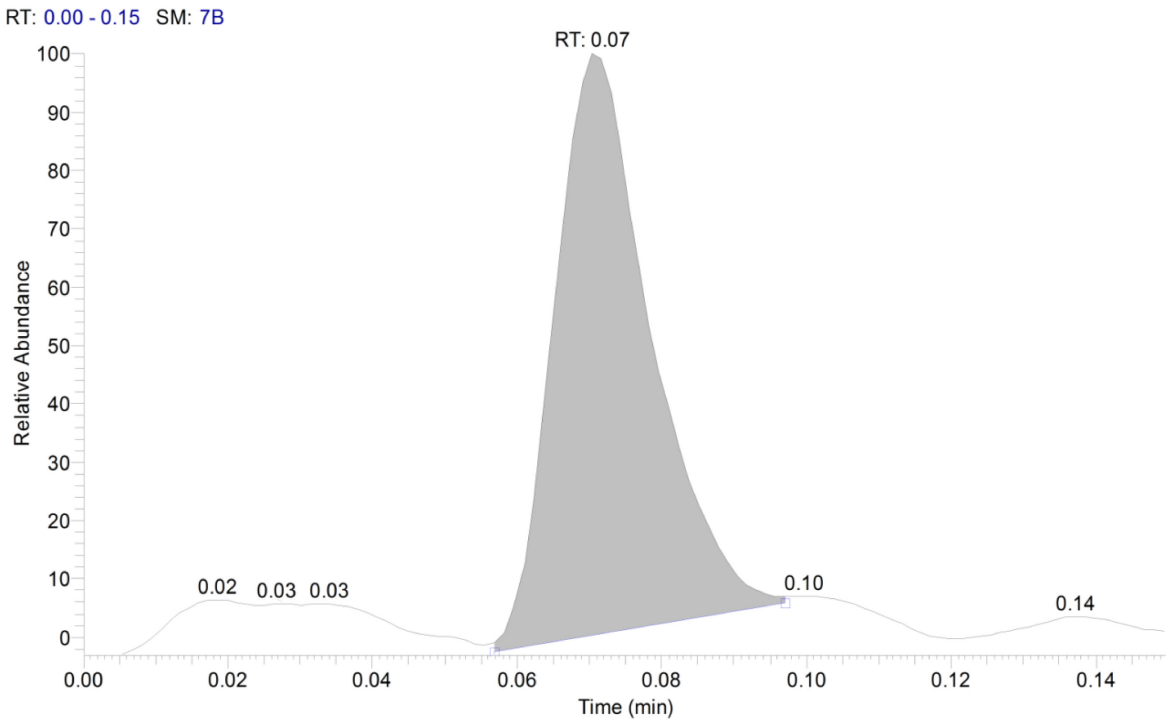


**Figure 4S-5.** Example of a LDTD signal of MMPB at LOQ concentration (1 μg $L^{-1}$).

# Chapitre 5. Détection à haute résolution et masse exacte (HRMS) de l'anatoxine-a dans les eaux de lacs utilisant la LDTD-APCI couplée au spectromètre de masse Q-Exactive

Une version de ce chapitre se trouve dans l'article intitulé :

High Resolution/Accurate Mass (HRMS) Detection of Anatoxin-a in Lake Water Using LDTD-APCI Coupled to a Q-Exactive Mass Spectrometer

Audrey Roy-Lachapelle, Morgan Solliec, Marc Sinotte, Christian Deblois et Sébastien Sauvé, *Talanta,* 2015. **132**; p. 836-844.

**Note sur ma contribution**

Ma participation aux travaux de recherche: J'ai conçu le design expérimental en collaboration avec le Prof. Sauvé et Morgan Solliec et j'ai réalisé les manipulations, l'analyse, l'interprétation des résultats.

Rédaction : J'ai rédigé l'article en m'appuyant sur les commentaires du Prof. Sauvé, mon directeur de thèse.

Collaboration des co-auteurs: Morgan Solliec m'a assisté dans le développement du projet et la rédaction de l'article, Marc Sinotte a contribué à l'écriture de l'article et Christian Deblois m'a fourni des résultats présentés dans l'article.

# Abstract

A new innovative analytical method combining ultra-fast analysis time with high resolution/accurate mass detection was developed to eliminate the misidentification of anatoxin-a (ANA-a), a cyanobacterial toxin, from the natural amino acid phenylalanine (PHE). This was achieved by using the laser diode thermal desorption-atmospheric pressure chemical ionization (LDTD-APCI) coupled to the Q-Exactive, a high resolution/accurate mass spectrometer (HRMS). This novel combination, the LDTD-APCI-HRMS, allowed for an ultra-fast analysis time (< 15 seconds/sample). A comparison of two different acquisition modes (full scan and targeted ion fragmentation) was made to determine the most rigorous analytical method using the LDTD-APCI interface. Method development focused toward selectivity and sensitivity improvement to reduce the possibility of false positives and to lower detection limits. The Q-Exactive mass spectrometer operates with resolving powers between 17 500 and 140 000 FWHM (*m/z* 200). Nevertheless, a resolution of 17 500 FWHM is enough to dissociate ANA-a and PHE signals. Mass accuracy was satisfactory with values below 1 ppm reaching precision to the fourth decimal. Internal calibration with standard addition was achieved with the isotopically-labeled ($D_5$) phenylalanine with good linearity ($R^2 > 0.999$). Enhancement of signal to noise ratios relative to a standard triple-quadrupole method was demonstrated with lower detection and quantification limit values of 0.2 and 0.6 µg $L^{-1}$ using the Q-Exactive. Accuracy and interday/intraday relative standard deviations were below 15%. The new method was applied to 8 different lake water samples with signs of cyanobacterial blooms. This work demonstrates the possibility of using an ultra-fast LDTD-APCI sample introduction system with an HRMS hybrid instrument for quantitative purposes with high selectivity in complex environmental matrices.

**Keywords :** High resolution mass spectrometry, LDTD-APCI, Anatoxin-a, Phenylalanine, Cyanobacteria

## 5.1 Introduction

Cyanotoxins are produced by cyanobacteria, commonly known as blue-green algae. They are encountered in natural waters after the proliferation of a cyanobacterial bloom favored in eutrophic and hypertrophic water [25, 47]. The principal families, with their most studied toxins, are the hepatotoxins (microcystins, nodularins, cylindrospermopsin), the neurotoxins (anatoxin-a, anatoxin-a(s), homoanatoxin-a, saxitoxins, BMAA), the cytotoxins (aplysiatoxin, debromoaplysiatoxin, lyngbyatoxin, cylindrospermopsin) and the endotoxins (lipopolysaccharides) [53, 191]. Among the neurotoxins, anatoxin-a (ANA-a) has a vast distribution with ten cyanobacteria genera responsible for their production - *Anabaena*, *Aphanizomenon*, *Arthrospira*, *Cylindrospermum*, *Microcystis*, *Nostoc*, *Planktothrix* (*Oscillatoria*), *Phormidium* and *Raphidiopsis* [47]. Our main target cyanotoxin, ANA-a, is an alkaloid compound ($pK_a$ 9.4, M.W. = 165.24 g $mol^{-1}$), stable under acidic conditions (pH = 2) but degradable under natural conditions at high pH and in contact with sunlight. Degradation products include the non-toxic metabolites dihydroanatoxin-a and epoxyanatoxin-a [25, 49]. ANA-a is a potent neuromuscular blocking agent with a high toxicity ($LD_{50}$) of 200-250 µg $kg^{-1}$ for mouse, causing irreversible inhibition of the acetylcholinesterase activity and accumulation of acetylcholine in the neuromuscular junctions. High doses of ingested ANA-a can cause continuous stimulation of the respiratory muscles, leading to asphyxiation [51]. Several animal mortality have been regularly attributed to ANA-a for cattle, wildlife, and pets, and some documented confirmations have also been published [196, 197]. Although the World Health Organisation (WHO) has not established guidelines for ANA-a concentrations in drinking and recreational waters, several jurisdictions have implemented such guidelines into their risk management of this neurotoxin. To date, Canada and New Zealand tolerate concentrations below 3.7 µg $L^{-1}$ and 6 µg $L^{-1}$ respectively in drinking water. In addition, three U.S. states, California, Oregon and Washington, tolerate concentrations from 1 µg $L^{-1}$ for drinking water and as high as 100 µg $L^{-1}$ for recreational waters [86]. Lower amount of ANA-a are produced in natural blooms compared to other cyanotoxins (e.g. microcystins), but due its non-negligible toxicity, it is important to assess the presence of the toxin in drinking and recreational waters for public and animal safety [53, 269].

Most of the techniques developed for the detection of ANA-a are based on liquid chromatography coupled with tandem mass spectrometry (LC-MS/MS).[4, 10-12] Spectroscopic detection methods are avoided mainly for the lack of sensitivity due to the instability of ANA-a in contact with UV light and the impossibility to detect the degradation products [143, 270-272]. Therefore, mass spectrometric detection following a chromatographic separation gives higher accuracy, sensitivity as well as selectivity. Unfortunately, phenylalanine (PHE), an essential amino acid present in natural waters, is an isobaric interference of ANA-a and they cannot be resolved by using a triple-quadrupole mass spectrometer [273]. Indeed, given their similar molecular masses and identical fragmentation prior to mass spectrometric detection, their similar liquid chromatography (LC) retention time can potentially lead to the misidentification of ANA-a. Different LC strategies have been proposed to achieve sufficient separation of ANA-a and PHE, but further work is needed since the required analyses are long and costly [122, 124, 143, 274]. The use of high resolution mass spectrometry (HRMS) for cyanotoxins was presented for the first time by James *et al.* [179] with the study of the fragmentation pathways of ANA-a, using a hybrid quadrupole time-of-flight mass spectrometer (QqTOF-MS) and a quadrupole ion-trap mass spectrometer (QIT-MS). According to the mass difference of ANA-a and PHE, a resolution of 4500 FWHM (full width at half maximum) is needed to achieve a mass separation to 10% valley. These instruments have sufficient resolving power to distinguish the signals compared to the minimal resolution needed [177]. Given the different MS instruments and hybrids, the use of HRMS becomes interesting to reduce the presence of false positives due to isobaric interferences and improve the selectivity of ANA-a detection.

Previously, a technique was proposed using laser diode thermal desorption-atmospheric pressure chemical ionization-tandem mass spectrometry (LDTD-APCI-MS/MS) for the analysis of ANA-a in natural waters [159]. The LDTD is a sample introduction apparatus using thermal desorption prior to atmospheric pressure ionization that significantly reduces the analysis time by eliminating the liquid chromatography step. The analytical approach requires a simple sample preparation method by eliminating the time consuming extraction procedures normally required for ANA-a and it is combined with the LDTD-APCI prior to MS detection allowing for an analysis time of 15 s/sample [47, 155]. This analytical

pathway gave a robust alternative for the high throughput analysis of ANA-a in water containing cyanobacterial blooms. However, the isobaric interference, PHE, was an issue since there is no chromatographic separation before ionization. The problem was solved by the use of a pseudo-separation of both compounds using the LDTD laser power, given that the desorption of ANA-a takes place at a temperature lower than PHE [159].

In order to resolve the PHE interference, a new approach is proposed, the LDTD-APCI-HRMS. It couples the LDTD interface with a high-resolution and accurate-mass (HR/AM) detection using a benchtop Orbitrap mass spectrometer, the Q-Exactive. The Orbitrap is combined to a high-performance quadrupole precursor selection and a higher energy collisional dissociation (HCD) cell, thereby giving a powerful tool for the screening of various compounds in environmental matrices. Moreover, the use of an S-lens increases the ion flux through the quadrupole, improving sensitivity and signal intensity [253]. Various HRMS mass spectrometers are known to be alternatives to triple quadrupole instruments with slightly higher instrument costs [177]. Time of flight (TOF) and QTOF have similar resolving power, up to 40 000 FWHM offering a mass accuracy lower than 5 ppm. On the other hand, Orbitrap and LTQ-Orbitrap instruments have better performances with resolving power up to 70 000 FWHM with mass accuracy lower than 2 ppm [177, 275-277]. Compared to other Orbitrap mass spectrometers, the performances of the Q-Exactive are slightly better with resolving power up to 140 000 FWHM and mass accuracy < 3 ppm with external mass calibration and < 1 ppm with internal mass calibration (use of a lock mass) [248]. Furthermore, the main advantage of the Q-Exactive hybrid resides in the quadrupole mass filter combined with a HCD cell offering the possibility of precursor ion fragmentations analogous to an MS/MS mass spectrometer, thus giving a high specificity in ion selection [187]. The Q-Exactive was previously used for peptides sequencing, metabolomics and relatively few studies explored the possibility of quantifying small molecules in environmental matrices [185, 187, 251]. The aim of this study was to develop and validate a new analytical method for the ANA-a detection in lake water using a novel instrument combination, the LDTD-APCI-HRMS, in order to resolve the isobaric interference from phenylalanine. The possibility to couple the LDTD as a sample introduction prior to detection with the Q-Exactive instrument for higher sensitivity and selectivity is demonstrated. The sensitivity and selectivity

of two different detection modes, full scan (FS) and targeted ion fragmentation (t-$MS^2$) are evaluated with the use of LDTD-APCI for an environmental water matrix. Several HRMS parameters were optimized to enhance mass resolution and accuracy, duty cycle and signal intensity. The method validation is done with the use of deuterated phenylalanine (PHE-$D_5$) as an internal standard. Under these conditions, the method detection limit and quantification limit (MDL and MQL), linear dynamic range, accuracy, precision and matrix effect were determined. The method was applied to real freshwater samples with cyanobacterial blooms and proved to be suitable for ANA-a detection in presence of PHE with a lower MDL relative to the previously developed analytical method using a triple-quadrupole MS instrument [159].

## 5.2 Materials and methods

### 5.2.1 Chemicals and reagents

(±)-Anatoxin-a/furamate salt standard, 99%, was purchased from Abcam Biochemicals (Cambridge, MA, USA). DL-Phenylalanine standard, 99%, was obtained from Sigma-Aldrich Chemical Co. (Oakville, ON, Canada). DL-Phenylalanine (Ring-$D_5$) standard, 98%, was obtained from Cambridge Isotope Laboratories, Inc. (Andover, MA, USA). Sodium hydroxide, 97%, and formic acid, 95%, were purchased from Sigma-Aldrich Chemical Co. (Oakville, ON, Canada). Methanol (MeOH) was of analytical grade purity from Fisher Scientific (Whitby, ON, Canada). Deionized/distilled water (dd-$H_2O$) was used for dilution. Compressed air (Ultra Zero Certified grade; ≤ 2 ppm water) used as carrier gas was purchased from MEGS Specialty Gases, Inc. (St-Laurent, QC, Canada).

### 5.2.2 Stock solution and cyanobacterial bloom samples

The solutions were prepared and stored according to previous protocol with modifications [159]. Stock standard solutions of ANA-a/furamate salt (100 mg $L^{-1}$) were prepared with acidified water (0.1 M formic acid, pH ~ 2) and were stored at -20 °C for a maximum of 4 months. A 100 mg $L^{-1}$ stock solution of DL-PHE was prepared daily in dd-$H_2O$. The DL-PHE-$D_5$ (100 mg $L^{-1}$) stock solution was prepared in dd-$H_2O$ and was stored at -20 °C for a maximum of one month [274]. All working solutions were prepared daily in dd-$H_2O$ with

pH adjusted to 2 with formic acid and diluted in MeOH (50:50 v/v). Environmental samples were provided by the monitoring program realized by the *Ministère du Développement Durable, de l'Environnement, et de lutte aux changements climatiques,* (MDDELCC – The province of Quebec Ministry of the Environment) (Québec, Canada). All targeted lakes were chosen for their high occurrence of cyanobacterial blooms in different regions from the province of Québec, Canada. ANA-a was previously quantified by LC-MS/MS by the Centre d'Expertise en Analyse Environnementale du Québec (CEAEQ), the analytical services of the MDDELCC. The samples were acidified for preservation (0.1 M formic acid, pH ~ 2) and then submitted to a freeze-thaw lysis three times to break the cells walls and leach the toxin, followed by a filtration using 0.45 µm nitrocellulose membrane obtained from Whatman (Florham Park, NJ, USA). The solutions were then prepared the same way as for the working solutions.

### 5.2.3 LDTD-APCI parameters

The desorption and ionisation of ANA-a, PHE and PHE-$D_5$ were performed using the T-960 LDTD-APCI ionization interface model and the instrument was controlled by LazSoft 4.0 software (Phytronix Technologies, Québec, QC, Canada) integrated with the Excalibur 2.2 Software (Thermo Fisher Scientific, Waltham, MA, USA). The LDTD apparatus was described in previous work.[21, 22, 31, 35] Briefly, 2 µL of sample is spotted into a LazWell 96-well sample metal plate. After complete solvent drying at 40 °C (about 5 minutes), the back of the sample well is heated by an infrared laser (980 nm, 20 W, continuous) in the LDTD instrument. After the sample desorption, a carrier gas flow (2 L $min^{-1}$), set at 50 °C to avoid temperature variation, transfers the gas phase molecules to positive APCI ionisation followed by the MS detection. In previous work, we used lower laser power for a pseudo-separation of ANA-a and PHE since the amino acid desorption is substantially decreased with a lower temperature compared to the targeted toxin [159]. In this study, a higher temperature is needed to desorb both compounds since the internal standard is the amino acid PHE labeled with deuterium (PHE-$D_5$). In this manner, tests of different laser powers, from 10 to 60%, were performed by spiking 250 µg $L^{-1}$ of ANA-a and 200 µg $L^{-1}$ of PHE-$D_5$ in blank water matrix from a lake sample (n=6). The laser pattern was optimized to the following settings: 2 s at 0%,

1s ramping from 0% to 45%, 2 s hold at 45%, 0.1 s from 45% to 0% and 2 s hold at 0%, with a total desorption time of 7 seconds per sample. APCI ionization in positive mode is within these parameters: ion sweep gas 0.3, sheath gas, auxiliary gas and skimmer offset are set to 0 (all arbitrary values), vaporizer temperature 0 °C and capillary temperature 350 °C.

### 5.2.4 HRMS parameters

Detection of compounds was performed using a Q-Exactive mass spectrometer controlled by the Excalibur 2.2 Software (Thermo Fisher Scientific, Waltham, MA, USA). Instrument calibration in positive mode was done within 24 hours to avoid mass shifts in detection with a direct infusion of a LTQ Velos ESI Positive Ion Calibration Solution (Pierce Biotechnology Inc. Rockford, IL, USA.). All the Q-Exactive parameters were optimized toward mass resolution and accuracy for better quantification, sensitivity and selectivity. The different optimization tests were performed by spiking 250 µg $L^{-1}$ of ANA-a and 200 µg $L^{-1}$ of PHE-$D_5$ in blank water matrix from a lake sample (n=6). Full scan (FS) and targeted MS/MS (t-$MS^2$) modes were optimized and compared to determine which was best suited for LDTD analysis in environmental water matrices. A lock mass (*m/z* 155.1185 – $C_8H_{14}N_2O$) was chosen from matrix background as internal standard for mass accuracy enhancement during spectral data acquisition. The mass range of FS mode was within *m/z* 100-200. The data were acquired at a resolving power of 35 000 FWHM at *m/z* 200. The automatic gain control (AGC) target for a maximum capacity in C-trap was set at $3 \cdot 10^6$ ions for a maximum injection time of 100 ms. As for t-$MS^2$, a mass inclusion list has to be used including the precursor ion masses and their expected retention time and a time of 0.2 min was set as the total analysis time. The precursor ions are filtered by the quadrupole which operates at an isolation width of 0.4 amu. A resolving power of 17 500 FWHM at *m/z* 200 was used. The AGC target was set at $10^5$ ions for a maximum injection time of 50 ms. All optimized collision energies, precursor ions and fragment ions are shown in **Tableau 5-1**.

**Tableau 5-1.** Parameters of HRMS detection.

| Compound | Ion type | Chemical Formula | Calculated exact mass (*m/z*) | Average experimental exact mass (*m/z*) | NCE[c] (%) | Mass Accuracy[d] (ppm) | Confirmation Ion[e] (*m/z*) |
|---|---|---|---|---|---|---|---|
| ANA-a | Precursor | $C_{10}H_{15}NO+H$ | 166.12319 | 166.1231 | 27 | 0.72 | 167.1253 |
| | Product[a] | $M-NH_3+H$ | 149.09664 | 149.0965 | | 0.67 | 150.0987 |
| | Product[b] | $M-NH_3-H_2O+H$ | 131.08608 | 131.0859 | | 0.68 | 132.0811 |
| PHE-$D_5$ | Precursor | $C_9H_6D_5NO_2+H$ | 171.11819 | 171.1181 | 32 | 0.65 | 171.1202 |
| | Product | $M-NH_3+H$ | 154.09164 | 154.0917 | | 0.70 | 154.0939 |
| PHE | Precursor | $C_9H_{11}NO_2+H$ | 166.08680 | 166.0867 | 31 | 0.72 | 167.0889 |
| | Product | $M-NH_3+H$ | 149.06025 | 149.0601 | | 0.77 | 150.0623 |
| | Product | $M-NH_3-H_2O+H$ | 131.04969 | 131.0496 | | 0.76 | 132.0519 |

[a] Quantification ion (most abundant MS/MS transition)
[b] Confirmation ion (second most abundant MS/MS transition)
[c] Fragmentation energy for precursor ion in HCD cell
[d] Accuracy of average measured mass
[e] Second abundant ion in isotopic pattern

### 5.2.5 Data analysis and method validation

All data treatment was performed using the Excalibur 2.2 Software (Thermo Fisher Scientific, Waltham, MA, USA). The method validation was done according to the recommendation of validation protocol for environmental chemistry analysis from the Québec's MDDELCC guidelines [207]. The second most abundant observed ion was used as confirmation ion for each target compounds in both detection modes (FS and t-$MS^2$) and the isotopic ratio was confirmed with < 10% of intensity variations (**Tableau 5-1**). Two fragment ions, with the highest signal intensity, were selected as quantification and confirmation ions (**Tableau 5-1**) and the relative intensities of their ratios were used for confirmation of the targeted compounds and to avoid false positives. The quantification ion, with the highest signal intensity, was used to establish the limits of detection and quantification. Mass scale stability was assessed by measuring the mass measurement accuracy of each ion (precursors and fragments) for each concentration level of the linear dynamic range of the calibration. Mass accuracy stability of measurements over time was evaluated in FS mode for ANA-a (250

µg $L^{-1}$) over a month for a total of 120 acquisitions. Selectivity was improved with the optimization of the extracted masses from acquisition data, and the mass tolerance was set to 5 ppm (± 2.5 ppm). The masses were selected at three points of a LDTD peak for a target compound, two at the extremities and one at the top. Each concentration level of the internal calibration was analyzed in triplicates using standard addition (ranging from 0.5 to 1 000 µg $L^{-1}$). Seven-point calibration curves were prepared with blank bloom water matrices for validation. The concentration of internal standard PHE-$D_5$, (200 µg $L^{-1}$), was selected for its capacity to correct the signal variation of ANA-a with three different concentrations on the calibration curve, 1, 50 and 750 µg $L^{-1}$ (data not shown). Method detection limit (MDL) and method quantification limit (MQL) were established by calculating 3 and 10 times respectively the standard deviation of the mean value of 6 spiked blank matrix samples (n=6) containing approximately 5 times the estimated concentration for detection limit (1 µg $L^{-1}$). Accuracy, interday/intraday variations, and matrix effects were determined with three different concentrations on the linearity range (1, 50 and 750 µg $L^{-1}$, n=6) in blank relevant matrix. Intraday repeatability was estimated over six weeks. Accuracy values were determined by the relative error (%) and precision values were defined as the relative standard deviation (%). The matrix effect was determined by comparing spiked blank relevant matrix with spiked pure solvent samples and the ratios gave the signal recovery and were expressed as percentage.

All validation parameters were determined for both scan modes (FS and t-$MS^2$) for performance comparison. Statistical comparison was used when needed with the Statistical Package for Social Science (SPSS 21.0, Chicago, IL) for Windows. ANOVA test and Tukey's post hoc tests were used with statistical significance defined as $P < 0.05$.

## 5.3 Results and discussion

### 5.3.1 Solutions pH and LDTD laser pattern optimization

The pH of the working solutions was optimized to consider the presence of PHE-$D_5$ with ANA-a in the samples and therefore increase signal intensity. The $pK_a$ of ANA-a is 9.4 and the $pK_a$'s of PHE, are 2.18 and 9.09 [48, 278]. The effect of the pH on signal intensity was

studied between pH 2 and 13. As shown in supplementary material **Figure 5S-1**, it is found that above neutral pH, signal intensities decrease. First, for ANA-a, it is known that it is unstable in alkaline conditions and degrades into its metabolites [25]. Also, with a pH lower than 9.4, the global charge state is positive, which improves ionization stability and reproducibility prior to MS detection. As for PHE-$D_5$, considering both pKa values, its global charge becomes negative in alkaline conditions with pH higher than 9.1. Finally, the pH in the working solutions was adjusted to 2, for higher stability and to improve the storage conditions of ANA-a.

The LDTD parameters were previously optimized and discussed for ANA-a, including deposition solvent, carrier gas flow and laser pattern including laser power [155, 159, 162]. However, the LDTD laser power was selected in order to have a minimum desorption of PHE without affecting ANA-a. In the proposed method, there is no need to separate the two compounds with laser desorption since the isobaric masses are distinguished through high resolution mass detection. Furthermore, the internal standard PHE-$D_5$, has to be desorbed with the same amount of energy as PHE. **Figure 5-1** presents the new condition results with the same correlation of signal intensity with the laser power (%) of ANA-a and PHE compared to the first optimization [159]. For optimal desorption of both compounds, laser power was set at 45% since PHE-$D_5$ signal does not significantly increase above a laser power of 40% ($P > 0.05$), but ANA-a signal significantly decreases for a laser power above 45% ($P < 0.05$). The parameters were optimized to the following settings: 2 s at 0%, 1s ramping from 0% to 45%, 2 s hold at 45%, 0.1 s from 45% to 0% and 2 s hold at 0%, for a total desorption time of 7 seconds. A slightly shorter pattern was used for analysis without affecting the desorption step.

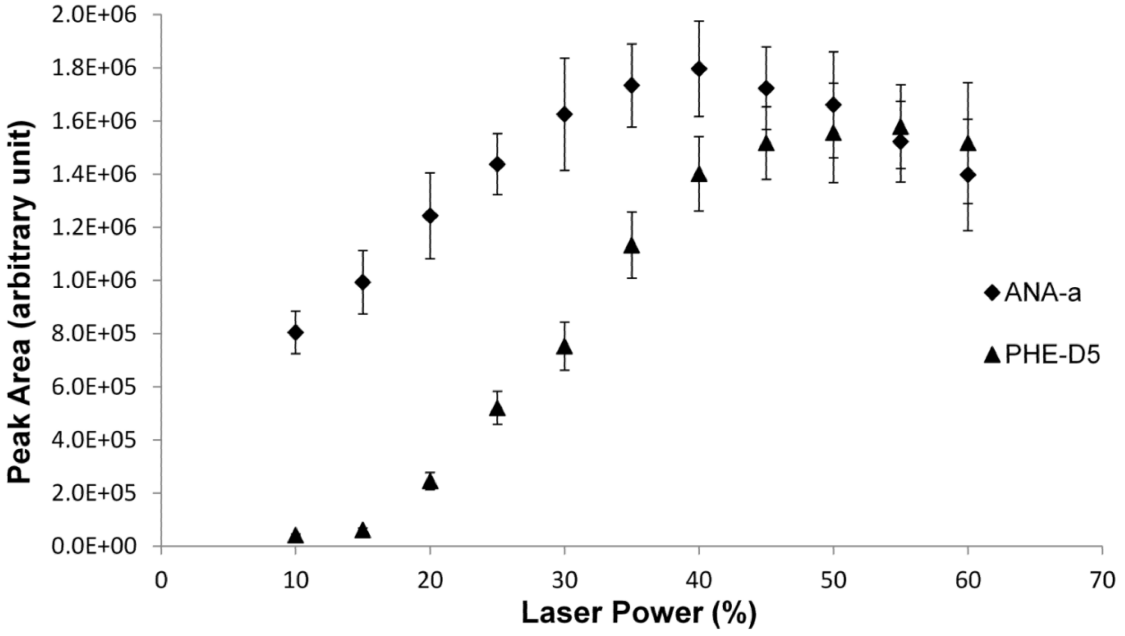


**Figure 5-1.** Effect of LDTD laser power on average peak area of the target compound, ANA-a and PHE-$D_5$. Vertical error bars represent standard deviations from the mean (n=6).

## 5.3.2 LDTD-APCI-HRMS parameters optimization

Signal intensity and selectivity are two major parameters when optimizing an analytical method in complex matrices with low concentrations of target analytes (µg $L^{-1}$ to low ng $L^{-1}$). According to the European Commission, the confirmation criteria for MS/MS detection consists of using two different transitions for a precursor ion. For HRMS detection operated in full scan mode at a resolution higher than 10 000 FWHM, the second-most abundant ion in isotopic pattern must be distinctive with 10% of peak height [279]. The Q-Exactive is a two dimensional Orbitrap and it can thus enhance selectivity using both criteria, thereby reducing the possibility of false positives in complex analytical conditions [254]. The LDTD is a sample introduction technique which eliminates the separation step prior to detection in order to increase sample analysis time as well as sample throughput and there is no criteria given using this apparatus for analysis confirmation with a hybrid HRMS detector. Considering these, the following optimization of different HRMS parameters are presented in both FS and t-$MS^2$ scan modes to determine the optimal detection method using the LDTD-APCI coupled with the Q-Exactive mass spectrometer.

A lock mass is used in HRMS detection, for internal mass correction of the measured accurate mass. According to the manufacturer recommendations, external and internal mass calibrations (with and without lock mass) give mass accuracies of < 1 ppm and < 3 ppm respectively, under defined conditions [248]. A lock mass is selected for its constant presence in samples and its signal must be stable throughout the analysis. **Figure 5S-2** presents the different lock masses used for mass correction and they were selected according to their detection in empty LDTD plate wells, pure solvent blanks and in the bloom water sample matrix background in FS mode (*m/z* 50-300), depending on their abundance and recurrence. The results show the distribution of mass shifts (n=12) of the precursor ion of ANA-a (*m/z* 166.1232) in FS mode including the maxima, minima, quartiles and median corrected with different lock mass target. Each exact masses used are presented with their corresponding molecular formula. Without the use of a lock mass in complex matrix, the mass shift of the target ion is higher than 3 ppm, however, *m/z* 131.1184, 155.1184 and 195.1487 make a significant correction to the accurate measured mass with mass shift lower than 3 ppm. The selected mass was *m/z* 155.1184 according to its capability to permit significant mass correction with mass shift lower than 1 ppm and with less mass variation (RSD < 15%) ($P$ < 0.05).

The Q-Exactive has the ability to temporarily trap the ions in the detector, unlike a triple quadrupole mass spectrometer which operates with a continuous path to the detection. For Orbitrap analyzers, the automatic gain control (AGC) is the total ion population injected and it has to be pre-defined as the AGC target. The injection time (IT) of the population to the detector will vary depending on the number of ions introduced to the mass analyzer. Therefore, the AGC target is selected to have a maximum of target ions travelling to the detector and which compete with the background molecules. Moreover, injection time will affect the duty cycle of the detection, which establishes the number of measurements essential for accurate quantification. A compromise between signal intensity and repeatability is made under specific conditions. For a FS scan, large amounts of background ions are analyzed with targeted compounds so the AGC target should be high enough to “trap” these ions and increase their signal intensity. As for the t-$MS^2$ scans, much fewer ions are transferred to the Orbitrap analyzer, since only targeted precursors are transferred to the C-trap and then

fragmented [185, 253]. **Figure 5S-3** presents the variation of signal intensity of ANA-a and PHE-$D_5$ for different AGC targets with different maximum ion time injections of both FS and t-$MS^2$ scan modes. The selected AGC targets were $3 \cdot 10^6$ ions for a maximum of 100 ms and $10^5$ ions for a maximum of 50 ms respectively. These results were selected in accordance with the previous explanations.

The main novelty of the Q-Exactive mass spectrometer compared to other Orbitrap analyzers is the use of a high-performance quadrupole precursor selection and a HCD cell which enables SIM and MS/MS experiments. The use of a precursor mass filter and fragmentation leads to great improvements of selectivity in complex matrices for a HRMS instrument. As for triple quadrupole mass analysis, two fragments were selected, one for quantification and one for confirmation. The optimized energies with their respective fragments are presented in **Tableau 5-1**.

The selectivity of HRMS analysis is principally determined by the resolving power (RP) and the mass tolerance (MT) [185, 254]. First, using higher RP enables a better mass accuracy, thus a higher selectivity. Yet, increasing the RP decrease the number of acquisitions for an analysis due to duty cycles [254]. For quantitative measurements with acceptable RSDs, it is generally agreed that a LC peak must count at least seven acquisition points [253]. This notion is also considered for a LDTD acquisition peak. The LDTD desorption is faster than a usual elution time for a LC peak for a target compound. Therefore, the number of acquisition points in relation with RP was studied to yield the best compromise between selectivity and repeatability. The tested RP were between 17 500 and 140 000 FWHM (*m/z* 200) for both FS and t-$MS^2$ scan modes with results shown in **Figure 5-2**. As previously explained, the number of acquisition points decreases with the increase of RP for both scan modes. Accordingly, due to a decrease of duty cycle for t-$MS^2$ analysis, less data is acquisitioned. With these criteria, the selected RP for FS scans was 35 000 FWHM (*m/z* 200) and 17 500 FWHM (*m/z* 200) for t-$MS^2$. Second, by narrowing the mass tolerance of a monitored ion in a mass extraction window, selectivity is greatly enhanced by reducing the presence of false positives. However, mass tolerance must consider the accuracy of a target mass given that minimizing a mass tolerance window can eliminate the presence of masses outside the established range. **Figure**

**5-3** presents the optimization of the mass tolerance for the mass extraction of the ANA-a quantification fragment in t-$MS^2$ mode. An adequate mass tolerance was chosen to be 5 ppm (± 2.5 ppm), by comparing mass tolerances between 1 and 10 ppm. With mass windows smaller than 5 ppm, there is a mass distortion and there is no difference on the signal with a larger window. According to Kaufmann *et al.* [254], with FS scans using an Exactive mass spectrometer, the resolving power must be higher than 50 000 (*m/z* 200) with a MT of maximum 5 ppm for a comparable selectivity with conventional MS/MS experiments with SRM acquisitions. Unfortunately, the FS mode using the LDTD-APCI interface, in this case, does not permit quantitative analysis with resolving power higher than 35 000 FWHM (*m/z* 200) because of the limited amount of data points during the acquisition (the peak width is approximately 0.5 sec). On the other hand, considering that the t-$MS^2$ scan mode can be compared to a traditional SRM experiment for its levels of ion selection, the use of a resolving power of 17 500 FWHM (*m/z* 200) with a MT of 5 ppm is more selective than FS acquisitions and should be more selective than a common SRM experiment considering the high mass discrimination.

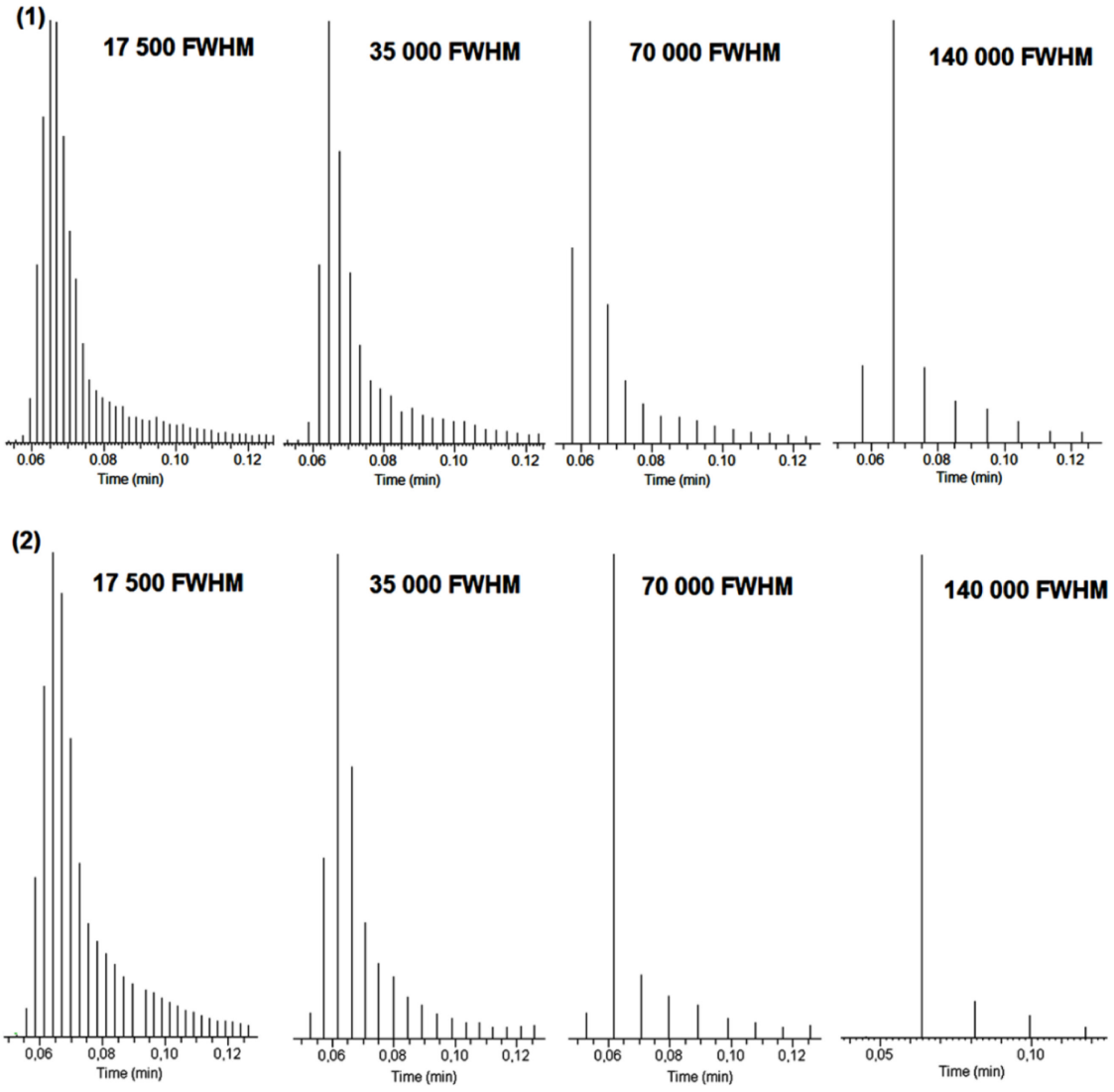


**Figure 5-2.** Examples of the number of data acquisition for a LDTD peak of ANA-a with the different resolving powers scanned by (1) FS mode and (2) t-$MS^2$ mode.

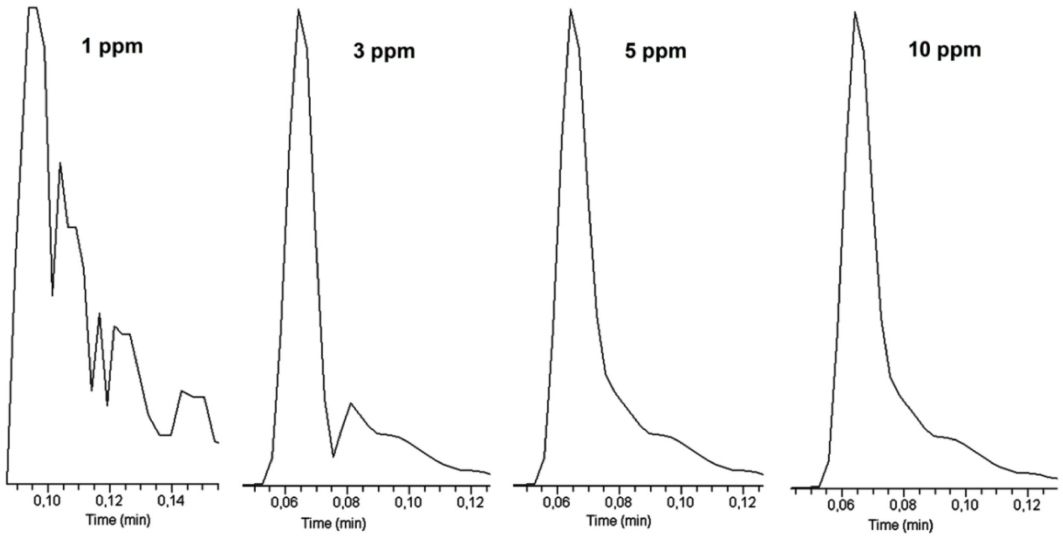


**Figure 5-3.** Effect of different mass tolerances from the mass extraction of the ANA-a quantification fragment (*m/z* 149.0965) by t-$MS^2$ mode and impact on the LDTD peak shape distortion.

### 5.3.3 Data analysis and method validation

To confirm the signal resolution of ANA-a and PHE, a FS data acquisition was recorded at 17 500 FWHM (*m/z* 200). The respective signal of ANA-a and PHE are presented at the left of the mass spectrum (**Figure 5-4**) and they are complete separated. This is in accordance with the resolution needed (> 4500 FWHM) to dissociate the two signals considering their difference in mass values. To the right, the characteristic isotopes of the two compounds appear with relative heights of approximately 10%. The use of isotopically-labeled phenylalanine (PHE-$D_5$) as internal standard was justified by the unavailability of isotopically-labeled ANA-a and by its structural analogy. Moreover, PHE-$D_5$ has also been successfully used as internal standard in previous work [274]. We used a seven-point internal calibration curve based on a standard addition by spiking ANA-a in blank relevant matrix with a linear dynamic range between 0.5 and 1 000 µg $L^{-1}$ analyzed in triplicates. The concentration of PHE-$D_5$ used in every measure is 200 µg $L^{-1}$ and was optimised considering the lowest variability of signal ratio (ANA-a/ PHE-$D_5$) throughout the calibration curve (data not shown). **Tableau 5-2** summarizes the validation parameters for the two experience modes. With the Q-

Exactive operating in t-$MS^2$ (targeted ion fragmentation), the MDL and MQL (n=6) were lower than for the FS (full scan) mode with values of 0.2 and 0.6 µg $L^{-1}$ compared to 0.5 and 1.5 µg $L^{-1}$. Overall, these results are an improvement compared to previous values obtained using a triple quadrupole mass spectrometer which ranged from 1 to 4 µg $L^{-1}$ [159]. Accuracy, expressed as relative errors (RE - %), intraday/interday precisions, expressed as relative standard deviations (RSD - %) and matrix effect expressed as the percentage of signal recovery of replicate measurements (n=6), are summarized in **Tableau 5-3** and were evaluated with three concentration levels from the calibration curve, 1, 50 and 750 µg $L^{-1}$ in blank relevant matrix. Overall, the data showed similar accuracy for both scan modes at higher concentrations with ≤ 15% RE. However, at the lowest concentration, FS mode showed lower accuracy with > 15% RE. The t-$MS^2$ experiment offered less measurement variability (≤ 10% RSD) compared to FS experiment (≤ 15%RSD). As for the signal recovery of ANA-a for FS mode at higher concentrations and for t-$MS^2$ mode for all concentrations, results showed no significant matrix effect in the analysis with values ranging from 96 to 108% with a precision < 15%. However, at the lowest concentration for FS mode, the signal recovery was 172% with a precision of 16% showing that significant signal enhancement due to matrix effect occurs at low concentrations with this scan mode. Two fragments ions of ANA-a were selected and their second most abundant isotope was monitored for ion confirmation to avoid false positives for HRMS analysis (**Tableau 5-1**). The mass accuracy for all ions monitored in HRMS is shown in **Tableau 5-1** and the values were deemed acceptable (0.65-0.76 ppm) compared to instrument standard values for internal calibration with lock mass (< 1 ppm). Mass scale stability is shown in **Figure 5S-4** and mass accuracy variation is stable with average mass accuracies of < 0.8 ppm and RSD variation of < 10%. The assessment of mass accuracy stability of measurements over time is shown on **Figure 5S-5** with 120 acquisitions. An average mass accuracy of < 0.8 ppm with RSD variation of < 15% over 4 weeks of analysis shows an acceptable stability of exact mass measurements. Finally, the developed method was tested on positive cyanobacterial bloom samples of 8 different lakes around the province of Québec, Canada, obtained during the proliferation season. The detection was done with the two optimized scan modes and the selectivity was evaluated by comparing the new quantification approaches with a parallel certified standard LC-MS/MS analysis performed by

the CEAEQ (**Tableau 5-4**). Except for sample no 5, all concentrations were reported below our determined limits of detection (< 0.1-0.01 µg $L^{-1}$). For the t-$MS^2$ analytical method, the only positive sample was no 5, with a concentration of 0.21 µg $L^{-1}$, which is similar to the value reported by the CEAEQ (< 0.2 µg $L^{-1}$). Inversely, the FS method gives considerably higher concentration of ANA-a for samples no 1, 2, 5 and 7 with values ranging from 1.1 to 2.5 µg $L^{-1}$ and these samples had the characteristic of being high in cyanobacteria biomass. The presented results clearly show the presence of false positives in the FS scan analysis and the lack of selectivity of the analytical method. Furthermore, the validation was done with only one sample from the lot. Normally, reported concentrations are very low, around the concentrations of our tested samples. This is in agreement with the low occurrence of ANA-a production in cyanobacterial blooms [47, 53]. Nonetheless, the evaluated MDL and MQL of the present developed method are substantially lower than the pertinent guidelines in Canada (3.7 µg $L^{-1}$) making it a valid approach for the screening ANA-a for risk management purposes. Globally, an analytical pathway using precursor selection and fragmentation is the method of choice for a quantitative detection using the LDTD-APCI-HRMS with the Q-Exactive mass spectrometer instrument with confirmed selectivity and sensitivity. Moreover, high resolution mass spectrometry is a method of choice for the resolution of isobaric interferences as demonstrated with the signal separation of ANA-a and the amino acid phenylalanine.

**Tableau 5-2.** Comparison of method validation parameters for experience modes (FS and t-$MS^2$).

| Experimental mode | $R^2$ | Linearity range (µg $L^{-1}$) | MDL (µg $L^{-1}$) | MQL (µg $L^{-1}$) | Standard avg. RSD (%) |
|---|---|---|---|---|---|
| FS | 0.998 | 1.5 – 1 000 | 0.5 | 1.5 | 10 |
| t-$MS^2$ | 0.999 | 0.5 – 1 000 | 0.2 | 0.6 | 5 |

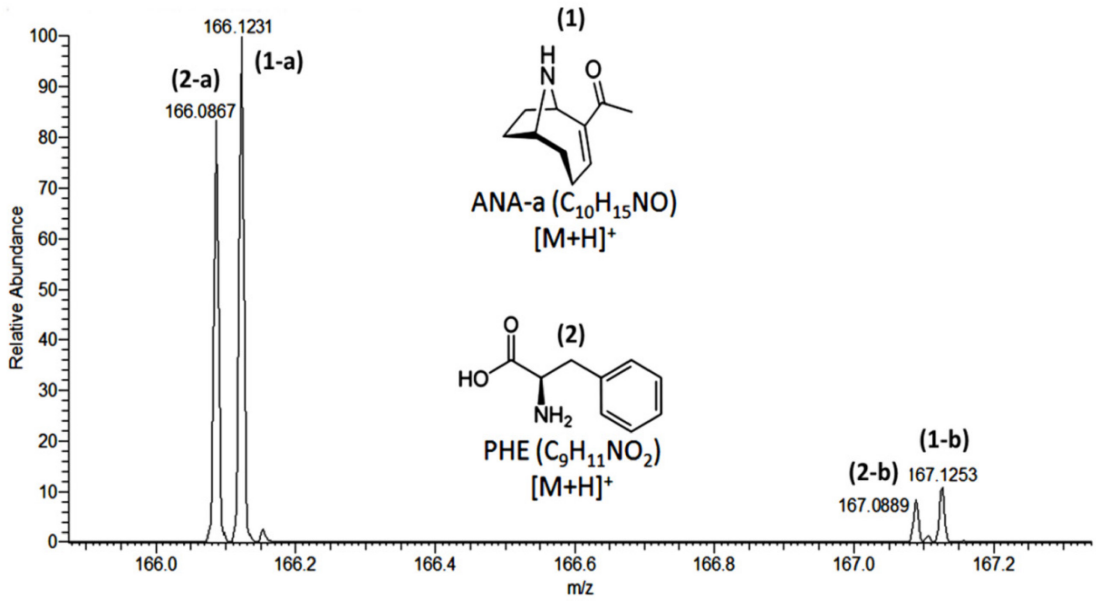


**Figure 5-4.** Mass spectrum of (1) ANA-a and (2) PHE acquisitioned in FS scan mode with a resolving power of 17 500 FWHM (*m/z* 200). (1-a) and (2-a) are the resolved signals and (1-b) and (2-b) are the signals of the first characteristic isotopes of both compounds.

**Tableau 5-3.** Parameters for FS and t-$MS^2$ detection by LDTD-APCI-HR/MS in positive ionization mode (PI) → $[M+H]^+$.

| Experience Mode | QC concentrations (µg $L^{-1}$) | Accuracy (RE %) | Intraday (RSD %) | Interday (RSD %) | Signal recovery from matrix effect (%) |
|---|---|---|---|---|---|
| FS | 1 | 17 | 12 | 15 | 172 |
| | 50 | 13 | 10 | 12 | 108 |
| | 750 | 11 | 11 | 13 | 98 |
| t-$MS^2$ | 1 | 9 | 9 | 8 | 102 |
| | 50 | 6 | 10 | 9 | 96 |
| | 750 | 8 | 8 | 7 | 98 |

**Tableau 5-4.** Anatoxin-a detection in lake samples using LDTD-APCI-HR/MS and LC-MS/MS.

| No. Sample | Location | Date | ANA-a detection FS (µg $L^{-1}$) | ANA-a detection t-$MS^2$ (µg $L^{-1}$) | ANA-a detection by LC-MS/MS (µg $L^{-1}$) |
|---|---|---|---|---|---|
| 1 | Estrie | 2013-06-14 | 2.5 (11) | ND | < 0.1 |
| 2 | Estrie | 2013-06-14 | 1.1 (9) | ND | < 0.02 |
| 3 | Saguenay | 2013-06-20 | ND | ND | < 0.01 |
| 4 | Saguenay | 2013-06-20 | ND | ND | < 0.01 |
| 5 | Abitibi-Témiscamingue | 2013-06-24 | 1.9 (10) | 0.21 (7) | < 0.2 |
| 6 | Abitibi-Témiscamingue | 2013-07-31 | ND | ND | < 0.01 |
| 7 | Abitibi-Témiscamingue | 2013-07-31 | 1.6 (12) | ND | < 0.02 |
| 8 | Montérégie | 2013-08-01 | ND | ND | < 0.01 |

ND – Not detected

## 5.4 Conclusion

A new analytical method was explored, the LDTD-APCI-HRMS, using a mass spectrometric hybrid, the Q-Exactive. This method was successfully used to resolve the misidentification of the cyanobacterial toxin, anatoxin-a, from the essential amino acid, phenylalanine. Two scan modes were explored (FS and t-$MS^2$) to determine the best detection method for selective, sensitive and quantitative analysis. FS mode did not show good results in terms of selectivity given an important presence of false positives in charged complex matrices. On the other hand, the use of t-$MS^2$ greatly increases the selectivity of compound detection. An internal calibration with standard addition was also validated with the isotopically-labeled phenylalanine (PHE-$D_5$) as internal standard. The method was validated and deemed linear with correlation coefficients ($R^2$) above 0.999. MDL and MQL ranged from 0.2 to 1.5 µg $L^{-1}$, and with better sensitivity compared to the previous study of ANA-a analysis using the LDTD-APCI-MS/MS. Accuracy and precision values were below 15% and the signal recovery showed no significant matrix effect with values ranging from 96 to 108% except for FS detection at the lowest concentration which showed a precision higher than 15%

and a signal enhancement with a recovery of 172%. With the use of a lock mass, mass accuracy was below 1 ppm with low variation (< 15%). The LDTD-APCI-HRMS is a powerful tool for the screening of anatoxin-a at lower concentrations than established guidelines (3.7 µg $L^{-1}$) in natural and recreational water with simple sample preparation, fast quantification responses (< 15 seconds/samples), high-throughput analysis and high selectivity. Compared to traditional MS/MS and HRMS detection, the Q-Exactive has the advantage of combining high-performance precursor selection with a high resolution and accurate mass detection. It would be possible, for future work, to adapt this analytical technique for the detection of ANA-a in different matrices such as plant extract and animal tissues given that such performances are attractive for fast trace level detection of contaminants in complex environmental matrices.

## 5.5 Acknowledgments

The Fond de Recherche Québec Nature et technologies and the Natural Sciences and Engineering Research Council of Canada (NSERC) are acknowledged for financial support. We thank Thermo Fisher Scientific and Phytronix Technologies for their support. We also thank Paul Fayad and Sung Vo Duy for their technical help and scientific support.

## 5.6 Supplementary material

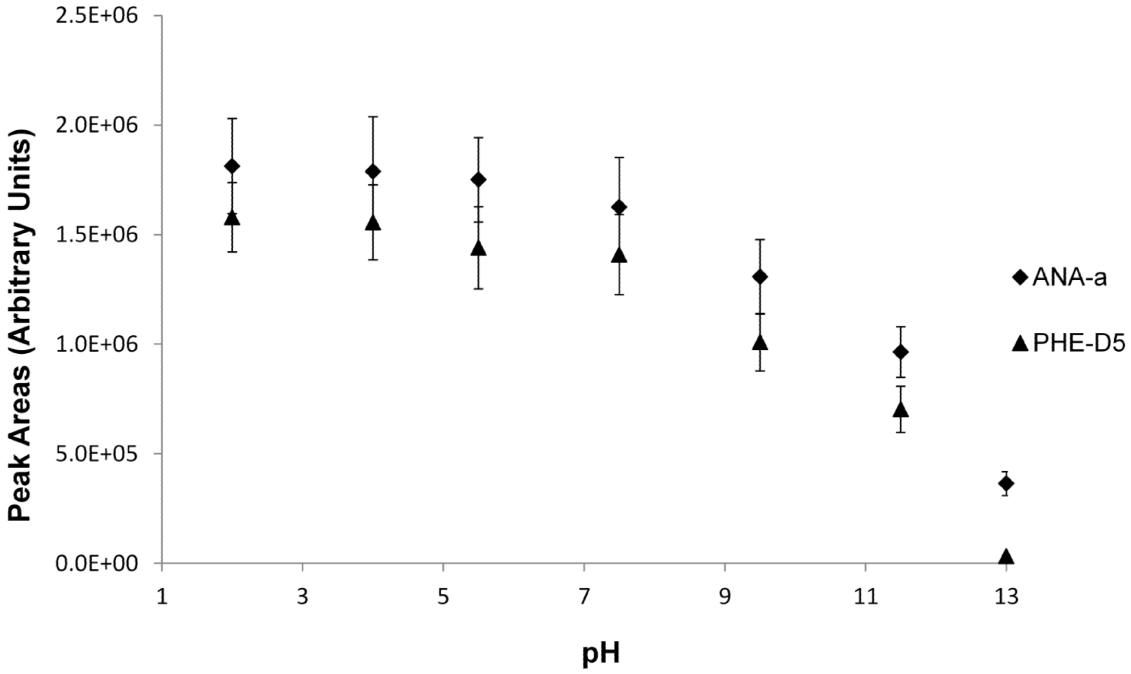


**Figure 5S-1.** pH effect on ANA-a and PHE-$D_5$ signal intensity.

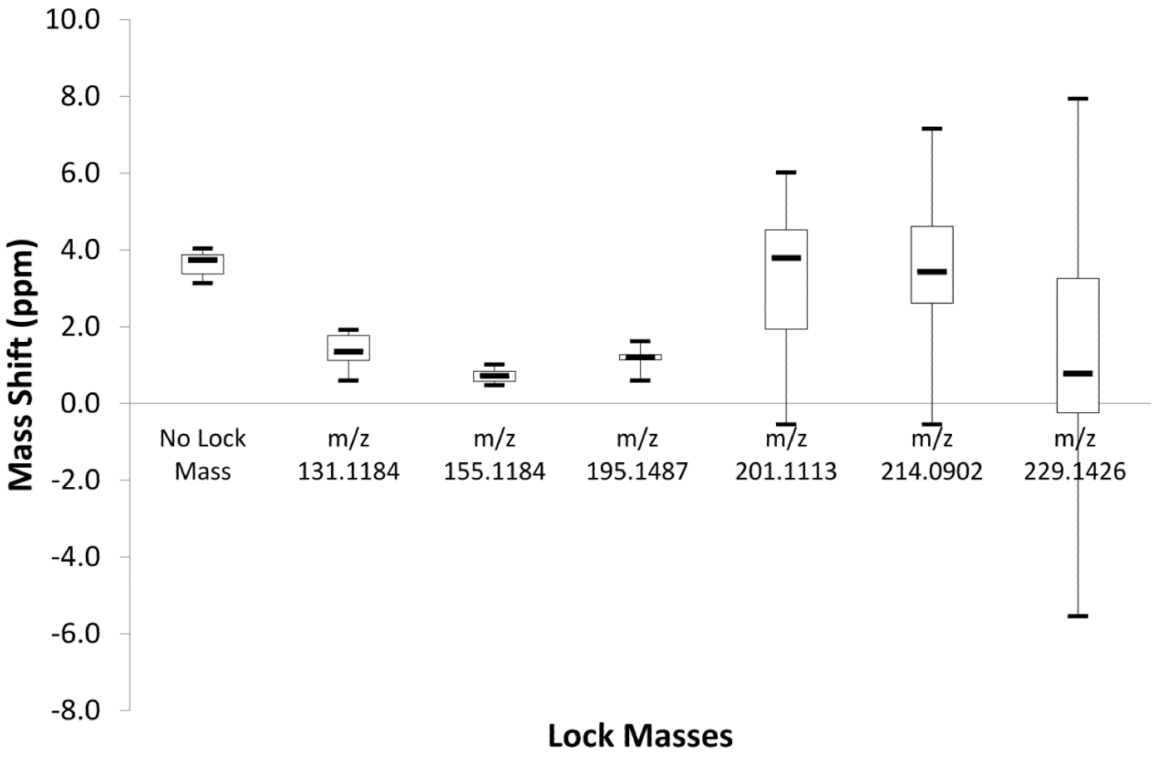


**Figure 5S-2.** Mass errors of ANA-a (*m/z* 166.1231) measured in FS mode corrected with different lock masses. Results include maxima, minima, quartiles and median (n=12).

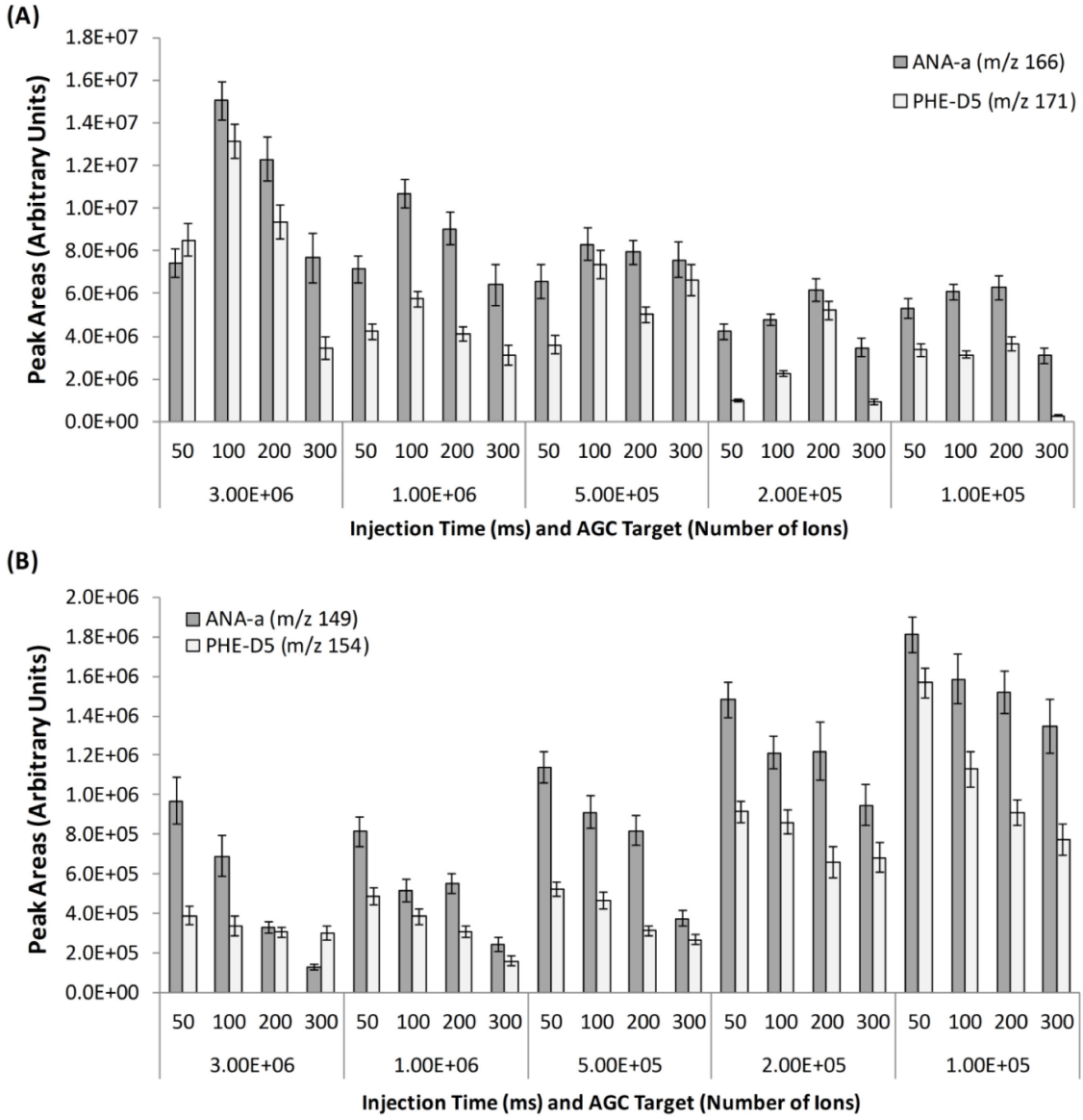


**Figure 5S-3.** Effect of the automatic gain control (AGC) target and maximum injection time (IT) on the quantity of ions going through the ion trap in terms of signal intensity. The experiment was undertaken in (1) FS and (2) t-$MS^2$ scan modes. Vertical error bars represent standard deviations from the mean (n=6).

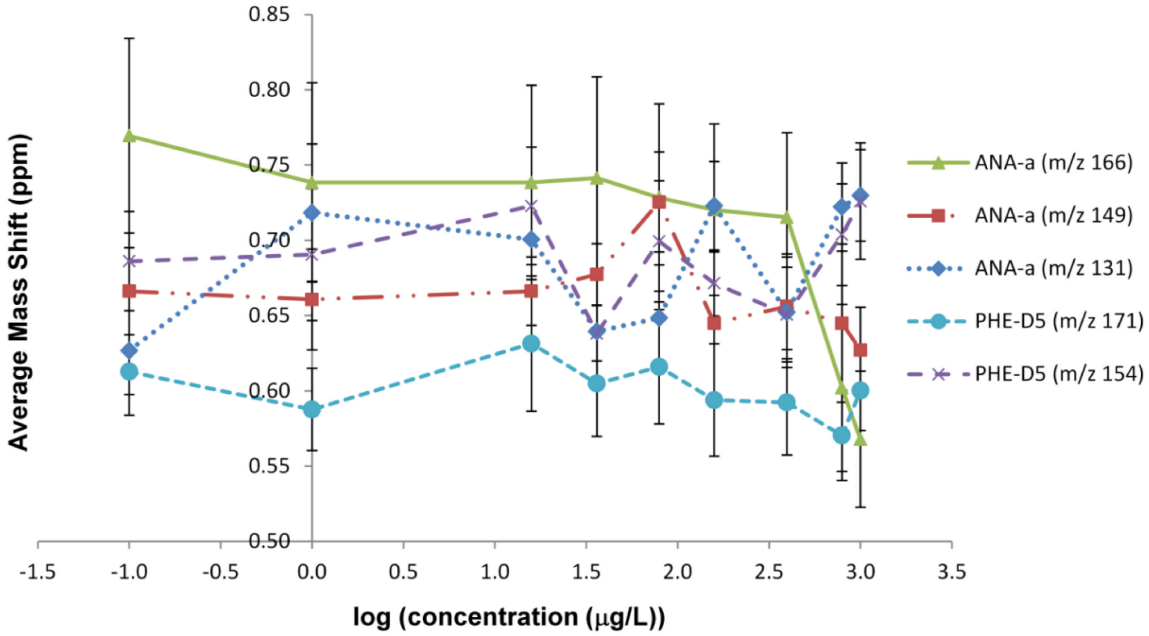


**Figure 5S-4.** Mass scale stability represented with the mass accuracy of the different concentration levels of the calibration curves. The different ions of ANA-a and PHE-$D_5$ are presented from FS and t-$MS^2$ scan modes. Concentrations are presented as the log (concentration (μg $L^{-1}$)) for better representation. Vertical error bars represent standard deviations from the mean (n=6).

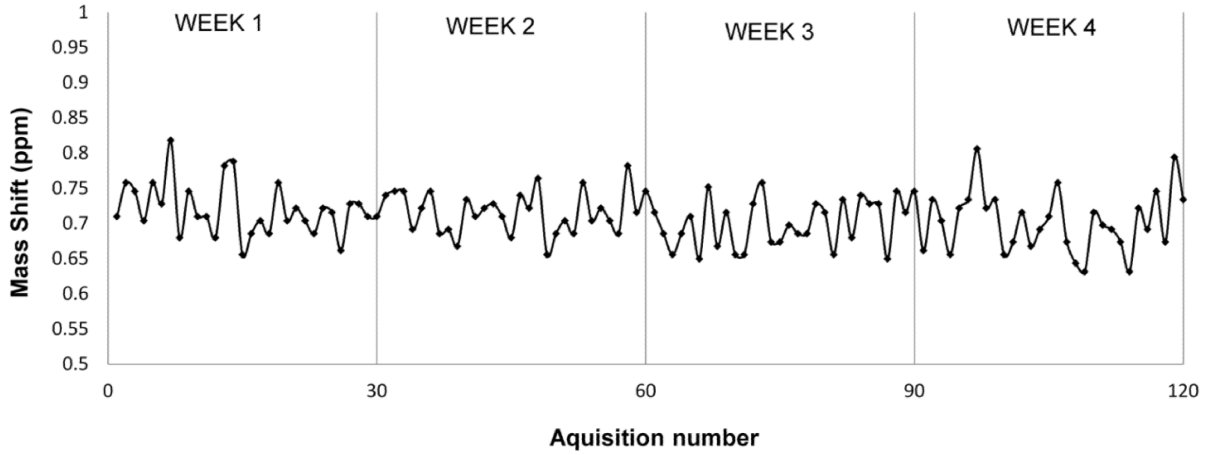


**Figure 5S-5.** Acquisition of the mass errors of ANA-a (*m/z* 166.1231) experimental mass using FS scan mode with resolving power of 35 000 FWHM (*m/z* 200) with internal correction (use of lock mass). The data were taken for 4 weeks consecutively for a total of 120 acquisitions.

# Chapitre 6. Analyse des microcystines totales dans les tissus de poisson utilisant la désorption thermique à diode laser couplée à une ionisation à pression atmosphérique et à la spectrométrie de masse à haute résolution (LDTD-APCI-HRMS)

Une version de ce chapitre se trouve dans l'article intitulé :

Total microcystins analysis in fish tissue using laser thermal desorption-atmospheric pressure chemical ionization-high resolution mass spectrometry (LDTD-APCI-HRMS)

Audrey Roy-Lachapelle, Morgan Solliec, Marc Sinotte, Christian Deblois et Sébastien Sauvé, *Journal of Agricultural and Food Chemistry,* 2015. **63**(33); p. 7440-7449.

**Note sur ma contribution**

Ma participation aux travaux de recherche: J'ai conçu le design expérimental en collaboration avec le Prof. Sauvé et Morgan Solliec et j'ai réalisé les manipulations, l'analyse, l'interprétation des résultats.

Rédaction : J'ai rédigé l'article en m'appuyant sur les commentaires du Prof. Sauvé, mon directeur de thèse.

Collaboration des co-auteurs: Morgan Solliec m'a assisté dans le développement du projet et la rédaction de l'article, Marc Sinotte a contribué à l'écriture de l'article et Christian Deblois m'a fourni des résultats présentés dans l'article.

# Abstract

Microcystins (MCs) are cyanobacterial toxins encountered in aquatic environments worldwide. Over 100 MC variants have been identified and have the capacity to covalently bind to animal tissue. This study presents a new approach for cell-bound and free microcystins analysis in fish tissue using sodium hydroxide as a digestion agent and Lemieux oxidation to obtain the 2-methyl-3-methoxy-4-phenylbutyric acid (MMPB) moiety, common to all microcystin congeners. The use of laser diode thermal desorption-atmospheric pressure chemical ionization coupled to with Q-Exactive mass spectrometer (LDTD-APCI-HRMS) led to an analysis time of approximately 10 seconds per sample and high-resolution detection. Digestion/oxidation and solid phase extraction recoveries ranged from 70 to 75% and 86 to 103%, respectively. Method detection and quantification limits values were 2.7 and 8.2 μg $kg^{-1}$, respectively. Fish samples from cyanobacteria-contaminated lakes were analyzed and concentrations ranging from 2.9 to 13.2 μg $kg^{-1}$ were reported.

**Keywords:** Microcystins, fish, cyanotoxins, LDTD-APCI, HRMS

## 6.1 Introduction

Cyanobacteria—commonly known as blue green algae—are encountered worldwide, mostly in eutrophic water bodies [190]. Although they are essentially harmless in small numbers, some species generate harmful algal blooms (HABs) that are linked to the production of many types of potent toxins associated with human and animal health concerns [280]. Some cyanotoxins are known for their bioaccumulation and potential for biomagnification in the food chain [281]. Knowing that cyanobacteria in surface waters are part of the diet of aquatic animals, the associated toxins are ultimately available to upper trophic levels, possiblyincreasing exposure and health threats to higher organisms [281, 282]. Microcystins (MCs) are the most known and widespread cyanotoxins and are generated by at least 20 cyanobacteria genera [283]. The cyclic structure of MCs (**Figure 6-1**) includes uncommon amino acids such as the β-amino acid Adda (3-amino-9-methoxy-2,6,8-trimethyl-10-phenyldeca-4(E),6(E)-dienoic acid), which is responsible for the toxic activities . In the polypeptide cycle, two amino acids (X and Z) have multiple combinations, causing the MCs to be found in multiple variants. More recently, new MCs were identified, indicating that all the sites from the peptide ring can be areas of adenylation, and over 100 different structures have been identified [32, 194, 284]. They all have hepatotoxic properties, meaning that they will primarily accumulate in the liver when ingested at high doses. While bioaccumulating in the liver, the toxins inhibit protein phosphatases PP1 and 2A through covalent and non-covalent binding, ultimately leading to liver necrosis and death at high doses. Tumour-promoting effects have been demonstrated at lower exposure, and studies have shown links between MCs and hepatic cancer in human populations [24, 285, 286]. The World Health Organization (WHO) proposed a maximum lifetime tolerable daily intake (TDI) for humans of 0.04 μg/kg/day for MC-LR [6, 287].

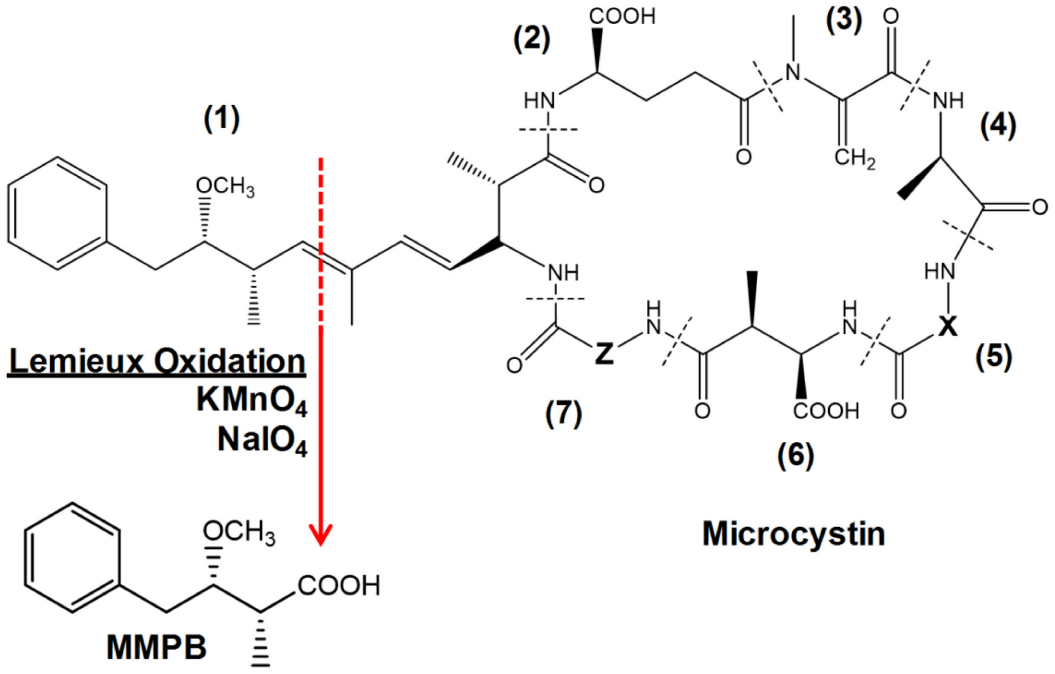


**Figure 6-1.** Lemieux oxidation applied to Microcystin-LR releasing the Adda moiety, the 2-methyl-3-methoxy-4-phenylbutyric acid (MMPB) for total microcystins analysis. Microcystin structure includes (1) Adda, (2) D-glutamic acid, (3) N-methyldehydroalanine, (4) D-alanine, (5) variable L-amino acid, (6) D-methylaspartic acid and (7) variable L-amino acid.

MCs are present in fish tissue in two different forms: 1) the free fraction consisting of the dissolved and reversibly bound MCs to tissues and 2) the covalently bound fraction associated with PP or cysteine-containing peptides within tissues. Extracting the bound fraction has been a challenge for tissue extraction procedures in fish exposed to MCs [130]. Conventional extraction methods involve organic solvents using aqueous or acidified methanol (MeOH). However, solvent extraction yielded poor recovery values since only the free fraction of MCs was recovered and detected [129]. A different approach was explored to analyse the total MCs in fish tissue via Lemieux oxidation (**Figure 6-1**) in order to release the oxidative product of Adda, the 2-methyl-3-methoxy-4-phenylbutyric acid (MMPB) [130, 131, 268]. Common to all congeners, MMPB makes it possible to quantify the total MCs and has been successfully used for analyses in water by our research group and other laboratories [104, 107, 288, 289]. As for fish tissue analysis, a method was proposed using trypsinization

followed by Lemieux oxidation and SPE cleanup and MMPB was detected using liquid chromatography coupled with mass spectrometry (LC-MS) [130, 131, 268]. However, the results from oxidation recoveries, SPE extraction efficiency and signal recovery from matrix effects gave poor values. Moreover, the global procedures were laborious: up to 20 hours of sample preparation required for the trypsinization step and long LC-MS analysis times with over 40-minute runs [130].

We have developed a new approach to detect total MCs (free and protein-bound) in fish tissues. First, the tissue was digested with sodium hydroxide followed by Lemieux oxidation. A different SPE procedure was proposed to enhance recovery values and decrease the amount of salts in the extracts. Finally, the MMPB moiety was analyzed using a technology known as laser diode thermal desorption (LDTD) coupled with atmospheric pressure chemical ionisation (APCI), and the detection was done with a high-resolution mass spectrometer, the Q-Exactive (HRMS). The LDTD has ultra-fast analysis times (<15 seconds/sample), works with small amount of samples (2-10 µL) per analysis and requires only a small volume of solvents since there is no liquid chromatography. In a previous study, the LDTD was successfully used to analyze MMPB in water samples with a triple quadrupole mass spectrometer detector (MS/MS) [288]. Anatoxin-a was also detected with this technology for its direct determination in water using both MS/MS and HRMS [159, 250]. The LDTD was also successfully applied to small molecules in different matrices, including wastewater, sludge, sediment, soil and biological matrices [155, 160, 162-164, 290]. For this method, the Q-Exactive was chosen for two reasons: the sensitivity is higher than a standard triple quadrupole, thus giving better limits of detection and quantification, and the selectivity is better since the mass spectrometer enables precursor fragmentation and exact mass detection. Indeed, this hybrid Orbitrap detector combines a quadrupole precursor selection with a high energy collisional dissociation cell (HCD) making it possible to fragment selected precursor ions. Also, with a resolving power of up to 140,000 full width half maximum (FWHM) at *m/z* 200, the mass accuracy obtained with the Q-Exactive is between 1 and 3 ppm [248].

The objective of this study was to develop a new analytical method for the detection of all the MC variants and to improve their extraction in fish tissue in order to get a more realistic quantification for prudent risk management. By applying this method to samples of fish exposed to cyanotoxins, we aimed to determine the possible undervaluation from their quantification by conventional analytical methods based on the analysis of individual MCs using available standards.

## 6.2 Materials and methods

### 6.2.1 Chemicals, reagents and stock solutions

2-methyl-3-methoxy-4-phenylbutyric acid sodium salt (MMPB, purity ≥ 94%) was purchased from Wako Pure Chemical Industries, Ltd. (Osaka, Japan). 4-phenylbutyric acid (4-PB, purity ≥ 99%) was obtained from Sigma-Aldrich (Oakville, ON, Canada). Ampoules of certified standard solutions of microcystin-LR (MC-LR, 10.2 µM aqueous methanol (1:1, v/v)) were obtained from the Certified Reference Materials Program (NRC, Halifax, NS, Canada). Potassium permanganate ($KMnO_4$, purity ≥ 99,0%), sodium (meta)periodate ($NaIO_4$, purity ≥ 99,0%), sodium bisulfite (purity ≥ 95%), sodium hydroxide (NaOH, purity ≥ 98%), hydrochloric acid (HCl, ACS reagent 37%) and sulfuric acid standard solution (1.000 M) were obtained from Sigma-Aldrich (Oakville, ON, Canada). All solvents were high performance liquid chromatography (HPLC) grade from Fisher Scientific (Whitby, ON, Canada). Deionized/distilled water (dd-$H_2O$) was used for recovery evaluation. Individual stock standard solutions were prepared in methanol (MeOH) at a concentration of 100 mg $L^{-1}$ and kept at -20°C for 12 months for the MMPB standards and a maximum of 6 months for the 4-PB standards, according to compound stability [288]. Compressed air (Ultra Zero Certified grade; ≤ 2 ppm water) was used as a carrier gas for the LDTD desorption and obtained from MEGS Specialty Gases, Inc. (St-Laurent, QC, Canada).

### 6.2.2 Fish tissue samples

Environmental samples were provided by the monitoring program of the *Ministère du Développement durable, de l'Environnement et de la Lutte aux changements climatiques*

(MDDELCC), Québec provincial environment ministry (Québec, QC, Canada) as part of an MC project to monitor fish in natural lakes where cyanobacterial blooms occur. Fish were caught on August 20, 2009, and on October 14 and 15, 2009 in three different lakes in the province of Québec, Canada: Lac Vert, Lac Roxton and Lac Noir. All three lakes were affected by cyanobacterial blooms. Eight different species were caught and kept at -20°C until homogenisation and analysis: rainbow smelt, white sucker, brook trout, yellow perch, walleye, pike, brown bullhead and lake whitefish. The analysis was first performed by the government monitoring program of the *Centre d'expertise en analyse environnementale du Québec* (CEAEQ). Fish tissue (muscle and whole fish) was weighed and dried using diatomaceous earth, followed by slow elution with acidified MeOH with formic acid. The solvent was evaporated, and the samples were reconstituted in the mobile phase and filtered using 0.2 µm nylon filters submitted to ultracentrifugation. An aliquot was used for LC-MS/MS analysis. Four microcystins quantified were quantified: MC-LA, MC-LR, MC-RR and MC-YR.

### 6.2.3 NaOH digestion and Lemieux oxidation

Frozen homogenized fish tissue was used instead of freeze-dried tissue in order to make direct comparisons with MCs previously found in the samples using the CEAEQ's standard analytical procedure. Thus, 1 g of wet weight and homogenized fish tissue was submitted to a freeze-thaw lysis three times in order to break the remaining cells and leach the toxins. The tissues were then digested in 5 mL NaOH solution (50 mM) for 2 hours. The pH was adjusted to 9 using an HCl solution (100 mM) and oxidants were added in solution with $KMnO_4$ (50mM) and $NaIO_4$ (50mM). The reaction was conducted at room temperature for 2 h in the absence of light. Saturated $NaHSO_3$ solution was added until the purple color turned white in order to quench the reaction. A 10% sulfuric acid solution was used to acidify the solution (pH ~ 2).

### 6.2.4 Solid phase extraction procedures

Before the solid phase extraction (SPE) step, suspensions were transferred in centrifuge tubes and submitted to sonication for 15 minutes. They were then centrifuged for 15 minutes at 3,000 rpm, and the supernatants were filtered using 0.2 µm nylon filters from Whatman

(Florham Park, NJ, USA) prior to extraction. A polymeric hydrophobic sorbent consisting of styrene-divinylbenzene (Strata SDB-L) was used as an SPE cartridge from Phenomenex (Torrance, CA, USA) with 500 mg bed mass and a volume of 6 mL. The procedure was carried out using a 12-position manifold from Phenomenex (Torrance, CA, USA). The SPE was performed with the filtered aliquots of sample supernatants with the pH already adjusted to 2. The SPE cartridges were conditioned with 5 mL of methanol (MeOH) for sorbent activation followed by 5 mL of acidified water with 0.1% formic acid (HPLC grade). The samples were then loaded on the cartridge columns by gravity. The cartridges were washed twice with 5 mL of water with 0.1% formic acid containing 10% MeOH (v/v). Elution was performed with 5 mL of MeOH into glass conical-bottom centrifuge tubes. The eluates were completely dried under a gentle stream of nitrogen at room temperature with a nine-port Reacti-Vap unit (Pierce, Rockford, IL, USA). The dried fractions were then reconstituted in acetonitrile (ACN) and directly submitted to LDTD-APCI-HRMS detection.

### 6.2.5 LDTD-APCI-HRMS

Compound desorption was achieved with a T-960 LDTD-APCI ionization interface model, and the instrument was controlled using LazSoft 4.0 software (Phytronix Technologies, Québec, QC, Canada) integrated with Excalibur 2.2 software (Thermo Fisher Scientific, Waltham, MA, USA). The LDTD instrument was described in previous work [155, 164, 288]. In this experiment, 4 µL aliquots from extract samples were spotted into a LazWell 96-well sample metal plate. After complete solvent drying at 40 °C for 5 minutes, the back of the sample well was heated by an infrared laser (980 nm, 20 W, continuous) in the LDTD instrument. The sample is desorbed and a carrier gas flow of 2 L $min^{-1}$ was then set at a temperature of 50°C to avoid temperature variations and transfer the gas phase molecules to negative APCI ionization followed by HRMS detection. Finally, the laser power is expressed as a percentage, and the laser pattern was optimized to the following settings: 2 s at 0%, 2 s ramping from 0% to 40%, 1 s hold at 40%, 0.1 s from 40% to 0% and 2 s hold at 0%, with a total desorption time of 7 seconds per sample. APCI ionization in negative mode is within these parameters: ion sweep gas 0.3, sheath gas, auxiliary gas and skimmer offset are set to 0 (all arbitrary values), vaporizer temperature 0 °C and capillary temperature 350 °C.

The detection was performed using a Q-Exactive mass spectrometer controlled by the Excalibur 2.3 software (Thermo Fisher Scientific, Waltham, MA, USA). Instrument calibration in negative mode was done every 5 days to avoid mass shifts in detection with a direct infusion of a LTQ Velos ESI Negative Ion Calibration Solution (Pierce Biotechnology Inc. Rockford, IL, USA). The Q-Exactive parameters were selected toward mass resolution and accuracy for better quantification, sensitivity and selectivity. The targeted ion fragmentation (t-$MS^2$) mode was used for MMPB quantification and normalized collision energy (NCE) was optimized. Standard solutions of MMPB and 4-PB at a concentration of 100 µg $L^{-1}$ were directly infused with a syringe at a flow rate of 0.01 mL $min^{-1}$. The fragment ions and their collision energies (NCE) were chosen using Q-Exactive Tune 2.3 software (Thermo Fisher Scientific, Waltham, MA). The precursor ions were filtered by the quadrupole, which operates at an isolation width of 0.4 amu. The optimized collision energies, precursor ions and fragment ions are presented in **Tableau 6-1**. A resolving power of 17,500 FWHM at *m/z* 200 was used with an automatic gain control (AGC) target set at $1 \cdot 10^5$ ions for a maximum injection time of 50 ms. For more technical details, please refer to previous studies [185, 249, 250, 253].

**Tableau 6-1.** Parameters of HRMS detection.

| Compound | Chemical Formula | Calculated exact mass (*m/z*) | Experimental exact mass (*m/z*) | NCE[d] (%) | Mass Accuracy[e] (ppm) | Confirmation Ion[f] (*m/z*) |
|---|---|---|---|---|---|---|
| MMPB | $C_{12}H_{16}O_3$-H[a] | 207.10212 | 207.1019 | 25 | 1.2 | 208.1042 |
| | $C_9H_{11}O$[b] | 135.08099 | 135.0808 | | 1.5 | 135.0829 |
| | $C_7H_7$[c] | 91.05478 | 91.0547 | | 1.1 | 91.0571 |
| 4-PB | $C_{10}H_{12}O_2$-H | 163.07590 | 163.0756 | 30 | 1.7 | 163.0780 |
| | $C_7H_7$ | 91.05478 | 91.0546 | | 1.5 | 91.0568 |

[a] Precursor ion
[b] Quantification ion (most abundant MS/MS transition)
[c] Confirmation ion (second most abundant MS/MS transition)
[d] Fragmentation energy for precursor ion in HCD cell
[e] Accuracy of average measured mass
[f] Second abundant ion in isotopic pattern

### 6.2.6 Method validation

Data treatment was carried out using Excalibur 2.3 software (Thermo Fisher Scientific, Waltham, MA, USA). The method validation was done according to the recommendations of the validation protocol for environmental chemistry analysis from the MDDELCC ministry guidelines. The two fragment ions with the highest signal intensity were selected as the quantification and confirmation ions. The quantification ion was used to establish the method limits of detection and quantification. Compound confirmation could be done with the ratio of their relative intensities in order to avoid false positives. The second most abundant ion from the isotopic pattern and the isotopic ratio with <10% intensity variations were used for confirmation. A mass tolerance window was set to 5 ppm (± 2.5 ppm) for the extracted masses from acquisition in order to get a good selectivity in data analysis. The reaction recovery yield values for fish tissue digestion and oxidation were evaluated using a blank matrix, which consisted of fish that were not in contact with cyanobacterial bloom at three MMPB concentrations: (25, 250 and 1 000 µg $kg^{-1}$). The fish tissue was spiked with MC-LR and the corresponding MMPB concentrations prior to digestion and oxidation. To obtain a relevant matrix with interactions between the fish tissue and the added MC, the blank homogenates were incubated for 3 hour prior to the extraction procedure. The mean peak area values were compared with those obtained by spiking the digested and oxidized fish tissue with MMPB

before SPE. The recovery values of the SPE method and the matrix effects were also evaluated using blank fish tissue at three concentrations: (25, 250 and 1 000 µg $kg^{-1}$). Extraction recoveries were determined with the mean peak area of MMPB spiked prior to extraction in matrix-containing (blank fish tissue) samples compared to matrix-containing samples spiked post-extraction. The matrix effects were evaluated with the mean peak area of MMPB spiked prior to extraction in matrix-containing samples compared to spiked matrix-free (dd-$H_2O$) samples prior to extraction. All recovery values were evaluated in triplicate, and the results are reported as percentages. A seven-point internal calibration curve was prepared with blank fish tissue by standard addition with concentration levels ranging from 15 to 2 500 µg $kg^{-1}$. The concentration of internal standard (IS) 4-PB was selected at 500 µg $kg^{-1}$ for its capacity for signal correction (data not shown). The method detection limit (MDL) and method quantification limit (MQL) were established by calculating 3 and 10 times the standard deviation of the mean value of 6 spiked blank fish tissue samples containing approximately 5 times the estimated concentration for detection limit (15 µg $kg^{-1}$), respectively. Accuracy—expressed as relative error (RE-%)—and interday/intraday—expressed as the relative standard deviation (RSD-%)—were determined with three different concentrations on the linearity range (25, 250 and 1 000 µg $kg^{-1}$, n=6) in blank fish tissue samples. Intraday repeatability was estimated over three weeks. Statistical comparison was used when needed with the Statistical Package for Social Sciences (SPSS 21.0, Chicago, IL) for Windows. ANOVA and Tukey's post hoc tests were used with statistical significance defined as $P < 0.05$.

## 6.3 Results and discussion

### 6.3.1 Digestion and oxidation

The extraction of total MCs through MMPB from biological matrices was previously explored with the use of trypsinization and Lemieux oxidation followed by SPE clean-up [130, 131]. For higher extraction efficiency, our study first considered the possibility of NaOH as a digestion reagent to break down the tissu and thus allow the free and bound MCs to react to Lemieux oxidation and then be converted to MMPB. MCs are known to be stable in a wide range of pH as well as high temperatures and sunlight [34]. Since MCs can withstand higher

alkaline and acidic pH, NaOH was then used as a digestion agent for fish tissue without affecting MC stability. The optimization was developed by spiking MC-LR in blank fish tissue before the digestion and oxidation with the corresponding MMPB concentration (1 000 µg $kg^{-1}$) recovered after SPE clean-up, and this concentration was chosen for its higher signal intensity and therefore easier optimization. Different NaOH concentrations between 10 and 100 mM were studied and submitted to different digestion periods ranging from 30 minutes to 5 hours (n=3). The results are shown in **Figure 6-2a**. The optimal results were 50 mM of NaOH used for 2 hours, which yielded in higher MMPB signals and less variability. Longer digestion durations did not significantly increase the MMPB signal ($P > 0.05$), and the faster digestion time was therefore preferred. Finally, higher concentrations enhance salt concentration in solution and can reduce LDTD desorption due to the presence of a salt layer in the wells and may also induce ion suppression during the charge transfer of APCI ionization [155, 171, 174].

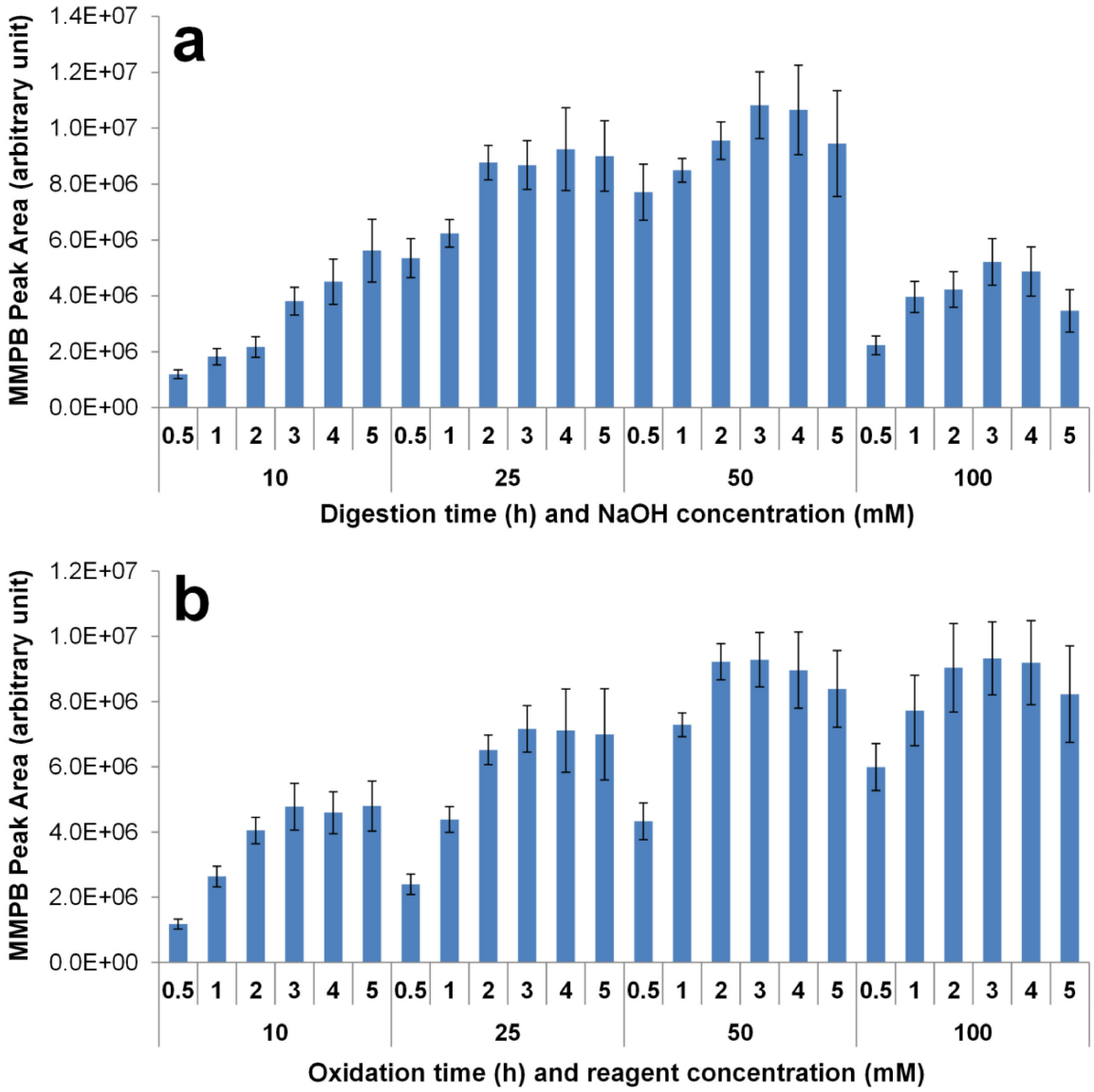


**Figure 2.** Optimization of (a) the digestion and (b) the oxidation by varying the reaction time (first x-axis) and the reagents concentration (second x-axis). $KMnO_4$ and $NaIO_4$ concentrations were identical during the oxidation. Vertical error bars represent standard deviations from the mean (n = 3).

Lemieux oxidation was previously used in bloom water matrices in a previous work and was optimized according to three parameters: pH, oxidation time and reagent concentration. The reaction medium was alkaline with a pH of 9 with 100 mM HCl after digestion. This was set as the most efficient pH value used for MC oxidation in previous

studies. However, since the oxidation takes place in fish tissue, reagent concentration and oxidation time were reassessed in order to obtain the best reaction yield. $KMnO_4$ and $NaIO_4$ were tested with concentrations between 10 and 100 mM, and each concentration was tested for an oxidation time between 30 minutes and 5 hours (n=3). The results are shown in **Figure 6-2b**. The optimal values were the use of 50 mM of reagents at a reaction time of 2 hours. Reaction conditions were similar to those in the previous study, with a reaction time of 2 hours instead of 1 being the only difference. The lower reaction time and reagent concentrations were selected for faster sample preparation and to limit ion suppression from ionization due to the high amount of salts in the matrix. The digestion and oxidation reaction recovery values were determined together, using blank fish tissue spiked before digestion with MC-LR, and the results were compared with blank fish tissue spiked after oxidation with the corresponding MMPB concentrations (25, 250 and 1 000 µg $kg^{-1}$). Recovery yield values are shown in **Tableau 6-2** with their respective standard deviations (SD) and values ranging from 70 to 75%. These results represent a significant improvement as compared to previous studies using trypsinization prior to Lemieux oxidation with results ranging from 5 to 40% [131, 268].

**Tableau 6-2.** Validation parameters using internal calibration with three different concentrations (n = 6).

| Concentrations (µg $kg^{-1}$) | Accuracy RE (%) | Intraday RSD (%) | Interday RSD (%) | Digestion/ oxidation recovery ± SD (%) | SPE recovery ± SD (%) | Signal recovery from matrix effects ± SD (%) |
|---|---|---|---|---|---|---|
| 25 | 10 | 6 | 7 | 70 ± 7 | 91 ± 6 | 92 ± 7 |
| 250 | 6 | 4 | 5 | 75 ± 9 | 95 ± 9 | 90 ± 10 |
| 1 000 | 5 | 5 | 9 | 72 ± 6 | 98 ± 7 | 93 ± 9 |

## 6.3.2 Sample clean-up and elution

A solid phase extraction (SPE) clean-up was developed to isolate MMPB and 4-PB from the reaction mixtures. Extensive clean-up was necessary because of the fish tissue, which constitutes a highly complex matrix, and the high amounts of salts in the digestion and oxidations steps [268]. Indeed, the presence of proteins, lipids and salts can induce ion suppression during APCI ionization due to charge transfer limitations and thus affecting signal

intensity [171]. In the analysis of MMPB in animal tissues, reverse phase or ion-exchange SPE sorbents are generally used for clean-up [130, 131, 268]. In this study, SDB-L sorbent was tested to enhance MMPB recovery and limit the elution of contaminants from the matrix. The SDB-L SPE targets hydrophobic and aromatic analytes which is appropriate for MMPB since its structure includes an aromatic cycle. The $pK_a$ of MMPB being 4.63, the molecule is in neutral state in acidic conditions and can be adsorbed on the SDB-L sorbent. As for the procedure, SPE sorbents were washed twice with 5 mL of $H_2O$ with 0.1% formic acid 10% MeOH to eliminate a maximum of interfering compounds and salts from the matrix. The elution step was done with 5 mL of MeOH since the compounds did not need a change of polarity to be released from the sorbent. The recovery values for the SPE procedure were evaluated using blank fish tissues spiked before SPE and the mean peak area values were compared to blank fish tissue spiked after SPE. The recovery results were deemed satisfactory (ranging from 91 to 98%) and are shown in **Tableau 6-2** for the three concentration levels (25, 250 and 1 000 µg $kg^{-1}$). The matrix effects were determined by comparing the mean peak area of targeted compounds in matrix-containing samples spiked before extraction as compared to dd-$H_2O$ spiked before extraction. The signal recoveries are shown in **Tableau 6-2** and ranged from 90 to 93%, illustrating that the MMPB signal is not significantly affected by the matrix.

### 6.3.3 LDTD-APCI-HRMS

Different parameters were optimized in order to improve signal intensity for optimal MMPB detection by LDTD-APCI-HRMS. Several parameters from the LDTD desorption had to be reassessed. Indeed, in earlier work, an analytical method was developed and optimized to analyze MMPB by LDTD-APCI-MS/MS in lake water. However, fish tissue is a completely different matrix and the LDTD desorption may be affected if parameters such as deposition solvent, volume of deposition, laser power and laser pattern are not optimized. In this case, the carrier gas flow was not studied since changing the parameter did not lead to improvement. The different optimizations were done with post-extraction blank fish tissue spiked with 100 µg $L^{-1}$ of MMPB (n=6).

Firstly, the deposition solvent will affect compound desorption by LDTD depending on its solubility and on how the dried solvent will create layers of nanocrystals constituted of the

analytes and the matrix [155]. Therefore, deposition solvents were tested as solvents of reconstitution after the SPE clean-up and included ethyl acetate, isopropanol, methanol, hexane, acetone, water, ethanol and acetonitrile. As the results demonstrate in **Figure 6-3**, the optimal deposition solvent was acetonitrile (ACN). Indeed, the use of ACN considerably reduces the amount of proteins and amino acids available in the samples by their precipitation, thus reducing matrix complexity. Secondly, deposition volumes were evaluated in order to maximize the amount of analytes submitted to desorption, thus increasing the signal intensity. **Figure 6S-1** in Supplementary Information shows the results and a volume of 4 µL yields significantly higher signal intensity ($P < 0.05$) with a lower variability. With higher deposition volumes, higher variability is observed followed by a signal decrease. This is explained by the higher mass of analyte, which is concomitant with a higher presence of interfering compounds that can reduce LDTD desorption and also impact APCI ionization with ion suppression. Thirdly, the laser power is the amount of energy transferred to the back of the well of the LDTD plate expressed as a percentage (of maximum) and which influences the analytes' desorption rate. Laser power values were studied between 10 and 60% since higher power can burn the well, thus inducing compound degradation or fragmentation. The results in **Figure 6S-2** shows that 40% is the optimal laser power for higher MMPB desorption with minimal signal variability.

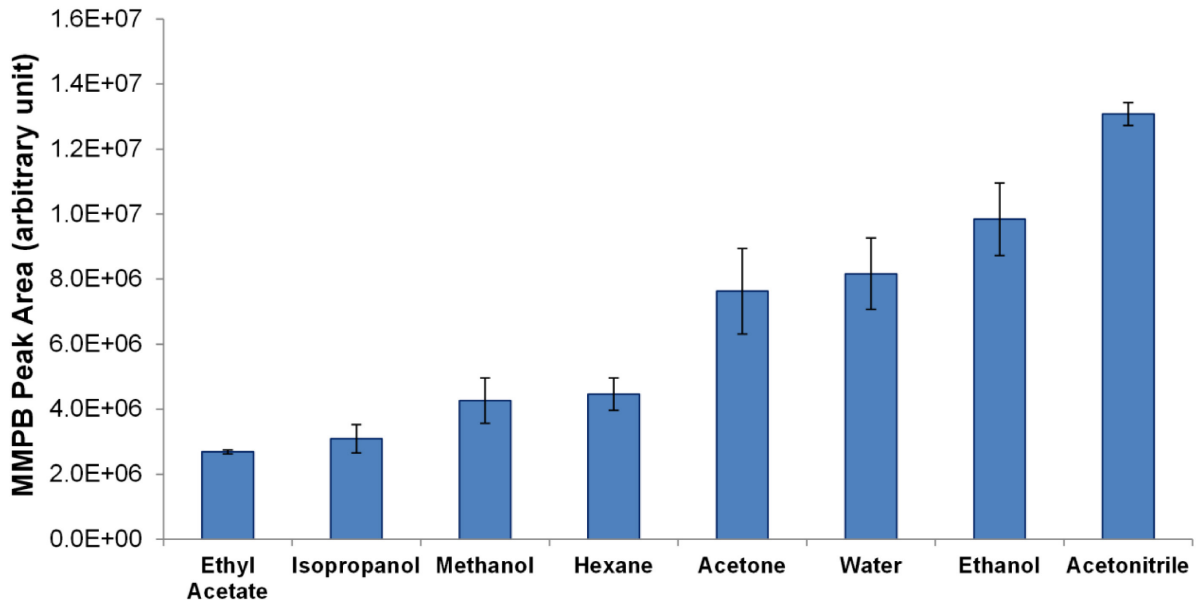


**Figure 6-3.** Effect of different solvents used for post SPE samples reconstitution and LDTD desorption after sample deposition in wells on MMPB mean peak area. Vertical error bars represent standard deviations from the mean (n = 6).

The laser pattern was studied, including the laser ramp time enhancement followed by the laser plateau time. The laser ramp time influences the shape of the LDTD peak and, by the same token, the number of acquisition data points per peak. Since LDTD desorption is fast, the HRMS detection can often lack data acquisition points for low-variability quantification (the criteria being at least 7 points) [253]. The laser plateau time influences the amount of compound that will desorb and the signal stability. The two parameters were evaluated together by varying them between 0.5 and 3 seconds (**Figure 6S-3**). The optimal values were a laser ramp time of 2 seconds with a laser plateau time of 1 s yielding more than 10 data acquisition points in a peak width of about 5 seconds (**Figure 6-4**). Higher laser plateau times caused signal instability and higher variability. The phenomenon also occurred with higher laser ramp time, at more than 3 seconds, when the beginning of a peak distortion was observed and caused higher signal variability. With 4 seconds of laser ramp time, peak distortion is obvious causing much higher signal variability (**Figure 6S-4**). No significant enhancement was observed with higher laser plateau and ramp time ($P > 0.05$).

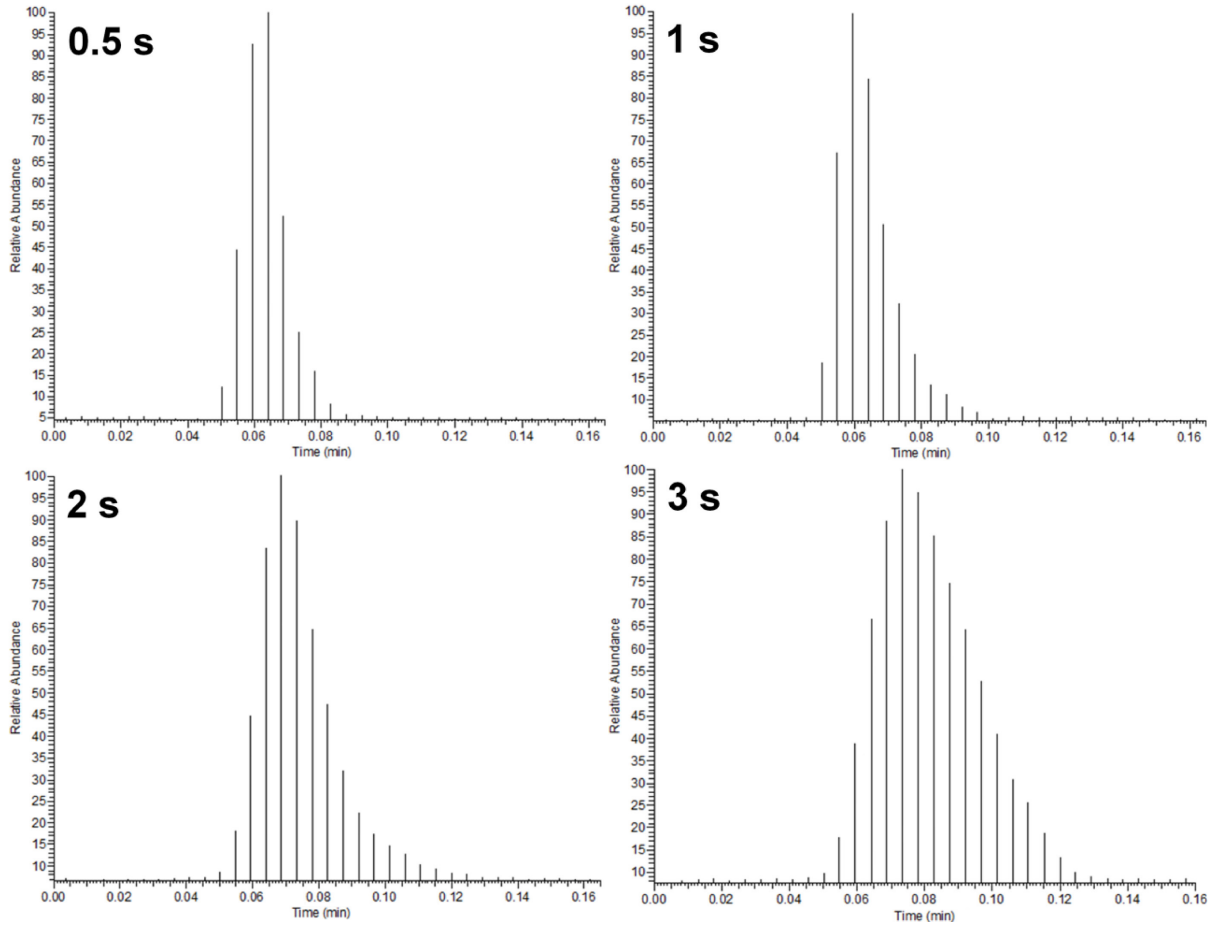


**Figure 6-4.** Number of data acquisition points for LDTD peaks of MMPB with different laser ramp times.

### 6.3.4 Method validation

The evaluation of the LDTD-APCI-HRMS method was done according to these parameters: linearity, sensitivity, accuracy, precision, selectivity and matrix effects, which were previously discussed in the sample clean-up and elution section. Due to the unavailability of isotopically-labeled MMPB, 4-phenylbutyric acid (4-PB) was used as the internal standard based on previous studies [268, 288]. All validation parameters were evaluated using spiked blank fish tissue to take matrix effects into account. A seven-point standard addition calibration curve spiked prior to the SPE procedure was used with a linear dynamic range between 15 and 2 500 µg $kg^{-1}$ analyzed in triplicate. The optimal concentration of 4-PB used as signal variation correction was set at 500 µg $kg^{-1}$ depending on the lowest variability

throughout the calibration linearity range (data not shown). Ultimately, correlation coefficients showed a good linearity with $R^2$ > 0.999. The method detection limit and method quantification limit (MDL and MQL) were 2.7 and 8.2 µg $kg^{-1}$, which is comparable to previous work. **Figure 6S-5** shows a sample LDTD peak signal obtained around the MQL (8 µg $kg^{-1}$) [268]. **Tableau 6-2** summarizes the validation parameters determined at three concentrations from the linearity range (25, 250 and 1 000 µg $kg^{-1}$). Values from the accuracy expressed as the relative errors (RE-%) and from intraday and interday precisions expressed as relative standard deviations (RSD-%) were equal to or lower than 10%, which means that the method was both selective and precise.

### 6.3.5 Fish tissue samples

The method was applied to determine the total MCs present in 49 samples of fish tissue caught in 3 different lakes of the province of Québec, Canada, where cyanobacterial blooms occurred during the growing season. **Tableaux 3** and **A-1** present the results obtained using three different analytical methods. The results from the method developed in this study are presented first. Then, the same samples were submitted to LDTD-APCI-MS/MS analysis using a previously developed method for total MCs in lake water [288]. The purpose here was to compare the sensitivity and selectivity of MS/MS detection with HRMS detection using LDTD-APCI technology. Finally, CEAEQ results using a standard analytical method for MCs in fish tissue are presented for the same samples. Of the 49 samples (**Tableau 6S-1**), 24 had a positive response to MCs, including 22 that were above the detection limit (**Tableau 6-3**). Concentrations varied between 2.7 and 13.2 µg $kg^{-1}$ of fresh fish tissues weight. Four samples (1 to 4) had relatively higher detected concentrations, which could be explained by the type of fish tissue. Indeed, three of these samples from a bottom feeder, the white sucker, included the viscera known to concentrate higher amount of MCs, but that are not generally consumed by fisherman. Interestingly, the second highest concentration was for a headed and gutted rainbow smelt, these small fish are eaten as is. Smelt's preferred habitat is the metalimnion, which is also the habitat of the blue green algae *Planktothrix* responsible for the Lac Vert's contamination by MCs. Smelt consume crustacean, zooplankton and insect larvae that are themselves algae consumers. Only four results were above the estimated MQL values,

although yellow perch and lake whitefish were quite close. Of the 24 samples with positive MC detection, only 5 were detected using the LDTD-APCI-MS/MS technique with relative differences in values of -13% on average. This difference was explained by the different response of matrix effects using MS/MS, for which the signal recovery was 82%. The detection and quantification limits of the method were 6.8 and 20.4 µg $kg^{-1}$, respectively. While these values are comparable with those obtained in previous studies, the use of HRMS offered better sensitivity (i.e. 2.7 and 8.2 µg $kg^{-1}$, respectively), which supports the choice of our detection method.

**Tableau 6-3.** Comparison of results from fish samples with detected MCs above method detection limit using three detection methods.

| No. Sample | Location | Fish specie | Fish part | Total MC via MMPB and HRMS ($\mu g\ kg^{-1}$)[a] (RSD - %) | Total MC via MMPB and MS/MS ($\mu g\ kg^{-1}$)[b] (RSD - %) | Total MC with standards ($\mu g\ kg^{-1}$)[c] |
|---|---|---|---|---|---|---|
| 1 | Lac Vert | Rainbow smelt | No head/viscera | **11.9 (7)** | 10.3 (9) | ND |
| 2 | Lac Vert | White sucker | Whole | 8.7 (8) | 7.5 (12) | ND |
| 3 | Lac Vert | White sucker | Whole | **13.2 (6)** | 11.9 (11) | 2.0 |
| 4 | Lac Vert | White sucker | Whole | **9.5 (10)** | 8.1 (11) | ND |
| 6 | Lac Vert | Brook trout | Muscle | 5.0 (10) | ND | ND |
| 7 | Lac Vert | Brook trout | Muscle | 4.5 (9) | ND | ND |
| 9 | Lac Roxton | Yellow perch | Muscle | 4.0 (10) | ND | ND |
| 11 | Lac Roxton | Yellow perch | Muscle | 3.1 (11) | ND | ND |
| 14 | Lac Roxton | Yellow perch | Muscle | 5.2 (9) | ND | ND |
| 17 | Lac Noir | Yellow perch | Muscle | 4.5 (7) | ND | ND |
| 18 | Lac Noir | Yellow perch | Muscle | 7.3 (11) | 6.9 (12) | ND |
| 20 | Lac Noir | Yellow perch | Muscle | 2.7 (12) | ND | ND |
| 22 | Lac Noir | Walleye | Muscle | 4.4 (8) | ND | ND |
| 24 | Lac Noir | Walleye | Muscle | 2.9 (10) | ND | ND |
| 27 | Lac Noir | Walleye | Muscle | 3.4 (9) | ND | ND |
| 33 | Lac Noir | Brown bullhead | Muscle | 3.8 (9) | ND | ND |
| 35 | Lac Noir | Brown bullhead | Muscle | 5.2 (8) | ND | ND |
| 38 | Lac Noir | Lake whitefish | Muscle | 7,1 (8) | ND | ND |
| 40 | Lac Noir | Lake whitefish | Muscle | 6,2 (9) | ND | ND |
| 41 | Lac Noir | Lake whitefish | Muscle | 5.9 (7) | ND | ND |
| 44 | Lac Noir | Lake whitefish | Muscle | 7.3 (10) | ND | ND |
| 45 | Lac Noir | Lake whitefish | Muscle | 4.5 (11) | ND | ND |
| 46 | Lac Noir | Lake whitefish | Muscle | 3.0 (9) | ND | ND |
| 49 | Lac Noir | Yellow perch | Muscle | 3.7 (11) | ND | ND |

ND – Not detected
[a]Total microcystins determined via MMPB using LDTD-APCI-HRMS.
[b]Total microcystins determined via MMPB using LDTD-APCI-MS/MS.
[c]Microcystins determined via the summation of all microcystins for which standards allowed detection and quantification (i.e. MC-LA, MC-LR, MC-RR and MC-YR) using LC-MS/MS.
[d]Values in bold represent concentrations above the MQL.

Using the CEAEQ's standard analytical method, only one sample showed the positive detection of MCs at 2.0 µg $kg^{-1}$ of MC-YR congener. This value represents 15% of the recovered total MCs from the same sample. The detection limit of each studied MC variant was 1 µg $kg^{-1}$, and detection method sensitivity therefore cannot explain this discrepancy. Two reasons may explain the substantial underestimation of MCs. First it is possible that the extraction method may not be able to release the covalently bound MCs from the tissue. Williams *et al.* provided experimental evidence, using Lemieux oxidation, MMPB-GC/MS, radiolabeled MMPB and MeOH extraction-PPase to demonstrate that a substantial amount of MCs were covalently bound *in viv*o [291, 292]. MeOH extraction actually recovered ≈24% of the total MC-LR measured with MMPB in liver from salmons intraperitoneally injected. This underestimation is similar to what this study obtained for whole fish in the only sample with a detection using the conventional extraction method. Other authors estimated that as much as 60 to 90% of total MCs could be covalently bound [291-294]. Second, other variants and variant isomers present in the samples could have been missed altogether. Indeed, some tissue samples from the same lake and date had MC detections suspected by CEAEQ to be YR isomer (data not shown). Due to the absence of appropriate standards for LC-MS/MS, the CEAEQ analytical laboratory could not certify the identification and concentration of the suspected isomer, although its characteristics were so close to the available standard that it was deemed with a very high probability to be an isomer of MC-YR. As was recently demonstrated with total MCs in water [288], this study also illustrates the inherent risk of relying on a limited number of standards when trying to assess total MC contamination in tissue. Our results show the importance of analyzing total MCs in fish tissue using proper sample preparation and extraction methods along with selective and sensitive detection methods.

### 6.3.6 Risk assessment

The maximum lifetime TDI for humans (i.e. 0.04 µg/kg/day) set out by the WHO has been used in several exposure scenarios to estimate the potential risk for fish consumers. Scenarios aiming to protect at-risk groups (e.g. children [295] or important consumers of locally caught fish [296]) are expected to be the most stringent. Assuming that no exposure

would come from drinking water or recreational exposure, the TDI would transfer into ≈8 μg $kg^{-1}$ of fish for a 60-kg adult who consumes 300 g of fish per day on average [296, 297], or to ≈24 μg $kg^{-1}$ for those who consume 100 g per day [298]. Some of the results presented in **Tableau 6-3** would then exceed the TDI if fish consumption is high enough. These results are noteworthy since only one of the 49 samples was over the detection limit (i.e. 1 μg $kg^{-1}$) of the initial LC-MS/MS analysis. However, it was observed that only three samples were detected above the estimated MQL (8.2 μg $kg^{-1}$). Though further studies are required to improve sensitivity, the findings here were satisfactory for MCs detection around the WHO's TDI.

Likewise, assuming that 15% of the total MCs were detected in studies analyzing only unbound concentrations, several studies including this one would have MC levels above the WHO's TDI using our method [298-302]. Overall these results suggest that certain groups may be at a higher risk than previously estimated and that more research on the toxicity of total MCs is needed. Moreover, the WHO has classified MCs as a "possible human carcinogenic" (Class II-B) [303]. It is therefore important to enhance our ability to estimate the total concentration from all sources of exposure to this class of pollutants since cancer may develop after a long latency period and possibly at relatively low exposure levels.

Although the variants, isomers, conjugates and covalently-bound MCs probably all have different toxicological properties that have yet to be understood, a method to analyze quickly total MCs is nevertheless essential to make prudent exposure measurements while research progress. Furthermore, this new method for total MCs in tissue would be helpful in a tiered approach to screen out samples that do not contain these toxins, enabling resource allocation where other variants could be playing an unnoticed role in toxicity. Though many studies have explored the availability of MCs in aquatic animal consumption after cooking and digestion, the bioavailability and toxicity of bound MCs are still poorly understood [193, 304, 305]. However, findings showed that serious risk to animal and human health is most likely possible and that contamination monitoring could prevent eventual poisoning cases. It would therefore be beneficial to understand the fate, transportation, and accumulation of MCs in the food web, with or without other analyses and assays [306].

## 6.4 Conclusion

In conclusion, a new approach to detect total microcystins (MCs) in fish tissue has been demonstrated and validated using LDTD-APCI-HRMS. MCs are known to covalently bind with animal tissue, and effective sample preparation is therefore necessary to analyze both free and bound fractions and the possible MCs congeners. We explored the possibility of using sodium hydroxide as a digestive agent for fish tissue prior to a well-known oxidation step, Lemieux oxidation, for total MCs analysis. A new approach for sample clean-up was also explored using an SDB-L SPE cartridge for recovery enhancement and eliminating the salts present in solution. The use of LDTD-APCI has already been reported for the analysis of MMPB in water but HRMS detection with the Q-Exactive was chosen for better sensitivity and selectivity. The use of LDTD-APCI-HRMS enabled ultra-fast analysis times at 10 s per sample. Digestion and oxidation were optimized and recoveries ranged from 70 to 75% respectively. SPE recoveries ranged from 86 to 103%, and signal recoveries from matrix effects ranged from 90 to 93%. An internal calibration was used with 4-PB and the validated method gave linear correlation coefficients ($R^2$) of 0.999, MDL and MQL were 2.7 and 8.2 μg $kg^{-1}$, respectively. Accuracy and interday/intraday variation coefficients for target compounds were below 10%. Interday and intraday precision was evaluated below 10%. Of a total of 49 fish samples from lakes with HABs, 25 (51%) had a positive response for total microcystins with concentrations ranging from 2.9 to 13.2 μg $kg^{-1}$ fresh weight in tissue. Using standardized extraction and LC-MS/MS methods, only one sample (2%) had a microcystin response with a concentration of 2 μg $kg^{-1}$ of MC-YR. For that sample, the total MCs were seven times higher than the initial value. These results suggest that MC concentration in fish tissues could be significantly underestimated using standard analytical methods and that a suitable extraction method combined with total MC detection is required for prudent risk management.

## 6.5 Acknowledgments

This research was carried out with the financial support of the the Fond de recherche Québec–Nature et technologies and the Natural Sciences and Engineering Research Council of Canada (NSERC). The authors would also like to thank Thermo Fisher Scientific and Phytronix Technologies for their support as well as Paul B. Fayad and Sung Vo Duy for their technical and scientific expertise.

## 6.6 Supplementary material

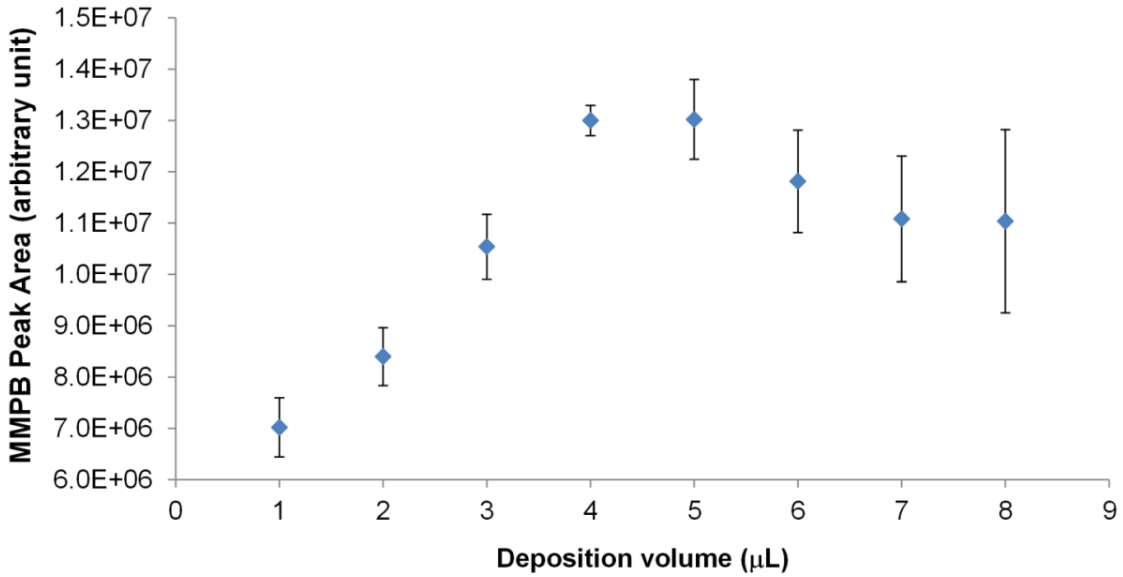


**Figure 6S-1.** Effect of deposition volume on average peak area of target compound, MMPB. Vertical error bars represent standard deviations from the mean (n = 6).

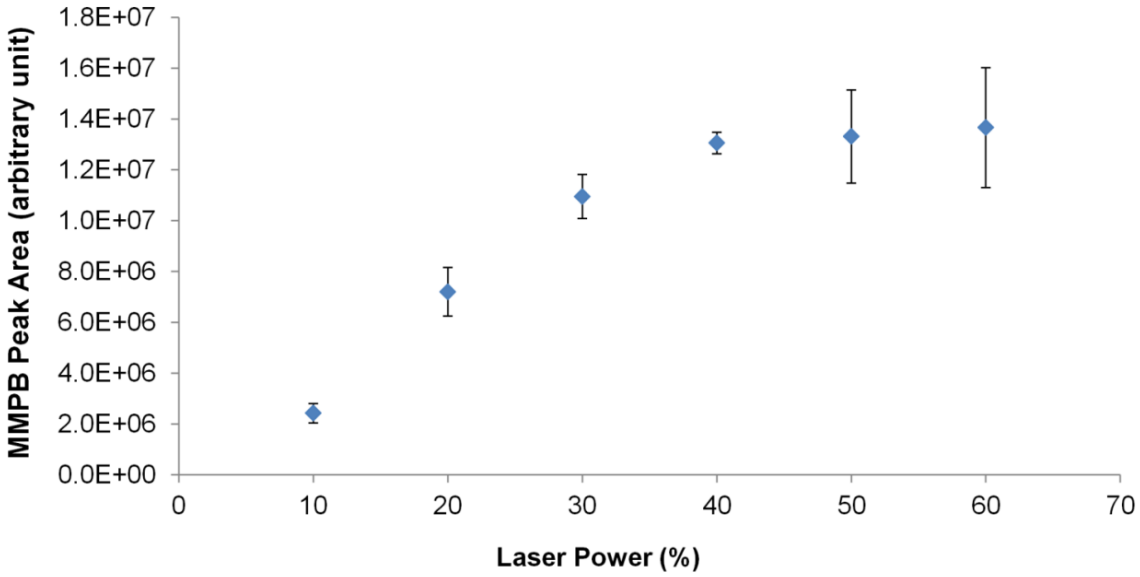


**Figure 6S-2.** Effect of LDTD laser power on average peak area of target compound, MMPB. Vertical error bars represent standard deviations from the mean (n = 6).

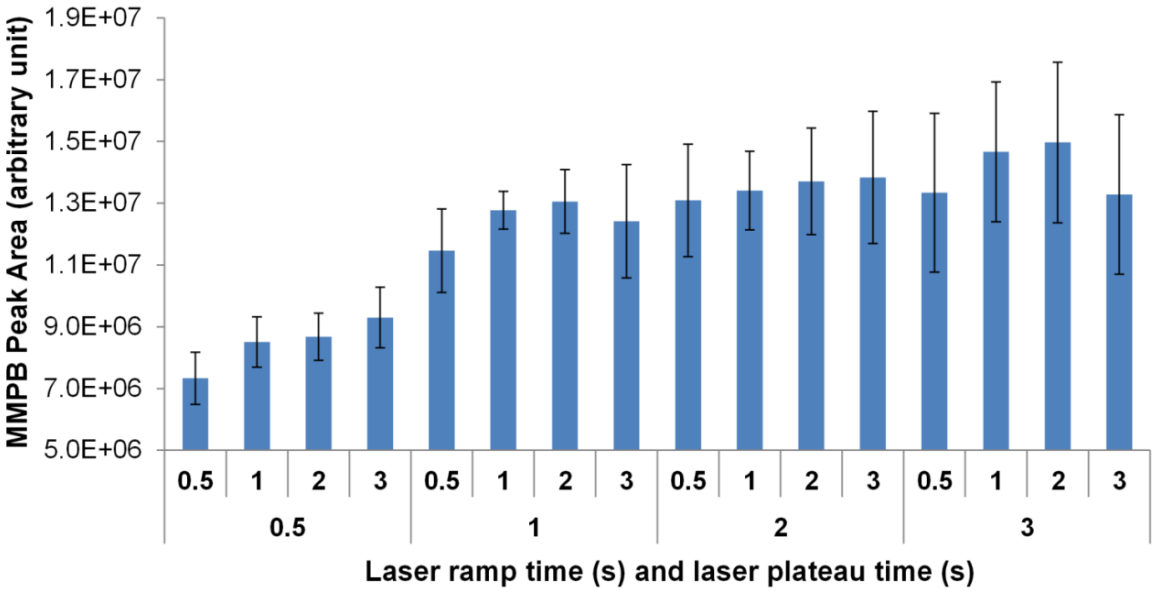


**Figure 6S-3.** Effect of the laser ramp time (first x-axis) and laser plateau time (second x-axis) on average peak area of target compound, MMPB. Vertical error bars represent standard deviations from the mean (n = 6).

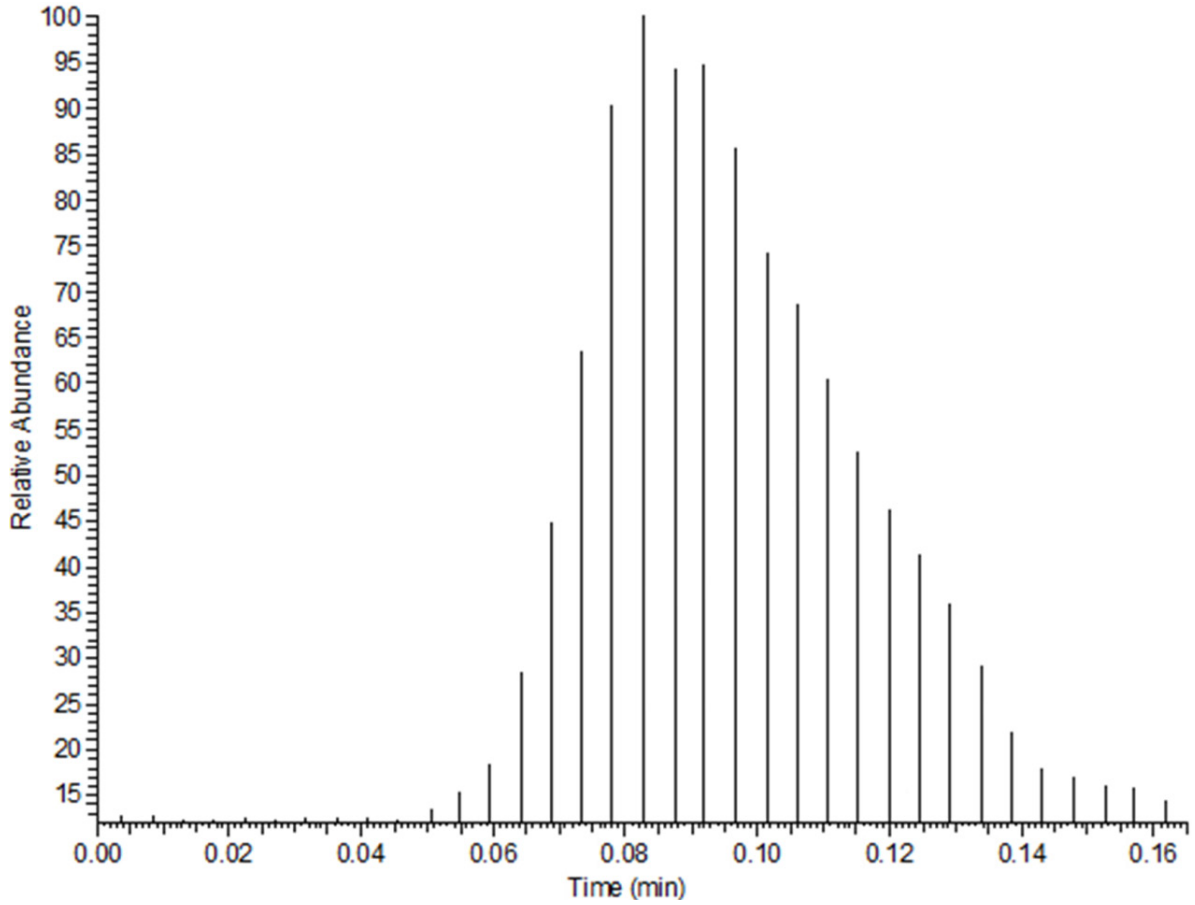


**Figure 6S-4.** Example of peak distortion when laser ramp time from the LDTD is 4 seconds.

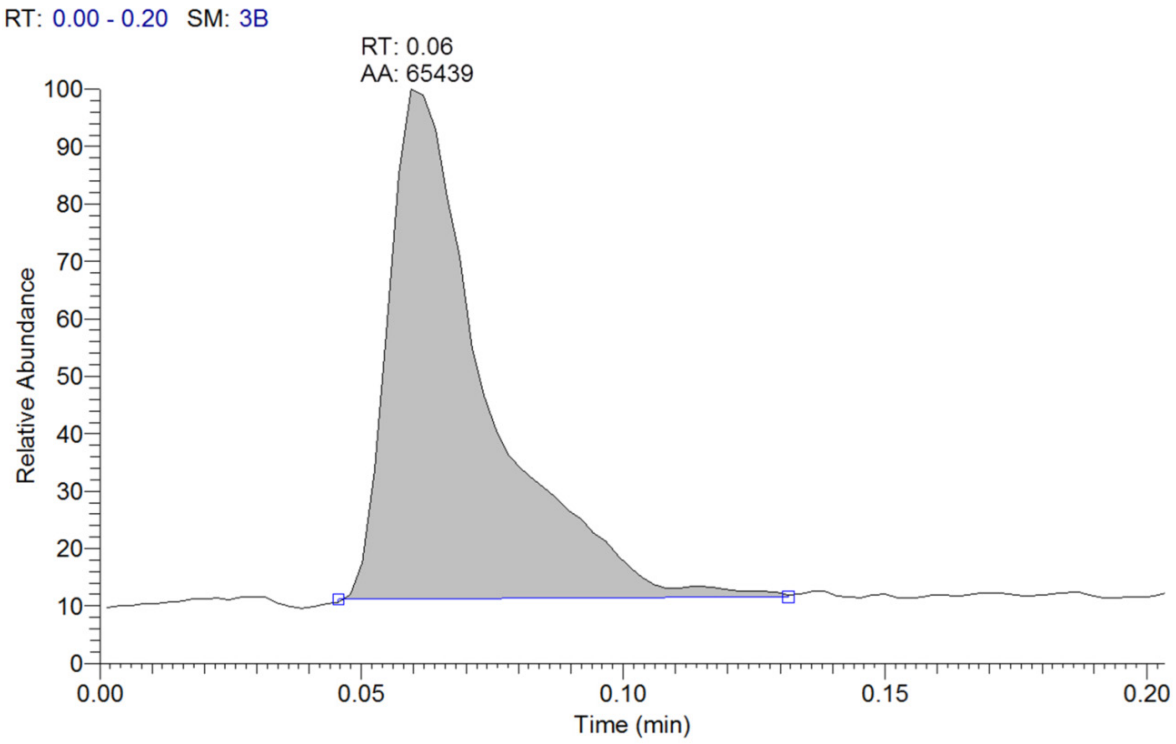


**Figure 6S-5.** Example of a LDTD signal of MMPB around the MQL concentration (8 µg $kg^{-1}$).

**Tableau 6S-1.** Comparison of microcystins detection in fish samples using three detection methods.

| No. Sample | Location | Fish specie | Fish part | Total MC via MMPB and HRMS ($\mu g\ kg^{-1}$)[a] (RSD - %) | Total MC via MMPB and MS/MS ($\mu g\ kg^{-1}$)[b] (RSD - %) | Total MC with standards ($\mu g\ kg^{-1}$)[c] |
|---|---|---|---|---|---|---|
| 1 | Lac Vert | Rainbow smelt | No head/viscera | **11.9 (7)** | **10.3 (9)** | ND |
| 2 | Lac Vert | White sucker | Whole | **8.7 (8)** | **7.5 (12)** | ND |
| 3 | Lac Vert | White sucker | Whole | **13.2 (6)** | **11.9 (11)** | **2.0** |
| 4 | Lac Vert | White sucker | Whole | **9.5 (10)** | **8.1 (11)** | ND |
| 5 | Lac Vert | Brook trout | Muscle | ND | ND | ND |
| 6 | Lac Vert | Brook trout | Muscle | **5.0 (10)** | ND | ND |
| 7 | Lac Vert | Brook trout | Muscle | **4.5 (9)** | ND | ND |
| 8 | Lac Roxton | Yellow perch | Muscle | ND | ND | ND |
| 9 | Lac Roxton | Yellow perch | Muscle | **4.0 (10)** | ND | ND |
| 10 | Lac Roxton | Yellow perch | Muscle | ND | ND | ND |
| 11 | Lac Roxton | Yellow perch | Muscle | **3.1 (11)** | ND | ND |
| 12 | Lac Roxton | Yellow perch | Muscle | ND | ND | ND |
| 13 | Lac Roxton | Yellow perch | Muscle | ND | ND | ND |
| 14 | Lac Roxton | Yellow perch | Muscle | **5.2 (9)** | ND | ND |
| 15 | Lac Roxton | Yellow perch | Muscle | ND | ND | ND |
| 16 | Lac Noir | Yellow perch | Muscle | ND | ND | ND |
| 17 | Lac Noir | Yellow perch | Muscle | **4.5 (7)** | ND | ND |
| 18 | Lac Noir | Yellow perch | Muscle | **7.3 (11)** | **6.9 (12)** | ND |
| 19 | Lac Noir | Yellow perch | Muscle | ND | ND | ND |
| 20 | Lac Noir | Yellow perch | Muscle | **2.7 (12)** | ND | ND |
| 21 | Lac Noir | Walleye | Muscle | ND | ND | ND |
| 22 | Lac Noir | Walleye | Muscle | **4.4 (8)** | ND | ND |
| 23 | Lac Noir | Walleye | Muscle | ND | ND | ND |
| 24 | Lac Noir | Walleye | Muscle | **2.9 (10)** | ND | ND |
| 25 | Lac Noir | Walleye | Muscle | ND | ND | ND |
| 26 | Lac Noir | Walleye | Muscle | ND | ND | ND |
| 27 | Lac Noir | Walleye | Muscle | **3.4 (9)** | ND | ND |
| 28 | Lac Noir | Walleye | Muscle | ND | ND | ND |
| 29 | Lac Noir | Pike | Muscle | ND | ND | ND |
| 30 | Lac Noir | Pike | Muscle | ND | ND | ND |
| 31 | Lac Noir | Pike | Muscle | ND | ND | ND |
| 32 | Lac Noir | Brown bullhead | Muscle | ND | ND | ND |
| 33 | Lac Noir | Brown bullhead | Muscle | **3.8 (9)** | ND | ND |
| 34 | Lac Noir | Brown bullhead | Muscle | ND | ND | ND |
| 35 | Lac Noir | Brown bullhead | Muscle | **5.2 (8)** | ND | ND |
| 36 | Lac Noir | Brown bullhead | Muscle | ND | ND | ND |
| 37 | Lac Noir | Lake whitefish | Muscle | ND | ND | ND |
| 38 | Lac Noir | Lake whitefish | Muscle | **7,1 (8)** | ND | ND |
| 39 | Lac Noir | Lake whitefish | Muscle | ND | ND | ND |
| 40 | Lac Noir | Lake whitefish | Muscle | **6,2 (9)** | ND | ND |
| 41 | Lac Noir | Lake whitefish | Muscle | **5.9 (7)** | ND | ND |

**Tableau 6S-1.** *Continued.*

| No. Sample | Location | Fish Specie | Fish part | Total MC via MMPB and HRMS ($\mu g\ kg^{-1}$)[a] (RSD - %) | Total MC via MMPB and MS/MS ($\mu g\ kg^{-1}$)[b] (RSD - %) | Total MC with standards ($\mu g\ kg^{-1}$)[c] |
|---|---|---|---|---|---|---|
| 42 | Lac Noir | Lake whitefish | Muscle | ND | ND | ND |
| 43 | Lac Noir | Lake whitefish | Muscle | ND | ND | ND |
| 44 | Lac Noir | Lake whitefish | Muscle | **7.3 (10)** | ND | ND |
| 45 | Lac Noir | Lake whitefish | Muscle | **4.5 (11)** | ND | ND |
| 46 | Lac Noir | Lake whitefish | Muscle | **3.0 (9)** | ND | ND |
| 47 | Lac Noir | Lake whitefish | Muscle | ND | ND | ND |
| 48 | Lac Noir | Lake whitefish | Muscle | ND | ND | ND |
| 49 | Lac Noir | Yellow perch | Muscle | **3.7 (11)** | ND | ND |

ND – Not detected

[a]Total microcystins determined via MMPB using LDTD-APCI-HRMS.

[b]Total microcystins determined via MMPB using LDTD-APCI-MS/MS.

[c]Microcystins determined via the summation of all microcystins for which standards allowed detection and quantification (i.e. MC-LA, MC-LR, MC-RR and MC-YR) using LC-MS/MS.

# Chapitre 7. Conclusion

## 7.1 Conclusions générales

La présence des cyanobactéries est une menace constante de par leur production de métabolites secondaires, les cyanotoxines. Ces composés possèdent des toxicités variables allant de simples problèmes d'irritation à des symptômes graves reliés à des troubles neurodégénératifs et de lésions d'organes. Quelques normes internationales ont été établies afin de contrôler le contact avec des sources d'eaux contaminées, mais le manque d'information sur la plupart des cyanotoxines limite l'implantation d'une réglementation globale. Avec l'augmentation des épisodes d'efflorescences de cyanobactéries et la vaste distribution des cyanotoxines, des méthodes analytiques performantes sont nécessaires pour mieux comprendre leurs impacts et en gérer les risques. De nombreuses méthodes analytiques ont été développées au cours des dernières décennies pour la détection et la quantification des cyanotoxines, mais étant donné leurs propriétés chimiques complexes et variées, regrouper toutes les espèces en une seule méthode d'analyse demeure un défi. Le **Tableau 7-1** présente les caractéristiques des méthodes analytiques proposées dans cette thèse et les méthodes comparables développées antérieurement.

**Tableau 7-1.** Comparaison entre les méthodes analytiques de la thèse et les méthodes analytiques antérieures.

| Méthode | MC eau | MMPB eau | MMPB poisson | ANA-a | CYN | STX | BMAA | Commentaires |
|---|---|---|---|---|---|---|---|---|
| UHPLC-MS/MS[a] | 0,01 – 0,02 µg $L^{-1}$ | NA | NA | 0,01 µg $L^{-1}$ | 0,02 µg $L^{-1}$ | NA | NA | Sensible, sélectif, robuste<br>Dispendieux, standards peu disponibles, temps d'analyse plus courts (jusqu'à 10 min) |
| UHPLC-HRMS[b] | NA | NA | NA | 0,007 µg $L^{-1}$ | 0,01 µg $L^{-1}$ | 0,01 µg $L^{-1}$ | 0,008 µg $L^{-1}$ | Sensible, très sélectif (masse exacte), robuste et fiable<br>Dispendieux, standards peu disponibles, temps d'analyse plus courts (jusqu'à 10 min) |
| LDTD-MS/MS[c] | NA | 0,2 µg $L^{-1}$ | NA | NA | NA | NA | NA | Temps d'analyse ultra-rapides (15 s), robuste, sensible<br>Dispendieux, aucune séparation chromatographique |
| LDTD-HRMS[d] | NA | NA | 2.7 µg $kg^{-1}$ | 0,2 µg $L^{-1}$ | NA | NA | NA | Temps d'analyse ultra-rapides (15 s), robuste, sensible, sélectif (masse exacte)<br>Dispendieux, aucune séparation chromatographique |
| ELISA | 0,006 – 0,2 µg $L^{-1}$ | NA | NA | NA | 0,04 µg $L^{-1}$ | 0,003 – 0,01 µg $L^{-1}$ | NA | Sensible, peu dispendieux, rapide<br>Peu reproductible, sélectivité croisée |
| HPLC-MS/MS | 0,02 – 1,5 µg $L^{-1}$ | 0,002 - 0,1 µg $L^{-1}$ | 0,2 – 1 µg $kg^{-1}$ | 0,008 µg $L^{-1}$ | 0,2 µg $L^{-1}$ (C18)<br>0,01 µg $L^{-1}$ (HILIC) | 0,425 µg $L^{-1}$ | 0,4 µg $L^{-1}$ (HILIC) | Sensible, sélectif, robuste et fiable<br>Dispendieux, standards peu disponibles, longs temps d'analyse (jusqu'à 30 min) |
| UHPLC-MS/MS | 0,002 – 0,2 µg $L^{-1}$ | NA | NA | 0,13 µg $L^{-1}$ | 0,17 µg $L^{-1}$ (C18) | NA | 0,025 µg $L^{-1}$ (C18) | Sensible, sélectif, robuste et fiable<br>Dispendieux, standards peu disponibles, temps d'analyse plus courts (jusqu'à 10 min) |

[a] Méthode analytique en référence au Chapitre 2
[b] Méthode analytique en référence au Chapitre 3
[c] Méthode analytique en référence au Chapitre 4
[d] Méthode analytique en référence aux Chapitres 5 et 6

En tenant compte de cette problématique, diverses méthodes analytiques ont été développées et validées pour l'analyse des cyanotoxines incluant les MC, l'ANA-a, le CYN, les STX et le BMAA dans les eaux de lac contaminés et les poissons. Une première approche pour l'analyse de six MC (MC-RR, YR, LR, LY, LW et LF) ainsi que ANA-a et CYN a été développée à l'aide d'une extraction sur phase solide en ligne couplée à la chromatographie liquide, à une ionisation par nébulisation électrostatique chauffée et une détection par spectrométrie de masse en tandem (SPE-LC-HESI-MS/MS). La méthode permet l'analyse de plusieurs toxines en une analyse simple et rapide (8 minute par échantillon) dans des eaux contaminées en cyanobactéries tout en séparant ANA-a de son interférant isobare, la phénylalanine. En raison des faibles limites de détection (0,01-0,02 $\mu g\ L^{-1}$), la méthode a permis de détecter plusieurs congénères de MC et ANA-a dans 12 échantillons analysés avec des concentrations souvent plus élevées dans l'eau brute que les recommandations de l'Organisation Mondiale de la Santé (OMS - 1 $\mu g\ L^{-1}$) pour la MC-LR (entre 1,2 et 36 $\mu g\ L^{-1}$) dans l'eau potable. Cette méthode permet principalement de faire l'analyse rapide de 8 cyanotoxines aux propriétés physicochimiques diverses avec une grande sensibilité, se comparant avec les performances obtenues avec les méthodes analytiques antérieures (**Tableau 7-1**). L'amélioration se veut principalement dans l'étendue des cyanotoxines analysées en incluant CYN et la séparation analytique d'ANA-a et PHE. Par contre, certains congénères des MC ne sont pas présents dans la méthode analytique. Il est parfois difficile et coûteux de se procurer plusieurs étalons différents des cyanotoxines. Dans ce cas-ci, la MC-LA n'était pas inclue dans l'analyse, bien qu'elle est souvent dominante dans des eaux contaminées par des MC. Il serait donc important d'inclure cette toxine lors de travaux futurs afin d'avoir une détection plus représentative des cyanotoxines.

Une méthode d'analyse a été développée pour la détection des cyanotoxines BMAA, ANA-a, CYN et STX dans des eaux de lacs à l'aide d'une détection par LC-HESI couplée à la spectrométrie de masse à haute résolution (HRMS) soit par le Q-Exactive. Le développement analytique a consisté en l'utilisation d'une préconcentration à l'aide de la SPE manuelle et d'une dérivatisation à l'aide de chlorure de dansyle permettant une chromatographie simplifiée et une fragmentation spécifique des composés. De plus, l'étude de deux isomères de constitution du BMAA, le DAB et l'AEG, a permis de détecter le BMAA de manière

spécifique grâce à la séparation chromatographique et la détection à haute résolution. Une possible surévaluation par la coélution de BMAA et AEG a été évitée par l'élucidation de fragments spécifiques par détection en masse exacte. Des limites de détection entre 0,007 et 0,01 µg $L^{-1}$ ont été obtenues, une amélioration comparativement aux méthodes analytiques antérieures (**Tableau 7-1**) et les diverses toxines ont été détectées à basses concentrations dans les échantillons analysés à l'exception de STX. Le BMAA a finalement été détecté à des concentrations entre 0,01 et 0,3 µg $L^{-1}$. L'avantage principal de cette approche est l'inclusion de plusieurs cyanotoxines aux propriétés complexes dans une même analyse. En effet, cette méthode propose pour la premières fois une analyse du BMAA, avec trois autres cyanotoxines alcaloïdes utilisant une dérivatisation chimique. De plus, la HRMS s'est montré plus performante quant à la sélectivité des analyses. Il serait par contre important, dans un travail futur, d'améliorer la séparation chromatographique des composés BMAA et AEG.

Les dernières approches analytiques incluent la détection des MC et d'ANA-a grâce à une méthode ultra-rapide d'introduction d'échantillons par désorption thermique à diode laser couplée à une ionisation chimique à pression atmosphérique (LDTD-APCI). Malgré qu'elle soit souvent moins sensible lorsqu'aucune étape de préconcentration n'est utilisée, cette interface élimine l'utilisation de LC et permet des temps d'analyse de moins de 15 secondes par échantillon en plus de simplifier les étapes de préparations d'échantillons. La première partie consistait en l'analyse des MC totales dans les eaux de lacs contaminés par LDTD-APCI-MS/MS. On retrouve plus de 100 congénères différents des MC, mais seulement près de 12 congénères sont disponibles sur le marché comme étalons. À l'aide d'une oxydation de Lemieux à base de permanganate de potassium et de periodate de sodium, il a été possible détacher un fragment communs à toutes les MC, le MMPB, et ainsi permettre une analyse globale de tous les congénères. La méthode proposée possède une limite de détection 0,2 µg $L^{-1}$ qui est en concordance avec la limite de l'OMS étant de 1 µg $L^{-1}$. Ensuite, des échantillons contaminés en cyanobactéries ont été analysés afin de comparer les résultats avec les analyses standards du Centre d'expertise en analyse environnementale du Québec (CEAEQ), afin d'évaluer le risque de sous-estimation d'une analyse par MC ciblées. Des concentrations entre 1 et 425 µg $L^{-1}$ ont été obtenues et une sous-évaluation allant de 5 à 85 % a permis de suggérer

que la présence d'isomères et de d'autres congénères des MC ne sont pas pris en compte dans les analyses de routines par LC-MS/MS.

La deuxième partie consiste en l'analyse ultra-rapide d'ANA-a dans les eaux de lacs à l'aide de la LDTD-APCI-HRMS. La méthode analytique a été développée sans extraction ni préconcentration, mais avec une filtration et une modification de pH en solution permettant ainsi des temps d'analyse très rapides. L'utilisation de la HRMS a permis de résoudre une interférence isobare à l'ANA-a, la phénylalanine. En effet, autant les masses précurseurs et fragments des deux molécules ne peuvent être résolues à l'aide de MS et MS/MS. Par contre, le pouvoir de résolution de la HRMS permet de distinguer les deux composés et de permettre l'élimination d'une séparation chromatographique et d'une analyse par LDTD. La méthode analytique possède une limite de détection de 0,2 $\mu g\ L^{-1}$ et la toxine a été détectée dans un échantillon avec une concentration de 0,21 $\mu g\ L^{-1}$. Comparativement aux méthodes développées par chromatographie inclues dans cette thèse et aux méthodes antérieures proposées dans la littérature, les limites de détections sont plus élevées (**Tableau 7-1**) et cette méthode ne se distingue par sa sensibilité. Par contre, l'avantage réside par la grande rapidité d'analyse permettant une détection quasi instantanée d'une contamination dans un lac ciblé.

Finalement, la méthode des MC totales a été adaptée pour l'analyse de poissons en utilisant la LDTD-APCI-HRMS pour la détection afin d'améliorer la sélectivité et la sensibilité. Les matrices de poisson étant complexes et les MC se liant de manière irréversible sur les tissus, une méthode d'extraction a été développée comprenant une digestion à base d'hydroxyde de sodium et une oxydation de Lemieux. De cette manière, les MC ont pu être converties en MMPB et une étape manuelle de SPE a par la suite permis de purifier les échantillons pour finalement les soumettre à l'analyse. La méthode a permis d'obtenir une limite de détection de 2,7 $\mu g\ kg^{-1}$ et une comparaison de l'analyse de différents poissons provenant de lacs au travers du Québec a été faite entre la méthode développée, la même méthode appliquée à la MS/MS et les analyses standards du CEAEQ. L'utilisation de la HRMS a permis une amélioration de la sensibilité des analyses étant donné que la limite de détection en MS/MS était de 6,8 $\mu g\ kg^{-1}$. De plus, des concentrations considérablement plus élevées ont été observées par la méthode analytique développée, obtenant des concentrations

entre 2,9 et 13,2 µg $kg^{-1}$ pour la moitié des poissons analysés tandis que la méthode standard a permis de détecter uniquement la MC-LY dans un seul échantillon à 2 µg $kg^{-1}$. Ces résultats supposent la présence de MC liées non analysés ainsi que la possible présence de congénères et d'isomères des MC non analysés par la méthode conventionnelle utilisant une extraction liquide et une analyse par LC-MS/MS.

Cette thèse présente de nouvelles stratégies analytiques dans le but de faire une analyse plus étendue des cyanotoxines par le biais de méthodes sélectives et sensibles. Les méthodes chromatographiques avaient pour premier but l'amélioration des analyses multi-toxines en incluant plus de cyanotoxines en une seule méthode analytiques. La LDTD a été ensuite proposée afin d'obtenir des temps d'analyses ultra-rapides, mais elle se voit limitée sur les types de toxines analysables. En effet, les molécules plus polaires peuvent être difficilement vaporisées ou ionisées par l'APCI en plus d'être plus facilement soumis à des faux positifs. Le BMAA, par exemple, est très polaire et ne s'ionise pas en APCI. De plus, il ne peut être analysé par cette technique, car une séparation chromatographique est nécessaire afin d'éliminer les faux positifs causés par ses isomères de conformation. Aussi, les MC étant très peu volatiles, ne peuvent être analysés utilisant la LDTD sans recourir à une dérivatisation. Les analyses, par le biais du MMPB, ont permis la détection du spectre total des MC. Par la suite, l'utilisation de la HRMS s'est vue, pour la première fois, un outil intéressant quant à la sélectivité des méthodes analytiques quantitatives ciblant les cyanotoxines. En effet, une détection à masse exacte permet de distinguer le signal de nos analytes d'une majeure partie des interférences isobares.

## 7.2 Perspectives

Malgré que l'étude des cyanobactéries et des cyanotoxines date de plusieurs décennies, leur détection et leur compréhension demeure un défi de taille. Globalement, la prédiction des efflorescences des points de vue spatial et temporel est encore aujourd'hui très difficile, principalement causé par la mécompréhension des mécanismes de production spécifiques des cyanobactéries et des cyanotoxines. De plus, les changements climatiques et l'eutrophisation des milieux naturels augmentent la production et la variabilité des efflorescences

cyanobactériennes. Ce manque de données rend la gestion de risques difficile en temps réel sur la présence de cyanobactéries et de cyanotoxines en milieu aquatique.

Étant donné la difficulté de prédiction de la présence des cyanotoxines, il est important d'utiliser des méthodes analytiques simples, sensibles et rapides pour leur détection simultanée. Cependant, due à leur complexité, aucune méthode biologique ou physicochimique n'a permis à date de détecter toutes les cyanotoxines en une analyse. En effet, vu la diversité de leurs propriétés physicochimiques, il est difficile de développer des méthodes d'extraction ou de séparations chromatographiques qui permettent de cibler et combiner toutes les cyanotoxines du même coup.

Le développement de futures méthodes analytiques des cyanotoxines fait face à plusieurs défis. Comme mentionné précédemment, la grande variété des propriétés physicochimiques rend difficile, à ce jour, la capacité de détecter et quantifier la majorité des cyanotoxines en une seule analyse. Ces composés possèdent, tout d'abord, des conditions de dégradation différentes en fonction du pH, de la température ou de la lumière. Les conditions d'entreposage d'échantillon, d'extraction des composés et d'analyse doivent donc être soigneusement choisies. La distribution et la disponibilité des cyanotoxines peuvent aussi influencer les capacités d'extraction. En effet, ces toxines se retrouvent de manière intra et extra cellulaires, ce qui doit être pris en compte étant donné que cette distribution peut influencer la quantité retrouvée de manière soluble dans un échantillon. La complexité de matrices influence aussi leur distribution. En effet, l'hydrophobicité des cyanotoxines est très variées et certaines vont facilement s'adsorber sur la matière en suspension, tandis que d'autres resteront parfaitement solubles. Le matériel choisi pour l'entreposage est tout aussi critique. Par exemple, il a été observé que les MC peuvent s'adsorber sur certaines surfaces en plastique, tel le polypropylène, tandis que le BMAA s'adsorbe facilement sur des surfaces en verre [141, 307]. En plus d'interactions physiques, certaines toxines peuvent s'accumuler dans les tissus biologiques et même se lier de manière irréversible comme nous montre l'exemple des MC au **Chapitre 6**. Une méthode d'extraction plus agressive peut être optimale pour les MC dans les tissus, mais pourrait considérablement influencer la récupération de d'autre cyanotoxines sensibles aux conditions choisies. D'un point de vue analytique, la disponibilité d'étalons pour les cyanotoxines et leurs congénères est très limitée et demeure un important

obstacle quant à l'analyse quantitative des cyanotoxines. Finalement, le but ultime de toute méthode analytique est de faire des analyses robustes à faibles coûts. À ce jour, les méthodes analytiques à la fois sensibles et sélectives des cyanotoxines sont longues et très coûteuses incluant généralement les techniques chromatographiques couplées à la MS. L'utilisation de dispositifs pour des analyses peu coûteuses sur le terrain, tel l'ELISA, sont limités en termes de sélectivité et de variétés de cyanotoxines analysées.

Des méthodes analytiques plus efficaces par la suite permettraient un suivi rapide des cyanotoxines en fonction des normes établies. La découverte de nouvelles stratégies d'extractions, de nouvelles méthodes chromatographiques et l'avancement technologique des méthodes de détection en sont la clé. Comme démontré aux chapitres précédents, l'utilisation de dérivatisation peut être une option envisageable afin d'uniformiser les propriétés chimiques des cyanotoxines et finalement les regrouper en une analyse. Ensuite, l'utilisation d'une détection par HRMS de manière quantitative, ayant été proposée dans plusieurs chapitres, est envisageable pour des projets futurs grâce à la grande sélectivité qu'elle procure. En améliorant les procédés analytiques des cyanotoxines, on rend accessible des outils permettant de mieux comprendre leur nature et leur caractéristique et ultimement mieux comprendre leurs impacts pour les humains.

Finalement, l'étude des cyanotoxines demeure un sujet d'actualité et même pour de nombreux travaux futurs en chimie analytique, mais aussi dans de nombreux domaines tant biologique, écologique, économique et politique malgré les défis de taille qu'elles imposent. En effet, leur présence peut influencer les activités récréatives locales, la pêche de poissons, crustacés et mollusques locale ou industrielle et même l'alimentation en eaux potable. Il demeure donc primordial d'améliorer le suivi des cyanotoxines afin de prévenir tout contact pouvant causer des problèmes de l'ordre de la santé publique.

# Bibliographie


1. Hartman, H. Photosynthesis and the origin of life. *Origins of Life and Evolution of the Biosphere*, 1998. **28**(4-6): p. 515-521.
2. Hoiczyk, E. et Hansel, A. Cyanobacterial cell walls: news from an unusual prokaryotic envelope. *Journal of Bacteriology*, 2000. **182**(5): p. 1191-1199.
3. Mur, R., Skulberg, O.M. et Utkilen, H. Cyanobacteria in the environment, publié dans *Toxic Cyanobacteria in Water: A guide to their public health consequences, monitoring and management*, Chorus, I. et Bartram, J., Éditeurs. 1999, E & FN Spon: London. p. 1-30.
4. Whitton, B.A. et Potts, M. Introduction to the cyanobacteria, publié dans *Ecology of Cyanobacteria II*, Whitton, B.A., Éditeur. 2012, Springer: Dordrecht. p. 1-13.
5. Garcia-Pichel, F., Belnap, J., Neuer, S. et Schanz, F. Estimates of global cyanobacterial biomass and its distribution. *Algological Studies*, 2003. **109**(1): p. 213-227.
6. Chorus, I. et Bartram, J. (Éditeurs), *Toxic cyanobacteria in water : a guide to their public health consequences, monitoring, and management*, 1999, E & FN Spon: London. 416 p.
7. Izaguirre, G., Hwang, C.J., Krasner, S.W. et McGuire, M.J. Geosmin and 2-methylisoborneol from cyanobacteria in three water supply systems. *Applied and Environmental Microbiology*, 1982. **43**(3): p. 708-714.
8. Funari, E. et Testai, E. Human health risk assessment related to cyanotoxins exposure. *CRC Critical Reviews in Toxicology*, 2008. **38**(2): p. 97-125.
9. Flores, E., Herrero, A., Wolk, C.P. et Maldener, I. Is the periplasm continuous in filamentous multicellular cyanobacteria? *Trends in Microbiology*, 2006. **14**(10): p. 439-443.
10. Paerl, H.W. et Otten, T.G. Harmful cyanobacterial blooms: causes, consequences, and controls. *Microbial Ecology*, 2013. **65**(4): p. 995-1010.
11. Merel, S., Walker, D., Chicana, R., Snyder, S., Baures, E. et Thomas, O. State of knowledge and concerns on cyanobacterial blooms and cyanotoxins. *Environment International*, 2013. **59**: p. 303-327.
12. van Apeldoorn, M.E., Van Egmond, H.P., Speijers, G.J. et Bakker, G.J. Toxins of cyanobacteria. *Molecular Nutrition & Food Research*, 2007. **51**(1): p. 7-60.
13. Chevalier, P., Pilote, R. et Leclerc, J.-M. Risques à la santé publique découlant de la présence de cyanobactéries (algues bleues) toxiques et de microcystines dans trois bassins versants du sud-ouest québécois tributaires du fleuve Saint-Laurent. *Institut National de Santé Publique du Québec*, 2001: p. 153.
14. Zamyadi, A., Ho, L., Newcombe, G., Bustamante, H. et Prevost, M. Fate of toxic cyanobacterial cells and disinfection by-products formation after chlorination. *Water Research*, 2012. **46**(5): p. 1524-1535.
15. Falconer, I.R. et Humpage, A.R. Cyanobacterial (Blue-Green algal) toxins in water supplies: Cylindrospermopsins. *Environmental Toxicology*, 2006. **21**(4): p. 299-304.
16. Wilhelm, S.W., Bullerjahn, G.S., Eldridge, M.L., Rinta-Kanto, J.M., Poorvin, L. et Bourbonniere, R.A. Seasonal hypoxia and the genetic diversity of prokaryote populations in the central basin hypolimnion of Lake Erie: evidence for abundant

cyanobacteria and photosynthesis. *Journal of Great Lakes Research*, 2006. **32**(4): p. 657-671.
17. Codd, G.A. Cyanobacterial toxins, the perception of water quality, and the prioritisation of eutrophication control. *Ecological Engineering*, 2000. **16**(1): p. 51-60.
18. O'neil, J., Davis, T.W., Burford, M.A. et Gobler, C. The rise of harmful cyanobacteria blooms: the potential roles of eutrophication and climate change. *Harmful Algae*, 2012. **14**: p. 313-334.
19. Paerl, H.W. et Paul, V.J. Climate change: links to global expansion of harmful cyanobacteria. *Water Research*, 2012. **46**(5): p. 1349-1363.
20. Stevens, S., Nierzwicki-Bauer, S. et Balkwill, D. Effect of nitrogen starvation on the morphology and ultrastructure of the cyanobacterium Mastigocladus laminosus. *Journal of Bacteriology*, 1985. **161**(3): p. 1215-1218.
21. Adams, D.G., Carr, N.G. et Wilcox, M. The developmental biology of heterocyst and akinete formation in cyanobacteria. *Critical Reviews in Microbiology*, 1981. **9**(1): p. 45-100.
22. Tomitani, A., Knoll, A.H., Cavanaugh, C.M. et Ohno, T. The evolutionary diversification of cyanobacteria: molecular–phylogenetic and paleontological perspectives. *Proceedings of the National Academy of Sciences*, 2006. **103**(14): p. 5442-5447.
23. Kaebernick, M. et Neilan, B.A. Ecological and molecular investigations of cyanotoxin production. *FEMS Microbiology Ecology*, 2001. **35**(1): p. 1-9.
24. Pearson, L., Mihali, T., Moffitt, M., Kellmann, R. et Neilan, B. On the Chemistry, Toxicology and Genetics of the Cyanobacterial Toxins, Microcystin, Nodularin, Saxitoxin and Cylindrospermopsin. *Marine Drugs*, 2010. **8**(5): p. 1650-1680.
25. Neilan, B.A., Pearson, L.A., Muenchhoff, J., Moffitt, M.C. et Dittmann, E. Environmental conditions that influence toxin biosynthesis in cyanobacteria. *Environmental Microbiology*, 2013. **15**(5): p. 1239-1253.
26. Westrick, J.A., Szlag, D.C., Southwell, B.J. et Sinclair, J. A review of cyanobacteria and cyanotoxins removal/inactivation in drinking water treatment. *Analytical and Bioanalytical Chemistry*, 2010. **397**(5): p. 1705-1714.
27. Ferrão-Filho, A.d.S. et Kozlowsky-Suzuki, B. Cyanotoxins: bioaccumulation and effects on aquatic animals. *Marine Drugs*, 2011. **9**(12): p. 2729-2772.
28. Carmichael, W.W. Health effects of toxin-producing cyanobacteria:"The CyanoHABs". *Human and Ecological Risk Assessment: An International Journal*, 2001. **7**(5): p. 1393-1407.
29. Dittmann, E., Fewer, D.P. et Neilan, B.A. Cyanobacterial toxins: biosynthetic routes and evolutionary roots. *Fems Microbiology Reviews*, 2013. **37**(1): p. 23-43.
30. Dawson, R. The toxicology of microcystins. *Toxicon*, 1998. **36**(7): p. 953-962.
31. Jurczak, T., Tarczynska, M., Karlsson, K. et Meriluoto, J. Characterization and diversity of cyano-bacterial hepatotoxins (microcystins) in blooms from polish freshwaters identified by liquid chromatography-electrospray ionisation mass spectrometry. *Chromatographia*, 2004. **59**(9-10): p. 571-578.
32. Puddick, J., Prinsep, M.R., Wood, S.A., Kaufononga, S.A., Cary, S.C. et Hamilton, D.P. High levels of structural diversity observed in microcystins from Microcystis CAWBG11 and characterization of six new microcystin congeners. *Marine Drugs*, 2014. **12**(11): p. 5372-5395.

33. Rivasseau, C., Martins, S. et Hennion, M.-C. Determination of some physicochemical parameters of microcystins (cyanobacterial toxins) and trace level analysis in environmental samples using liquid chromatography. *Journal of Chromatography A*, 1998. **799**(1): p. 155-169.
34. Song, W., De La Cruz, A.A., Rein, K. et O'Shea, K.E. Ultrasonically induced degradation of microcystin-LR and-RR: Identification of products, effect of pH, formation and destruction of peroxides. *Environmental Science & Technology*, 2006. **40**(12): p. 3941-3946.
35. Runnegar, M., Falconer, I. et Silver, J. Deformation of isolated rat hepatocytes by a peptide hepatotoxin from the blue-green alga Microcystis aeruginosa. *Naunyn-Schmiedeberg's Archives of Pharmacology*, 1981. **317**(3): p. 268-272.
36. Fujiki, H. et Suganuma, M. Tumor promotion by inhibitors of protein Z phosphatases 1 and 2A: The okadaic acid class of compounds. *Advances in Cancer Research*, 1993. **61**: p. 143-194.
37. An, J. et Carmichael, W.W. Use of a colorimetric protein phosphatase inhibition assay and enzyme linked immunosorbent assay for the study of microcystins and nodularins. *Toxicon*, 1994. **32**(12): p. 1495-1507.
38. Sainis, I., Fokas, D., Vareli, K., Tzakos, A.G., Kounnis, V. et Briasoulis, E. Cyanobacterial cyclopeptides as lead compounds to novel targeted cancer drugs. *Marine Drugs*, 2010. **8**(3): p. 629-657.
39. MacKintosh, R.W., Dalby, K.N., Campbell, D.G., Cohen, P.T., Cohen, P. et MacKintosh, C. The cyanobacterial toxin microcystin binds covalently to cysteine-273 on protein phosphatase 1. *FEBS Letters*, 1995. **371**(3): p. 236-240.
40. Beattie, K.A., Kaya, K. et Codd, G.A. The cyanobacterium Nodularia PCC 7804, of freshwater origin, produces [L-Har 2] nodularin. *Phytochemistry*, 2000. **54**(1): p. 57-61.
41. Rinehart, K.L., Harada, K., Namikoshi, M., Chen, C., Harvis, C.A., Munro, M.H., Blunt, J.W., Mulligan, P.E. et Beasley, V.R. Nodularin, microcystin, and the configuration of adda. *Journal of the American Chemical Society*, 1988. **110**(25): p. 8557-8558.
42. Gehringer, M.M., Adler, L., Roberts, A.A., Moffitt, M.C., Mihali, T.K., Mills, T.J., Fieker, C. et Neilan, B.A. Nodularin, a cyanobacterial toxin, is synthesized in planta by symbiotic Nostoc sp. *The ISME Journal*, 2012. **6**(10): p. 1834-1847.
43. Yoshizawa, S., Matsushima, R., Watanabe, M.F., Harada, K.-i., Ichihara, A., Carmichael, W.W. et Fujiki, H. Inhibition of protein phosphatases by microcystis and nodularin associated with hepatotoxicity. *Journal of Cancer Research and Clinical Oncology*, 1990. **116**(6): p. 609-614.
44. Ohta, T., Sueoka, E., Iida, N., Komori, A., Suganuma, M., Nishiwaki, R., Tatematsu, M., Kim, S.-J., Carmichael, W.W. et Fujiki, H. Nodularin, a potent inhibitor of protein phosphatases 1 and 2A, is a new environmental carcinogen in male F344 rat liver. *Cancer Research*, 1994. **54**(24): p. 6402-6406.
45. Annila, A., Lehtimäki, J., Mattila, K., Eriksson, J.E., Sivonen, K., Rantala, T.T. et Drakenberg, T. Solution structure of nodularin an inhibitor of serine/threonine-specific protein phosphatases. *Journal of Biological Chemistry*, 1996. **271**(28): p. 16695-16702.

46. Sipiä, V., Kankaanpää, H., Pflugmacher, S., Flinkman, J., Furey, A. et James, K. Bioaccumulation and detoxication of nodularin in tissues of flounder (Platichthys flesus), mussels (Mytilus edulis, Dreissena polymorpha), and clams (Macoma balthica) from the northern Baltic Sea. *Ecotoxicology and Environmental Safety*, 2002. **53**(2): p. 305-311.
47. Osswald, J., Rellan, S., Gago, A. et Vasconcelos, V. Toxicology and detection methods of the alkaloid neurotoxin produced by cyanobacteria, anatoxin-a. *Environment International*, 2007. **33**(8): p. 1070-1089.
48. Koskinen, A.M.P. et Rapoport, H. Synthetic and conformational studies on anatoxin-a - a potent acetylcholine agonist. *Journal of Medicinal Chemistry*, 1985. **28**(9): p. 1301-1309.
49. James, K.J., Furey, A., Sherlock, I.R., Stack, M.A., Twohig, M., Caudwell, F.B. et Skulberg, O.M. Sensitive determination of anatoxin-a, homoanatoxin-a and their degradation products by liquid chromatography with fluorimetric detection. *Journal of Chromatography A*, 1998. **798**(1-2): p. 147-157.
50. Hiller, S., Krock, B., Cembella, A. et Luckas, B. Rapid detection of cyanobacterial toxins in precursor ion mode by liquid chromatography tandem mass spectrometry. *Journal of Mass Spectrometry*, 2007. **42**(9): p. 1238-1250.
51. Fawell, J.K., Mitchell, R.E., Hill, R.E. et Everett, D.J. The toxicity of cyanobacterial toxins in the mouse: II Anatoxin-a. *Human & Experimental Toxicology*, 1999. **18**(3): p. 168-173.
52. Namikoshi, M., Murakami, T., Fujiwara, T., Nagai, H., Niki, T., Harigaya, E., Watanabe, M.F., Oda, T., Yamada, J. et Tsujimura, S. Biosynthesis and transformation of homoanatoxin-a in the cyanobacterium Raphidiopsis mediterranea Skuja and structures of three new homologues. *Chemical Research in Toxicology*, 2004. **17**(12): p. 1692-1696.
53. Kaushik, R. et Balasubramanian, R. Methods and approaches used for detection of cyanotoxins in environmental samples: A review. *Critical Reviews in Environmental Science and Technology*, 2013. **43**(13): p. 1349-1383.
54. Matsunaga, S., Moore, R.E., Niemczura, W.P. et Carmichael, W.W. Anatoxin-a (s), a potent anticholinesterase from Anabaena flos-aquae. *Journal of the American Chemical Society*, 1989. **111**(20): p. 8021-8023.
55. Hall, S., Strichartz, G., Moczydlowski, E., Ravindran, A. et Reichardt, P. The saxitoxins: sources, chemistry, and pharmacology, publié dans *Marine Toxins: Origin, Structure, and Molecular Pharmacology*, Hall, S. et Strichartz, G., Éditeurs. 1990, ACS Symposium Series v. 418, American Chemical Society: Washington. p. 29-65.
56. Kalaitzis, J.A., Chau, R., Kohli, G.S., Murray, S.A. et Neilan, B.A. Biosynthesis of toxic naturally-occurring seafood contaminants. *Toxicon*, 2010. **56**(2): p. 244-258.
57. Kientz, C.E. Chromatography and mass spectrometry of chemical warfare agents, toxins and related compounds: state of the art and future prospects. *Journal of Chromatography A*, 1998. **814**(1): p. 1-23.
58. Alfonso, A., Louzao, M., Vieytes, M. et Botana, L. Comparative study of the stability of saxitoxin and neosaxitoxin in acidic solutions and lyophilized samples. *Toxicon*, 1994. **32**(12): p. 1593-1598.

59. Andrinolo, D.o., Michea, L.F. et Lagos, N. Toxic effects, pharmacokinetics and clearance of saxitoxin, a component of paralytic shellfish poison (PSP), in cats. *Toxicon*, 1999. **37**(3): p. 447-464.
60. Alonso, E., Alfonso, A., Vieytes, M.R. et Botana, L.M. Evaluation of toxicity equivalent factors of paralytic shellfish poisoning toxins in seven human sodium channels types by an automated high throughput electrophysiology system. *Archives of Toxicology*, 2015: p. 1-10.
61. Bourke, A., Hawes, R., Neilson, A. et Stallman, N. An outbreak of hepato-enteritis (the Palm Island mystery disease) possibly caused by algal intoxication. *Toxicon*, 1983. **21**: p. 45-48.
62. de la Cruz, A.A., Hiskia, A., Kaloudis, T., Chernoff, N., Hill, D., Antoniou, M.G., He, X.X., Loftin, K., O'Shea, K., Zhao, C., Pelaez, M., Han, C., Lynch, T.J. et Dionysiou, D.D. A review on cylindrospermopsin: the global occurrence, detection, toxicity and degradation of a potent cyanotoxin. *Environmental Science-Processes & Impacts*, 2013. **15**(11): p. 1979-2003.
63. Kiss, T., Vehovszky, A., Hiripi, L., Kovacs, A. et Vörös, L. Membrane effects of toxins isolated from a cyanobacterium, Cylindrospermopsis raciborskii, on identified molluscan neurones. *Comparative Biochemistry and Physiology Part C: Toxicology & Pharmacology*, 2002. **131**(2): p. 167-176.
64. Runnegar, M.T., Kong, S.-M., Zhong, Y.-Z., Ge, J.-L. et Lu, S.C. The role of glutathione in the toxicity of a novel cyanobacterial alkaloid cylindrospermopsin in cultured rat hepatocytes. *Biochemical and Biophysical Research Communications*, 1994. **201**(1): p. 235-241.
65. Runnegar, M.T., Kong, S.-M., Zhong, Y.-Z. et Lu, S.C. Inhibition of reduced glutathione synthesis by cyanobacterial alkaloid cylindrospermopsin in cultured rat hepatocytes. *Biochemical Pharmacology*, 1995. **49**(2): p. 219-225.
66. Banker, R., Carmeli, S., Werman, M., Teltsch, B., Porat, R. et Sukenik, A. Uracil moiety is required for toxicity of the cyanobacterial hepatotoxin cylindrospermopsin. *Journal of Toxicology and Environmental Health Part A*, 2001. **62**(4): p. 281-288.
67. Shaw, G.R., Seawright, A.A., Moore, M.R. et Lam, P.K. Cylindrospermopsin, a cyanobacterial alkaloid: evaluation of its toxicologic activity. *Therapeutic Drug Monitoring*, 2000. **22**(1): p. 89-92.
68. Saker, M.L., Metcalf, J.S., Codd, G.A. et Vasconcelos, V.M. Accumulation and depuration of the cyanobacterial toxin cylindrospermopsin in the freshwater mussel Anodonta cygnea. *Toxicon*, 2004. **43**(2): p. 185-194.
69. Nagai, H., Yasumoto, T. et Hokama, Y. Aplysiatoxin and debromoaplysiatoxin as the causative agents of a red alga Gracilaria coronopifolia poisoning in Hawaii. *Toxicon*, 1996. **34**(7): p. 753-761.
70. Werner, K.A., Marquart, L. et Norton, S.A. Lyngbya dermatitis (toxic seaweed dermatitis). *International Journal of Dermatology*, 2012. **51**(1): p. 59-62.
71. Taylor, M.S., Stahl-Timmins, W., Redshaw, C.H. et Osborne, N.J. Toxic alkaloids in Lyngbya majuscula and related tropical marine cyanobacteria. *Harmful Algae*, 2014. **31**: p. 1-8.
72. Cox, P.A., Banack, S.A., Murch, S.J., Rasmussen, U., Tien, G., Bidigare, R.R., Metcalf, J.S., Morrison, L.F., Codd, G.A. et Bergman, B. Diverse taxa of cyanobacteria produce beta-N-methylamino-L-alanine, a neurotoxic amino acid (vol

102, pg 5074, 2005). *Proceedings of the National Academy of Sciences of the United States of America*, 2005. **102**(27): p. 9734-9734.
73. Vega, A. et Bell, E.A. α-Amino-β-methylaminopropionic acid, a new amino acid from seeds of Cycas circinalis. *Phytochemistry*, 1967. **6**(5): p. 759-762.
74. Bradley, W.G. et Mash, D.C. Beyond Guam: The cyanobacteria/BMAA hypothesis of the cause of ALS and other neurodegenerative diseases. *Amyotrophic Lateral Sclerosis*, 2009. **10**: p. 7-20.
75. Glover, W.B., Liberto, C.M., McNeil, W.S., Banack, S.A., Shipley, P.R. et Murch, S.J. Reactivity of beta-methylamino-L-alanine in complex sample matrixes complicating detection and quantification by mass spectrometry. *Analytical Chemistry*, 2012. **84**(18): p. 7946-7953.
76. Lobner, D., Piana, P.M.T., Salous, A.K. et Peoples, R.W. beta-N-methylamino-L-alanine enhances neurotoxicity through multiple mechanisms. *Neurobiology of Disease*, 2007. **25**(2): p. 360-366.
77. Pablo, J., Banack, S.A., Cox, P.A., Johnson, T.E., Papapetropoulos, S., Bradley, W.G., Buck, A. et Mash, D.C. Cyanobacterial neurotoxin BMAA in ALS and Alzheimer's disease. *Acta Neurologica Scandinavica*, 2009. **120**(4): p. 216-225.
78. Jiang, L.Y., Aigret, B., De Borggraeve, W.M., Spacil, Z. et Ilag, L.L. Selective LC-MS/MS method for the identification of BMAA from its isomers in biological samples. *Analytical and Bioanalytical Chemistry*, 2012. **403**(6): p. 1719-1730.
79. Nelson, K.E., Levy, M. et Miller, S.L. Peptide nucleic acids rather than RNA may have been the first genetic molecule. *Proceedings of the National Academy of Sciences*, 2000. **97**(8): p. 3868-3871.
80. Banack, S.A., Metcalf, J.S., Jiang, L., Craighead, D., Ilag, L.L. et Cox, P.A. Cyanobacteria produce N-(2-aminoethyl) glycine, a backbone for peptide nucleic acids which may have been the first genetic molecules for life on earth. *Plos one*, 2012. **7**(11): p. e49043.
81. Stewart, I., Schluter, P.J. et Shaw, G.R. Cyanobacterial lipopolysaccharides and human health–a review. *Environmental Health*, 2006. **5**(1): p. 7.
82. Carmichael, W. A world overview—One-hundred-twenty-seven years of research on toxic cyanobacteria—Where do we go from here?, publié dans *Cyanobacterial harmful algal blooms: State of the science and research needs*. 2008, Springer. p. 105-125.
83. Jochimsen, E.M., Carmichael, W.W., An, J., Cardo, D.M., Cookson, S.T., Holmes, C.E., Antunes, M.B., de Melo Filho, D.A., Lyra, T.M. et Barreto, V.S.T. Liver failure and death after exposure to microcystins at a hemodialysis center in Brazil. *New England Journal of Medicine*, 1998. **338**(13): p. 873-878.
84. Falconer, I.R. An overview of problems caused by toxic blue-green algae (cyanobacteria) in drinking and recreational water. *Environmental Toxicology*, 1999. **14**(1): p. 5-12.
85. World Health Organization. *Guidelines for drinking-water quality*. 4th ed. 2011, World Health Organization: Geneva. 541 p.
86. Chorus, I. *Current approaches to Cyanotoxin risk assessment, risk management and regulations in different countries*, Chorus, I., Éditeur. 2012, Federal Environment Agency: Dessau-Roßlau. 151 p.
87. Wolf, H.U. et Frank, C. Toxicity assessment of cyanobacterial toxin mixtures. *Environmental Toxicology*, 2002. **17**(4): p. 395-399.

88. Jaeg, J.-P. Microcystines: intoxication des animaux domestiques et sécurité des aliments d'origine animale. *Revue de Médecine Vétérinaire*, 2007. **1**(2): p. 46-58.
89. Nicholson, B.C. et Burch, M.D. *Evaluation of analytical methods for detection and quantification of cyanotoxins in relation to Australian drinking water guidelines*, Nicholson, B.C. et Burch, M.D., Éditeurs. 2001, National Health and Medical Research Council of Australia: Canberra. 64 p.
90. Kayagaki, N., Kawasaki, A., Ebata, T., Ohmoto, H., Ikeda, S., Inoue, S., Yoshino, K., Okumura, K. et Yagita, H. Metalloproteinase-mediated release of human Fas ligand. *The Journal of Experimental Medicine*, 1995. **182**(6): p. 1777-1783.
91. Gurbuz, F., Metcalf, J.S., Codd, G.A. et Karahan, A.G. Evaluation of enzyme-linked immunosorbent assays (ELISAs) for the determination of microcystins in cyanobacteria. *Environmental Forensics*, 2012. **13**(2): p. 105-109.
92. Rivasseau, C. et Hennion, M.-C. Potential of immunoextraction coupled to analytical and bioanalytical methods (liquid chromatography, ELISA kit and phosphatase inhibition test) for an improved environmental monitoring of cyanobacterial toxins. *Analytica Chimica Acta*, 1999. **399**(1): p. 75-87.
93. Metcalf, J., Hyenstrand, P., Beattie, K. et Codd, G. Effects of physicochemical variables and cyanobacterial extracts on the immunoassay of microcystin-LR by two ELISA kits. *Journal of Applied Microbiology*, 2000. **89**(3): p. 532-538.
94. Bláhová, L., Oravec, M., Maršálek, B., Šejnohová, L., Šimek, Z. et Bláha, L. The first occurrence of the cyanobacterial alkaloid toxin cylindrospermopsin in the Czech Republic as determined by immunochemical and LC/MS methods. *Toxicon*, 2009. **53**(5): p. 519-524.
95. Micheli, L., Di Stefano, S., Moscone, D., Palleschi, G., Marini, S., Coletta, M., Draisci, R. et Delli Quadri, F. Production of antibodies and development of highly sensitive formats of enzyme immunoassay for saxitoxin analysis. *Analytical and Bioanalytical Chemistry*, 2002. **373**(8): p. 678-684.
96. Stevens, D. et Krieger, R. Stability studies on the cyanobacterial nicotinic alkaloid snatoxin-A. *Toxicon*, 1991. **29**(2): p. 167-179.
97. Kaya, K. et Sano, T. Total microcystin determination using erythro-2-methyl-3-(methoxy-d(3))-4-phenylbutyric acid (MMPB-d(3)) as the internal standard. *Analytica Chimica Acta*, 1999. **386**(1-2): p. 107-112.
98. Duncan, M.W., Villacreses, N.E., Pearson, P.G., Wyatt, L., Rapoport, S.I., Kopin, I.J., Markey, S.P. et Smith, Q.R. 2-amino-3-(methylamino)-propanoic acid (BMAA) pharmacokinetics and blood-brain barrier permeability in the rat. *Journal of Pharmacology and Experimental Therapeutics*, 1991. **258**(1): p. 27-35.
99. Svrcek, C. et Smith, D.W. Cyanobacteria toxins and the current state of knowledge on water treatment options: a review. *Journal of Environmental Engineering and Science*, 2004. **3**(3): p. 155-185.
100. Falconer, I.R., Burch, M.D., Steffensen, D.A., Choice, M. et Coverdale, O.R. Toxicity of the blue-green alga (cyanobacterium) Microcystis aeruginosa in drinking water to growing pigs, as an animal model for human injury and risk assessment. *Environmental Toxicology and Water Quality*, 1994. **9**(2): p. 131-139.
101. Kokociński, M., Dziga, D., Spoof, L., Stefaniak, K., Jurczak, T., Mankiewicz-Boczek, J. et Meriluoto, J. First report of the cyanobacterial toxin cylindrospermopsin in the shallow, eutrophic lakes of western Poland. *Chemosphere*, 2009. **74**(5): p. 669-675.

102. Li, R., Carmichael, W.W., Brittain, S., Eaglesham, G.K., Shaw, G.R., Liu, Y. et Watanabe, M.M. First report of the cyanotoxins cylindrospermopsin and deoxycylindrospermopsin from Raphidiopsis curvata (Cyanobacteria). *Journal of Phycology*, 2001. **37**(6): p. 1121-1126.
103. Lee, H.S., Jeong, C.K., Lee, H.M., Choi, S.J., Do, K.S., Kim, K. et Kim, Y.H. On-line trace enrichment for the simultaneous determination of microcystins in aqueous samples using high-performance liquid chromatography with diode-array detection. *Journal of Chromatography A*, 1999. **848**(1): p. 179-184.
104. Wu, X., Xiao, B., Li, R., Wang, Z., Chen, X. et Chen, X. Rapid quantification of total microcystins in cyanobacterial samples by periodate-permanganate oxidation and reversed-phase liquid chromatography. *Analytica Chimica Acta*, 2009. **651**(2): p. 241-247.
105. Welker, M., Bickel, H. et Fastner, J. HPLC-PDA detection of cylindrospermopsin—opportunities and limits. *Water Research*, 2002. **36**(18): p. 4659-4663.
106. Harada, K.i., Oshikata, M., Shimada, T., Nagata, A., Ishikawa, N., Suzuki, M., Kondo, F., Shimizu, M. et Yamada, S. High-performance liquid chromatographic separation of microcystins derivatized with a highly fluorescent dienophile. *Natural Toxins*, 1997. **5**(5): p. 201-207.
107. Wang, C., Tian, C., Tian, Y., Feng, B., We, S., Li, Y., Wu, X. et Xiao, B. A sensitive method for the determination of total microcystins in water and sediment samples by liquid chromatography with fluorescence detection. *Analytical Methods*, 2015. **7**(2): p. 759-765.
108. James, K.J., Sherlock, I.R. et Stack, M.A. Anatoxin-a in Irish freshwater and cyanobacteria, determined using a new fluorimetric liquid chromatographic method. *Toxicon*, 1997. **35**(6): p. 963-971.
109. Molica, R.J., Oliveira, E.J., Carvalho, P.V., Costa, A.N., Cunha, M.C., Melo, G.L. et Azevedo, S.M. Occurrence of saxitoxins and an anatoxin-a (s)-like anticholinesterase in a Brazilian drinking water supply. *Harmful Algae*, 2005. **4**(4): p. 743-753.
110. Cianca, R.C.C., Pallares, M.A., Barbosa, R.D., Adan, L.V., Martins, J.M.L. et Gago-Martínez, A. Application of precolumn oxidation HPLC method with fluorescence detection to evaluate saxitoxin levels in discrete brain regions of rats. *Toxicon*, 2007. **49**(1): p. 89-99.
111. Combes, A., El Abdellaoui, S., Sarazin, C., Vial, J., Mejean, A., Ploux, O., Pichon, V. et Grp, B. Validation of the analytical procedure for the determination of the neurotoxin beta-N-methylamino-L-alanine in complex environmental samples. *Analytica Chimica Acta*, 2013. **771**: p. 42-49.
112. Al-Sammak, M.A., Hoagland, K.D., Snow, D.D. et Cassada, D. Methods for simultaneous detection of the cyanotoxins BMAA, DABA, and anatoxin-alpha in environmental samples. *Toxicon*, 2013. **76**: p. 316-325.
113. Barco, M., Rivera, J. et Caixach, J. Analysis of cyanobacterial hepatotoxins in water samples by microbore reversed-phase liquid chromatography–electrospray ionisation mass spectrometry. *Journal of Chromatography A*, 2002. **959**(1): p. 103-111.
114. Takino, M., Daishima, S. et Yamaguchi, K. Analysis of anatoxin-a in freshwaters by automated on-line derivatization–liquid chromatography–electrospray mass spectrometry. *Journal of Chromatography A*, 1999. **862**(2): p. 191-197.

115. Hormazábal, V., Østensvik, Ø., Underdal, B. et Skulberg, O.M. Simultaneous determination of the cyanotoxins anatoxin A, microcystin desmethyl-3, LR, RR, and YR in fish muscle using liquid chromatography-mass spectrometry. *Journal of Liquid Chromatography & Related Technologies*, 2000. **23**(2): p. 185-196.
116. Li, A.F., Tian, Z.J., Li, J., Yu, R.C., Banack, S.A. et Wang, Z.Y. Detection of the neurotoxin BMAA within cyanobacteria isolated from freshwater in China. *Toxicon*, 2010. **55**(5): p. 947-953.
117. Esterhuizen-Londt, M., Downing, S. et Downing, T.G. Improved sensitivity using liquid chromatography mass spectrometry (LC-MS) for detection of propyl chloroformate derivatised beta-N-methylamino-L-alanine (BMAA) in cyanobacteria. *Water SA*, 2011. **37**(2): p. 133-138.
118. Pietsch, C., Wiegand, C., Amé, M.V., Nicklisch, A., Wunderlin, D. et Pflugmacher, S. The effects of a cyanobacterial crude extract on different aquatic organisms: evidence for cyanobacterial toxin modulating factors. *Environmental Toxicology*, 2001. **16**(6): p. 535-542.
119. Mekebri, A., Blondina, G. et Crane, D. Method validation of microcystins in water and tissue by enhanced liquid chromatography tandem mass spectrometry. *Journal of Chromatography A*, 2009. **1216**(15): p. 3147-3155.
120. Amé, M.V., Galanti, L.N., Menone, M.L., Gerpe, M.S., Moreno, V.J. et Wunderlin, D.A. Microcystin–LR,–RR,–YR and–LA in water samples and fishes from a shallow lake in Argentina. *Harmful Algae*, 2010. **9**(1): p. 66-73.
121. Beltran, E., Ibanez, M., Sancho, J.V. et Hernandez, F. Determination of six microcystins and nodularin in surface and drinking waters by on-line solid phase extraction-ultra high pressure liquid chromatography tandem mass spectrometry. *Journal of Chromatography A*, 2012. **1266**: p. 61-68.
122. Oehrle, S.A., Southwell, B. et Westrick, J. Detection of various freshwater cyanobacterial toxins using ultra-performance liquid chromatography tandem mass spectrometry. *Toxicon*, 2010. **55**(5): p. 965-972.
123. Spoof, L., Vesterkvist, P., Lindholm, T. et Meriluoto, J. Screening for cyanobacterial hepatotoxins, microcystins and nodularin in environmental water samples by reversed-phase liquid chromatography–electrospray ionisation mass spectrometry. *Journal of Chromatography A*, 2003. **1020**(1): p. 105-119.
124. Bogialli, S., Bruno, M., Curini, R., Di Corcia, A. et Lagana, A. Simple and rapid determination of anatoxin-a in lake water and fish muscle tissue by liquid-chromatography-tandem mass spectrometry. *Journal of Chromatography A*, 2006. **1122**(1-2): p. 180-185.
125. Jiang, L.Y., Johnston, E., Aberg, K.M., Nilsson, U. et Ilag, L.L. Strategy for quantifying trace levels of BMAA in cyanobacteria by LC/MS/MS. *Analytical and Bioanalytical Chemistry*, 2013. **405**(4): p. 1283-1292.
126. Fan, H., Qiu, J., Fan, L. et Li, A. Effects of growth conditions on the production of neurotoxin 2, 4-diaminobutyric acid (DAB) in Microcystis aeruginosa and its universal presence in diverse cyanobacteria isolated from freshwater in China. *Environmental Science and Pollution Research*, 2014. **22**(8): p. 5943-5951.
127. Vasas, G., Gaspar, A., Pager, C., Suranyi, G., Máthé, C., Hamvas, M.M. et Borbely, G. Analysis of cyanobacterial toxins (anatoxin-a, cylindrospermopsin, microcystin-LR) by capillary electrophoresis. *Electrophoresis*, 2004. **25**(1): p. 108-115.

128. Baptista, M.S., Cianca, R.C.C., Lopes, V.R., Almeida, C.M.R. et Vasconcelos, V.M. Determination of the non protein amino acid beta-N-methylamino-L-alanine in estuarine cyanobacteria by capillary electrophoresis. *Toxicon*, 2011. **58**(5): p. 410-414.
129. Smith, J.L. et Boyer, G.L. Standardization of microcystin extraction from fish tissues: A novel internal standard as a surrogate for polar and non-polar variants. *Toxicon*, 2009. **53**(2): p. 238-245.
130. Cadel-Six, S., Moyenga, D., Magny, S., Trotereau, S., Edery, M. et Krys, S. Detection of free and covalently bound microcystins in different tissues (liver, intestines, gills, and muscles) of rainbow trout (Oncorhynchus mykiss) by liquid chromatography-tandem mass spectrometry: Method characterization. *Environmental Pollution*, 2014. **185**: p. 333-339.
131. Neffling, M.R., Lance, E. et Meriluoto, J. Detection of free and covalently bound microcystins in animal tissues by liquid chromatography-tandem mass spectrometry. *Environmental Pollution*, 2010. **158**(3): p. 948-952.
132. Falconer, I.R. Measurement of toxins from blue-green algae in water and foodstuffs, publié dans *Algal Toxins in Seafood and Drinking Water*, Falconer, I.R., Éditeur. 1993, Academic Press: London. p. 165-175.
133. Almeida, V.P., Cogo, K., Tsai, S.M. et Moon, D.H. Colorimetric test for the monitoring of microcystins in cyanobacterial culture and environmental samples from southeast-Brazil. *Brazilian Journal of Microbiology*, 2006. **37**(2): p. 192-198.
134. Nicholson, B., Papageorgiou, J., Humpage, A., Steffensen, D., Monis, P., Linke, T., Fanok, S., Shaw, G., Eaglesham, G. et Davis, B. *Determination and Significance of Emerging Algal Toxins (Cyanotoxins)*, American Water Works Association., Éditeur. 2007, IWA Publishing: New York. 140 p.
135. Metcalf, J.S. et Codd, G.A. Analysis of cyanobacterial toxins by immunological methods. *Chemical Research in Toxicology*, 2003. **16**(2): p. 103-112.
136. Tillmanns, A.R., Pick, F.R. et Aranda-Rodriguez, R. Sampling and analysis of microcystins: implications for the development of standardized methods. *Environmental Toxicology*, 2007. **22**(2): p. 132-143.
137. McElhiney, J., Drever, M., Lawton, L.A. et Porter, A.J. Rapid isolation of a single-chain antibody against the cyanobacterial toxin microcystin-LR by phage display and its use in the immunoaffinity concentration of microcystins from water. *Applied and Environmental Microbiology*, 2002. **68**(11): p. 5288-5295.
138. Sano, T., Nohara, K., Shiraishi, F. et Kaya, K. A method for micro-determination of total microcystin content in waterblooms of cyanobacteria (blue-green algae). *International Journal of Environmental Analytical Chemistry*, 1992. **49**(3): p. 163-170.
139. Harada, K., Murata, H., Qiang, Z., Suzuki, M. et Kondo, F. Mass spectrometric screening method for microcystins in cyanobacteria. *Toxicon*, 1996. **34**(6): p. 701-710.
140. Msagati, T.A., Siame, B.A. et Shushu, D.D. Evaluation of methods for the isolation, detection and quantification of cyanobacterial hepatotoxins. *Aquatic Toxicology*, 2006. **78**(4): p. 382-397.
141. Cohen, S.A. Analytical techniques for the detection of alpha-amino-beta-methylaminopropionic acid. *Analyst*, 2012. **137**(9): p. 1991-2005.
142. Lawton, L.A., Edwards, C. et Codd, G.A. Extraction and high-performance liquid chromatographic method for the determination of microcystins in raw and treated waters. *Analyst*, 1994. **119**(7): p. 1525-1530.

143. Furey, A., Crowley, J., Hamilton, B., Lehane, M. et James, K.J. Strategies to avoid the mis-identification of anatoxin-a using mass spectrometry in the forensic investigation of acute neurotoxic poisoning. *Journal of Chromatography A*, 2005. **1082**(1): p. 91-97.
144. Moollan, R.W., Rae, B. et Verbeek, A. Some comments on the determination of microcystin toxins in waters by high-performance liquid chromatography. *Analyst*, 1996. **121**(2): p. 233-238.
145. Lawton, L.A., Edwards, C., Beattie, K.A., Pleasance, S., Dear, G.J. et Codd, G.A. Isolation and characterization of microcystins from laboratory cultures and environmental samples of Microcystis aeruginosa and from an associated animal toxicosis. *Natural Toxins*, 1995. **3**(1): p. 50-57.
146. Hoffmann, E.d. et Stroobant, V. *Spectrométrie de masse : cours et exercices corrigés*. 3e éd. ed. Sciences sup Chimie, Hoffmann, E.d., Éditeur. 2005, Dunod: Paris. 425 p.
147. Dell'Aversano, C., Eaglesham, G.K. et Quilliam, M.A. Analysis of cyanobacterial toxins by hydrophilic interaction liquid chromatography–mass spectrometry. *Journal of Chromatography A*, 2004. **1028**(1): p. 155-164.
148. Dahlmann, J., Budakowski, W.R. et Luckas, B. Liquid chromatography–electrospray ionisation-mass spectrometry based method for the simultaneous determination of algal and cyanobacterial toxins in phytoplankton from marine waters and lakes followed by tentative structural elucidation of microcystins. *Journal of Chromatography A*, 2003. **994**(1): p. 45-57.
149. Gagnon, A. et Pick, F.R. Effect of nitrogen on cellular production and release of the neurotoxin anatoxin-a in a nitrogen-fixing cyanobacterium. *Frontiers in Microbiology*, 2012. **3**(211): p. 1-7.
150. Welker, M., Fastner, J., Erhard, M. et von Dohren, H. Applications of MALDI-TOF MS analysis in cyanotoxin research. *Environmental Toxicology*, 2002. **17**(4): p. 367-374.
151. Aráoz, R., Guérineau, V., Rippka, R., Palibroda, N., Herdman, M., Laprevote, O., Von Döhren, H., De Marsac, N.T. et Erhard, M. MALDI-TOF-MS detection of the low molecular weight neurotoxins anatoxin-a and homoanatoxin-a on lyophilized and fresh filaments of axenic Oscillatoria strains. *Toxicon*, 2008. **51**(7): p. 1308-1315.
152. Welker, M., Christiansen, G. et von Döhren, H. Diversity of coexisting Planktothrix (cyanobacteria) chemotypes deduced by mass spectral analysis of microystins and other oligopeptides. *Archives of Microbiology*, 2004. **182**(4): p. 288-298.
153. Wu, J., Hughes, C.S., Picard, P., Letarte, S., Gaudreault, M., Lévesque, J.F., Nicoll-Griffith, D.A. et Bateman, K.P. High-throughput cytochrome P450 inhibition assays using laser diode thermal desorption-atmospheric pressure chemical ionization-tandem mass spectrometry. *Analytical Chemistry*, 2007. **79**(12): p. 4657-4665.
154. Picard, P., Tremblay, P. et Paquin, E.R. Laser Diode Thermal Desorption Ionization Source (LDTD) : Fundamental Aspects, publié dans *56th American Society for Mass Spectrometry Conference*. 2008: Denver, CO, USA.
155. Fayad, P.B., Prévost, M. et Sauvé, S. Laser diode thermal desorption/atmospheric pressure chemical ionization tandem mass spectrometry analysis of selected steroid hormones in wastewater: method optimization and application. *Analytical Chemistry*, 2010. **82**(2): p. 639-45.
156. Jiang, Q., Shi, H. et Zhao, M. Free energy of crystal–liquid interface. *Acta Materialia*, 1999. **47**(7): p. 2109-2112.

157. Daves Jr, G.D. Mass spectrometry of involatile and thermally unstable molecules. *Accounts of Chemical Research*, 1979. **12**(10): p. 359-365.
158. Beuhler, R., Flanigan, E., Greene, L. et Friedman, L. Proton transfer mass spectrometry of peptides. Rapid heating technique for underivatized peptides containing arginine. *Journal of the American Chemical Society*, 1974. **96**(12): p. 3990-3999.
159. Lemoine, P., Roy-Lachapelle, A., Prévost, M., Tremblay, P., Solliec, M. et Sauvé, S. Ultra-fast analysis of anatoxin-A using laser diode thermal desorption-atmospheric pressure chemical ionization-tandem mass spectrometry: Validation and resolution from phenylalanine. *Toxicon*, 2013. **61**: p. 165-74.
160. Solliec, M., Massé, D. et Sauvé, S. Analysis of trimethoprim, lincomycin, sulfadoxin and tylosin in swine manure using laser diode thermal desorption-atmospheric pressure chemical ionization-tandem mass spectrometry. *Talanta*, 2014. **128**: p. 23-30.
161. Swales, J.G., Temesi, D.G., Denn, M. et Murphy, K. Determination of paracetamol in mouse, rat and dog plasma samples by laser diode thermal desorption-APCI-MS/MS. *Bioanalysis*, 2012. **4**(11): p. 1327-1335.
162. Boisvert, M., Fayad, P.B. et Sauvé, S. Development of a new multi-residue laser diode thermal desorption atmospheric pressure chemical ionization tandem mass spectrometry method for the detection and quantification of pesticides and pharmaceuticals in wastewater samples. *Analytica Chimica Acta*, 2012. **754**: p. 75-82.
163. Viglino, L., Prévost, M. et Sauvé, S. High throughput analysis of solid-bound endocrine disruptors by LDTD-APCI-MS/MS. *Journal of Environmental Monitoring*, 2011. **13**(3): p. 583-90.
164. Segura, P.A., Tremblay, P., Picard, P., Gagnon, C. et Sauvé, S. High-throughput quantitation of seven sulfonamide residues in dairy milk using laser diode thermal desorption-negative mode atmospheric pressure chemical ionization tandem mass spectrometry. *Journal of Agricultural and Food Chemistry*, 2010. **58**(3): p. 1442-1446.
165. Byrdwell, W.C. Atmospheric pressure chemical ionization mass spectrometry for analysis of lipids. *Lipids*, 2001. **36**(4): p. 327-346.
166. Horning, E., Horning, M., Carroll, D., Dzidic, I. et Stillwell, R. New picogram detection system based on a mass spectrometer with an external ionization source at atmospheric pressure. *Analytical Chemistry*, 1973. **45**(6): p. 936-943.
167. Sunner, J., Nicol, G. et Kebarle, P. Factors determining relative sensitivity of analytes in positive mode atmospheric pressure ionization mass spectrometry. *Analytical Chemistry*, 1988. **60**(13): p. 1300-1307.
168. Horning, E., Carroll, D., Dzidic, I., Lin, S.-N., Stillwell, R. et Thenot, J.-P. Atmospheric pressure ionization mass spectrometry: Studies of negative ion formation for detection and quantification purposes. *Journal of Chromatography A*, 1977. **142**: p. 481-495.
169. King, R., Bonfiglio, R., Fernandez-Metzler, C., Miller-Stein, C. et Olah, T. Mechanistic investigation of ionization suppression in electrospray ionization. *Journal of the American Society for Mass Spectrometry*, 2000. **11**(11): p. 942-950.
170. Beaudry, F. et Vachon, P. Electrospray ionization suppression, a physical or a chemical phenomenon? *Biomedical Chromatography*, 2006. **20**(2): p. 200-205.
171. Sangster, T., Spence, M., Sinclair, P., Payne, R. et Smith, C. Unexpected observation of ion suppression in a liquid chromatography/atmospheric pressure chemical

ionization mass spectrometric bioanalytical method. *Rapid Communications in Mass Spectrometry*, 2004. **18**(12): p. 1361-1364.
172. Jessome, L.L. et Volmer, D.A. Ion suppression: a major concern in mass spectrometry. *LCGC Solutions for Separation Scientists*, 2006. 1-5.
173. Picard, P., Tremblay, P. et Paquin, E.R. Mechanisms involved in positive atmospheric pressure chemical ionization (APCI) of an LDTD source, publié dans *56th ASMS Conference on Mass Spectrometry and Allied Topics*. 2009: Denver, CO, USA.
174. Badjagbo, K., Picard, P., Moore, S. et Sauvé, S. Direct atmospheric pressure chemical ionization-tandem mass spectrometry for the continuous Real-time trace analysis of benzene, toluene, ethylbenzene, and xylenes in ambient air. *Journal of the American Society for Mass Spectrometry*, 2009. **20**(5): p. 829-836.
175. Beattie, I., Smith, A., Weston, D.J., White, P., Szwandt, S. et Sealey, L. Evaluation of laser diode thermal desorption (LDTD) coupled with tandem mass spectrometry (MS/MS) for support of in vitro drug discovery assays: Increasing scope, robustness and throughput of the LDTD technique for use with chemically diverse compound libraries. *Journal of Pharmaceutical and Biomedical Analysis*, 2012. **59**: p. 18-28.
176. Harris, D.C. *Quantitative Chemical Analysis*, Fiorillo, J., Quinn, D., Treadway, K., Szczepanski, T. et Byrd, M.L., Éditeurs. 2010, Clancy Marshall: New York. 750 p.
177. Balogh, M.P. Debating resolution land mass accuracy in mass spectrometry. *Spectroscopy*, 2004. **19**(10): p. 34-40.
178. Hu, Q., Noll, R.J., Li, H., Makarov, A., Hardman, M. et Graham Cooks, R. The Orbitrap: a new mass spectrometer. *Journal of Mass Spectrometry*, 2005. **40**(4): p. 430-443.
179. James, K.J., Crowley, J., Hamilton, B., Lehane, M., Skulberg, O. et Furey, A. Anatoxins and degradation products, determined using hybrid quadrupole time-of-flight and quadrupole ion-trap mass spectrometry: forensic investigations of cyanobacterial neurotoxin poisoning. *Rapid Communications in Mass Spectrometry*, 2005. **19**(9): p. 1167-1175.
180. Xian, F., Hendrickson, C.L. et Marshall, A.G. High resolution mass spectrometry. *Analytical Chemistry*, 2012. **84**(2): p. 708-719.
181. Kamleh, A., Barrett, M., Wildridge, D., Burchmore, R., Scheltema, R. et Watson, D. Metabolomic profiling using Orbitrap Fourier transform mass spectrometry with hydrophilic interaction chromatography: a method with wide applicability to analysis of biomolecules. *Rapid Communications in Mass Spectrometry*, 2008. **22**(12): p. 1912-1918.
182. Scigelova, M. et Makarov, A. Orbitrap mass analyzer–overview and applications in proteomics. *Proteomics*, 2006. **6**(S2): p. 16-21.
183. Wang, J., Chow, W., Chang, J. et Wong, J.W. Ultrahigh-performance liquid chromatography electrospray ionization Q-Orbitrap mass spectrometry for the analysis of 451 pesticide residues in fruits and vegetables: method development and validation. *Journal of Agricultural and Food Chemistry*, 2014. **62**(42): p. 10375-10391.
184. Liu, X., Ser, Z. et Locasale, J.W. Development and quantitative evaluation of a high-resolution metabolomics technology. *Analytical Chemistry*, 2014. **86**(4): p. 2175-2184.
185. Fedorova, G., Randak, T., Lindberg, R.H. et Grabic, R. Comparison of the quantitative performance of a Q-Exactive high-resolution mass spectrometer with that of a triple

quadrupole tandem mass spectrometer for the analysis of illicit drugs in wastewater. *Rapid Communications in Mass Spectrometry*, 2013. **27**(15): p. 1751-1762.
186. Rochat, B. Quantitative/qualitative analysis using LC-HRMS: the fundamental step forward for clinical laboratories and clinical practice. *Bioanalysis*, 2012. **4**(14): p. 1709-1711.
187. Michalski, A., Damoc, E., Hauschild, J.P., Lange, O., Wieghaus, A., Makarov, A., Nagaraj, N., Cox, J., Mann, M. et Horning, S. Mass spectrometry-based proteomics using Q Exactive, a high-performance benchtop quadrupole orbitrap mass spectrometer. *Molecular & Cellular Proteomics*, 2011. **10**(9).
188. Hurtaud-Pessel, D., Jagadeshwar-Reddy, T. et Verdon, E. Development of a new screening method for the detection of antibiotic residues in muscle tissues using liquid chromatography and high resolution mass spectrometry with a LC-LTQ-Orbitrap instrument. *Food Additives & Contaminants: Part A*, 2011. **28**(10): p. 1340-1351.
189. Cotton, J., Leroux, F., Broudin, S., Marie, M.n., Corman, B., Tabet, J.-C., Ducruix, C.l. et Junot, C. High-resolution mass spectrometry associated with data mining tools for the detection of pollutants and chemical characterization of honey samples. *Journal of Agricultural and Food Chemistry*, 2014. **62**(46): p. 11335-11345.
190. Codd, G.A., Morrison, L.F. et Metcalf, J.S. Cyanobacterial toxins: risk management for health protection. *Toxicology and Applied Pharmacology*, 2005. **203**(3): p. 264-272.
191. Drobac, D., Tokodi, N., Simeunovic, J., Baltic, V., Stanic, D. et Svircev, Z. Human exposure to cyanotoxins and their effects on health. *Arhiv Za Higijenu Rada I Toksikologiju*, 2013. **64**(2): p. 305-316.
192. Wu, X.Q., Wang, C.B., Xiao, B.D., Wang, Y., Zheng, N. et Liu, J.S. Optimal strategies for determination of free/extractable and total microcystins in lake sediment. *Analytica Chimica Acta*, 2012. **709**: p. 66-72.
193. Papadimitriou, T., Kagalou, I., Stalikas, C., Pilidis, G. et Leonardos, I.D. Assessment of microcystin distribution and biomagnification in tissues of aquatic food web compartments from a shallow lake and evaluation of potential risks to public health. *Ecotoxicology*, 2012. **21**(4): p. 1155-1166.
194. Bortoli, S. et Volmer, D. Account: Characterization and identification of microcystins by mass spectrometry. *European Journal of Mass Spectrometry*, 2014. **20**(1): p. 1-19.
195. Institut National de Santé Publique du Québec. Propositions de critères d'intervention et de seuils d'alerte pour les cyanobactéries. *l'Eau, G.S.s.*, 2005. Québec. 4 p.
196. Faassen, E.J., Harkema, L., Begeman, L. et Lurling, M. First report of (homo)anatoxin-a and dog neurotoxicosis after ingestion of benthic cyanobacteria in The Netherlands. *Toxicon*, 2012. **60**(3): p. 378-384.
197. Puschner, B., Hoff, B. et Tor, E.R. Diagnosis of anatoxin-a poisoning in dogs from North America. *Journal of Veterinary Diagnostic Investigation*, 2008. **20**(1): p. 89-92.
198. Aranda-Rodriguez, R., Jin, Z., Harvie, J. et Cabecinha, A. Evaluation of three field test kits to detect microcystins from a public health perspective. *Harmful Algae*, 2015. **42**: p. 34-42.
199. Humpage, A., Froscio, S., Lau, H.-M., Murphy, D. et Blackbeard, J. Evaluation of the Abraxis Strip Test for Microcystins™ for use with wastewater effluent and reservoir water. *Water research*, 2012. **46**(5): p. 1556-1565.

200. Zhou, Y., Tian, X.L., Li, Y.S., Pan, F.G., Zhang, Y.Y., Zhang, J.H., Wang, X.R., Ren, H.L., Lu, S.Y., Li, Z.H., Liu, Z.S., Chen, Q.J. et Liu, J.Q. Development of a monoclonal antibody-based sandwich-type enzyme-linked immunosorbent assay (ELISA) for detection of abrin in food samples. *Food Chemistry*, 2012. **135**(4): p. 2661-2665.
201. Yen, H.-K., Lin, T.-F. et Liao, P.-C. Simultaneous detection of nine cyanotoxins in drinking water using dual solid-phase extraction and liquid chromatography–mass spectrometry. *Toxicon*, 2011. **58**(2): p. 209-218.
202. Lucci, P. et Núñez, O. On-line solid-phase extraction for liquid chromatography with mass spectrometry analysis of pesticides. *Journal of Separation Science*, 2014. **37**(20): p. 2929-2939.
203. Gago-Ferrero, P., Mastroianni, N., Diaz-Cruz, M.S. et Barcelo, D. Fully automated determination of nine ultraviolet filters and transformation products in natural waters and wastewaters by on-line solid phase extraction-liquid chromatography-tandem mass spectrometry. *Journal of Chromatography A*, 2013. **1294**: p. 106-116.
204. Fayad, P.B., Prevost, M. et Sauve, S. On-line solid-phase extraction coupled to liquid chromatography tandem mass spectrometry optimized for the analysis of steroid hormones in urban wastewaters. *Talanta*, 2013. **115**: p. 349-360.
205. Barco, M., Flores, C., Rivera, J. et Caixach, J. Determination of microcystin variants and related peptides present in a water bloom of Planktothrix (Oscillatoria) rubescens in a Spanish drinking water reservoir by LC/ESI-MS. *Toxicon*, 2004. **44**(8): p. 881-886.
206. Lawrence, J.F., Niedzwiadek, B., Menard, C., Lau, B.P.Y., Lewis, D., Kuper-Goodman, T., Carbone, S. et Holmes, C. Comparison of liquid chromatography/mass spectrometry, ELISA, and phosphatase assay for the determination of microcystins in blue-green algae products. *Journal of AOAC International*, 2001. **84**(4): p. 1035-1044.
207. Centre d'expertise en analyse environnementale du Québec. Protocole pour la validation d'une méthode d'analyse en chimie. *Centre d'Expertise en Analyse Environnementale du Québec*, 2009(DR-12-VMC): p. 30.
208. Centre d'Expertise en Analyse Environnementale du Québec. Identification, dénombrement et estimation du biovolume des cyanobactéries et des algues. *Ministère du Développement Durable, de l'Environnement et de la Lutte contre les Changement Climatiques*, 2012(MA. 800 – Cya.alg 1.0): p. 22.
209. Kaloudis, T., Zervou, S.-K., Tsimeli, K., Triantis, T.M., Fotiou, T. et Hiskia, A. Determination of microcystins and nodularin (cyanobacterial toxins) in water by LC–MS/MS. Monitoring of Lake Marathonas, a water reservoir of Athens, Greece. *Journal of Hazardous Materials*, 2013. **263**: p. 105-115.
210. Jiang-qi, Q., Qing-jing, Z., Cheng-xia, J., Pan, L. et Mu, Y. Optimisation of microcystin extraction for their subsequent analysis by HPLC-MS/MS method in urban lake water. *International Journal of Environmental Science and Development*, 2013. **4**(5): p. 600-603.
211. Guzmán-Guillén, R., Prieto, A.I., González, A.G., Soria-Díaz, M.E. et Cameán, A.M. Cylindrospermopsin determination in water by LC-MS/MS: Optimization and validation of the method and application to real samples. *Environmental Toxicology and Chemistry*, 2012. **31**(10): p. 2233-2238.

212. Rodrigues, M., Reis, M. et Mateus, M. Liquid chromatography/negative electrospray ionization ion trap MS 2 mass spectrometry application for the determination of microcystins occurrence in Southern Portugal water reservoirs. *Toxicon*, 2013. **74**: p. 8-18.
213. Schäfer, A.I., Akanyeti, I. et Semião, A.J. Micropollutant sorption to membrane polymers: A review of mechanisms for estrogens. *Advances in Colloid and Interface Science*, 2011. **164**(1): p. 100-117.
214. Poole, C.F., Gunatilleka, A.D. et Sethuraman, R. Contributions of theory to method development in solid-phase extraction. *Journal of Chromatography A*, 2000. **885**(1): p. 17-39.
215. Yang, M., Fazio, S., Munch, D. et Drumm, P. Impact of methanol and acetonitrile on separations based on π–π interactions with a reversed-phase phenyl column. *Journal of Chromatography A*, 2005. **1097**(1): p. 124-129.
216. Howard, K.L. et Boyer, G.L. Quantitative analysis of cyanobacterial toxins by matrix-assisted laser desorption ionization mass spectrometry. *Analytical Chemistry*, 2007. **79**(15): p. 5980-5986.
217. Akcaalan, R., Mazur-Marzec, H., Zalewska, A. et Albay, M. Phenotypic and toxicological characterization of toxic Nodularia spumigena from a freshwater lake in Turkey. *Harmful Algae*, 2009. **8**(2): p. 273-278.
218. Cox, P.A., Banack, S.A., Murch, S.J., Rasmussen, U., Tien, G., Bidigare, R.R., Metcalf, J.S., Morrison, L.F., Codd, G.A. et Bergman, B. Diverse taxa of cyanobacteria produce β-N-methylamino-L-alanine, a neurotoxic amino acid. *Proceedings of the National Academy of Sciences of the United States of America*, 2005. **102**(14): p. 5074-5078.
219. Banack, S.A., Murch, S.J. et Cox, P.A. Neurotoxic flying foxes as dietary items for the Chamorro people, Marianas Islands. *Journal of Ethnopharmacology*, 2006. **106**(1): p. 97-104.
220. Cox, P.A., Banack, S.A. et Murch, S.J. Biomagnification of cyanobacterial neurotoxins and neurodegenerative disease among the Chamorro people of Guam. *Proceedings of the National Academy of Sciences of the United States of America*, 2003. **100**(23): p. 13380-13383.
221. Rao, S.D., Banack, S.A., Cox, P.A. et Weiss, J.H. BMAA selectively injures motor neurons via AMPA/kainate receptor activation. *Experimental Neurology*, 2006. **201**(1): p. 244-252.
222. Cox, P.A., Richer, R., Metcalf, J.S., Banack, S.A., Codd, G.A. et Bradley, W.G. Cyanobacteria and BMAA exposure from desert dust: a possible link to sporadic ALS among Gulf War veterans. *Amyotrophic Lateral Sclerosis*, 2009. **10**(S2): p. 109-117.
223. Humpage, A.R. et Falconer, I.R. Oral toxicity of the cyanobacterial toxin cylindrospermopsin in male Swiss albino mice: Determination of no observed adverse effect level for deriving a drinking water guideline value. *Environmental Toxicology*, 2003. **18**(2): p. 94-103.
224. Shimizu, Y. Microalgal metabolites. *Chemical Reviews*, 1993. **93**(5): p. 1685-1698.
225. Wiberg, G. et Stephenson, N. Toxicologic studies on paralytic shellfish poison. *Toxicology and Applied Pharmacology*, 1960. **2**(6): p. 607-615.
226. Botana, L.M., (Éditeur), *Seafood and Freshwater Toxins: Pharmacology, Physiology, and Detection*, 2000, CRC Press: New York. 1215 p.

227. Fitzgerald, D.J., Cunliffe, D.A. et Burch, M.D. Development of health alerts for cyanobacteria and related toxins in drinking water in South Australia. *Environmental Toxicology*, 1999. **14**(1): p. 203-209.
228. Esterhuizen, M. et Downing, T.G. beta-N-methylamino-L-alanine (BMAA) in novel South African cyanobacterial isolates. *Ecotoxicology and Environmental Safety*, 2008. **71**(2): p. 309-313.
229. Snyder, L.R., Hoggard, J.C., Montine, T.J. et Synovec, R.E. Development and application of a comprehensive two-dimensional gas chromatography with time-of-flight mass spectrometry method for the analysis of L-beta-methylamino-alanine in human tissue. *Journal of Chromatography A*, 2010. **1217**(27): p. 4639-4647.
230. Banack, S.A., Johnson, H.E., Cheng, R. et Cox, P.A. Production of the neurotoxin BMAA by a marine cyanobacterium. *Marine Drugs*, 2007. **5**(4): p. 180-196.
231. Scott, P.M., Niedzwiadek, B., Rawn, D.F.K. et Lau, B.P.Y. Liquid chromatographic determination of the cyanobacterial toxin beta-N-methylamino-L-alanine in algae food supplements, freshwater fish, and bottled water. *Journal of Food Protection*, 2009. **72**(8): p. 1769-1773.
232. Banack, S.A., Metcalf, J.S., Spacil, Z., Downing, T.G., Downing, S., Long, A., Nunn, P.B. et Cox, P.A. Distinguishing the cyanobacterial neurotoxin beta-N-methylamino-L-alanine (BMAA) from other diamino acids. *Toxicon*, 2011. **57**(5): p. 730-738.
233. Faassen, E.J., Gillissen, F. et Lurling, M. A Comparative Study on Three Analytical Methods for the Determination of the Neurotoxin BMAA in Cyanobacteria. *Plos One*, 2012. **7**(5): p. e36667.
234. Rosen, J. et Hellenas, K.E. Determination of the neurotoxin BMAA (beta-N-methylamino-L-alanine) in cycad seed and cyanobacteria by LC-MS/MS (liquid chromatography tandem mass spectrometry). *Analyst*, 2008. **133**(12): p. 1785-1789.
235. Kruger, T., Monch, B., Oppenhauser, S. et Luckas, B. LC-MS/MS determination of the isomeric neurotoxins BMAA (beta-N-methylamino-L-alanine) and DAB (2,4-diaminobutyric acid) in cyanobacteria and seeds of Cycas revoluta and Lathyrus latifolius. *Toxicon*, 2010. **55**(2-3): p. 547-557.
236. Spacil, Z., Eriksson, J., Jonasson, S., Rasmussen, U., Ilag, L.L. et Bergman, B. Analytical protocol for identification of BMAA and DAB in biological samples. *Analyst*, 2010. **135**(1): p. 127-132.
237. Christensen, S.J., Hemscheidt, T.K., Trapido-Rosenthal, H., Laws, E.A. et Bidigare, R.R. Detection and quantification of beta-methylamino-L-alanine in aquatic invertebrates. *Limnology and Oceanography-Methods*, 2012. **10**: p. 891-898.
238. Li, A.F., Fan, H., Ma, F.F., McCarron, P., Thomas, K., Tang, X.H. et Quilliam, M.A. Elucidation of matrix effects and performance of solid-phase extraction for LC-MS/MS analysis of b-N-methylamino-L-alanine (BMAA) and 2,4-diaminobutyric acid (DAB) neurotoxins in cyanobacteria. *Analyst*, 2012. **137**(5): p. 1210-1219.
239. Salomonsson, M.L., Hansson, A. et Bondesson, U. Development and in-house validation of a method for quantification of BMAA in mussels using dansyl chloride derivatization and ultra performance liquid chromatography tandem mass spectrometry. *Analytical Methods*, 2013. **5**(18): p. 4865-4874.
240. McCarron, P., Logan, A.C., Giddings, S.D. et Quilliam, M.A. Analysis of β-N-methylamino-L-alanine (BMAA) in spirulina-containing supplements by liquid chromatography-tandem mass spectrometry. *Aquatic Biosystems*, 2014. **10**(1): p. 5.

241. Faassen, E.J., Gillissen, F., Zweers, H.A.J. et Lurling, M. Determination of the neurotoxins BMAA (beta-N-methylamino-L-alanine) and DAB (alpha-,gamma-diaminobutyric acid) by LC-MSMS in Dutch urban waters with cyanobacterial blooms. *Amyotrophic Lateral Sclerosis*, 2009. **10**: p. 79-84.
242. Seiler, N. Use of the dansyl reaction in biochemical analysis. *Methods of Biochemical Analysis*, 1970. **18**: p. 259-337.
243. Simmaco, M., De Biase, D., Barra, D. et Bossa, F. Automated amino acid analysis using precolumn derivatization with dansylchloride reversed-phase high-performance liquid chromatography. *Journal of Chromatography A*, 1990. **504**: p. 129-138.
244. Loukou, Z. et Zotou, A. Determination of biogenic amines as dansyl derivatives in alcoholic beverages by high-performance liquid chromatography with fluorimetric detection and characterization of the dansylated amines by liquid chromatography-atmospheric pressure chemical ionization mass spectrometry. *Journal of Chromatography A*, 2003. **996**(1-2): p. 103-113.
245. Guo, K. et Li, L. Differential C-12/C-13-isotope dansylation labeling and fast liquid chromatography/mass spectrometry for absolute and relative quantification of the metabolome. *Analytical Chemistry*, 2009. **81**(10): p. 3919-3932.
246. Lin, H., Tian, Y.A., Zhang, Z.J., Wu, L.L. et Chen, Y. Quantification of piperazine phosphate in human plasma by high-performance liquid chromatography-electrospray ionization tandem mass spectrometry employing precolumn derivatization with dansyl chloride. *Analytica Chimica Acta*, 2010. **664**(1): p. 40-48.
247. Santa, T. Derivatization reagents in liquid chromatography/electrospray ionization tandem mass spectrometry. *Biomedical Chromatography*, 2011. **25**(1-2): p. 1-10.
248. Thermo Fisher Scientific. *Operating Manual*. Q Exactive ™, Thermo Fisher Scientific., Éditeur. Vol. Revision C - 1288120. 2012: Bremen. 238 p.
249. Solliec, M., Roy-Lachapelle, A. et Sauve, S. Quantitative performance of liquid chromatography coupled to Q-Exactive high resolution mass spectrometry (HRMS) for the analysis of tetracyclines in a complex matrix. *Analytica Chimica Acta*, 2015. **853**: p. 415-424.
250. Roy-Lachapelle, A., Solliec, M., Sinotte, M., Deblois, C. et Sauvé, S. High resolution/accurate mass (HRMS) detection of anatoxin-a in lake water using LDTD–APCI coupled to a Q-Exactive mass spectrometer. *Talanta*, 2015. **132**: p. 836-844.
251. Bateman, K.P., Kellmann, M., Muenster, H., Papp, R. et Taylor, L. Quantitative-qualitative data acquisition using a benchtop Orbitrap mass spectrometer. *Journal of the American Society for Mass Spectrometry*, 2009. **20**(8): p. 1441-1450.
252. Meriluoto, J.A. et Spoof, L.E. Cyanotoxins: sampling, sample processing and toxin uptake, publié dans *Cyanobacterial harmful algal blooms: State of the science and research needs*, Hudnell, H.K., Éditeur. 2008, Springer: New York. p. 483-499.
253. Zhang, Y., Hao, Z., Kellmann, M. et Huhmer, A. HR/AM targeted peptide quantitation on a Q Exactive MS: A unique combination of high selectivity, sensitivity, and throughput. *Thermo Fisher Scientific Application Note*, 2012. **554**: p. 1-12.
254. Kaufmann, A., Butcher, P., Maden, K., Walker, S. et Widmer, M. Comprehensive comparison of liquid chromatography selectivity as provided by two types of liquid chromatography detectors (high resolution mass spectrometry and tandem mass spectrometry): "Where is the crossover point?". *Analytica Chimica Acta*, 2010. **673**(1): p. 60-72.

255. Falconer, I.R. et Humpage, A.R. Health risk assessment of cyanobacterial (blue-green algal) toxins in drinking water. *International Journal of Environmental Research and Public Health*, 2005. **2**(1): p. 43-50.
256. Rinehart, K.L., Harada, K., Namikoshi, M., Chen, C., Harvis, C.A., Munro, M.H.G., Blunt, J.W., Mulligan, P.E., Beasley, V.R., Dahlem, A.M. et Carmichael, W.W. Nodularin, microcystin, and the configuration of adda. *Journal of the American Chemical Society*, 1988. **110**(25): p. 8557-8558.
257. Mackintosh, R.W., Dalby, K.N., Campbell, D.G., Cohen, P.T.W., Cohen, P. et Mackintosh, C. The cyanobacterial toxin microcystin binds covalently to cysteine-273 on protein phosphatase 1. *FEBS Letters*, 1995. **371**(3): p. 236-240.
258. Zamyadi, A., McQuaid, N., Prevost, M. et Dorner, S. Monitoring of potentially toxic cyanobacteria using an online multi-probe in drinking water sources. *Journal of Environmental Monitoring*, 2012. **14**(2): p. 579-588.
259. Meriluoto, J. Chromatography of microcystins. *Analytica Chimica Acta*, 1997. **352**(1-3): p. 277-298.
260. Mountfort, D.O., Holland, P. et Sprosen, J. Method for detecting classes of microcystins by combination of protein phosphatase inhibition assay and ELISA: comparison with LC-MS. *Toxicon*, 2005. **45**(2): p. 199-206.
261. Wang, J., Pang, X.L., Ge, F. et Ma, Z.Y. An ultra-performance liquid chromatography-tandem mass spectrometry method for determination of microcystins occurrence in surface water in Zhejiang Province, China. *Toxicon*, 2007. **49**(8): p. 1120-1128.
262. Tsuji, K., Masui, H., Uemura, H., Mori, Y. et Harada, K. Analysis of microcystins in sediments using MMPB method. *Toxicon*, 2001. **39**(5): p. 687-692.
263. Young, F.M., Metcalf, J.S., Meriluoto, J.A.O., Spoof, L., Morrison, L.F. et Codd, G.A. Production of antibodies against microcystin-RR for the assessment of purified microcystins and cyanobacterial environmental samples. *Toxicon*, 2006. **48**(3): p. 295-306.
264. Zeck, A., Eikenberg, A., Weller, M.G. et Niessner, R. Highly sensitive immunoassay based on a monoclonal antibody specific for [4-arginine]microcystins. *Analytica Chimica Acta*, 2001. **441**(1): p. 1-13.
265. Heudi, O., Barteau, S., Picard, P., Tremblay, P., Picard, F. et Kretz, O. Laser diode thermal desorption-positive mode atmospheric pressure chemical ionization tandem mass spectrometry for the ultra-fast quantification of a pharmaceutical compound in human plasma. *Journal of Pharmaceutical and Biomedical Analysis*, 2011. **54**(5): p. 1088-1095.
266. Wu, X.Q., Xiao, B.D., Gong, Y., Wang, Z., Chen, X.G. et Li, R.H. Kinetic study of the 2-methyl-3-methoxy-4-phenylbutanoic acid produced by oxidation of microcystin in aqueous solutions. *Environmental Toxicology and Chemistry*, 2008. **27**(10): p. 2019-2026.
267. Gomis, V., Ruiz, F., Marcilla, A. et Pascual, M.D. Equilibrium for the ternary-system water plus sodium-chloride plus ethyl-acetate at 30-degrees-C. *Journal of Chemical and Engineering Data*, 1993. **38**(4): p. 589-590.
268. Ott, J.L. et Carmichael, W.W. LC/ESI/MS method development for the analysis of hepatotoxic cyclic peptide microcystins in animal tissues. *Toxicon*, 2006. **47**(7): p. 734-741.

269. Dorr, F.A., Rodriguez, V., Molica, R., Henriksen, P., Krock, B. et Pinto, E. Methods for detection of anatoxin-a(s) by liquid chromatography coupled to electrospray ionization-tandem mass spectrometry. *Toxicon*, 2010. **55**(1): p. 92-99.
270. Wong, S.H. et Hindin, E. Detecting an algal toxin by high-pressure liquid-chromatography. *Journal American Water Works Association*, 1982. **74**(10): p. 528-529.
271. Harada, K., Kimura, Y., Ogawa, K., Suzuki, M., Dahlem, A.M., Beasley, V.R. et Carmichael, W.W. A new procedure for the analysis and purification of naturally-occurring anatoxin-a from the blue-green-alga anabaena-flos-aquae. *Toxicon*, 1989. **27**(12): p. 1289-1296.
272. Afzal, A., Oppenlander, T., Bolton, J.R. et El-Din, M.G. Anatoxin-a degradation by Advanced Oxidation Processes: Vacuum-UV at 172 nm, photolysis using medium pressure UV and UV/H2O2. *Water Research*, 2010. **44**(1): p. 278-286.
273. Gugger, M., Lenoir, S., Berger, C., Ledreux, A., Druart, J.C., Humbert, J.F., Guette, C. et Bernard, C. First report in a river in France of the benthic cyanobacterium Phormidium favosum producing anatoxin-a associated with dog neurotoxicosis. *Toxicon*, 2005. **45**(7): p. 919-928.
274. Dimitrakopoulos, I.K., Kaloudis, T.S., Hiskia, A.E., Thomaidis, N.S. et Koupparis, M.A. Development of a fast and selective method for the sensitive determination of anatoxin-a in lake waters using liquid chromatography-tandem mass spectrometry and phenylalanine-d(5) as internal standard. *Analytical and Bioanalytical Chemistry*, 2010. **397**(6): p. 2245-2252.
275. Makarov, A., Denisov, E., Kholomeev, A., Baischun, W., Lange, O., Strupat, K. et Horning, S. Performance evaluation of a hybrid linear ion trap/orbitrap mass spectrometer. *Analytical Chemistry*, 2006. **78**(7): p. 2113-2120.
276. Jiwan, J.L.H., Wallemacq, P. et Herent, M.F. HPLC-high resolution mass spectrometry in clinical laboratory? *Clinical Biochemistry*, 2011. **44**(1): p. 136-147.
277. Moulard, Y., Bailly-Chouriberry, L., Boyer, S., Garcia, P., Popot, M.A. et Bonnaire, Y. Use of benchtop exactive high resolution and high mass accuracy orbitrap mass spectrometer for screening in horse doping control. *Analytica Chimica Acta*, 2011. **700**(1-2): p. 126-136.
278. Haynes, W.M. *CRC Handbook of Chemistry and Physics*. 94th ed, Taylor & Francis Limited., Éditeur. 2013-2014, CRC Press: Boca Raton. 2668 p.
279. The Commission of the European Communities. Commission decision of 12 August 2002 implementing Council Directive 96/23/EC concerning the performance of analytical methods and the interpretation of results. *Official Journal of the European Communities*, 2002: p. 8-36.
280. McLean, T.I. et Sinclair, G.A. Harmful Algal Blooms, publié dans *Environmental Toxicology*, Laws, E.A., Éditeur. 2013, Springer: New York. p. 319-360.
281. Christoffersen, K. Ecological implications of cyanobacterial toxins in aquatic food webs. *Phycologia*, 1996. **35**(6S): p. 42-50.
282. Qiu, T., Xie, P., Ke, Z., Li, L. et Guo, L. In situ studies on physiological and biochemical responses of four fishes with different trophic levels to toxic cyanobacterial blooms in a large Chinese lake. *Toxicon*, 2007. **50**(3): p. 365-376.
283. Metcalf, J.S. et Codd, G.A. Cyanotoxins, publié dans *Ecology of Cyanobacteria II*. 2012, Springer. p. 651-675.

284. del Campo, F.F. et Ouahid, Y. Identification of microcystins from three collection strains of Microcystis aeruginosa. *Environmental Pollution*, 2010. **158**(9): p. 2906-2914.
285. Svirčev, Z., Baltić, V., Gantar, M., Juković, M., Stojanović, D. et Baltić, M. Molecular aspects of microcystin-induced hepatotoxicity and hepatocarcinogenesis. *Journal of Environmental Science and Health Part C*, 2010. **28**(1): p. 39-59.
286. Žegura, B., Štraser, A. et Filipič, M. Genotoxicity and potential carcinogenicity of cyanobacterial toxins–a review. *Mutation Research/Reviews in Mutation Research*, 2011. **727**(1): p. 16-41.
287. World Health Organization. Cyanobacterial toxins: microcystin-LR in drinking-water, publié dans *Guidelines for drinking-water quality*, World Health Organization., Éditeur. 2003: Geneva. p. 1-14.
288. Roy-Lachapelle, A., Fayad, P.B., Sinotte, M., Deblois, C. et Sauve, S. Total microcystins analysis in water using laser diode thermal desorption-atmospheric pressure chemical ionization-tandem mass spectrometry. *Analytica Chimica Acta*, 2014. **820**: p. 76-83.
289. Suchy, P. et Berry, J. Detection of total microcystin in fish tissues based on lemieux oxidation and recovery of 2-methyl-3-methoxy-4-phenylbutanoic acid (MMPB) by solid-phase microextraction gas chromatography-mass spectrometry (SPME-GC/MS). *International Journal of Environmental Analytical Chemistry*, 2012. **92**(12): p. 1443-1456.
290. Darwano, H., Duy, S.V. et Sauvé, S. A new protocol for the analysis of pharmaceuticals, pesticides, and hormones in sediments and suspended particulate matter from rivers and municipal wastewaters. *Archives of Environmental Contamination and Toxicology*, 2014. **66**(4): p. 582-593.
291. Williams, D.E., Craig, M., Dawe, S.C., Kent, M.L., Holmes, C.F. et Andersen, R.J. Evidence for a covalently bound form of microcystin-LR in salmon liver and dungeness crab larvae. *Chemical Research in Toxicology*, 1997. **10**(4): p. 463-469.
292. Williams, D.E., Craig, M., Dawe, S.C., Kent, M.L., Andersen, R.J. et Holmes, C.F. 14 C-labelled microcystin-LR administered to Atlantic salmon via intraperitoneal injection provides in vivo evidence for covalent binding of microcystin-LR in salmon livers. *Toxicon*, 1997. **35**(6): p. 985-989.
293. Nasri, H., El Herry, S. et Bouaïcha, N. First reported case of turtle deaths during a toxic Microcystis spp. bloom in Lake Oubeira, Algeria. *Ecotoxicology and Environmental Safety*, 2008. **71**(2): p. 535-544.
294. Lance, E., Josso, C., Dietrich, D., Ernst, B., Paty, C., Senger, F., Bormans, M. et Gérard, C. Histopathology and microcystin distribution in Lymnaea stagnalis (Gastropoda) following toxic cyanobacterial or dissolved microcystin-LR exposure. *Aquatic Toxicology*, 2010. **98**(3): p. 211-220.
295. Weirich, C.A. et Miller, T.R. Freshwater harmful algal blooms: toxins and children's health. *Current Problems in Pediatric and Adolescent Health Care*, 2014. **44**(1): p. 2-24.
296. Dyble, J., Gossiaux, D., Landrum, P., Kashian, D.R. et Pothoven, S. A kinetic study of accumulation and elimination of microcystin-LR in yellow perch (Perca flavescens) tissue and implications for human fish consumption. *Marine Drugs*, 2011. **9**(12): p. 2553-2571.

297. Deblois, C.P., Mochon, A. et Juneau, P. Toxines de cyanobactéries dans les perchaudes: Analyse exploratoire dans quatre lacs du bassin de la rivière Yamaska. *Le Naturaliste Canadien*, 2008. **132**(1): p. 56-59.
298. Poste, A.E., Hecky, R.E. et Guildford, S.J. Evaluating microcystin exposure risk through fish consumption. *Environmental Science & Technology*, 2011. **45**(13): p. 5806-5811.
299. Schmidt, J.R., Shaskus, M., Estenik, J.F., Oesch, C., Khidekel, R. et Boyer, G.L. Variations in the microcystin content of different fish species collected from a eutrophic lake. *Toxins*, 2013. **5**(5): p. 992-1009.
300. Jia, J., Luo, W., Lu, Y. et Giesy, J.P. Bioaccumulation of microcystins (MCs) in four fish species from Lake Taihu, China: Assessment of risks to humans. *Science of The Total Environment*, 2014. **487**: p. 224-232.
301. Amrani, A., Nasri, H., Azzouz, A., Kadi, Y. et Bouaïcha, N. Variation in cyanobacterial hepatotoxin (microcystin) content of water samples and two species of fishes collected from a shallow lake in Algeria. *Archives of Environmental Contamination and Toxicology*, 2014. **66**(3): p. 379-389.
302. Zhang, D., Xie, P., Liu, Y., Chen, J. et Liang, G. Bioaccumulation of the hepatotoxic microcystins in various organs of a freshwater snail from a subtropical Chinese lake, Taihu Lake, with dense toxic Microcystis blooms. *Environmental Toxicology and Chemistry*, 2007. **26**(1): p. 171-176.
303. Grosse, Y., Baan, R., Straif, K., Secretan, B., El Ghissassi, F., Cogliano, V. et Group, W.I.A.f.R.o.C.M.W. Carcinogenicity of nitrate, nitrite, and cyanobacterial peptide toxins. *The Lancet Oncology*, 2006. **7**(8): p. 628-629.
304. Freitas, M., Azevedo, J., Carvalho, A.P., Campos, A. et Vasconcelos, V. Effects of storage, processing and proteolytic digestion on microcystin-LR concentration in edible clams. *Food and Chemical Toxicology*, 2014. **66**: p. 217-223.
305. Guzmán-Guillén, R., Prieto, A.I., Moreno, I., Soria, M.E. et Cameán, A.M. Effects of thermal treatments during cooking, microwave oven and boiling, on the unconjugated microcystin concentration in muscle of fish (Oreochromis niloticus). *Food and Chemical Toxicology*, 2011. **49**(9): p. 2060-2067.
306. Schmidt, J.R., Wilhelm, S.W. et Boyer, G.L. The Fate of Microcystins in the Environment and Challenges for Monitoring. *Toxins*, 2014. **6**(12): p. 3354-3387.
307. Hyenstrand, P., Metcalf, J., Beattie, K. et Codd, G. Effects of adsorption to plastics and solvent conditions in the analysis of the cyanobacterial toxin microcystin-LR by high performance liquid chromatography. *Water Research*, 2001. **35**(14): p. 3508-3511.